

**Dependency of non-invasive brain stimulation effects on
real-time EEG-based measurements of instantaneous
excitability in human motor cortex**

**Thesis submitted as requirement to fulfill the degree
„Doctor of Philosophy“ (Ph.D.)**

**at the
Faculty of Medicine
Eberhard Karls Universität
Tübingen**

**by
Desideri, Debora**

2020

Dean:	Professor Dr. B. Pichler
First reviewer:	Professor Dr. U. Ziemann
Second reviewer:	Professor Dr. M. Siegel
Third reviewer:	Professorin Dr. D. Saur

Date of oral examination: 01.12.2020

Table of contents

1. Introduction.....	1
1.1 Transcranial magnetic stimulation.....	2
1.2 Electroencephalography and brain oscillations.....	4
1.3 Real-time EEG-triggered TMS.....	5
1.3.1 Effect of μ -phase on corticospinal excitability and plasticity.....	6
1.3.2 Effect of μ -phase on cortical excitability.....	9
1.3.3 Effect of μ -phase on cortical plasticity.....	10
1.3.4 Cortical EEG responses to realistic sham versus real TMS.....	11
2. Results.....	12
2.1 Real-time EEG-defined excitability states determine efficacy of TMS- induced plasticity in human motor cortex	13
2.2 Phase of sensorimotor μ -oscillation modulates cortical responses to TMS of the human motor cortex	43
2.3 Nil effects of μ -rhythm phase-dependent burst-rTMS on cortical excitability in humans: a resting-state EEG and TMS-EEG study.....	60
2.4 Comparison of cortical EEG responses to realistic sham versus real TMS of human motor cortex	78
3. Discussion	88
4. Summary.....	93
5. Bibliography.....	95
6. German summary.....	102
7. Declaration of contribution of others.....	105
Acknowledgments.....	106

1. Introduction

The combination of non-invasive brain stimulation (NIBS) and biological signal recordings has been gaining significant attention in neuroscience very recently. In particular, integrating NIBS with brain imaging techniques has revealed to be a promising tool for studying and modulating neural networks in humans (Mutanen et al., 2013; Premoli et al., 2014; Veniero et al., 2013). Brain imaging can be used to investigate the physiological dynamics underlying NIBS effects, both in research and clinical settings. Nevertheless, the use of NIBS as a therapeutic tool is still limited due to the inconsistent response to NIBS based treatments across sessions and subjects (Goldsworthy et al., 2014; Lopez-Alonso et al., 2014; Vernet et al., 2014; Wiethoff et al., 2014). Several *in vitro* studies, as well as animal and human research, suggest that the state of the stimulated brain circuit at the time of the stimulation may play an important role in the response to NIBS (Huerta & Lisman, 1995; Massimini et al., 2005; Siegle & Wilson, 2014). This makes of brain imaging an interesting tool in the perspective of trying to reduce inter-subject variability and improve effect size of NIBS interventions, as it offers access to brain activity that can be used to define brain states of interest for the specific network under investigation.

Among the different brain imaging techniques, electroencephalography (EEG) is particularly appealing due to its millisecond temporal resolution, which allows capturing changes in brain state in real-time. Interaction with ongoing brain dynamics on a time scale of milliseconds can be achieved with transcranial magnetic stimulation (TMS), a NIBS method that is able to activate neurons in a relatively restricted cortical region (Hallett, 2007).

In this work, we combine EEG and TMS and introduce a novel real-time EEG-triggered TMS approach to study and modulate cortical and corticospinal responses to TMS. Our aim is to lay the groundwork for the establishment of more effective neurorehabilitation protocols that use a brain state-based approach to promote the restoration of dysfunctional networks. For our studies, we select the primary motor cortex as target cortical site, a choice dictated by the future perspective of translating the findings of our research to stroke patients with hand paresis.

1.1 Transcranial magnetic stimulation

Transcranial magnetic stimulation (TMS) is a procedure that uses a temporally changing magnetic field generated by a coil placed on the head to non-invasively induce an electric current in a small region of the cerebral cortex (Barker et al., 1985). Applied at appropriate intensities, TMS can lead to the generation of action potentials (Hallett, 2007). When the primary motor cortex (M1) is stimulated above a certain threshold, i.e. the resting motor threshold (RMT), responses of corticospinal neurons, i.e. the motor evoked potentials (MEPs), can be recorded in peripheral muscles using electromyography (EMG) (Barker et al., 1985; Hallett, 2007). Due to this unique feature to provide an easily accessible readout of its reactivity to a TMS pulse, the motor cortex has been the most targeted brain area in TMS research. In fact, the amplitude and latency of MEPs can be used to quantify the excitability state of the corticospinal system and to assess effects of functional changes and/or experimental interventions on excitability (Hallett, 2007).

Application of several TMS pulses in a certain temporal pattern, i.e. repetitive TMS (rTMS), is a widely used experimental intervention that can induce lasting changes in the excitability of the stimulated cortical site and in the cortical areas functionally connected to it (for a review Fitzgerald et al., 2006). Low frequency (1 Hz) rTMS protocols usually lead to a decreased MEPs amplitude with respect to the pre-rTMS value (Chen et al., 1997; Fitzgerald et al., 2005; Romero et al., 2002). On the other hand, after high frequency (≥ 5 Hz) rTMS MEPs amplitude usually increases with respect to the pre-rTMS value (Pascual-Leone et al., 1994; Peinemann et al., 2004; Quartarone et al., 2005). Another widely used rTMS intervention is the so-called theta burst stimulation (TBS), the basic element thereof being a burst of three TMS pulses at 50 Hz repeated every 200 ms (Huang & Rothwell, 2004). Different TBS protocols are established arranging the basic element, i.e. triplet at 50 Hz, according to different patterns: intermittent TBS (iTBS) is obtained using a 2 s train of TBS repeated every 10 s for a duration of 190 s; intermediate TBS (imTBS) uses a 5 s train of TBS repeated every 15 s for a total duration of 110 s; continuous TBS (cTBS) is an uninterrupted 40 s train of TBS (Huang et al., 2005). In the original publication by Huang and colleagues,

the specific pattern of the TBS intervention determined increase (iTBS), decrease (cTBS) or no change (imTBS) in MEP amplitude (Huang et al., 2005). Since its introduction, TBS has become a very popular protocol because it proved to be able to induce long-lasting changes in corticospinal excitability with a relatively short duration of the rTMS intervention and a limited number of pulses compared to other rTMS paradigms.

The mechanisms underlying rTMS aftereffects on cortical excitability are not completely understood yet, but the observed excitability changes are thought to be based on similar synaptic plasticity mechanisms as long-term potentiation (LTP) and long-term depression (LTD) observed in *in vitro* studies (Fitzgerald et al., 2006). This led to the idea of using rTMS to treat patients with neurological (Fregni et al., 2006; Mansur et al., 2005; Nowak et al., 2008; Talelli et al., 2007) and psychiatric (Bakker et al., 2015; Daskalakis et al., 2002; Padberg et al., 1999) network disorders that may originate from altered synaptic function. Despite some encouraging outcomes, most of the rTMS studies both in healthy participants and patients suffer from high variability across sessions and subjects (Goldsworthy et al., 2014; Lopez-Alonso et al., 2014; Vernet et al., 2014), limiting the efficacy of rTMS in providing a successful treatment in clinical settings.

Animal studies suggest that this variability is not randomness but a result of ongoing brain dynamics. In the cat visual cortex, ongoing neural activity deterministically accounts for the variability of visually evoked activity (Arieli et al., 1996) and explains the amount of neuronal firing after TMS (Pasley et al., 2009). Both *in vitro* and animal experiments, where stimulation was triggered during specific phases of endogenous theta oscillations in hippocampus, revealed that either LTP or LTD could be induced with the otherwise identical stimulation protocol (Huerta & Lisman, 1995), or the encoding vs. retrieval aspects of a memory task could be selectively enhanced (Siegle & Wilson, 2014). These results strongly suggest that synchronizing the stimulation to a particular state of the targeted brain area may help enhance effect size and control directionality of rTMS-induced plasticity.

1.2 Electroencephalography and brain oscillations

Electroencephalography (EEG) is a technique that allows to non-invasively record the electrical activity of the brain by means of electrodes placed on the scalp (H. Berger, 1929). At the cellular level, communication between neurons occurs via electrical currents traveling along the neurons' membrane, i.e. action potentials. Action potentials represent the largest variations of neuronal membrane potential and are the driving element of synaptic transmission. However, EEG does not detect action potentials, because their extracellular amplitude is too small and their duration is too short for multiple action potentials to sum up and generate a signal that can be recorded on the scalp. An action potential reaching the synaptic terminal triggers the release of neurotransmitters which activate specific postsynaptic receptors and lead to the generation of a postsynaptic potential. Postsynaptic potentials can be excitatory (EPSPs) or inhibitory (IPSPs), depending on the type of neurotransmitter and receptor, and last up to several tens of ms. Due to their longer duration, multiple postsynaptic potentials can overlap and add up generating a signal that can be recorded extracellularly on the scalp (Buzsáki et al., 2012; Nunez & Srinivasan, 2006).

A crucial factor for the superimposition of postsynaptic potentials is the spatial disposition of neurons in the cortex (Nunez & Silberstein, 2000). Because of their structured arrangement with their long apical dendrites oriented perpendicularly to the cortical surface, large pyramidal neurons situated in deep layers of the cortex are thought to be the main generators of the EEG signal (Buzsáki et al., 2012; Gloor, 1985; Nunez & Srinivasan, 2006). Due to their anatomical configuration, cortical pyramidal neurons act like electric dipoles, the direction of which is determined by the location of the synaptic input. Postsynaptic potentials at superficial excitatory synapses or at deep inhibitory synapses are registered as negative deflections on the surface EEG, whereas postsynaptic potentials at deep excitatory synapses or at superficial inhibitory synapses result in positive deflections (Kirschstein & Köhling, 2009; Zschocke & Hansen, 2012). The EEG signal is thus the superimposition of all EPSPs and IPSPs of cortical pyramidal neurons that result in a dipole orthogonal to the scalp. Given that the charge carriers of the EPSPs (Na^+ and Ca^{2+}) have a bigger electrochemical gradient than

the charge carriers of the IPSPs (Cl^- and K^+), the EPSPs are predominant in the EEG signal (Kirschstein & Köhling, 2009; Zschocke & Hansen, 2012).

The synchronized activity of thousands of large pyramidal neurons generates characteristic oscillatory patterns in the scalp EEG (Buzsáki, 2006; Buzsáki et al., 2012). EEG oscillations have peculiar frequency ranges and spatial distribution and are associated with different brain states or functions (Buzsáki, 2006). Slower EEG waves, i.e. delta (δ , 0.5 – 4 Hz) and theta (θ , 4 – 7 Hz) oscillations, exhibit larger amplitudes, whereas faster EEG waves, i.e. alpha (α , 7 – 13 Hz), mu (μ , 8 – 12 Hz), beta (β , 13 – 30 Hz) and gamma (γ , > 30 Hz) oscillations, present lower amplitudes with increasing frequency (Buzsáki, 2006). Brain oscillations are thought to play a fundamental role in information processing, perception, motor coordination, memory, sleep and consciousness (Gray et al., 1989; Gupta et al., 2016; Massimini et al., 2003; Rutishauser et al., 2010; Salenius et al., 1997). In particular, they are believed to functionally orchestrate the response of cortical neurons to synaptic inputs in a phase-dependent manner (Buzsáki & Draguhn, 2004). Different phases of an oscillation represent therefore different states of a neuronal assembly where neurons are more or less responsive to inputs, i.e. more or less excitable.

1.3 Real-time EEG-triggered TMS

In the last few years, EEG has gained increasing attention in the TMS field, as a tool to access cortical responses to TMS. Through the combination of TMS with EEG (TMS-EEG) it has been possible to record and characterize TMS evoked cortical potentials (TEPs, Bonato et al., 2006; Ilmoniemi et al., 1997; Komssi et al., 2004; Paus et al., 2001; Premoli et al., 2014) and TMS related modulation of spontaneous oscillatory activity (Fecchio et al., 2017; Fuggetta et al., 2005; Premoli et al., 2017; Rosanova et al., 2009) not only from the motor cortex, but also from other cortical regions. Providing access to direct cortical responses, TMS-EEG has also allowed the quantification of rTMS induced LTP-/LTD-like changes at the cortical level (Casula et al., 2014; Chung et al., 2017; Esser et al., 2006).

Recently, several researchers have been starting using TMS-EEG also to assess the influence of pre-stimulus brain activity on responses to TMS and they

showed that the current brain state affects MEP size as well as amplitude and spatiotemporal distribution of EEG responses to TMS (B. Berger et al., 2014; Bergmann et al., 2012; Keil et al., 2014; Mäki & Ilmoniemi, 2010; Massimini et al., 2005; Romei et al., 2008; Sauseng et al., 2009). However, most of these results have been obtained *post hoc* sorting the TMS trials according to pre-stimulus EEG features and present therefore some limitations. The first limitation is that often *post hoc* trial sorting cannot provide unequivocal results because of the contamination of the EEG signal by the stimulus artifact. This is a problem particularly for the estimation of pre-stimulus oscillatory phase. The second important limitation is that a *post hoc* trial sorting approach cannot be employed in the case of rTMS, where the intervention itself must be synchronized to a predefined brain state.

To overcome these limitations, we have constructed a real-time EEG-triggered TMS set-up based on a customized Simulink model (The Mathworks, USA) that is able to synchronize TMS with specific phases of the ongoing μ -oscillation generated in the left sensorimotor cortex (Zrenner et al., 2018).

The μ -rhythm is the dominant oscillation in the frequency spectrum of sensorimotor areas at rest (Hari, 2006; Neuper et al., 2005). Several studies indicate that pre-stimulus activity in the 8 – 12 Hz frequency band is associated with inhibitory control and that this control may occur in a phase-dependent manner (Jensen & Mazaheri, 2010). Previous animal and human research showed that neural spiking activity in the sensorimotor cortex is highest during the negative peak of the local μ -oscillation (Haegens et al., 2011), while the tactile perceptual threshold is decreased (Ai & Ro, 2014). These findings support the notion that the phase of the locally generated μ -oscillation plays an important role in information processing. With the present work, we wanted to assess the impact of μ -phase on cortical and corticospinal excitability and on rTMS induced plasticity measured with EMG and EEG.

1.3.1 Effect of μ -phase on corticospinal excitability and plasticity

In our publication “*Real-time EEG-defined excitability states determine efficacy of TMS-induced plasticity in human motor cortex*”, we investigated the role of the phase of the endogenous μ -oscillation in the modulation of

corticospinal excitability and in the induction of corticospinal plasticity measured with the amplitude of MEPs (Zrenner et al., 2018).

To address our scientific question, we tested two groups of right-handed volunteers. Each group underwent a first experimental session where the effect of μ -phase on corticospinal excitability was tested by means of single TMS pulses applied to the left M1 in the position and orientation to elicit MEPs in a selected target muscle of the right hand. For the first group (12 subjects) TMS was triggered either by the negative or the positive phase of the ongoing μ -oscillation, while for the second group (11 subjects) TMS was triggered either by the negative peak, the positive peak or random phase of the ongoing μ -oscillation.

In both groups, corticospinal excitability was significantly modulated by the phase of the μ -oscillation. In particular, for the first group of participants MEP amplitude was on average 14.2% larger when TMS was applied at the negative vs. the positive peak of the μ -oscillation. For the second group of participants, the effect of μ -phase was confirmed with an average MEP amplitude 36.5% larger in the negative vs. positive peak condition, and 22.4% larger in the random phase vs. positive peak condition.

Effect of μ -phase on corticospinal plasticity was tested using a rTMS protocol with a burst of three TMS pulses at 100 Hz as basic element and a total of 200 bursts per intervention. During the intervention, bursts were synchronized to a preselected brain state. Each experimental session consisted of 2 pre-rTMS and 3 post-rTMS blocks in which single TMS pulses were delivered to the left M1 and MEPs were recorded.

The first group of participants underwent six rTMS experimental sessions, in which the following brain states were used to trigger the rTMS triplets: positive peak or negative peak of the local μ -rhythm (Main Experiment), positive peak or negative peak of distal occipital α -rhythm (Control Experiment 1), replay of positive peak or negative peak μ -rhythm rTMS sequence from Main Experiment independent of ongoing μ -rhythm (Control Experiment 2). The Main Experiment investigated the effects of sensorimotor μ -phase on corticospinal plasticity. Control Experiment 1 served to demonstrate that the phase-dependent effects on corticospinal plasticity observed in the Main Experiment were produced only

when a locally generated oscillation is used to trigger the rTMS triplets. Control Experiment 2 was used to show that the results in the Main Experiment depended on the synchronization between stimulus and brain state and were not caused by the temporal properties of the rTMS sequence.

The second group of participants underwent three rTMS experimental sessions, in which the following brain states were used to trigger the rTMS triplets: positive peak, negative peak or random phase of the local μ -rhythm (Control Experiment 3). Control Experiment 3 was designed to validate, generalize and extend the results of the Main Experiment.

The major findings of these experiments are the following: in the Main Experiment and Control Experiment 3 rTMS induced a long-lasting (>30 minutes) increase of corticospinal excitability with respect to the average pre-rTMS MEP amplitude when consistently synchronized with the negative peak of the μ -oscillation (high excitable state), whereas no significant change was observed in the positive peak and random phase triggered rTMS sessions. Moreover, no effect of α -phase was observed in Control Experiment 1, suggesting that phase-dependent differential plasticity effects are obtained when rTMS is synchronized to endogenous oscillations originating from the same neural network that is targeted by rTMS. Finally, nil effects of rTMS in Control Experiment 2 support the notion that the direction of the induced plasticity critically depends on the synchronization between stimulus and brain state and is not caused by the temporal properties of the rTMS sequence.

These results confirm that the negative peak of the endogenous μ -oscillation represents a state of higher excitability of the corticospinal system, where the dendritic trees of the stimulated pyramidal neurons receive predominantly excitatory inputs and are closer to firing threshold. More importantly, we showed for the first time in the human brain that the efficacy and directionality of the induced plasticity effects are critically dependent on the synchronization of the rTMS intervention with the instantaneous state of the stimulated cortical network.

While our first study focused on corticospinal excitability and plasticity, our following publications "*Phase of sensorimotor μ -oscillation modulates cortical*

responses to TMS of the human motor cortex” and “*Nil effects of μ -rhythm phase-dependent burst-rTMS on cortical excitability in humans: a resting-state EEG and TMS-EEG study*” focused on cortical excitability and plasticity.

1.3.2 *Effect of μ -phase on cortical excitability*

In “*Phase of sensorimotor μ -oscillation modulates cortical responses to transcranial magnetic stimulation of the human motor cortex*”, we investigated the role of the phase of the endogenous μ -oscillation in the modulation of cortical excitability (Desideri et al., 2019).

Cortical excitability has been quantified with EEG using TEPs and TMS induced oscillations. TEPs represent the evoked part of the cortical response to TMS and are characterized by a series of positive and negative deflections at different latencies with a characteristic spatial distribution (Bonato et al., 2006; Komssi et al., 2004; Premoli et al., 2014). For the motor cortex, the most investigated TEP components are P25, N45, P70, N100, P180 and N280, where P and N indicate positive and negative deflections, respectively, and the number following them indicates the approximate latency of their occurrence. TMS-induced oscillations represent modulations of spontaneous cortical oscillatory activity that are not necessary time-locked to the TMS stimulus and are therefore canceled out in the analysis of TEPs. These responses can be uncovered with a time-frequency representation analysis and for the motor cortex they are typically expressed as an early (up to approximately 200 ms) power increase followed by a late (up to approximately 600 ms) power decrease in the α and β frequency bands (Gordon et al., 2018; Premoli et al., 2017). In our previous study, we showed that corticospinal excitability is enhanced at the negative vs. positive peak of the μ -oscillation, therefore we expected to observe a similar result at the cortical level, reflected by the amplitude of the TEPs and by the power of the TMS-induced oscillations.

To evaluate the impact of pre-stimulus μ -phase on cortical responses to TMS, we applied TMS to the left M1 on 12 healthy participants in three different conditions: a suprathreshold condition with a stimulation intensity of 110% RMT, a subthreshold condition with a stimulation intensity of 90% RMT and a realistic

sham condition. In all conditions, TMS has been triggered either by the positive peak, the negative peak or random phase of the endogenous μ -oscillation. The inclusion of a subthreshold stimulation intensity allowed us to disentangle between phase-dependent modulation of brain responses evoked by TMS vs. sensory re-afferent feedback caused by MEPs. The realistic sham TMS condition allowed us to exclude a significant contribution of the auditory and scalp somatosensory inputs associated with TMS to the μ -phase-dependent modulation of direct brain responses evoked by TMS.

The main findings of this study are the following: 100% RMT TMS applied at the negative vs. the positive peak of the μ -rhythm was associated with higher absolute amplitudes of the P70 and N100 TEP components. Enhancement of the N100 was confirmed with negative peak-triggered 90% RMT TMS, while the phase of the μ -rhythm did not influence evoked responses elicited by sham TMS. TMS-induced EEG oscillations were not significantly modulated by the phase of the ongoing μ -oscillation in any of the investigated conditions.

We demonstrated that TEPs can capture excitability fluctuations in the stimulated cortical site and can, therefore, represent a valuable tool to quantify the responsiveness of brain areas that don't provide other objective readouts.

1.3.3 Effect of μ -phase on cortical plasticity

In “*Nil effects of μ -rhythm phase- dependent burst-rTMS on cortical excitability in humans: a resting-state EEG and TMS-EEG study*”, we analyzed the EEG and TMS-EEG data from the plasticity sessions of our first publication (Zrenner et al., 2018) to assess whether μ -phase-synchronized rTMS induced long-lasting changes on EEG-based measures of cortical excitability alongside with the induced changes in corticospinal excitability (Desideri et al., 2018).

We analyzed resting-state EEG in the motor cortex ipsi- and contralateral to the stimulation, and single-pulse TMS-evoked and -induced EEG responses in the stimulated motor cortex. Oscillatory activity has been analyzed in the μ - and β -bands, both for resting-state EEG and for TMS related power modulation, while local mean field power (LMFP) has been used for the analysis of TEPs.

We found that none of these EEG measures were significantly modulated by any of the tested rTMS interventions. In particular, negative vs. positive peak μ -

phase-synchronized rTMS did not produce any consistent differential modulation at the cortical level, despite the presence of a significant differential and reproducible effect on MEP amplitude.

We concluded that EEG may not always be an appropriate tool to capture excitability changes induced by rTMS, as these changes happen at the molecular and synaptic level and include both excitatory and inhibitory components that cannot be differentiated at the macroscopic level by EEG.

1.3.4 *Cortical EEG responses to realistic sham versus real TMS*

In addition to the activation of cortical neurons and fibers, TMS also causes indirect brain responses through auditory and somatosensory stimulation. These responses are unwanted and may contribute significantly to the overall EEG signal, masking the effects of experimental interventions on direct cortical responses. In our publication "*Comparison of cortical EEG responses to realistic sham versus real TMS of human motor cortex*", we intended to assess the differences in cortical responses between real TMS at intensities above and below RMT and a realistic sham stimulation (Gordon et al., 2018).

To this aim, we used part of the data collected for our study "*Phase of sensorimotor μ -oscillation modulates cortical responses to transcranial stimulation of the human motor cortex*" (Desideri et al., 2019). In particular, we focused on the random phase TMS trials of the 110% RMT, 90% RMT and realistic sham stimulation conditions and analyzed TEPs and TMS-induced oscillations.

We found a significant difference in the amplitude of TEPs across conditions, with TEPs from 110% RMT showing overall highest amplitudes and realistic sham lowest amplitudes. Moreover, sham stimulation had only minor effects on TMS-induced oscillations compared to the pre-stimulus baseline, while TMS at 90% RMT and 110% RMT resulted in a significant early increase (50-200 ms) followed by a decrease (200-500 ms) in α and β power. TMS at 110% RMT led to an additional increase in β power at late latencies (650-800 ms).

These findings reinforce the evidence that cortical responses to TMS observed with EEG are mostly unrelated to sensory evoked potentials associated with TMS.

2. Results

This section consists of the four original manuscripts and the related supplementary materials that resulted from the research conducted in the framework of this doctoral thesis. All results presented are first or co-first author papers that have been published in peer-reviewed journals.

2.1 Real-time EEG-defined excitability states determine efficacy of TMS-induced plasticity in human motor cortex



Real-time EEG-defined excitability states determine efficacy of TMS-induced plasticity in human motor cortex



Christoph Zrenner¹, Debora Desideri¹, Paolo Belardinelli, Ulf Ziemann*

Department of Neurology & Stroke, Hertie Institute for Clinical Brain Research, University of Tübingen, Hoppe-Seyler-Str. 3, 72076, Tübingen, Germany

ARTICLE INFO

Article history:

Received 16 October 2017

Received in revised form

19 November 2017

Accepted 20 November 2017

Available online 24 November 2017

Keywords:

Brain-state dependent stimulation

EEG-TMS

μ -Rhythm

Repetitive transcranial magnetic stimulation

Corticospinal excitability

LTP-like plasticity

ABSTRACT

Background: Rapidly changing excitability states in an oscillating neuronal network can explain response variability to external stimulation, but if repetitive stimulation of always the same high- or low-excitability state results in long-term plasticity of opposite direction has never been explored *in vivo*.

Objective/hypothesis: Different phases of the endogenous sensorimotor μ -rhythm represent different states of corticospinal excitability, and repetitive transcranial magnetic stimulation (rTMS) of always the same high- vs. low-excitability state results in long-term plasticity of different direction.

Methods: State-dependent electroencephalography-triggered transcranial magnetic stimulation (EEG-TMS) was applied to target the EEG negative vs. positive peak of the sensorimotor μ -rhythm in healthy subjects using a millisecond resolution real-time digital signal processing system. Corticospinal excitability was indexed by motor evoked potential amplitude in a hand muscle.

Results: EEG negative vs. positive peak of the endogenous sensorimotor μ -rhythm represent high- vs. low-excitability states of corticospinal neurons. More importantly, otherwise identical rTMS (200 triple-pulses at 100 Hz burst frequency and ~1 Hz repetition rate), triggered consistently at this high-excitability vs. low-excitability state, leads to long-term potentiation (LTP)-like vs. no change in corticospinal excitability.

Conclusions: Findings raise the intriguing possibility that real-time information of instantaneous brain state can be utilized to control efficacy of plasticity induction in humans.

© 2017 Elsevier Inc. All rights reserved.

Introduction

Transcranial magnetic stimulation (TMS) evokes action potentials in cortex with a spatiotemporal precision of millimeters and milliseconds [1], enabling specific, non-invasive and safe interaction with ongoing network dynamics of the human brain [2,3] at a mesoscopic scale [4,5].

Responses of corticospinal neurons to TMS are indexed by motor evoked potentials (MEPs) recorded by electromyography (EMG) from muscles [1,6]. A salient feature of MEPs is their substantial trial-to-trial amplitude variability [7,8]. Also, long-term changes of MEP amplitude induced by repetitive TMS protocols show extensive intra- and interindividual variability [9–11]. Studies of animal preparations suggest that this variability is not due to noise but reflects dynamics of brain state. In cat visual cortex, the variability of

evoked activity is deterministically explained by ongoing neural activity [12]. In *in vitro* rat hippocampal slice experiments, the phase of ongoing theta-oscillations at the time of stimulation with a single 100 Hz quadruplet pulse determines the direction of synaptic plasticity, i.e., long-term potentiation (LTP) vs. depotentiation of LTP [13,14]. In human motor physiology, however, this insight has been largely ignored: 30 years of TMS for probing and modulating human brain networks have disregarded the continuously fluctuating brain states at the time of stimulation, with very few exceptions [15].

For the purpose of the present study, we have constructed a millisecond-resolution electroencephalography (EEG)-triggered TMS set-up that synchronizes TMS with specific phase of ongoing μ -oscillations in the alpha-band (8–12 Hz) from the sensorimotor cortex. μ -oscillations constitute the most prominent rhythm in the frequency spectrum of sensorimotor cortex at rest [16,17]. Furthermore, μ -oscillations are associated with phase-dependent inhibitory control [18], where neuronal spiking activity is reduced during the positive peak of local μ -oscillations [16], and tactile perceptual threshold is increased [19].

* Corresponding author.

E-mail address: ulf.ziemann@uni-tuebingen.de (U. Ziemann).

¹ These authors have contributed equally to this work.

Effects of μ -rhythm phase on corticospinal excitability cannot be assessed by post-hoc trial sorting in a non-ambiguous way because the EEG is contaminated by the stimulus artefact, and phase estimation depends on reconstruction of the gap in the signal for which no unequivocal method exists. This explains why the published findings using post-hoc phase-bin sorting of stimulus artefact-contaminated EEG data are contradictory [20–22]. An alternative approach uses transcranial alternating current stimulation (tACS) to entrain oscillations in a stimulated network [23,24] and triggers TMS pulses concurrently to a defined tACS phase but has also resulted in contradictory findings [25–27], and it is uncertain if the entrained oscillations are identical to the ones that occur endogenously. In addition, recent intracranial recordings have casted serious doubt on whether at all it is possible to entrain neuronal activity in human cortex with contemporary tACS methods [28]. This is why we introduce the real-time EEG-TMS approach for testing the effects of instantaneous endogenous μ -rhythm phase on corticospinal excitability (MEP amplitude), and on long-term change of corticospinal excitability induced by phase-specific neuromodulatory repetitive TMS (rTMS) [29], where post-hoc sorting cannot be used in any case.

Methods

Main Experiment and Control Experiments 1 and 2

Subjects. The study protocol was approved by the local ethics committee at the medical faculty of the University of Tübingen (protocol 716/2014B02). Experiments conformed to the Declaration of Helsinki, and were performed in accordance with the current TMS safety guidelines [30]. All subjects gave written informed consent prior to participation. 29 male right-handed healthy volunteers, between 18 and 50 years and without a history of neurological or psychiatric disease or use of central nervous system active drugs, alcohol or nicotine were screened to identify 12 subjects (mean age \pm s.d. 26.5 ± 7.5 years; age range, 20–48 years, Edinburgh Handedness Inventory laterality score, 62 ± 21) that fulfilled all pre-established inclusion criteria (i–iv, see below). The planned sample size of $n = 12$ was based on previous non-invasive brain stimulation plasticity studies [31]. A power analysis for sample size estimation was not performed due to the exploratory nature of this study. Inclusion criteria: (i) Resting motor threshold (RMT) of the right abductor pollicis brevis (APB) or first dorsal interosseous (FDI) muscle $\leq 60\%$ of maximum stimulator output. In case of comparable RMT for the two muscles, APB was chosen as target muscle for subsequent analysis, otherwise the muscle with lower RMT was chosen. The RMT threshold criterion was selected to increase the probability of inducing corticospinal plasticity [11], and to ensure that the TMS stimulator would be capable of generating the rTMS protocol at the required intensity of 80% RMT (the highest intensity at which triple pulses could be generated by the stimulator at 100 Hz was 48% of maximum output). (ii) Stimulus intensity necessary to evoke MEP of 1 mV in peak-to-peak amplitude (SI_{1mV}) $\leq 130\%$ of RMT. MEPs of 1 mV amplitude typically occur in the steep part of the sigmoid response curve, where the sensitivity to detect changes in corticospinal excitability is highest [32]. (iii) Single peak in the alpha band (8–12 Hz) $> 25\%$ of total power in the CSD power spectrum of the C3 EEG signal overlying the left sensorimotor cortex with the subject at rest and eyes open (Supplementary Fig. 3a). This criterion ensured that the oscillation amplitude was sufficiently large to enable our algorithm to estimate instantaneous phase of the trigger signal with sufficient accuracy [33] (Fig. 4c, Supplementary Fig. 3d). (iv) μ -oscillatory activity present for > 300 ms prior to the trigger in the averaged non-stimulated phase-triggered epochs of the initial excitability session. This criterion

ensured that the triggers were locked to a physiological oscillation rather than band-pass filtered noise [34] (Supplementary Fig. 3e). 16/17 of the excluded subjects failed on the CSD power spectrum criterion, and 1/17 subject on the RMT criterion.

Experimental set-up. We constructed an EEG-TMS set-up that utilized an online output copy of the EEG signal, analyzed in real-time, to trigger TMS pulses depending on the instantaneous oscillatory phase of the recorded EEG signal (Fig. 1, Supplementary Figs. 1–2). An air-cooled TMS coil (Magstim 70 mm Double Air Film Coil, Magstim Ltd, UK) and a high-frequency magnetic stimulator (Magstim Super Rapid Plus, Magstim Ltd, UK) were used to deliver biphasic single cosine cycle pulses with 400 μ s period. The coil was oriented such that the second phase of the biphasic pulse induced an electrical field in the brain from lateral-posterior to medial-anterior, i.e., orthogonal to the central sulcus. This current orientation is considered highly effective in *trans*-synaptically activating the corticospinal neurons [35]. The magnetic stimulator was triggered through an external TTL pulse delivered by the real-time digital signal processing system through the Magstim Stimulator Interface Module. Stimulus intensity was set manually. The stimulator touch screen UI was used to configure the stimulator to either deliver upon triggering a single pulse (for measurement of corticospinal excitability indexed by MEP amplitude) or a train of 3 pulses with an inter-pulse-interval of 10 ms (100 Hz, for induction of corticospinal plasticity).

An individually MRI-guided stereoscopic neuronavigation system (Localite GmbH, Sankt Augustin, Germany) was used for maintaining a constant position of the TMS coil in 3D-space relative to the participant's head, for recording the position of the coil at each TMS pulse, and for recording the position of each EEG electrode relative to the head. Excellent consistency of TMS coil location and orientation across experimental sessions of each subject was demonstrated post-hoc by intra-class correlations of spatial coordinates and coil angles of ≥ 0.96 for each degree of freedom.

MEP in relaxed right hand muscles were elicited by TMS of the hand representation of the left M1 and recorded through bipolar EMG adhesive hydrogel electrodes (Kendall, Covidien) over the APB and the FDI muscle in a bipolar belly-tendon montage (5 kHz sampling rate, 0.16 Hz – 1.25 kHz bandpass filter). The motor “hot-spot” was identified as the coil position and orientation resulting, at a slightly suprathreshold stimulation intensity, in maximum MEP amplitudes [35]. The corresponding coil coordinates were stored using the neuronavigation software, in order to retrieve them in the subsequent experimental sessions. RMT was defined as the minimum stimulation intensity necessary to elicit MEPs $> 50 \mu$ V, and was determined to the nearest 1% of maximum stimulator output using the standard relative frequency method [35].

Scalp EEG was recorded from a 64-channel TMS compatible Ag/AgCl sintered ring electrode cap (EasyCap GmbH, Germany) in the International 10–20 system arrangement. A 24-bit 80-channel biosignal amplifier was used for EEG and EMG recordings (NeuroOne Tesla with Analog Out Option, Bittium Biosignals Ltd, Finland), data was acquired in AC mode with a head-stage sample rate of 80 kHz for subsequent analysis. The analog output option of the amplifier was configured to recreate from the digital data a filtered and amplified parallel analog signal (5 kHz sampling rate per channel, 0.16 Hz–1.25 kHz bandpass filter) from a user-selectable subset of 16 amplifier channels covering left sensorimotor cortex. Out of this subset, a configuration of EEG sensors centered on C3 surrounded by FC3, C1, CP3 and C5 was analyzed by the real-time system. The analog output stage consisted of a 16-bit digital-to-analog converter (DAC) system with a 10-kHz frequency and a signal conditioning stage to produce a low-pass filtered (500 Hz cut-off frequency, 24 dB/octave) scaled signal in the ± 5 V range, resolving sensor data at 0.1 μ V. The analog-to-digital conversion

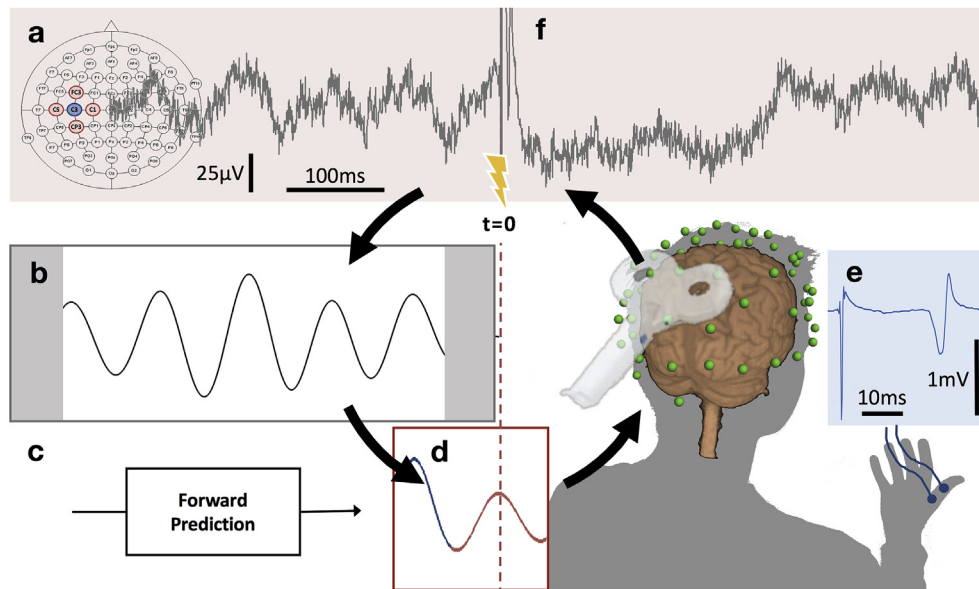


Fig. 1. μ -oscillation phase-triggered brain stimulation apparatus. (a) Scalp EEG raw data derived from a 5-point sum-of-difference operation centered on the C3 EEG electrode (Hjorth-C3) over left sensorimotor cortex is streamed to a real-time system with 3 ms latency where the processing algorithm is computed at a rate of 500 Hz. (b) A 500 ms sliding window of data is 8–12 Hz bandpass filtered forward and backward and edge artefacts (shaded) are removed. (c) Coefficients for an autoregressive model are calculated from the filtered data. (d) The signal is forward predicted (red trace), phase is estimated at time zero ($t = 0$) using a Hilbert transform and the TMS stimulator is triggered when a pre-set phase condition is met. (e) TMS of the hand area of left primary motor cortex produces a MEP in right hand muscles recorded with surface EMG. (f) Recovery of the μ -oscillation \sim 300 ms after the TMS pulse. (For interpretation of the references to colour in this figure legend, the reader is referred to the web version of this article.)

(ADC), digital filtering, DAC stage, and signal conditioning stage resulted in a constant latency of 3 ms between the signal at the EEG sensor and the signal at the analog output.

Real-time digital signal processing. Running in parallel to the wide-bandwidth 24-bit resolution 5 kHz recording and archiving of the raw EEG data, a real-time data acquisition, digital processing and TMS stimulator control system was implemented as a Simulink Real-Time model (Mathworks Ltd, USA, R2015a) executed on a dedicated xPC Target PC running the Simulink Real-Time operating system (DFI-ACP CL630-CRM mainboard). Biosignal data was acquired from the 16 channels of the analog output of the NeurOne amplifier through a compatible data acquisition card (UEI PD2-MF-64-500/16 L, United Electronic Instruments, USA) at a sample rate of 2 kHz, range of ± 5 V and resolution of 16 bit. The same card was also used to generate digital TTL output signals to trigger the TMS stimulator. Additional 8-bit synchronization signals were generated through the parallel port of the real-time PC, and both the stimulator trigger signals and the 8-bit triggers were acquired by the EEG amplifier and archived alongside the EEG/EMG data for subsequent analysis and sorting of epochs.

A multi-rate real-time model was programmed to process sliding windows of data at a fixed fundamental sample time step size of 0.5 ms. The sliding window was configured to have a length of 1000 samples (500 ms). The real-time system could be configured to trigger TMS pulses in a pre-determined sequence or, in accordance with EEG power and phase of the acquired analog EEG signal, at either the EEG positive or negative peak of the μ -rhythm as determined by the spatially filtered C3 electrode EEG signal. The parameters and execution of the real-time system were asynchronously controlled from a standard PC running Microsoft Windows 8 and Mathworks Matlab R2015a through an Ethernet connection. The sequence and timing of experimental blocks (Fig. 2) were controlled from a separate room through a customized automatic script in order to maintain consistency between experimental sessions and to keep the experimenter and subjects blinded to the stimulation condition.

Real-time μ -phase dependent brain stimulation. To isolate local sensorimotor μ -oscillations from signal contamination by volume conduction and interference from other sources of alpha oscillations, an orthogonal source derivation [33] was performed over a 500 ms sliding window: The mean was removed from each channel and a 5-point “sum-of-difference” operator centered on the C3 EEG electrode and the four nearest neighbors (C1, C5, FC3, CP3) was computed by the real-time system at a rate of 500 Hz. The resulting Hjorth-C3 signal was used for subsequent estimation of power and phase (Supplementary Fig. 1a). In order to estimate instantaneous phase at the edge of the sliding window (“time zero”), an autoregressive forward prediction method of the Hjorth-C3 signal was implemented [36]. Specifically, the sliding window was zero-phase forward and backward filtered (FIR 8–12 Hz bandpass filter, Supplementary Fig. 1b), trimmed by 64 ms segments on both ends to reduce edge effects, and the remaining 372 ms signal segment was used to generate the coefficients for an autoregressive forward prediction model (Yule-Walker, order 30), which served to iteratively compute a forecast 128 ms into the future, ± 64 ms around “time zero” (Supplementary Fig. 1c). Instantaneous phase was estimated by calculating the analytic signal from the 128 ms window using a fast Fourier transform (FFT)-based Hilbert transform (Supplementary Fig. 1d). Simultaneously, the power spectrum of the Hjorth-C3 signal was calculated from the entire sliding window using an autoregressive Yule-Walker model with order 200 to optimize spectral resolution in the alpha (8–12 Hz) frequency band [37]. A digital output (TTL) signal was generated to trigger the magnetic stimulator when the Hilbert transform crossed the target phase and a predetermined μ -power threshold was also exceeded (Supplementary Figs. 1-2).

The phase prediction algorithm was highly accurate on average, but it had a standard deviation of 54° over all trials (Fig. 4c). This variability is explained by the employed approach of forward-predicting a bandpass filtered signal that required a trade-off between the efficacy of the filter and the length of the prediction interval: A higher order FIR filter (covering more than 2 cycles,

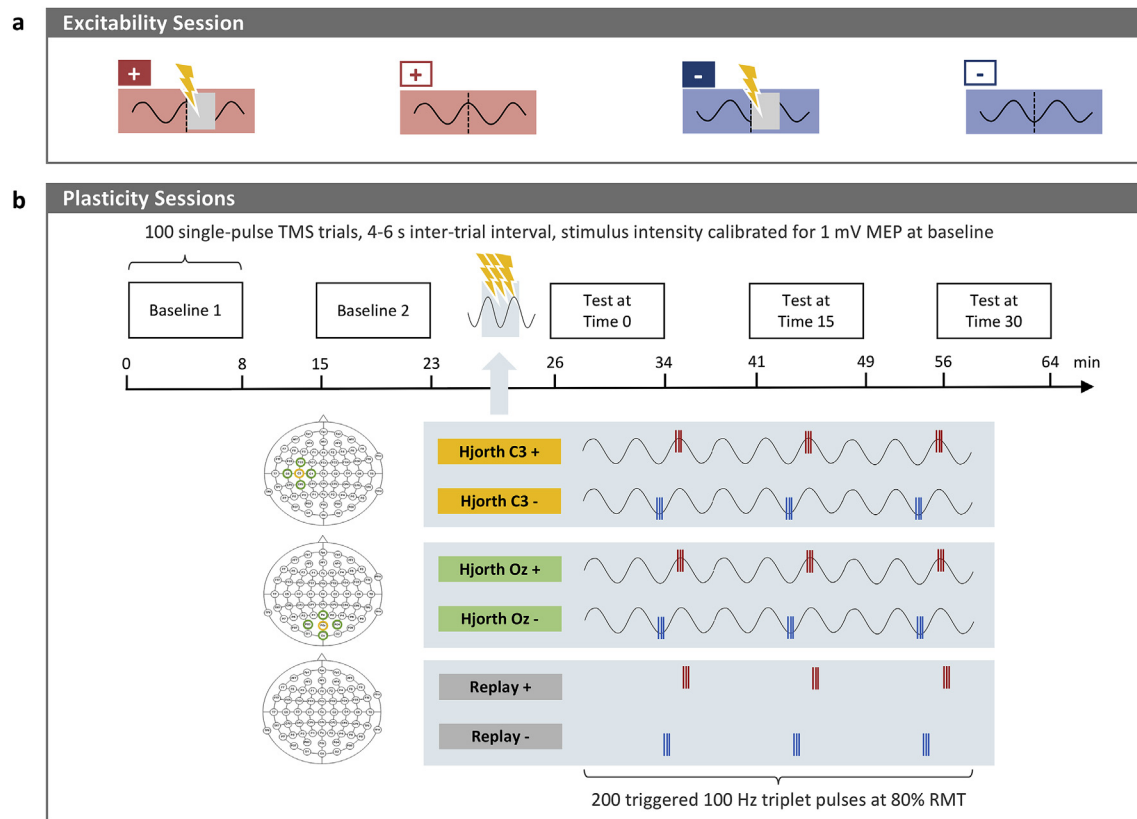


Fig. 2. Sessions in the Main Experiment and Control Experiments 1 and 2. (a) The first session (“excitability experiment”) assessed the effect of instantaneous phase of left sensorimotor μ -rhythm on corticospinal excitability in 4 randomized epoch conditions (~150 trials each): triggering (indicated by vertical dashed lines) and stimulating (indicated by yellow arrows), or triggering and non-stimulating on Hjorth-C3 EEG positive (+) or negative (-) peaks (600 trials in total; duration, ~20 min). The stimulated trials provided the corticospinal excitability data, quantified as peak-to-peak MEP amplitude from a right-hand muscle, while the triggered but non-stimulated trials enabled testing of phase-accuracy. (b) The subsequent sessions (“plasticity experiments”) tested the cumulative effects of different phase-specific rTMS interventions. Stimulation intensity was 80% of resting motor threshold, 200 triplets (3 pulses at 100 Hz) were applied, and mean duration \pm 1 s.d. was 192 ± 25 s (i.e., the mean triplet repetition rate \pm 1 s.d. was 1.01 ± 0.12 Hz). Corticospinal plasticity was tested by comparing MEP amplitudes in blocks of 100 single-pulse TMS trials 0, 15 and 30 min post-rTMS with those pre-rTMS (baseline 1 and baseline 2). Stimulus intensity was set prior to each session to elicit MEPs ~1 mV peak-to-peak amplitude, and this intensity was used throughout the experimental session. In the two sessions of the Main Experiment, TMS of the M1 was triggered by the Hjorth-C3 derived sensorimotor μ -rhythm either at the positive peak (Hjorth-C3 +) or the negative peak (Hjorth-C3 -). In Control Experiment 1 (two sessions), TMS of M1 was triggered by the Hjorth-Oz derived positive (Hjorth-Oz +) or negative peak (Hjorth-Oz -) of the occipital alpha-rhythm, to test topographical specificity of differential corticospinal plasticity induced by Hjorth-C3 triggered rTMS in the Main Experiment. In Control Experiment 2 (two sessions), replay of the identical rTMS sequences as in the Main Experiment (Replay +, Replay -) was applied, i.e. irrespective of power and phase of the ongoing μ -rhythm, to test the critical role of instantaneous brain state for corticospinal plasticity induction in the Main Experiment. All 12 subjects participated in the Main Experiment, and 11 and 8 of them in Control Experiments 1 and 2, respectively. For a given participant, the interval between consecutive sessions was ≥ 3 d, and the order of sessions was pseudo-randomized (with replay sessions always following Main Experiment sessions). (For interpretation of the references to colour in this figure legend, the reader is referred to the web version of this article.)

i.e. 200 at a sample rate of 1 kHz) isolates the μ -rhythm more accurately, but would also delay the signal longer (here, 100 ms) - any prediction error would then be amplified with the length of the delay that needs to be bridged and the prediction fails completely when the rhythm is not stable. A lower order filter (<100 at a sample rate of 1 kHz) enables faster adaptation to physiological slip of phase progression but does not remove frequencies outside of the pass band as effectively resulting in a noisy signal that doesn't oscillate symmetrically around zero. The parameters chosen for this study (two-pass FIR filter with order 128) worked satisfactory for subjects whose μ -(8-12 Hz) spectral component exceeded 25% of total power.

Experimental sessions. The initial session (excitability experiment) of the Main Experiment investigated the relationship of sensorimotor μ -rhythm phase and corticospinal excitability (Fig. 2a): At the beginning 5 min of resting-state EEG (eyes open, subjects instructed to relax and fixate a cross at eye level 1 m in front of them) were obtained. Thereafter, 4 trigger conditions (~150 trials each) were tested in randomized order with a minimum inter-trial interval of 2 s and a total of 600 trials. A trigger was

generated either by the Hjorth-C3 positive or negative peak, and either resulted (stimulated trials) or did not result in a TMS pulse (non-stimulated trials). Non-stimulated trials without a stimulus artefact were used to determine the actual phase at the time of the trigger and hence the accuracy of the real-time system (Fig. 4c). The non-stimulated trials were also voxel-wise correlated with source level activity to determine the anatomical origin of the Hjorth-C3 signal (Fig. 4a) and to provide CSD topographical plots (Fig. 4b) to demonstrate that the positive and negative peak of the EEG signal used for TMS-triggering were localized over left sensorimotor cortex. The stimulated trials provided the corticospinal excitability data for the Hjorth-C3 positive and negative peak conditions. Stimulation intensity was SI_{1mV} .

The subsequent sessions (plasticity experiments) investigated the effects of sensorimotor μ -rhythm phase on rTMS-induced plasticity (Fig. 2b). 200 triple pulses (3 pulses at 100 Hz) [14] with stimulus intensity of 80% RMT and minimum interval between triplets of 0.75 s were applied to the hand area of the left M1 for corticospinal plasticity induction. While 100 Hz quadruplets were used in the experiments in rat hippocampus [14], which

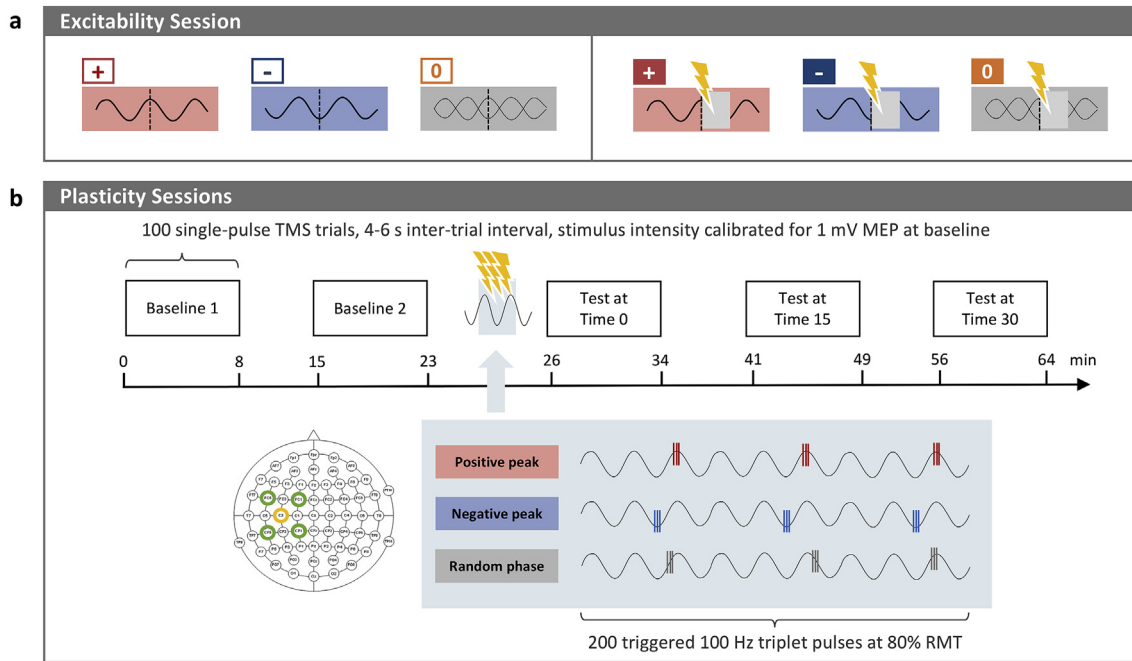


Fig. 3. Sessions in Control Experiment 3. (a) The first session assessed the effect of instantaneous phase of left sensorimotor μ -rhythm on corticospinal excitability in 3 randomly interleaved Hjorth-C3 triggered phase conditions: positive peak, negative peak, and random phase (100 trials per condition). A separate measurement with the identical set-up and the coil in place but the stimulator trigger cable unplugged was performed to obtain triggered non-stimulated trials for post-hoc assessment of phase-accuracy. (b) Subsequently, three plasticity sessions were performed in randomized order, ≥ 3 days apart from each other, to assess the cumulative effects of 200 rTMS triplets (3 pulses at 100 Hz; stimulus intensity 80% RMT) triggered by Hjorth-C3 positive peak, negative peak, or random phase. The mean duration ± 1 s.d. was 194 ± 16 s, (i.e., the mean triplet repetition rate ± 1 s.d. was 1.04 ± 0.08 Hz). Corticospinal plasticity was tested by comparing MEP amplitudes in blocks of 100 single-pulse TMS trials at 0, 15 and 30 min post-rTMS with those pre-rTMS (baseline 1 and baseline 2). Stimulus intensity for MEP amplitude testing was set at 120% RMT and this intensity was used throughout the experimental sessions.

covered on average 22.5% of the hippocampal 7.5 Hz theta oscillation cycle, we used triplets in order to cover a similar amount of the ~ 10 Hz sensorimotor μ -oscillation cycle. The triple pulses were

triggered by a combined criterion of μ -phase and power threshold. The phase condition was set, depending on the experimental session, to always trigger the first pulse of the triplets either at the

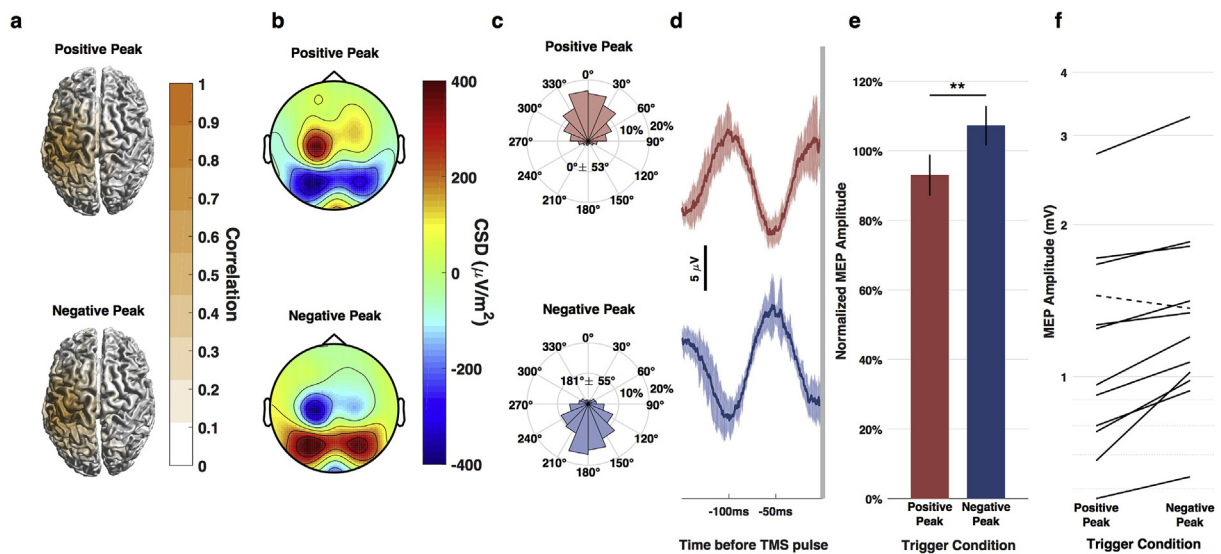


Fig. 4. Corticospinal excitability depends on the instantaneous phase of local sensorimotor μ -rhythm. (a) Group average ($n = 12$) voxel-wise correlation of source activity with Hjorth-C3 EEG signal for triggered non-stimulated positive and negative peak conditions, correlation coefficient (range, 0–1) indicated by the color bar. (b) Mean current source density (CSD) plots of the triggered non-stimulated positive and negative peak conditions, amplitudes (in $\mu\text{V}/\text{m}^2$) indicated by the color bar. (c) Distribution of actual phase angle at the time of the trigger of triggered non-stimulated trials of all subjects. Phase angles are binned (width, 22.5°) and frequencies are indicated (inner ring = 10%, outer ring = 20%). (d) Mean ± 1 s.d. of raw sensorimotor Hjorth-C3 EEG signal preceding TMS in the positive and negative peak condition, stimulus artefact shaded grey at right. (e) Mean ($n = 12$) ± 1 s.d. MEP amplitudes, evoked by TMS at Hjorth-C3 positive peak (red) vs. negative peak (blue), normalized to the individual mean, $**p = 0.001$ (two-tailed paired t-test). (f) Individual data showing larger MEP amplitude (in mV, logarithmic scale) at the Hjorth-C3 negative peak in all but one subject (dashed line). (For interpretation of the references to colour in this figure legend, the reader is referred to the web version of this article.)

Hjorth-C3 positive peak or negative peak of the ongoing μ -rhythm. The μ -power threshold was set manually before the beginning of the rTMS-intervention and was, if necessary, adjusted during the intervention to result in an interval between triplets ranging between 0.8 and 1.5 s, and a total duration of the plasticity induction protocol of 160–300 s (Supplementary Fig. 10). In the Main Experiment, mean (± 1 s.d.) μ -power threshold was $0.48 \pm 0.17 \mu\text{V}^2$ in the positive peak condition vs. $0.45 \pm 0.15 \mu\text{V}^2$ in the Hjorth-C3 negative peak condition ($t_{11} = 0.82$, $p = 0.43$, two-tailed paired t-test), and in Control Experiment 1: $0.57 \pm 0.28 \mu\text{V}^2$ in the positive peak condition vs. $0.55 \pm 0.26 \mu\text{V}^2$ in the Hjorth-Oz negative peak condition ($t_{10} = 0.82$, $p = 0.43$, two-tailed paired t-test).

Corticospinal plasticity was assessed by change in MEP amplitude in 3 blocks of 100 single-pulse TMS trials (inter-trial interval 5 ± 0.5 s) post-rTMS (0, 15 and 30 min post-rTMS) vs. 2 blocks pre-rTMS (baselines 1 and 2) (Fig. 2b). Single-pulse TMS for MEP amplitude assessment was applied without EEG information on the ongoing μ -rhythm. The two baseline blocks were obtained to demonstrate stability of the MEP measurements. The stimulator intensity for MEP measurements was kept constant at $SI_{1\text{mV}}$ throughout the experiment, as determined at the beginning of the experimental session. rTMS-induced changes in MEP amplitude could imply mechanisms at cortical, subcortical or even spinal level, but spinal excitability tested by H-reflexes or F waves consistently remained unchanged after various rTMS protocols in previous studies (for review [31]). This suggests that the rTMS-induced changes in MEP amplitude in the present experiments most likely originated at the level of motor cortex. However, we deliberately use the term “corticospinal plasticity” to not exclude the remote possibility of a contribution by spinal mechanisms.

In addition, the following control conditions were tested (Fig. 2b): In Control Experiment 1, rTMS over the hand area of the left M1 was triggered by the positive peak vs. negative peak of the sensor level Hjorth spatial filter centered on electrode Oz with POz, O2, Iz and O1 as nearest neighbors (Hjorth-Oz), i.e., the alpha-oscillations over visual cortex. The occipital alpha-power expressed in the CSD power spectrum of the signal from the Oz electrode at rest was $>25\%$ in each of the included participants (mean ± 1 s.d. $47 \pm 12\%$, range: 26%–67%). In Control Experiment 2, the identical rTMS sequences delivered in a given participant in the Main Experiment were replayed in the same participant, irrespective of instantaneous power and phase of the μ -rhythm. Control Experiment 1 tested the critical role of utilizing real-time EEG information from the local sensorimotor μ -rhythm for corticospinal plasticity induction in the Main Experiment. Control Experiment 2 provided essential information on the necessity of synchronizing rTMS with power and phase of the ongoing μ -rhythm for corticospinal plasticity induction in the Main Experiment. All 12 subjects participated in the main experiment, and 11 and 8 of them in Control Experiments 1 and 2, respectively. In a given participant, the interval between consecutive sessions was ≥ 3 d, the order of sessions was pseudo-randomized (with the replay conditions always following Main Experiment conditions), and sessions in a given participant were run always on the same time of day to avoid diurnal fluctuations in TMS-induced plasticity [38].

Data analysis and statistics. EMG and EEG data reprocessing was performed using the Fieldtrip open source toolbox [39], and customized analysis scripts on MATLAB® (Mathworks Ltd, USA, R2015a). EMG signals were zero-phase bandpass filtered (20–500 Hz) with a 3rd order Butterworth filter and an additional 3rd order zero-phase Butterworth notch filter (49–51 Hz) to reduce power line noise. Trials contaminated by involuntary muscle contraction in the 500 ms period prior to the TMS pulse (6.4% of the total) were discarded since pre-innervation increases MEP amplitude [1]. Single-trial peak-to-peak MEP amplitudes were

automatically determined in the retained trials within 20–40 ms after the TMS pulse. Statistical analyses were performed with IBM® SPSS® Statistics v.23. In the excitability experiment, the effect of μ -oscillation phase (Hjorth-C3 positive vs. negative peak) on MEP amplitude was tested using a two-tailed paired t-test. In the plasticity experiments, rmANOVAs were run on the ln-transformed baseline MEP amplitude data to demonstrate that there was no effect of Time (baseline 1 vs. baseline 2), Phase (positive vs. negative peak) or the interaction between Time and Phase. Since this was not the case (all $p > 0.05$), MEP amplitudes were averaged across baseline 1 and 2 for each individual experimental session, and post-rTMS MEP amplitudes (0, 15 and 30 min post-rTMS) were normalized to this average baseline. Then, three rmANOVAs with the within-subject effects of Time (0, 15 and 30 min post-rTMS) and Phase (Main Experiment: Hjorth-C3 positive peak vs. negative peak; Control Experiment 1: Hjorth-Oz positive peak vs. negative peak; Control Experiment 2: replay of Hjorth-C3 positive peak vs. negative peak) were performed on the normalized to average baseline MEP amplitudes. Mauchly's test was used to test for sphericity in all rmANOVAs, and the Greenhouse-Geisser correction was applied whenever sphericity was violated. *Post-hoc* paired two-tailed t-tests were applied in case of a significant main effect or interaction. For all tests, normal data distribution was verified by the Shapiro-Wilk test, and the significance level was $p < 0.05$.

Manual artefact rejection was performed in the stimulated and non-stimulated EEG trials (see above, excitability experiment). Epochs with artefacts in one or more channels were discarded. Single channels with artefact contamination in the majority of epochs were removed. A FastICA decomposition [40] was then applied. The resulting ICA components were visually inspected for topography, averaged time course and single trial time course. Components representing eye blinking, eye movements, and heartbeat were removed. After ICA cleaning, removed channels were spline-interpolated using the signals of the neighboring channels. EEG signals were re-referenced to an average-reference montage.

EEG source localization. Anatomical, T1-weighted MR images were acquired from all subjects with a Siemens Magnetom Prisma 3 T (voxel size = $1.0 \times 1.0 \times 1.0$ mm; FoV read = 250, FoV phase 93.8%, TR 2300 ms, TE = 4.18 ms, FA = 9.0°). The anatomical images were pre-processed with SPM [41]: the coordinate system of the MR image was realigned to the Montreal Neurological Institute coordinate system (MNI) and a correction for magnetic field inhomogeneities was applied. Segmentation of the anatomical image was performed for five different tissue types: skull, scalp, cerebrospinal fluid, grey and white matter. A Finite Element Model (FEM) of the head was created by means of a geometrical description based on hexahedrons and assigning the following respective conductivity values to the segmented tissues: 0.01 S/m, 0.43 S/m, 1.79 S/m, 0.33 S/m, 0.14 S/m [42]. A standard grid with 6 mm spatial resolution was linearly warped to the single subject head model for the dipole locations in the brain source space. Finally, the EEG electrode positions digitized by the neuro-navigation system were used for an accurate lead fields computation. A Linear Constrained Minimum Variance (LCMV) Beamformer [43] was then used to estimate the strength of neuronal activity at a particular spatial source location. Time-courses of each dipole in the grid were estimated in the 3 orthogonal directions. Then, the dipole moments were projected in the strongest direction, resulting in a single signal for each dipole in the grid.

Control experiment 3 (validation experiment)

Background. Control Experiment 3 was designed to validate, generalize and extend the results of the Main Experiment. The main

difference was the incorporation of an additional random phase trigger control condition that used the same 8–12 Hz power threshold criterion as the phase triggered conditions but instead of requiring a positive or negative peak phase detection event to occur, the stimulator was automatically triggered after a uniformly random delay between 0 and 100ms. The random phase condition differed from the two phase triggered conditions only in the distribution of phase angles (cf. Fig. 9b–c, Fig. 10a), but not in the pre-stimulus spectral power (Supplementary Fig. 6) or in the inter-trigger interval (Supplementary Fig. 10), and was included to provide a reference condition for any phase-specific effects. In all other regards, the Control Experiment 3 was substantially similar to the Main Experiment, differing only in the following methodological details.

Subjects. We performed a power analysis based on the data obtained in the Main Experiment (means and standard deviations in the Hjorth–C3 positive vs. negative peak conditions) to estimate the required sample size for Control Experiment 3. On a planned level of alpha of $p = 0.025$ (for a two-tailed t-test) and power ($1-\beta$) of $>90\%$ this resulted in a minimum of $n = 9$ subjects. To have a safety margin, we decided to include $n = 11$ subjects. We had to screen 30 additional right-handed healthy volunteers under the same study protocol, all without prior experience of TMS, and without a history of neurological or psychiatric disease, to identify 11 subjects (9 female, 2 male, mean age ± 1 s.d. 25.4 ± 3.7 years; age range, 21–32 years; Edinburgh Handedness Inventory laterality score, 91 ± 13) that fulfilled the following pre-established inclusion criteria: (i) RMT $\leq 67.5\%$ of maximum stimulator output. This intensity was chosen such that 80% RMT matched the maximum intensity at which the stimulator used in Control Experiment 3 was capable of generating 100 Hz rTMS pulses (54%). (ii) Spectral power in the alpha band (8–12 Hz) $> 25\%$ of total power in the CSD power spectrum of the C3 EEG signal with the subject at rest and eyes open (Supplementary Fig. 5a). (iii) A stable μ -oscillation for >300 ms in the average pre-stimulus EEG signal of the non-stimulated trials. 17/19 of the excluded subjects failed on the CSD power criterion, and 2/19 subjects on the RMT criterion.

Experimental set-up. A different stimulation set-up was used, consisting of a passively cooled TMS double coil (PMD70-pCool, 70 mm winding diameter, MAG & More, Germany) and a high-frequency magnetic stimulator (Research 100, MAG & More, Germany) customized to enable external triggering at up to 100 Hz and configured to deliver biphasic single cosine cycle pulses with 160 μ s period in the same polarity and orientation configuration as in the Main Experiment. Each TMS pulse was individually triggered through an external TTL trigger input from the real-time system. For MEP amplitude testing, stimulus intensity was set manually to 120% RMT. The same stereoscopic neuronavigation system (Localite GmbH, Germany) was used as in the Main Experiment, however, in MR-less mode, registering the subject's head to a standard Montreal Neurological Institute (MNI) brain anatomical dataset. Online EEG data acquired from a 64 channel EEG cap (Easycap GmbH, Germany), with a custom layout based on the 10–20 system but with a higher electrode density over sensorimotor cortex, was streamed from the EEG system (NeuroOne, Bittium Biosignals Ltd, Finland) main unit to the real-time system using the real-time “Digital Out” mode via UDP network protocol at a consistent rate of 1 data packet per millisecond. The original signal was then immediately available for real-time processing without degradation from passing through the analog intermediate stage used in the Main Experiment and the “Digital Out” mode also enabled use of the EEG amplifier in DC mode, which was chosen for Control Experiment 3 (5 kHz sampling rate, 1.25 kHz low-pass anti-aliasing filter).

Real-time digital signal processing. The real-time system was the same as used in the Main Experiment but to accept digital EEG data through a UDP connection at a rate of one packet per ms. Each packet contained 5 samples per channel which were down-sampled by averaging for subsequent real-time analysis at a temporal resolution of 1 ms. All 64 EEG channels were available to the real-time algorithm, a subset of 5 channels were used by the trigger algorithm.

Real-time μ -phase dependent brain stimulation. Local sensorimotor μ -rhythm was isolated using a Hjorth Laplacian orthogonal source derivation montage similar to the Main Experiment. However, instead of using the nearest neighboring electrodes surrounding C3, a slightly wider “diamond” shaped Hjorth-Laplace montage was chosen, with C3 at the center and CP1, CP5, FC1, and FC5 in the surrounding locations. The diamond shape was used to increase the size of the filter so that an off-center EEG source of the μ -rhythm could still be captured by the filter. The following changes were made to the phase detection algorithm as compared to the Main Experiment: (i) The sliding window used for phase detection was shortened to 400 ms to better cope with non-stationarity of the endogenous μ -rhythm. (ii) The band-pass filter stage was modified to only filter the signal in the forward direction, the resulting signal delay was then compensated in the autoregressive forecasting stage. (iii) The spectral power estimation algorithm was modified to use a Hann-windowed FFT over a longer time-window of 1024 ms of data with the threshold criterion being the difference in power between the alpha spectrum (8–12 Hz) relative to the average power across the 1–100 Hz range in units of dB, configurable by the experimenter during the experiment. Mean (± 1 s.d.) pre-EEG-triggered μ -power on Hjorth–C3 was $1.86 \pm 1.52 \mu\text{V}^2$ in the positive peak condition, $2.05 \pm 2.41 \mu\text{V}^2$ in the negative peak condition, and $1.80 \pm 1.79 \mu\text{V}^2$ in the random phase condition. These values were not different from each other (rmANOVA, $F_{2,20} = 0.266$, $p = 0.769$). (iv) An automatic artefact detection method was implemented to prevent a stimulus trigger from being generated within 400 ms of the EEG signal exceeding a set amplitude threshold of $\pm 40 \mu\text{V}$ at any of the 5 Hjorth-Laplace electrodes.

Experimental sessions. The same experimental sessions were conducted as in the Main Experiment, with the following changes: In the excitability experiment, the “random phase” control trigger condition was randomly interleaved with the “positive peak” and “negative peak” trigger conditions (Fig. 3a). Non-stimulated real-time triggered epochs were collected in a separate experimental block with the coil held in place over the motor hotspot but the stimulator trigger cable unplugged. A vacuum pillow (Vacuform, B. u.W. Schmidt GmbH, Germany) and a fixation arm (Magic Arm, Lino Manfrotto + Co. S. p.A. Italy) were used to immobilize the head and maintain a fixed coil position during the excitability experiment. In the plasticity experiment, all conditions were triggered by the C3–Hjorth signal over left sensorimotor cortex. In addition to the positive and negative peak conditions (to replicate the key result from the Main Experiment) a third random phase condition was included as a reference control (Fig. 3b). The three conditions were performed in separate sessions (≥ 3 d apart for a given participant) in a pseudo-randomized double-blind cross-over experimental design with exactly the same test and intervention blocks as in the Main Experiment. The coil was held in place manually during the plasticity experiment. Neuronavigation was used for all sessions to maintain coil position.

Data analysis and statistics. The exact same methods were used as in Main Experiment.

Results

Corticospinal excitability in main experiment

Phase-specific TMS of the μ -rhythm was achieved by low-latency acquisition of the filtered and amplified signal from the EEG electrodes overlying the hand area of the left sensorimotor cortex by a customized real-time signal-processing algorithm. Local cortical activity was isolated by computing the orthogonal source derivation by means of a 5-point central difference operator [33] centered on EEG electrode C3 (Hjorth-C3) over left sensorimotor cortex. A sliding window of data was zero-phase 8–12 Hz band-pass filtered to isolate the μ -rhythm. The signal was forward-predicted using an autoregressive model to enable instantaneous phase to be estimated at “time zero” [36], i.e., the time of the TMS trigger decision (Fig. 1a–d and Supplementary Figs. 1–2). Spectral power was simultaneously calculated within the sliding window in the alpha-frequency band. A TMS pulse was triggered when a pre-determined power threshold was met and a pre-specified phase angle was simultaneously crossed. MEP amplitudes were measured by surface EMG of right hand muscles (Fig. 1e).

Analysis of the Hjorth-C3 EEG signal of the triggered but non-stimulated EEG epochs (cf. Methods and Fig. 2a) showed best correlations with EEG activity at the source level in the hand knob area of left primary motor cortex (M1), or the directly adjacent primary somatosensory cortex in all subjects (Fig. 4a and Supplementary Fig. 3b). This verifies that the Hjorth-C3 EEG signal that was used for triggering single-pulse TMS in the excitability experiments, and rTMS in the plasticity experiments, originated from primary sensorimotor cortex. In addition, current source density (CSD) plots of the EEG signal ± 20 ms around the trigger in the non-stimulated trials showed a localized positivity (negativity) over the stimulated left M1 region in the positive (negative) Hjorth-C3 peak conditions (Fig. 4b and Supplementary Fig. 3c), further corroborating topographical specificity of our EEG-TMS approach.

Post-hoc analysis of the real-time triggered non-stimulated EEG epochs indicated accuracy of the real-time EEG-TMS system, with mean ± 1 s.d. phases of $0^\circ \pm 53^\circ$ and $181^\circ \pm 55^\circ$ for the positive and negative peak conditions, respectively (Fig. 4c and Supplementary Fig. 3d). Phase accuracy was also assessed by the average raw EEG signal preceding the TMS pulse in the stimulated positive and negative peak conditions (Fig. 4d).

The MEP amplitude evoked in the Hjorth-C3 negative peak condition was on average (± 1 s.d.) $14.2 \pm 11.2\%$ larger (range, -5.9% to 39.6%) than in the positive peak condition ($p = 0.001$, two-tailed paired t-test), indicating that corticospinal excitability varied with μ -rhythm phase (Fig. 2e–f). The effect size is comparable to the alpha-phase dependent modulation of cell firing rate of about 17% in monkey M1 [16].

The magnitude of this effect correlated with measures of “methodological efficacy”, indexed by the distance between TMS coil center position (overlying M1 hand area) and sensorimotor EEG electrode C3 (Fig. 5a), and correlation between the sensor level Hjorth-C3 signal and source activity at the stimulation site in M1 (Fig. 5b). These correlations strongly support the view that corticospinal excitability variation with phase depends specifically on the μ -oscillation originating at the site of stimulation.

Topographical specificity was tested further by dividing subjects into two groups (focal vs. broad Hjorth-Oz, $n = 6$ each, Supplementary Fig. 7a) based on analysis of their resting-state EEG (for methodological details, see legend of Supplementary Fig. 7), and a concern (cf. Fig. 7b) that EEG from occipital alpha-oscillations may have contaminated the Hjorth-C3 EEG signal. RmANOVA of the excitability data confirmed the significant effect of Phase ($F_{1,10} = 17.80$, $p = 0.002$), but did not reveal effects of Hjorth-Oz

Group ($F_{1,10} = 0.05$, $p = 0.82$) or Hjorth-Oz Group \times Phase interaction ($F_{1,10} = 0.18$, $p = 0.68$) (Supplementary Fig. 7b). This suggests that spread of occipital alpha-activity into the Hjorth-C3 EEG signal was not critical for the observed difference of corticospinal excitability between Hjorth-C3 positive vs. negative peaks of the μ -rhythm.

Pre-stimulus power of the μ -rhythm did not affect MEP amplitude in the Hjorth-C3 positive or negative peak conditions (Supplementary Fig. 4). This is at variance with a decreasing cell firing rate with increasing power of local alpha-oscillations in monkey M1 [16], and an inverse correlation between μ -power in the resting-state EEG of the pre-TMS period and MEP amplitude in humans [44–46]. This discrepancy may be explained by implementation of a μ -power threshold (see Methods) to ensure high accuracy of phase prediction, so that MEPs at low μ -power were not obtained. Further data that cover a larger μ -power range are required to clarify this issue. Furthermore, pre-stimulus power in other frequency bands (delta < 4 Hz, theta 4–7 Hz, beta 13–30 Hz, and gamma 31–45 Hz) was also unrelated to MEP amplitude (group data, all $r^2 < 0.002$).

Corticospinal plasticity in main experiment

Mean pre-stimulus EEG signals indicated good accuracy, on average, in the positive and negative peak conditions during the rTMS intervention (Fig. 6a).

RmANOVA demonstrated significant effects of Phase ($F_{1,11} = 7.01$, $p = 0.023$) and the interaction of Phase and Time ($F_{1,951,21,459} = 3.92$, $p = 0.036$), but not Time ($F_{1,357,14,923} = 0.08$, $p = 0.93$) on normalized MEP amplitude (Fig. 6b). These effects were explained by significantly larger MEP amplitudes in the Hjorth-C3 negative than positive peak condition 15 and 30 min post-rTMS ($p = 0.024$ and $p = 0.005$, respectively, two-tailed paired t-tests) (Fig. 6b–c). Moreover, MEP amplitudes in the negative peak condition were significantly increased 15 and 30 min post-rTMS compared to average baseline ($p = 0.014$ and $p = 0.010$, respectively, two-tailed paired t-tests) (Fig. 6b). In contrast, none of the post-rTMS MEP amplitudes in the positive peak condition were significantly different from average baseline (all $p > 0.05$, Fig. 6b–c). The time courses of the raw and baseline-normalized individual MEP amplitude data are shown in Supplementary Fig. 9a–b.

The absence of a significant difference of the mean inter-triplet-intervals in the rTMS sequences in the Hjorth-C3 positive vs. negative peak conditions (Supplementary Fig. 10a; $p = 0.47$, two-tailed paired t-test) strongly suggests that this differential plasticity effect cannot be accounted for by differences in pulse train stochastics of the rTMS sequence in the two conditions.

Moreover, pre-stimulus μ -power was not different during rTMS between Phase conditions (positive peak: $0.62 \pm 0.38 \mu V^2$; negative peak: $0.76 \pm 0.42 \mu V^2$; $p = 0.25$, two-tailed paired t-test), and pre-stimulus μ -power during rTMS did not predict the change in MEP amplitude (positive peak: $R^2 = 0.01$, $p = 0.73$; negative peak: $R^2 < 0.001$, $p = 0.98$). These nil findings demonstrate that ongoing μ -power was not relevant for the differential MEP change in the negative vs. positive peak conditions, nor for the magnitude of the LTP-like MEP increase in the negative peak condition.

Topographical specificity was assessed by dividing subjects into focal vs. broad Hjorth-Oz occipital alpha activity (see legend of Supplementary Fig. 7 for details). RmANOVA of normalized MEP amplitude confirmed the significant effect of Phase ($F_{1,10} = 6.60$, $p = 0.028$), but did not reveal effects of Time ($F_{2,20} = 0.10$, $p = 0.91$), Hjorth-Oz Group ($F_{1,10} = 0.15$, $p = 0.70$), Hjorth-Oz Group \times Phase interaction ($F_{1,10} = 0.87$, $p = 0.37$), or Hjorth-Oz Group \times Phase \times Time interaction ($F_{2,20} = 0.28$, $p = 0.97$) (Supplementary Fig. 7c), suggesting that possible spread of occipital alpha-activity

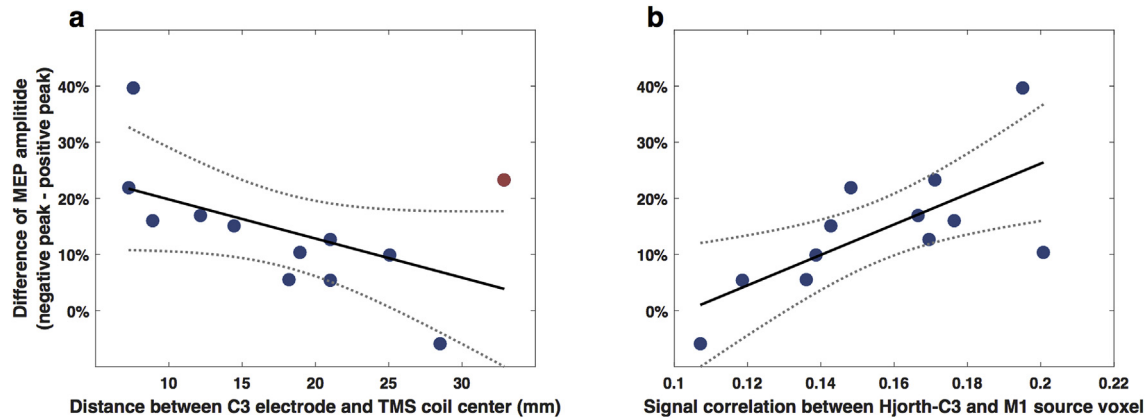


Fig. 5. Corticospinal excitability depends on local μ -oscillatory phase. (a) Individual percentage difference of MEP amplitude between the Hjorth-C3 negative minus positive peak condition normalized to the individual mean correlated inversely ($r^2 = 0.68$; $p = 0.002$) with the distance between the C3 EEG electrode and the center of the TMS coil. One outlier with distance >30 mm, where C3 was no longer the closest electrode to the center of the TMS coil, was excluded (marked red). (b) Individual difference of MEP amplitude between Hjorth-C3 negative vs. positive peak conditions correlated directly ($r^2 = 0.49$; $p = 0.01$) with the correlation between the Hjorth-C3 EEG sensor signal and the source-level activity at the voxel within the 6-mm source grid closest to the site of stimulation in superficial layers of M1. Data were normally distributed. Linear regression fit (solid line) with 95% c. i. (dotted lines). (For interpretation of the references to colour in this figure legend, the reader is referred to the web version of this article.)

into the Hjorth-C3 EEG signal was not critical for the observed difference of corticospinal plasticity induced by rTMS triggered on the Hjorth-C3 positive vs. negative peak of the μ -rhythm.

Finally, we assessed if μ -power was changed by the rTMS intervention. RmANOVA of the average baseline-normalized pre-

stimulus μ -power did not show effects of Phase ($F_{1,11} = 0.12$, $p = 0.74$), Time ($F_{2,22} = 1.26$, $p = 0.31$), or the interaction of Phase and Time ($F_{2,22} = 1.37$, $p = 0.22$, [Supplementary Fig. 11a](#)). It can be concluded that, in contrast to corticospinal excitability measured by MEP amplitude, power of the μ -rhythm was not altered by rTMS.

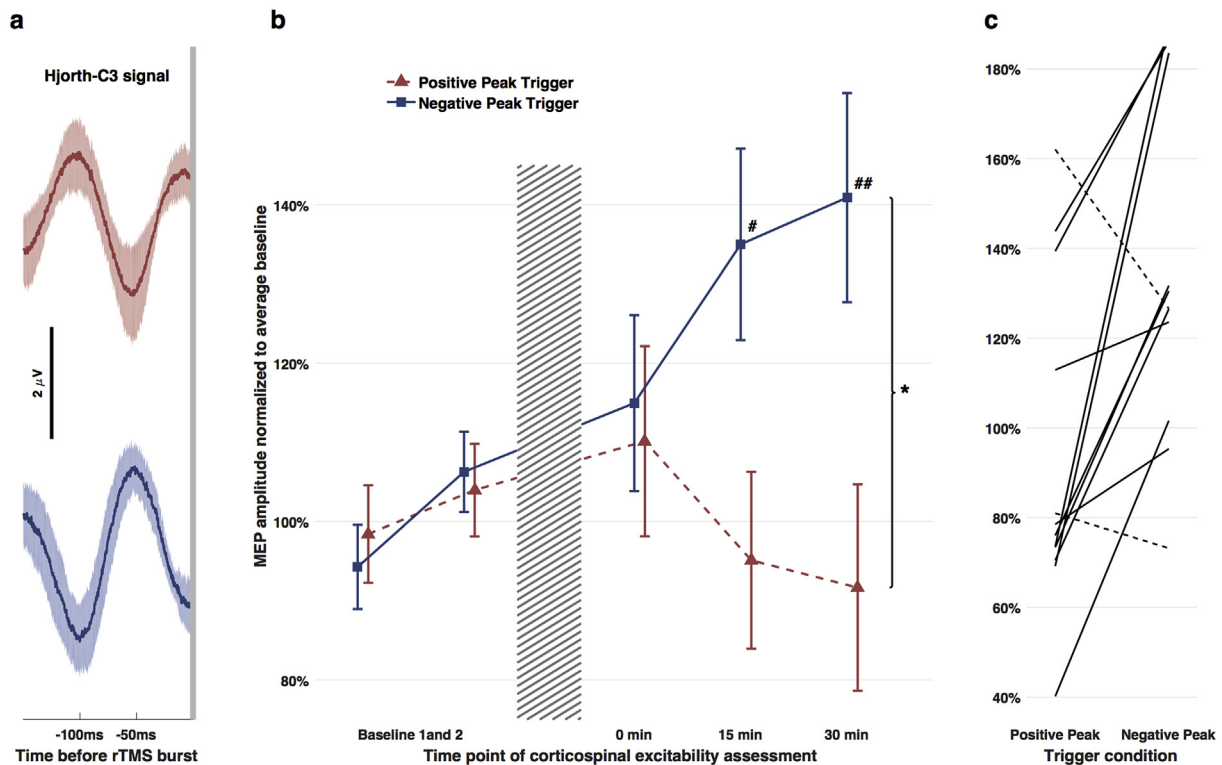


Fig. 6. | Efficacy of corticospinal plasticity depends on sensorimotor μ -rhythm phase. (a) Mean ($n = 12$) \pm 1 s.d. raw sensorimotor Hjorth-C3 EEG signal preceding rTMS in the positive (red) and negative peak conditions (blue), stimulus artefact shaded grey at right. (b) Time course of mean ($n = 12$) normalized to average baseline MEP amplitude \pm 1 s.e.m. with rTMS (hashed bar, 200×100 -Hz-triplets, intensity 80% of MEP threshold) triggered in separate sessions by the Hjorth-C3 positive peak (red triangles) or negative peak (blue squares) of ongoing μ -rhythm. * $p < 0.05$ effect of Phase in rmANOVA. # $p < 0.05$, ## $p = 0.01$ difference of post-rTMS MEP amplitude compared to average baseline (two-tailed paired t-tests). Mean \pm 1 s.d. absolute MEP amplitudes at baseline (averages of baseline 1 and 2) were 0.93 ± 0.12 mV and 1.18 ± 0.15 mV for the negative peak and positive peak conditions, respectively (values not different from each other, Wilcoxon signed-rank tests, $p = 0.27$). (c) Individual normalized to average baseline MEP amplitudes (means of the post-rTMS 15- and 30-min time points), with larger MEPs in the negative vs. positive peak condition in all but two subjects (dashed lines). (For interpretation of the references to colour in this figure legend, the reader is referred to the web version of this article.)

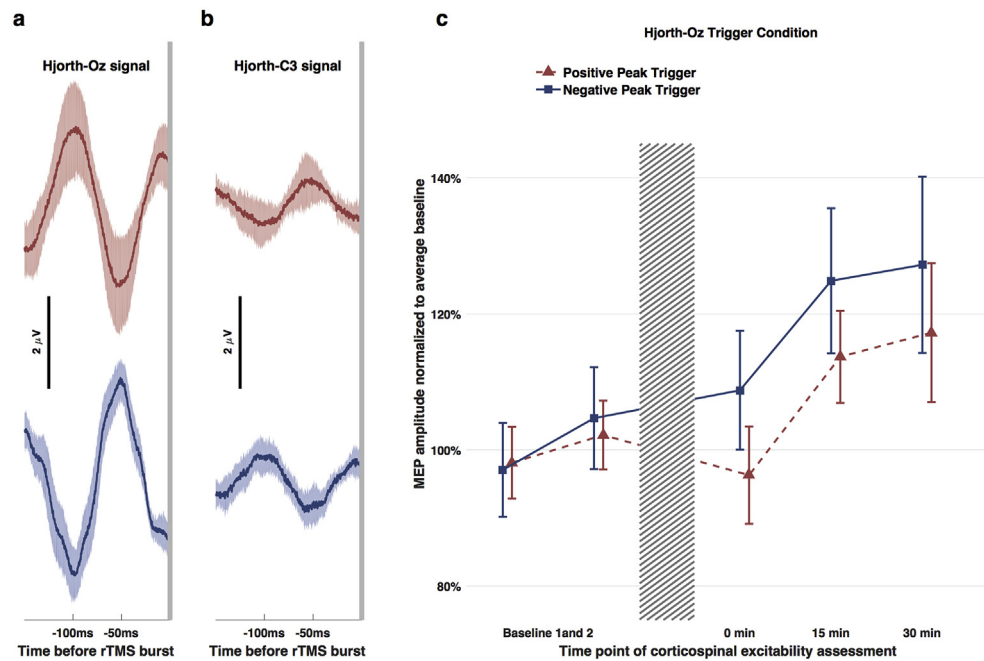


Fig. 7. Control Experiment 1. Mean ($n = 11$) \pm 1 s.d. pre-stimulus raw Hjorth-Oz EEG signal in the positive peak (red) and negative peak (blue) conditions used to trigger rTMS of M1 (a) and concurrent sensorimotor Hjorth-C3 EEG signal (b), stimulus artefact shaded grey at right. (c) Time course of mean ($n = 11$) normalized to average baseline MEP amplitude \pm 1 s. e.m. with rTMS of M1 (hashed bar, same protocol as in Main Experiment) triggered in separate sessions by the Hjorth-Oz positive peak (red triangles) or negative peak (blue squares) of ongoing occipital alpha-oscillations. (For interpretation of the references to colour in this figure legend, the reader is referred to the web version of this article.)

Control experiment 1

The pre-stimulus Hjorth-Oz EEG signal indicated accurate targeting, on average, of the positive and negative peaks during rTMS (Fig. 7a), while the pre-stimulus Hjorth-C3 EEG signal revealed reversed phases of lower amplitude (Fig. 7b). This anti-correlation may suggest contamination of the Hjorth-C3 EEG by occipital alpha-oscillations.

RmANOVA showed a significant effect of Time ($F_{3,30} = 7.28$, $p = 0.001$) but no effects of Phase ($F_{1,10} = 0.59$, $p = 0.46$), or the interaction of Phase and Time ($F_{3,30} = 0.29$, $p = 0.83$) on normalized MEP amplitude (Fig. 7c). None of the post-rTMS MEP amplitudes in the Hjorth-Oz positive or negative peak condition was different from average baseline (all $p > 0.05$, two-tailed paired t-tests). The distribution of inter-triplet-intervals was not different from the one in the Main Experiment (Supplementary Fig. 10b; $p = 0.42$, two-tailed paired t-test).

Why MEP amplitude increased irrespective of Hjorth-Oz alpha-rhythm phase can only be speculated upon. EEG-triggering was power-thresholded, and high alpha-power is associated with a state of low visual cortex excitability [47]. Paired-coil TMS experiments revealed inhibitory effective connectivity between visual cortex and M1 at rest and eyes open [48]. Therefore, it is possible that Hjorth-Oz EEG-triggering at high occipital alpha-power was coupled to a low-excitability state of visual cortex and, thus, a disinhibited, i.e., high-excitability state of M1, independent of occipital alpha-phase.

The findings of Control Experiment 1 suggest that EEG-triggering on endogenous oscillations originating from the same neural network that is targeted by rTMS is critical for inducing phase-dependent differential plasticity (see Main Experiment, Fig. 6b-c). In other words, such a phase-dependent differential effect on plasticity is not found if oscillations originating from a remote brain area (here, alpha-oscillations of visual cortex) are used for EEG-triggering.

Pre-stimulus μ -power was not different during rTMS between Phase conditions (positive peak: $0.65 \pm 0.47 \mu\text{V}^2$; negative peak: $0.77 \pm 0.58 \mu\text{V}^2$; $p = 0.60$, two-tailed paired t-test). Moreover, rmANOVA did not reveal any effect of rTMS on pre-stimulus μ -power: Phase ($F_{1,10} = 0.11$, $p = 0.75$), Time ($F_{1,139,11.39} = 0.53$, $p = 0.52$), Phase \times Time interaction ($F_{1,237,12.37} = 0.01$, $p = 0.99$, Supplementary Fig. 11b).

Control experiment 2

The average pre-stimulus Hjorth-C3 EEG signal was flat in both replay conditions (Fig. 8a), verifying randomness of phase targeting in this control experiment. RmANOVA did not reveal significant effects of Phase ($F_{1,7} = 0.74$, $p = 0.42$), Time ($F_{3,21} = 0.38$, $p = 0.77$), or the interaction of Phase and Time ($F_{3,21} = 0.63$, $p = 0.61$) (Fig. 8b) on normalized MEP amplitude.

These nil findings strongly suggest that consistent coupling of rTMS to instantaneous phase of the sensorimotor μ -alpha oscillation is essential for the differential plasticity effect obtained in the Main Experiment (cf. Fig. 6b-c).

Pre-stimulus μ -power was not different during rTMS between the positive ($0.57 \pm 0.39 \mu\text{V}^2$) and negative peak replay conditions ($0.64 \pm 0.48 \mu\text{V}^2$; $p = 0.79$, two-tailed paired t-test). Moreover, rmANOVA did not reveal any effect of rTMS on pre-stimulus μ -power: Phase ($F_{1,7} = 3.09$, $p = 0.12$), Time ($F_{2,14} = 0.65$, $p = 0.54$), Phase \times Time interaction ($F_{2,14} = 0.06$, $p = 0.94$, Supplementary Fig. 11c).

Corticospinal excitability in control experiment 3

CSD plots of the EEG signal ± 20 ms around the trigger in the non-stimulated trials showed a localized positivity (negativity) over the stimulated left M1 region in the positive (negative) Hjorth-C3 peak conditions, and no clear potential in the random phase condition (Fig. 9a), verifying spatial and conditional specificity of the EEG-TMS approach in this experiment. Mean \pm 1 s.d. phase

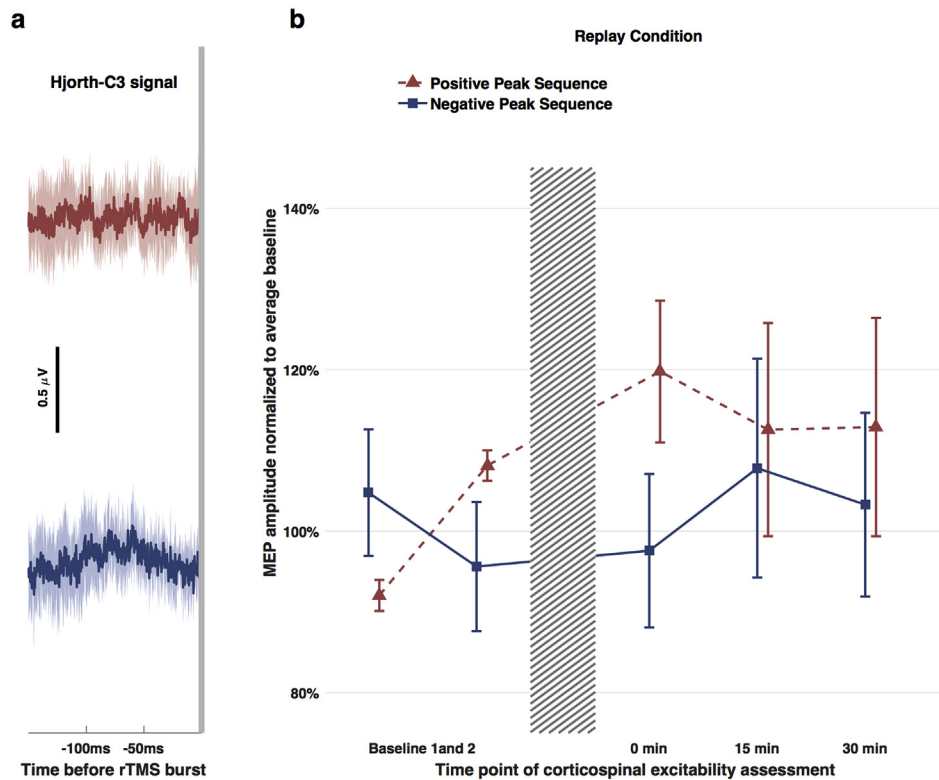


Fig. 8. Control Experiment 2. (a) Mean ($n = 8$) ± 1 s.d. pre-stimulus raw Hjorth-C3 EEG signal in the positive peak (red) and negative peak (blue) replay conditions, stimulus artefact shaded grey at right. RTMS of M1 was replayed from the sequences in the Main Experiment, i.e., uncoupled from power and phase of ongoing μ -rhythm. (b) Time course of mean ($n = 8$) normalized to average baseline MEP amplitude ± 1 s. e.m. with rTMS of M1 (hashed bar, same protocol as in Main Experiment) applied in separate sessions in the positive peak (red triangles) or negative peak (blue squares) replay conditions. (For interpretation of the references to colour in this figure legend, the reader is referred to the web version of this article.)

angles in the real-time triggered but non-stimulated trials were $5 \pm 58^\circ$ and $190 \pm 58^\circ$ in the positive and negative peak conditions, respectively, and uniformly distributed phases in the random phase condition (Fig. 9b). Also, the mean pre-stimulus EEG in the stimulated trials indicated good accuracy, on average, in the positive and negative peak conditions, while the flat signal in the random phase condition verifies randomness of phases (Fig. 9c).

RmANOVA revealed a significant effect of Phase ($F_{1,12,11,15} = 7.99$, $p = 0.014$) on normalized MEP amplitude. This was explained by significant differences between the negative vs. positive peak condition ($t_{10} = 2.99$, $p = 0.014$) and positive peak vs. random phase condition ($t_{10} = -3.86$, $p = 0.003$), while negative peak vs. random phase condition were not different ($t_{10} = 1.79$, $p = 0.10$, all two-sided paired t-tests) (Fig. 9d-e). MEP amplitude was on average $36.5 \pm 41.8\%$ (range, $-6.3\% - 143.6\%$) larger in the negative vs. positive peak condition, and on average $22.4 \pm 19.3\%$ (range, $3.9\% - 61.1\%$) larger in the random phase vs. positive peak condition.

Pre-stimulus μ -power did not affect MEP amplitude in the positive peak, negative peak or random phase conditions (Supplementary Fig. 6). Furthermore, pre-stimulus power in other frequency bands (delta < 4 Hz, theta 4–7 Hz, beta 13–30 Hz, and gamma 31–45 Hz) was also unrelated to MEP amplitude (group data, all $r^2 < 0.04$).

Data replicate the findings from the Main Experiment that the Hjorth-C3 negative peak condition reflects a high-excitability state of the corticospinal system relative to the positive peak condition. In addition, data indicate that excitability in the random phase condition is intermediate between the Hjorth-C3 negative and positive peak conditions. This is corroborated by an extended data sample ($n = 22$ subjects) in Supplementary Fig. 8.

The effect of μ -phase on MEP amplitude was particularly strong with small MEP amplitudes (cf. Figs. 4f and 9e). Regression analyses over all participants of the Main Experiment and Control Experiment 3 ($n = 22$, after exclusion of one outlier) revealed an inverse linear correlation between mean MEP amplitude (average of negative and positive peak conditions) and MEP ratio (negative peak/positive peak) with $R^2 = 0.211$, $p = 0.032$. Inclusion of mean MEP amplitude as a covariate in the comparison of MEP amplitudes between the negative and positive peak conditions still showed a significant effect of Phase ($F_{1,20} = 4.440$, $p = 0.048$). Altogether, these findings indicate that large MEPs are less sensitive to the modifying effect of μ -phase than small MEPs, and that a significant effect of μ -phase on corticospinal excitability is preserved in the present data set even when MEP amplitude is taken into account as a covariate.

Corticospinal plasticity in control experiment 3

The pre-stimulus EEG indicated good accuracy, on average, in the positive and negative peak conditions during rTMS, and the flat signal verified randomness of phases in the random phase condition (Fig. 10a).

RmANOVA showed a significant effect of Phase ($F_{2,20} = 5.54$, $p = 0.012$), but not Time ($F_{2,20} = 0.07$, $p = 0.93$) or the interaction of Phase and Time ($F_{4,40} = 0.35$, $p = 0.84$) on normalized MEP amplitude (Fig. 8b). Post-hoc pairwise comparisons of Phase showed significant differences for negative vs. positive EEG peak ($F_{1,10} = 9.09$, $p = 0.013$) and for negative peak vs. random phase ($F_{1,10} = 7.37$, $p = 0.022$) but not positive peak vs. random phase ($F_{1,10} = -0.16$, $p = 0.70$) (Fig. 10b-d). Moreover, MEP amplitudes in

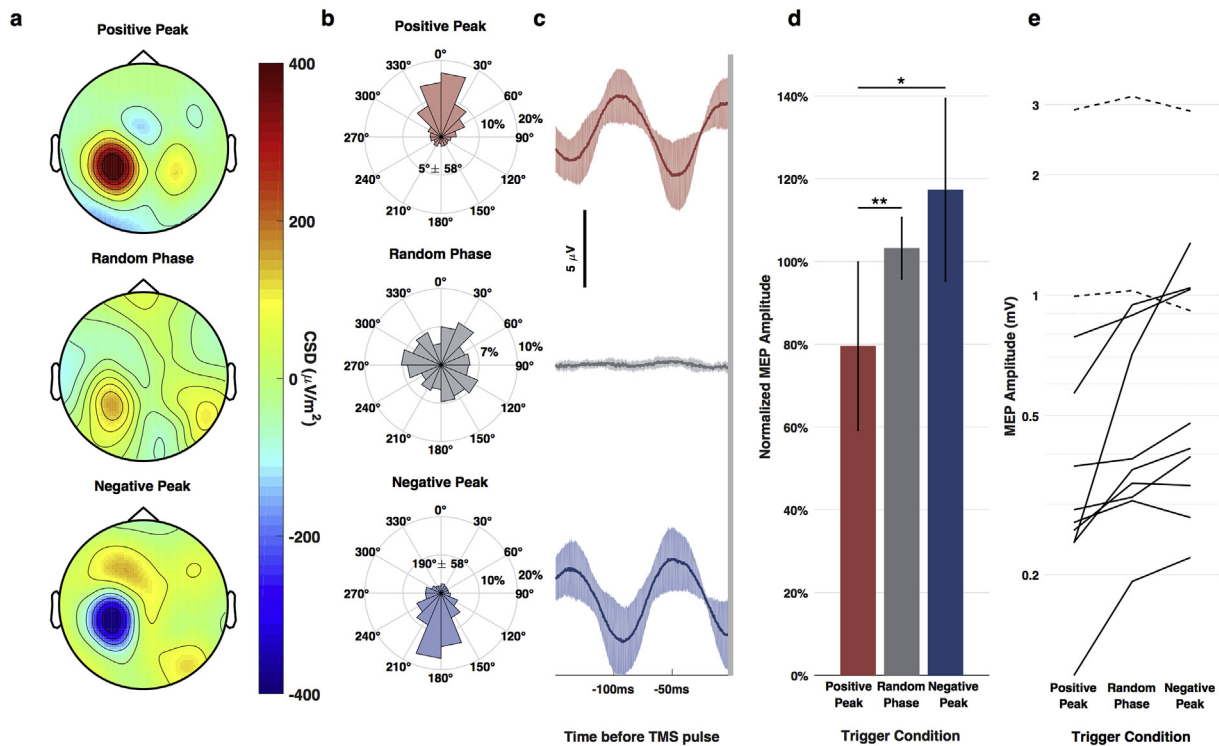


Fig. 9. Corticospinal excitability depends on instantaneous phase of sensorimotor μ -rhythm but not high μ -power. (a) Mean ($n = 11$) current source density (CSD) plots of the positive peak, random phase and negative peak condition, amplitudes (in $\mu\text{V}/\text{m}^2$) are indicated by the color bar. (b) Mean distribution of actual phase angle of triggered non-stimulated trials of positive peak, random phase and negative peak condition. Phase angles are binned (width, 22.5°) and frequencies indicated (inner ring 10%, outer ring 20% for positive and negative peak conditions; inner ring 7%, outer ring 10% for random phase condition). (c) Mean ($n = 11$) ± 1 s.d. raw sensorimotor Hjorth-C3 EEG signal preceding TMS in the positive, random phase and negative peak conditions, stimulus artefact shaded grey at right. (d) Mean ($n = 11$) ± 1 s.d. MEP amplitude, evoked by TMS at Hjorth-C3 positive peak (red) vs. random phase (grey) vs. negative peak (blue) condition, normalized to the individual mean. * $p < 0.05$, ** $p < 0.005$. (e) Individual data showing larger MEP amplitude (in mV, logarithmic scale) in the negative peak vs. positive peak condition in all but two subjects (dashed lines). (For interpretation of the references to colour in this figure legend, the reader is referred to the web version of this article.)

the negative peak condition were significantly increased at 0, 15 and 30 min post-rTMS compared to average baseline ($p = 0.002$, $p = 0.003$ and $p = 0.002$, respectively, two-tailed paired t -tests) (Fig. 10b), while post-rTMS MEP amplitudes in the positive peak and random phase conditions were not different from average baseline at any time point. The time courses of the individual raw and baseline-normalized MEP amplitude data are shown in Supplementary Fig. 9c-d.

Thus, Control Experiment 3 replicates the core finding of the Main Experiment of differential corticospinal plasticity in the Hjorth-C3 negative vs. positive peak conditions (Fig. 6b-c). In addition, it demonstrates that LTP-like corticospinal plasticity as observed in the negative peak condition does not occur in the random phase condition. This is a critically important extension of Control Experiment 2, because rTMS was triggered only when the power-threshold was exceeded in Control Experiment 3, whereas rTMS in the replay conditions of Control Experiment 2 was uncoupled from phase and power. Findings of Control Experiment 3 indicate that stimulating at high μ -power is not sufficient for inducing LTP-like corticospinal plasticity, and that consistent coupling of rTMS to the high-excitability state of the corticospinal system (i.e., the Hjorth-C3 negative peak) is a necessary requirement.

The temporal structure of the rTMS sequence was similar in the three phase conditions (mean inter-triplet-interval ± 1 s.d. positive peak: 1.02 ± 0.08 s; negative peak: 0.97 ± 0.06 s; random phase: 0.92 ± 0.08 s; Supplementary Fig. 10c), even though rmANOVA indicated a significant effect of Phase ($F_{2,20} = 5.71$, $p = 0.011$), and post-hoc testing revealed a significant difference between positive

peak and random phase conditions ($t_{10} = 2.84$, $p = 0.017$; two-sided paired t -test). Crucially, the temporal structure of the rTMS sequence in the negative peak condition did not differ from any of the other two sequences and, therefore, the observed differential plasticity (Fig. 10b) cannot be accounted for by differences in pulse train stochasticity between the rTMS sequences.

Pre-stimulus μ -power was not different during rTMS between the Phase conditions (rmANOVA : $F_{2,20} = 0.27$, $p = 0.77$; positive peak: $1.86 \pm 1.52 \mu\text{V}^2$; negative peak: $2.05 \pm 2.41 \mu\text{V}^2$; random phase condition: $1.80 \pm 1.79 \mu\text{V}^2$), and pre-stimulus μ -power during rTMS did not predict the post-rTMS MEP changes (positive peak: $R^2 = 0.19$, $p = 0.18$; negative peak: $R^2 < 0.001$, $p = 0.97$; random phase condition: $R^2 = 0.24$, $p = 0.13$), confirming that μ -power during rTMS was not relevant for the LTP-like corticospinal plasticity in the negative peak condition.

Similar to the Main Experiment, rmANOVA did not reveal any effect of rTMS on pre-stimulus μ -power: Phase ($F_{2,20} = 2.01$, $p = 0.16$), Time ($F_{2,20} = 0.02$, $p = 0.99$), and Phase with Time interaction ($F_{4,40} = 0.10$, $p = 0.98$, Supplementary Fig. 11d).

Discussion

We used here, for the first time, real-time millisecond-resolution brain-state dependent EEG-triggered TMS of human M1 to demonstrate that corticospinal excitability is modulated by phase of the ongoing sensorimotor μ -rhythm: the Hjorth-C3 negative peak of the μ -rhythm represents a high-excitability state, while the positive peak is a low-excitability state. Repeatedly stimulating at the high-excitability state with 100 Hz TMS triplets resulted in a

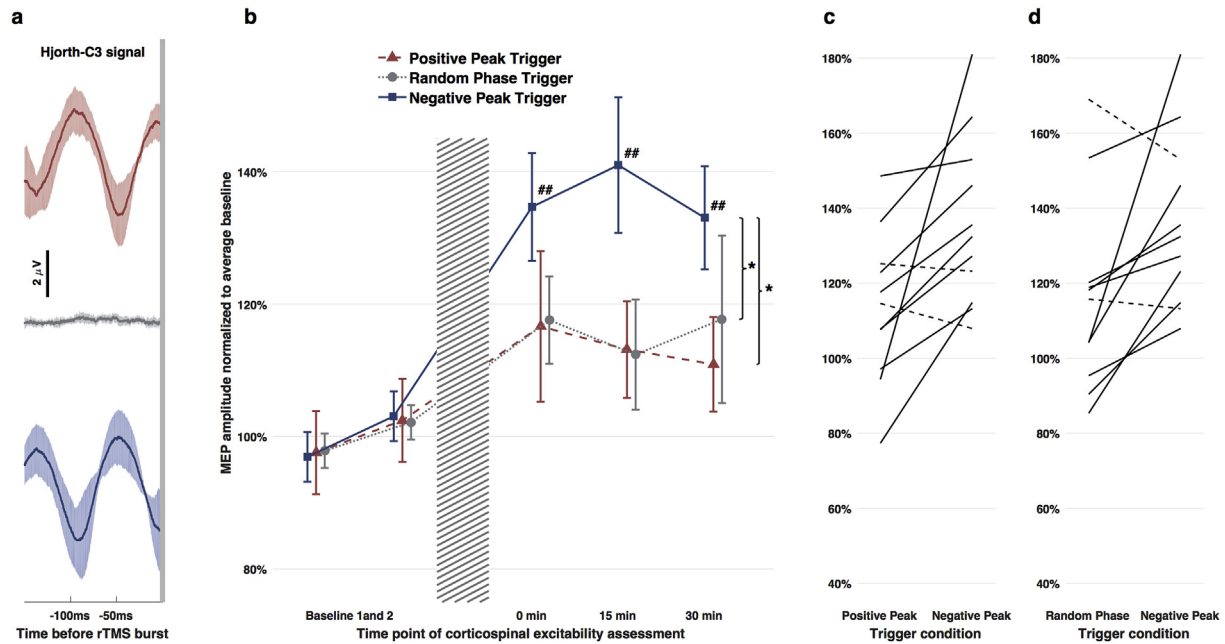


Fig. 10. LTP-like corticospinal plasticity occurs specifically in the Hjorth-C3 negative peak condition, but not in the positive peak or random phase conditions. (a) Mean ($n = 11$) ± 1 s.d. raw sensorimotor Hjorth-C3 EEG signal preceding TMS in the positive, random phase and negative peak conditions, stimulus artefact shaded grey at right. (b) Time course of mean ($n = 11$) normalized to average baseline MEP amplitude ± 1 s. e.m. with rTMS (hashed bar, same protocol as in Main Experiment) triggered in separate sessions by the Hjorth-C3 positive peak (red triangles), negative peak (blue squares) or at random phase (grey circles) of ongoing μ -rhythm. * $p < 0.05$ effect of Phase in rmANOVA. ** $p < 0.005$ difference of post-rTMS MEP amplitude compared to average baseline (two-tailed paired t-tests). Mean ± 1 s.d. absolute MEP amplitudes at baseline (averages of baseline 1 and 2) were 1.17 ± 0.35 mV, 1.24 ± 0.29 mV and 1.20 ± 0.19 mV for the negative peak, positive peak and random phase conditions, respectively (values not different from each other, Wilcoxon signed-rank tests, all $p > 0.15$). (c-d) Individual normalized to average baseline MEP amplitudes (means of the post-rTMS 0-, 15- and 30-min time points), with larger MEPs in the negative vs. positive peak condition (c) and negative peak vs. random phase condition (d) in all but two subjects each (dashed lines). (For interpretation of the references to colour in this figure legend, the reader is referred to the web version of this article.)

LTP-like increase in corticospinal excitability, while no change occurred if the same rTMS protocol was triggered at the low-excitability state, or at random μ -rhythm phase. Pooled analysis across the Main Experiment and Control Experiment 3 revealed that 21/23 (91.3%) subjects exhibited an LTP-like increase in the Hjorth-C3 negative peak condition. This is a significantly larger proportion than in recent studies that used “excitability-enhancing” non-invasive brain stimulation protocols without EEG information of ongoing brain state (range of LTP-responders, 52–61%) [9,10]. The effect size of the LTP-like increase in the Hjorth-C3 negative peak over the positive peak condition (data pooled from Main Experiment and Control Experiment 3) was large with Cohen’s $d = 1.32$ but not larger than in other studies that contrasted two different rTMS protocols expected to result in LTP- vs. long-term depression (LTD)-like corticospinal plasticity [49,50].

How may these effects be understood? Realistic modeling of the TMS-induced electrical field suggests that TMS over the M1 hand knob excites horizontal fibers in the upper cortical layers in the crowns of the pre- and postcentral gyrus [51,52], leading to trans-synaptic activation of the apical dendritic trees of pyramidal cells [53]. Synchronized excitatory post-synaptic currents at the apical dendrites of radially oriented pyramidal cells are the major generator of the negative deflections in the surface EEG [54]. These radially oriented pyramidal cells are most likely located in dorsal premotor and primary somatosensory cortex, and their excitation by TMS consecutively leads to activation of corticospinal neurons in M1 through dense direct cortico-cortical connections [55], as indicated by intracortical microstimulation experiments in monkeys [53] and paired-coil TMS experiments in humans [56]. In contrast, it is unlikely that the reported effects reflect μ -phase dependent excitability changes directly of corticospinal M1 neurons, as these are located in the anterior wall of the central sulcus

[57], so that their horizontally oriented apical dendrite vs. soma electrical dipoles remain largely undetected by Hjorth-C3 EEG.

Therefore, our corticospinal excitability data (Fig. 4e-f, Fig. 9d-e and Supplementary Fig. 8) are best explained by the supposition that a TMS pulse applied during the Hjorth-C3 derived negative peak of the μ -rhythm reaches the dendritic trees of pyramidal cells in dorsal premotor cortex or primary somatosensory cortex at a time when they already receive predominating excitatory input and are closer to firing threshold, leading to a higher fraction of them being recruited by the TMS pulse.

Very likely, the same mechanism also explains the critical dependence of LTP-like corticospinal plasticity on consistent stimulation with rTMS bursts during the high-excitability state (i.e., the Hjorth-C3 negative peak of the μ -rhythm): *In vitro* experiments point to dendritic membrane potentials as a pivotal determinant of the magnitude and direction of synaptic plasticity, where pairing of synaptic stimulation with an intracellular depolarization results in LTP, while pairing with hyperpolarization leads to LTD [58,59].

Linear and non-linear regression analyses to test for correlations between corticospinal excitability and rTMS-induced corticospinal plasticity differences between negative and positive peak did not reveal any significant relation in the Main Experiment or Control Experiment 3 (all $p > 0.20$). This may suggest that there is no such relation, that the relation is highly non-linear, as suggested by LTP/LTD experiments in rat visual cortex [58], or that inter-session variability has obscured such a relationship as excitability and plasticity measurements were obtained in different sessions on separate days.

One limitation of this work is that we did not provide evidence for or against the role of phase of oscillations in other frequency bands for regulation of corticospinal excitability and plasticity induction. While selecting the μ -rhythm for testing in the current

experiments was well grounded on previous research [16–19], other oscillations, in particular in the beta-band (13–30 Hz) have been suggested to play important roles in human sensorimotor cortex, e.g. during maintenance of tonic motor output or at rest [60,61]. However, tACS in the beta-band (20 Hz) of M1 had no effect on MEP amplitude [62], and single-pulse TMS testing of MEP amplitude during pre-defined phases of 20 Hz tACS resulted in contradictory findings [25–27]. Also, post-hoc trial sorting of MEP amplitude with respect to instantaneous phase in the beta-band has provided inconsistent results [20–22], signifying fundamental methodological problems with accurate phase estimation in stimulated trials. To clarify the role of sensorimotor oscillations in the beta-band on corticospinal excitability and plasticity induction will require controlled real-time beta-phase-triggered EEG-TMS experiments.

It is uncertain to what extent the current findings are generalizable to populations that have not been tested here, e.g. elderly subjects or patients. Also, the requirement of sufficient μ -power (>25% of total power in the CSD power spectrum of the C3 EEG signal overlying the left sensorimotor cortex) led to exclusion of >50% of the screened subjects (see Methods), and this could limit the broad applicability of the EEG-TMS technology presented in this work. We expect that individually optimized spatial filters that utilize more than 5 or even all available EEG channels will overcome the known limitations of the Hjorth Laplacian, and thereby improve the isolation of relevant brain rhythms, and screening success in subsequent EEG-TMS studies.

The μ -phase distribution had a relatively low precision with standard deviations of $\pm 50^\circ$ around the target phase (cf. Figs. 4c and 9b), in contrast to the time resolution of the EEG processing system of 1–2 ms. This discrepancy is due to fundamental signal processing limitations, chiefly the uncertainty introduced when isolating a specific biological EEG feature by filtering single-trial short-time mixed signal epochs in real-time. The resulting overall precision is determined by the signal-to-noise ratio, the temporal stability of the biological signal, and the parameters of the real-time phase estimation algorithm.

Single-pulse rTMS at ~ 1 Hz is known to result in LTD-like MEP decrease [63]. Therefore, we cannot exclude that a LTD-like effect caused by the ~ 1 Hz repetition rate of the 100 Hz triple-pulses has contributed to our findings, and may even have limited LTP-like corticospinal plasticity in the Hjorth-C3 negative peak conditions of the Main Experiment and Control Experiment 3. However, this possible effect does not impact the result that ongoing phase of μ -oscillations at the time of stimulation determined the resulting overall plasticity in otherwise identical stimulation protocols. A decisive clarification of this issue will require further experiments with a 100 Hz triplet repetition rate of e.g. 0.1 Hz that is not associated with any MEP change in single-pulse rTMS experiments [63].

In a similar vein, the triple-pulse burst frequency of 100 Hz (i.e., inter-pulse intervals of 10 ms) may have resulted in specific excitation of motor cortical circuits causing intracortical facilitation (ICF) [64]. The observed corticospinal plasticity effects may thus have been caused by μ -phase-dependent responsiveness of the ICF circuits to rTMS with 100 Hz triple-pulses. Hence, μ -phase-dependency of LTP-like effects may substantially differ when triple-pulses are given at intervals <5 ms (i.e., causing short-latency intracortical inhibition) [64,65], or at intervals of 50–200 ms that result in long-interval intracortical inhibition [66]. Further studies are necessary to resolve this question.

Finally, we have not provided evidence in detail that the long-lasting MEP amplitude increase in the Hjorth-C3 negative peak is an LTP-like phenomenon. However, this has been done in several previous studies on long-lasting increases in MEP amplitude induced by rTMS, and most researchers in this field accept the

notion that a long-lasting MEP increase induced by rTMS is LTP-like because it typically shows the characteristics of LTP as studied at the cellular level, i.e., duration >30 min, cooperativity, associativity, input-specificity and dependence on NMDA receptor activation (for reviews [31,67]).

In conclusion, we show here, for the first time in the human brain, that an otherwise identical rTMS protocol synchronized with an ongoing endogenous brain oscillation results in differential long-term changes of excitability of the stimulated neuronal circuit, depending on the targeted phase of this oscillation. In light of these findings, realizing the full therapeutic potential of brain stimulation for treatment of brain network disorders, such as stroke, epilepsy, Parkinson's disease, depression or schizophrenia will require an EEG-triggered approach that synchronizes each stimulus with the individual patient's instantaneous brain state. A multitude of increasingly sophisticated rTMS protocols has been developed in the past 30 years [31] but they suffer from high intra- and inter-individual variability and low effect sizes [9,10] because the applied pre-determined static TMS sequences are blind to the ever and rapidly changing instantaneous brain state [68]. In brain-state dependent stimulation the logic is turned around: Here, it is the ongoing cortical dynamics that drives the temporal pattern of the stimulus train such that the brain is always stimulated at a defined state that is conducive for a desired long-term change to occur: In the same way that beauty lies in the eye of the beholder, what a stimulus does to the brain is determined not simply by the nature of the stimulus, but by the nature of the brain receiving the stimulus, at that instant of time.

Competing financial interests

The authors declare no competing financial interests.

Author contributions

U.Z. and C.Z. created concept and design of the study; D.D. and P.B. performed the experiments; C.Z. and D.D. developed the real-time software; U.Z. P.B. D.D. and C.Z. jointly designed the experimental set-up, analyzed the data, created the figures and wrote the manuscript.

Acknowledgements

We thank Dr. Til Ole Bergmann for his comments on the experimental design and manuscript. This study was supported by DFG grant ZI 542/7-1 (to U.Z.), Industry-on-Campus Grant IoC 211 (to P.B., and D.D.), and University of Tübingen Fortune Junior Grant 2287-0-0 (to C.Z.).

Appendix A. Supplementary data

Supplementary data related to this article can be found at <https://doi.org/10.1016/j.brs.2017.11.016>.

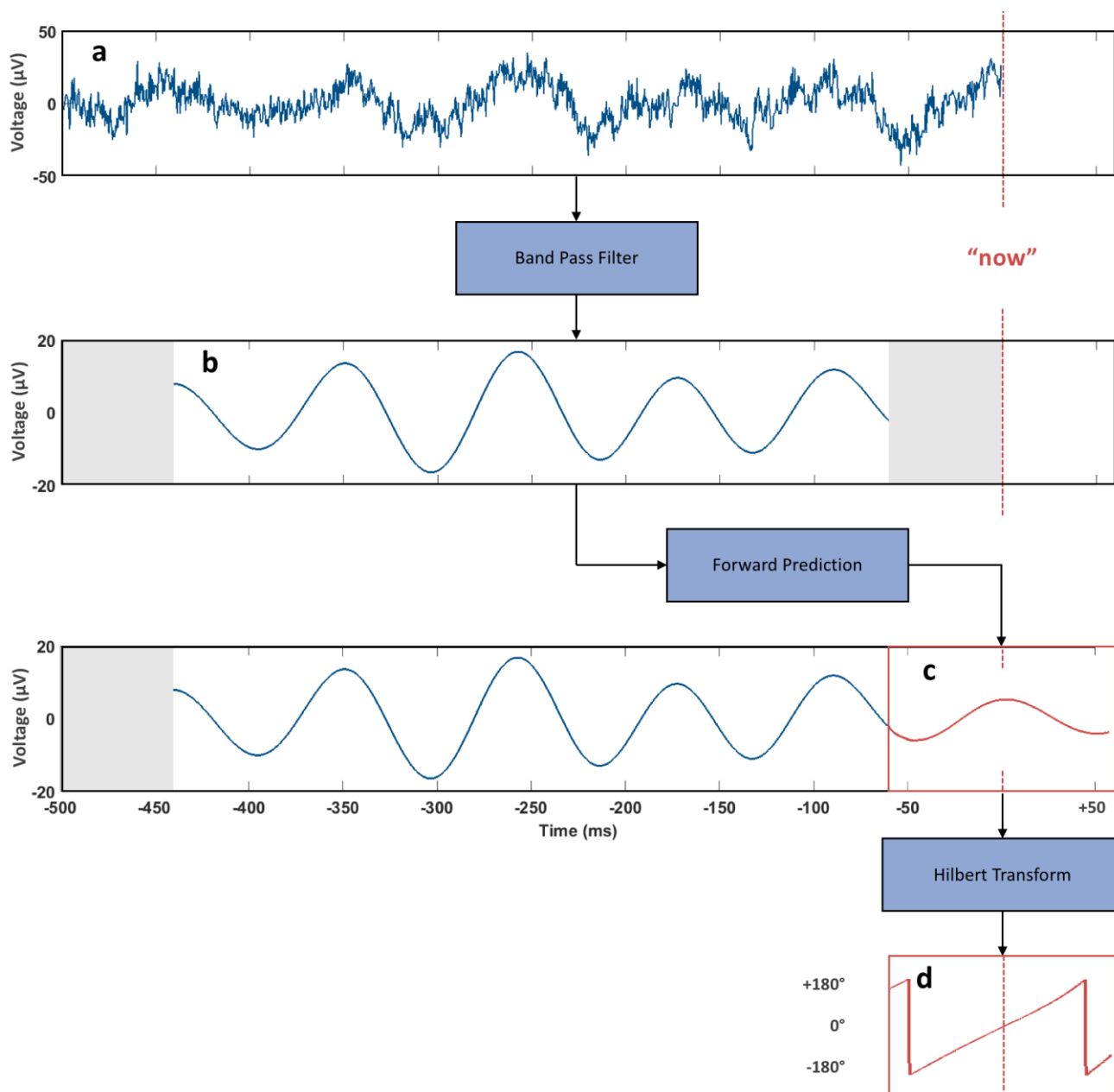
References

- [1] Hallett M. Transcranial magnetic stimulation: a primer. *Neuron* 2007;55:187–99.
- [2] Bergmann TO, Karabanov A, Hartwigsen G, Thielscher A, Siebner HR. Combining non-invasive transcranial brain stimulation with neuroimaging and electrophysiology: current approaches and future perspectives. *Neuroimage* 2016;140:4–19.
- [3] Thut G, Bergmann TO, Fröhlich F, et al. Guiding transcranial brain stimulation by EEG/MEG to interact with ongoing brain activity and associated functions: a position paper. *Clin Neurophysiol* 2017;128:843–57.

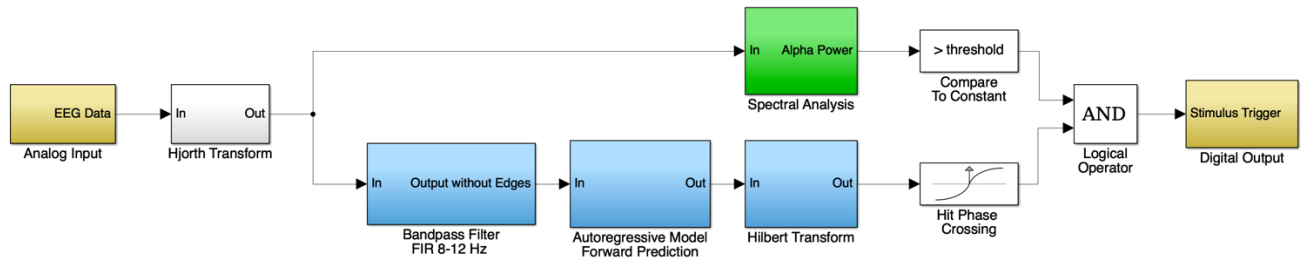
- [4] Allen EA, Pasley BN, Duong T, Freeman RD. Transcranial magnetic stimulation elicits coupled neural and hemodynamic consequences. *Science* 2007;317:1918–21.
- [5] Mueller JK, Grigsby EM, Prevosto V, et al. Simultaneous transcranial magnetic stimulation and single-neuron recording in alert non-human primates. *Nat Neurosci* 2014;17:1130–6.
- [6] Barker AT, Jalinous R, Freeston IL. Non-invasive magnetic stimulation of human motor cortex [letter]. *Lancet* 1985;1:1106–7.
- [7] Kiers L, Cros D, Chiappa KH, Fang J. Variability of motor potentials evoked by transcranial magnetic stimulation. *Electroencephalogr Clin Neurophysiol* 1993;89:415–23.
- [8] Ellaway PH, Davey NJ, Maskill DW, Rawlinson SR, Lewis HS, Anissimova NP. Variability in the amplitude of skeletal muscle responses to magnetic stimulation of the motor cortex in man. *Electroencephalogr Clin Neurophysiol* 1998;109:104–13.
- [9] Hamada M, Murase N, Hasan A, Balaratnam M, Rothwell JC. The role of interneuron networks in driving human motor cortical plasticity. *Cereb Cortex* 2013;23:1593–605.
- [10] Lopez-Alonso V, Cheeran B, Rio-Rodríguez D, Fernandez-Del-Olmo M. Inter-individual variability in response to non-invasive brain stimulation paradigms. *Brain Stimul* 2014;7:372–80.
- [11] Müller-Dahlhaus JF, Orekhov Y, Liu Y, Ziemann U. Interindividual variability and age-dependency of motor cortical plasticity induced by paired associative stimulation. *Exp Brain Res* 2008;187:467–75.
- [12] Arieli A, Sterkin A, Grinvald A, Aertsen A. Dynamics of ongoing activity: explanation of the large variability in evoked cortical responses. *Science* 1996;273:1868–71.
- [13] Huerta PT, Lisman JE. Heightened synaptic plasticity of hippocampal CA1 neurons during a cholinergically induced rhythmic state. *Nature* 1993;364:723–5.
- [14] Huerta PT, Lisman JE. Bidirectional synaptic plasticity induced by a single burst during cholinergic theta oscillation in CA1 in vitro. *Neuron* 1995;15:1053–63.
- [15] Bergmann TO, Mölle M, Schmidt MA, et al. EEG-guided transcranial magnetic stimulation reveals rapid shifts in motor cortical excitability during the human sleep slow oscillation. *J Neurosci* 2012;32:243–53.
- [16] Haegens S, Nacher V, Luna R, Romo R, Jensen O. alpha-Oscillations in the monkey sensorimotor network influence discrimination performance by rhythmic inhibition of neuronal spiking. *Proc Natl Acad Sci U. S. A* 2011;108:19377–82.
- [17] Hari R. Action-perception connection and the cortical mu rhythm. *Prog Brain Res* 2006;159:253–60.
- [18] Jensen O, Mazaheri A. Shaping functional architecture by oscillatory alpha activity: gating by inhibition. *Front Hum Neurosci* 2010;4:186.
- [19] Ai L, Ro T. The phase of prestimulus alpha oscillations affects tactile perception. *J Neurophysiol* 2014;111:1300–7.
- [20] Keil J, Timm J, Sanmiguel I, Schulz H, Obleser J, Schoenwiesner M. Cortical brain states and corticospinal synchronization influence TMS-evoked motor potentials. *J Neurophysiol* 2014;111:513–9.
- [21] Mäki H, Ilmoniemi RJ. EEG oscillations and magnetically evoked motor potentials reflect motor system excitability in overlapping neuronal populations. *Clin Neurophysiol* 2010;121:492–501.
- [22] Berger B, Minarik T, Liuzzi G, Hummel FC, Sauseng P. EEG oscillatory phase-dependent markers of corticospinal excitability in the resting brain. *Biomed Res Int* 2014;2014:936096.
- [23] Fröhlich F, McCormick DA. Endogenous electric fields may guide neocortical network activity. *Neuron* 2010;67:129–43.
- [24] Zaehle T, Rach S, Herrmann CS. Transcranial alternating current stimulation enhances individual alpha activity in human EEG. *PLoS One* 2010;5:e13766.
- [25] Guerra A, Pogosyan A, Nowak M, et al. Phase dependency of the human primary motor cortex and cholinergic inhibition cancelation during beta tACS. *Cereb Cortex* 2016;26:3977–90.
- [26] Nakazono H, Ogata K, Kuroda T, Tobimatsu S. Phase and frequency-dependent effects of transcranial alternating current stimulation on motor cortical excitability. *PLoS One* 2016;11, e0162521.
- [27] Raco V, Bauer R, Tharsan S, Gharabaghi A. Combining TMS and tACS for closed-loop phase-dependent modulation of corticospinal excitability: a feasibility study. *Front Cell Neurosci* 2016;10:143.
- [28] Lafon B, Henin S, Huang Y, et al. Low frequency transcranial electrical stimulation does not entrain sleep rhythms measured by human intracranial recordings. *Nat Commun* 2017;8:1199.
- [29] Zrenner C, Belardinelli P, Müller-Dahlhaus F, Ziemann U. Closed-loop neuroscience and non-invasive brain stimulation: a tale of two loops. *Front Cell Neurosci* 2016;10:92.
- [30] Rossi S, Hallett M, Rossini PM, Pascual-Leone A. Safety, ethical considerations, and application guidelines for the use of transcranial magnetic stimulation in clinical practice and research. *Clin Neurophysiol* 2009;120:2008–39.
- [31] Ziemann U, Paulus W, Nitsche MA, et al. Consensus: motor cortex plasticity protocols. *Brain Stimul* 2008;1:164–82.
- [32] Fuhl A, Müller-Dahlhaus F, Lücke C, Toennes SW, Ziemann U. Low doses of ethanol enhance LTD-like plasticity in human motor cortex. *Neuropsychopharmacology* 2015;40:2969–80.
- [33] Hjorth B. An on-line transformation of EEG scalp potentials into orthogonal source derivations. *Electroencephalogr Clin Neurophysiol* 1975;39:526–30.
- [34] Mazaheri A, Nieuwenhuis IL, van Dijk H, Jensen O. Prestimulus alpha and mu activity predicts failure to inhibit motor responses. *Hum Brain Mapp* 2009;30:1791–800.
- [35] Rossini PM, Burke D, Chen R, et al. Non-invasive electrical and magnetic stimulation of the brain, spinal cord, roots and peripheral nerves: basic principles and procedures for routine clinical and research application. An updated report from an I.F.C.N. Committee. *Clin Neurophysiol* 2015;126:1071–107.
- [36] Chen LL, Madhavan R, Rapoport BI, Anderson WS. Real-time brain oscillation detection and phase-locked stimulation using autoregressive spectral estimation and time-series forward prediction. *IEEE Trans Biomed Eng* 2013;60:753–62.
- [37] McFarland DJ, Wolpaw JR. Sensorimotor rhythm-based brain-computer interface (BCI): model order selection for autoregressive spectral analysis. *J Neural Eng* 2008;5:155–62.
- [38] Sale MV, Ridding MC, Nordstrom MA. Cortisol inhibits neuroplasticity induction in human motor cortex. *J Neurosci* 2008;28:8285–93.
- [39] Oostenveld R, Fries P, Maris E, Schoffelen JM. FieldTrip: open source software for advanced analysis of MEG, EEG, and invasive electrophysiological data. *Comput Intell Neurosci* 2011;2011:156869.
- [40] Hyvarinen A. Fast and robust fixed-point algorithms for independent component analysis. *IEEE Trans Neural Netw* 1999;10:626–34.
- [41] Penny WD, Friston KJ, Ashburner JT, Kiebel SJ, Nichols TE. Statistical parametric mapping: the analysis of functional brain images. Academic Press; 2011.
- [42] Oostendorp TF, van Oosterom A. The surface Laplacian of the potential: theory and application. *IEEE Trans Biomed Eng* 1996;43:394–405.
- [43] Van Veen BD, van Drongelen W, Yuchtman M, Suzuki A. Localization of brain electrical activity via linearly constrained minimum variance spatial filtering. *IEEE Trans Biomed Eng* 1997;44:867–80.
- [44] Zarkowski P, Shin CJ, Dang T, Russo J, Avery D. EEG and the variance of motor evoked potential amplitude. *Clin EEG Neurosci* 2006;37:247–51.
- [45] Sauseng P, Klimesch W, Gerloff C, Hummel FC. Spontaneous locally restricted EEG alpha activity determines cortical excitability in the motor cortex. *Neuropsychologia* 2009;47:284–8.
- [46] Lepage JF, Saint-Amour D, Theoret H. EEG and neuronavigated single-pulse TMS in the study of the observation/execution matching system: are both techniques measuring the same process? *J Neurosci Methods* 2008;175:17–24.
- [47] Romei V, Brodbeck V, Michel C, Amedi A, Pascual-Leone A, Thut G. Spontaneous fluctuations in posterior alpha-band EEG activity reflect variability in excitability of human visual areas. *Cereb Cortex* 2008;18:2010–8.
- [48] Strigaro G, Ruge D, Chen JC, et al. Interaction between visual and motor cortex: a transcranial magnetic stimulation study. *J Physiol* 2015;593:2365–77.
- [49] Ziemann U, Ilic TV, Pauli C, Meintzschel F, Ruge D. Learning modifies subsequent induction of LTP-like and LTD-like plasticity in human motor cortex. *J Neurosci* 2004;24:1666–72.
- [50] Jung NH, Gleich B, Gattinger N, et al. Quadri-pulse theta burst stimulation using ultra-high frequency bursts - a new protocol to induce changes in cortico-spinal excitability in human motor cortex. *PLoS One* 2016;11, e0168410.
- [51] Laakso I, Hirata A, Ugawa Y. Effects of coil orientation on the electric field induced by TMS over the hand motor area. *Phys Med Biol* 2014;59:203–18.
- [52] Bungert A, Antunes A, Espenhahn S, Thielscher A. Where does TMS stimulate the motor cortex? Combining electrophysiological measurements and realistic field estimates to reveal the affected cortex position. *Cereb Cortex* 2017;27:5083–94.
- [53] Amassian VE, Stewart M, Quirk GJ, Rosenthal JL. Physiological basis of motor effects of a transient stimulus to cerebral cortex. *Neurosurgery* 1987;20:74–93.
- [54] Buzsáki G, Anastassiou CA, Koch C. The origin of extracellular fields and currents—EEG, ECoG, LFP and spikes. *Nat Rev Neurosci* 2012;13:407–20.
- [55] Dum RP, Strick PL. Frontal lobe inputs to the digit representations of the motor areas on the lateral surface of the hemisphere. *J Neurosci* 2005;25:1375–86.
- [56] Groppa S, Schlaack BH, Munchau A, et al. The human dorsal premotor cortex facilitates the excitability of ipsilateral primary motor cortex via a short latency cortico-cortical route. *Hum Brain Mapp* 2012;33:419–30.
- [57] Geyer S, Ledberg A, Schleicher A, et al. Two different areas within the primary motor cortex of man. *Nature* 1996;382:805–7.
- [58] Artola A, Brocher S, Singer W. Different voltage-dependent thresholds for inducing long-term depression and long-term potentiation in slices of rat visual cortex. *Nature* 1990;347:69–72.
- [59] Sjöström PJ, Häusser M. A cooperative switch determines the sign of synaptic plasticity in distal dendrites of neocortical pyramidal neurons. *Neuron* 2006;51:227–38.
- [60] Baker SN. Oscillatory interactions between sensorimotor cortex and the periphery. *Curr Opin Neurobiol* 2007;17:649–55.
- [61] Pfurtscheller G, Lopes da Silva FH. Event-related EEG/MEG synchronization and desynchronization: basic principles. *Clin Neurophysiol* 1999;110:1842–57.
- [62] Rjosk V, Kaminski E, Hoff M, et al. Transcranial alternating current stimulation at beta frequency: lack of immediate effects on excitation and

- interhemispheric inhibition of the human motor cortex. *Front Hum Neurosci* 2016;10:560.
- [63] Chen R, Classen J, Gerloff C, et al. Depression of motor cortex excitability by low-frequency transcranial magnetic stimulation. *Neurology* 1997;48:1398–403.
- [64] Ziemann U, Rothwell JC, Ridding MC. Interaction between intracortical inhibition and facilitation in human motor cortex. *J Physiol* 1996;496:873–81.
- [65] Kujirai T, Caramia MD, Rothwell JC, et al. Corticocortical inhibition in human motor cortex. *J Physiol (Lond)* 1993;471:501–19.
- [66] Valls-Sole J, Pascual-Leone A, Wassermann EM, Hallett M. Human motor evoked responses to paired transcranial magnetic stimuli. *Electroencephalogr Clin Neurophysiol* 1992;85:355–64.
- [67] Cooke SF, Bliss TV. Plasticity in the human central nervous system. *Brain* 2006;129:1659–73.
- [68] Womelsdorf T, Schoffelen JM, Oostenveld R, et al. Modulation of neuronal interactions through neuronal synchronization. *Science* 2007;316:1609–12.

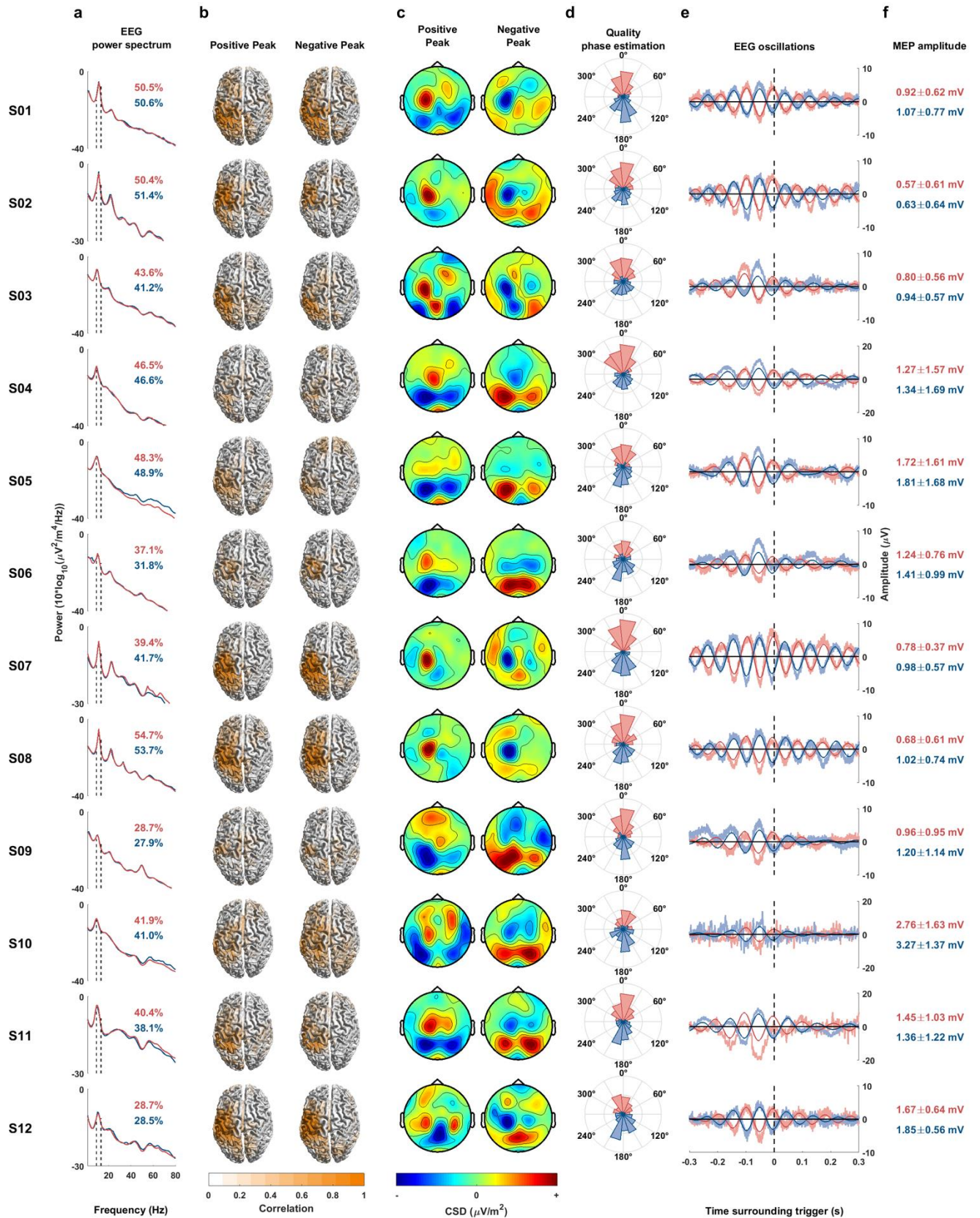
Supplementary Figures



Supplementary Figure 1 | Real-time μ -rhythm phase estimation. (a) Sliding window of 500 ms duration of raw EEG signal after 5-point sum-of-difference operation centered on the C3 EEG electrode to isolate left sensorimotor μ -rhythm. (b) The same window after zero-phase (forward and backward) FIR 8-12 Hz bandpass filtering with 64 ms edge artefacts trimmed on either side (grey shaded). (c) Autoregressive model estimation from the remaining segment to perform a 128 ms time-series forward-prediction. (d) Hilbert transformation of the 128 ms data segment surrounding time zero ("now") to obtain the phase angle. The entire process is implemented in a real-time signal processing system and executed at a rate of 500 Hz.

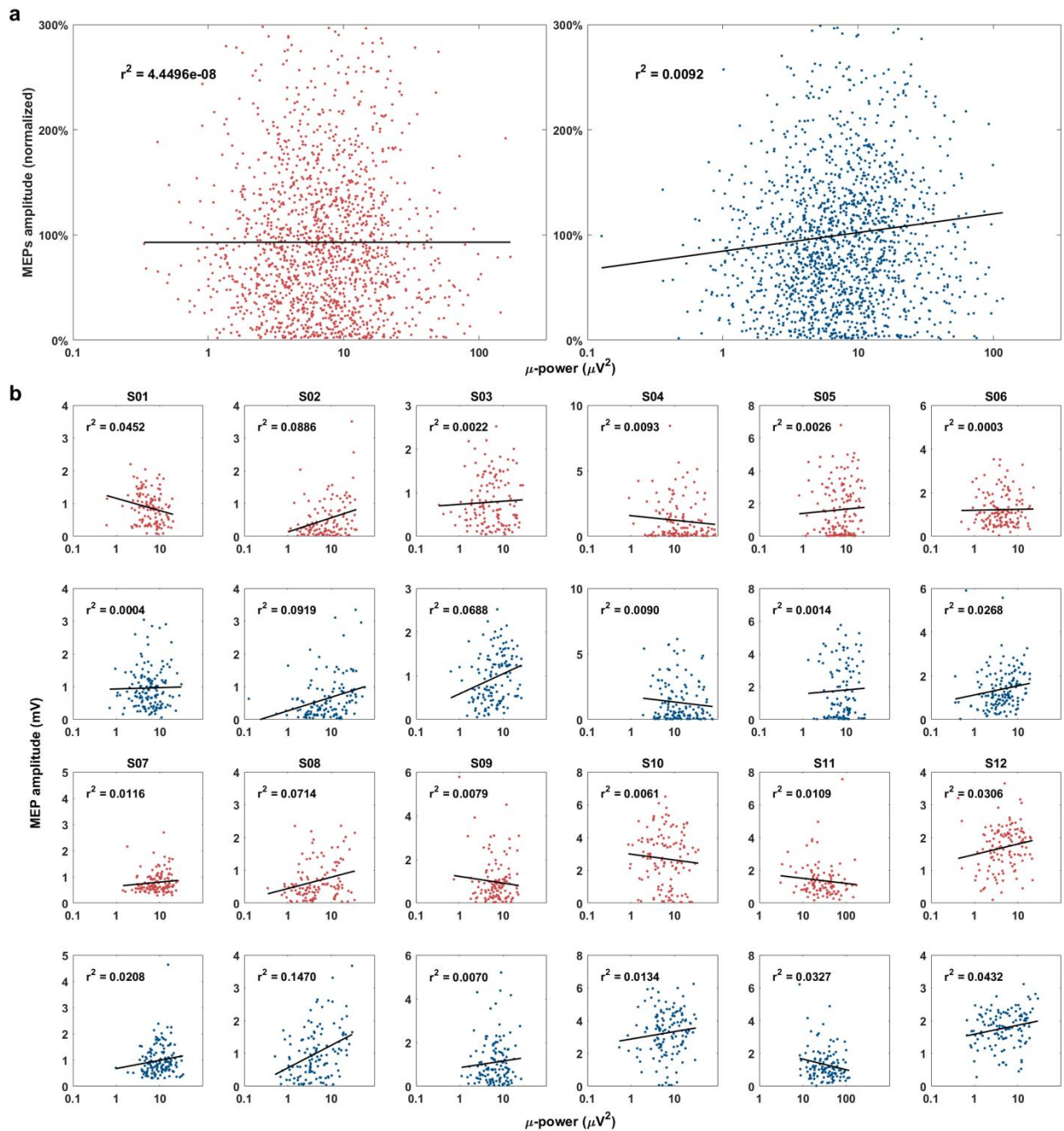


Supplementary Figure 2 | Simulink Real-Time Model. The graphically designed digital signal processing algorithm is compiled into an executable binary. EEG data is acquired through a data acquisition card from the analog output stream of the EEG main unit at a sample rate of 1 kHz. A sliding window of 500 ms is de-meant and a 5-point sum-of-difference operator is applied (“Hjorth Transform”). The resulting frame of data is further processed in two parallel streams. In one processing stream (shown at the top), a spectral analysis is performed to estimate the power in the 8-12 Hz alpha spectrum (green box). In the second processing stream (shown at the bottom, blue boxes), the frame of data is filtered forward and backward by a FIR 8-12 Hz bandpass filter and the edges are removed. The resulting (shorter) vector of EEG data is then iteratively forward predicted by an autoregressive forecasting model. The resulting vector is used to perform a Hilbert transform and the phase angle is determined from this signal at “time zero”. If both the spectral alpha power exceeds a threshold and simultaneously a pre-determined phase angle is crossed (positive peak or negative peak), a TTL trigger signal is sent to the stimulus generator through a digital output of the data acquisition card.

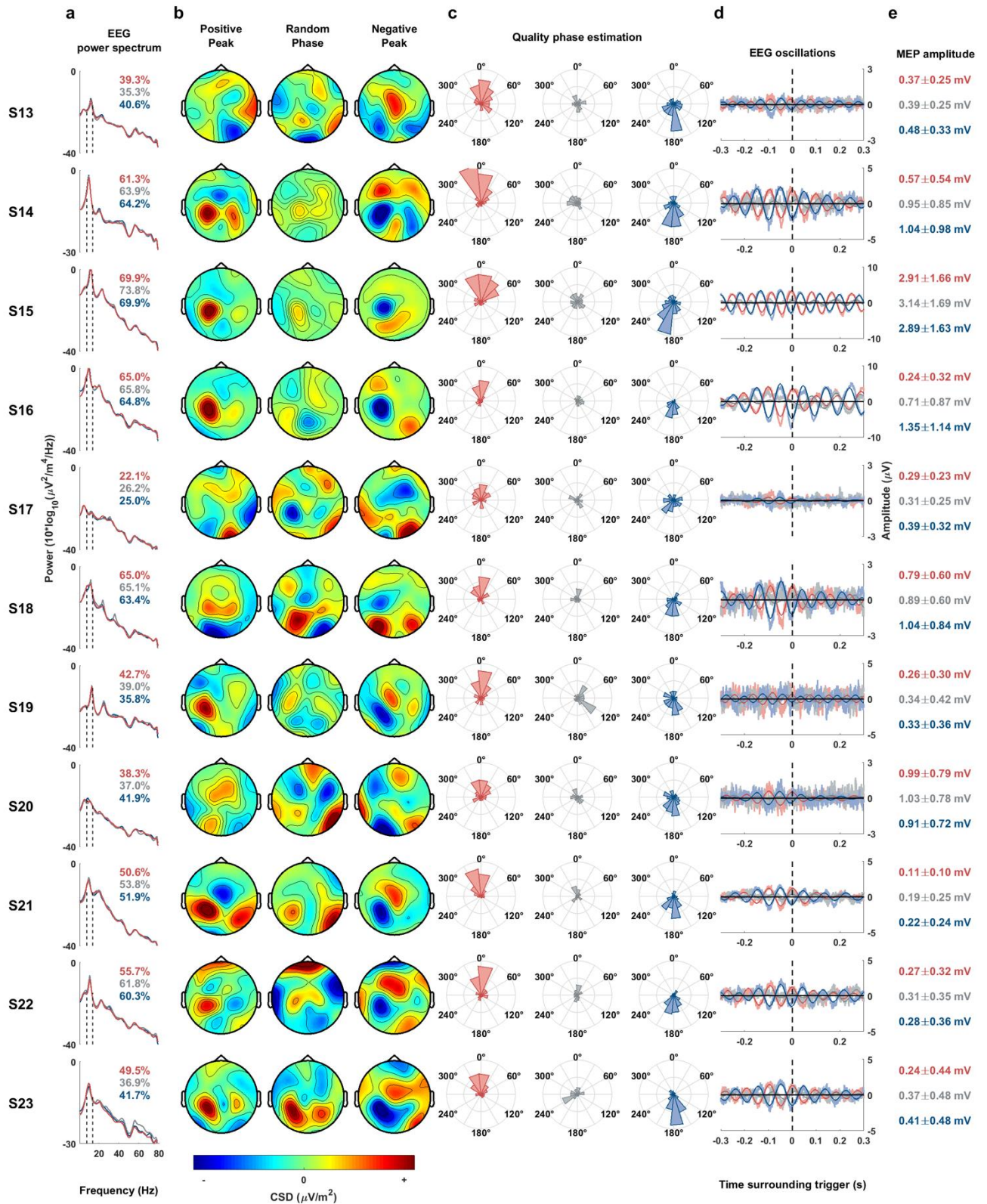


Supplementary Figure 3 | Individual data (subjects S1-S12) of the Hjorth-C3 derived estimation of the sensorimotor μ -rhythm for triggering TMS pulses in the Main Experiment. (a) EEG power spectrum derived from the CSD C3 signal estimated from the triggered but non-stimulated trials (1 s window, positive peak trigger in red, negative peak trigger in blue). Note high within-subject consistency across the positive vs. negative peak conditions of alpha-peak power (individual alpha range indicated by vertical dashed lines) given as percentage of total power in the spectrum. (b) Anatomical correlation between voxel-wise source-level signal and the Hjorth-C3 derived sensorimotor μ -rhythm used for triggering, demonstrating that the origin of the Hjorth-C3 signal is the hand representation area in sensorimotor cortex (hand knob in M1, or adjacent primary somatosensory cortex)

in all subjects. The color bar denotes the correlation coefficient. **(c)** Individual current source density (CSD) plots of the triggered non-stimulated positive and negative peak conditions. Amplitudes are individually scaled and centered at $0 \mu\text{V}/\text{m}^2$, individual maximum negativity (blue) and maximum positivity (red) are indicated by the color bar. **(d)** Distribution of actual phases determined from real-time triggered non-stimulated epochs of the Hjorth-C3 positive and negative peak conditions, shaded red and blue, respectively. Radius axis of the rose plots is 15% for the inner and 30% for the outer ring in all subjects. **(e)** Average amplitude ± 0.3 s around the time of the real-time trigger (time = 0) for positive peak (red) and negative peak (blue) conditions, showing the average raw Hjorth-C3 signal, and after FIR 8-12 Hz bandpass filtering. Note that at least 2 cycles of the μ -oscillation can be detected in the pre-trigger period in all of the subjects. **(f)** Individual mean (± 1 s.d.) absolute MEP amplitudes (in mV) in the positive peak (in red font), and negative peak condition (blue). Data correspond to the normalized to the individual mean MEP data in Fig. 2f.

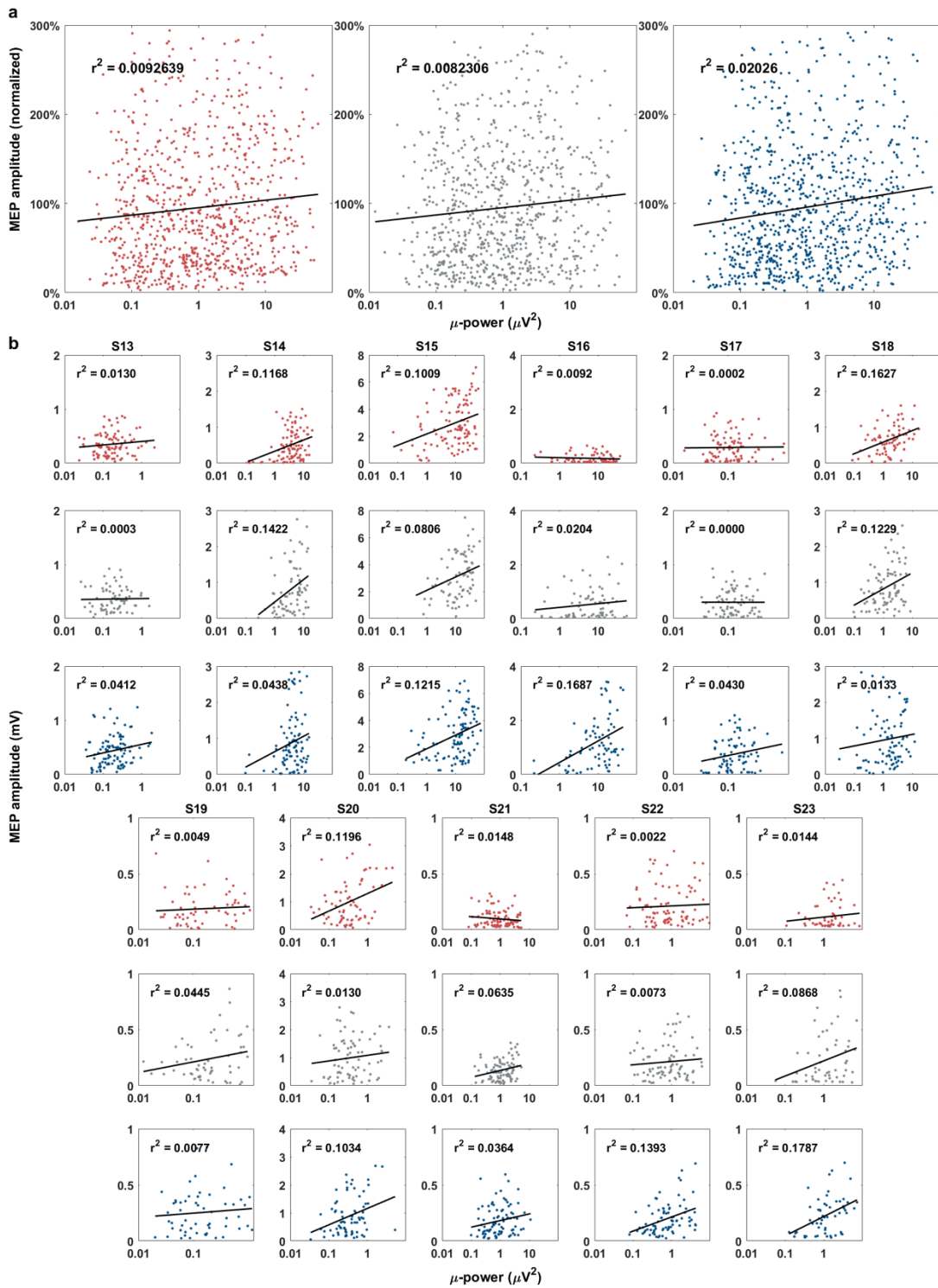


Supplementary Figure 4 | Relation of pre-stimulus μ -power and MEP amplitude in the Main Experiment. Spectral power was estimated from the 500 ms window of EEG data preceding TMS by performing FFT on the Hjorth-C3 EEG signal overlying left sensorimotor cortex. **(a)** Group data normalized to the mean MEP for each subject and condition (y-axis); pre-stimulus μ -power is given in μV^2 (logarithmized x-axis). Left: Hjorth-C3 positive peak condition, right: Hjorth-C3 negative peak condition. Linear regression analysis indicated that <1% of the variability of MEP amplitude is explained by pre-stimulus μ -power. **(b)** Individual scatter plots of pre-stimulus power (in μV^2) vs. MEP amplitude (in mV) for each subject (S01-S12) in the Hjorth-C3 positive peak (red) and Hjorth-C3 negative peak condition (blue). All data were normally distributed. Note that even at individual level pre-stimulus μ -power never explained >10% of MEP amplitude variability.



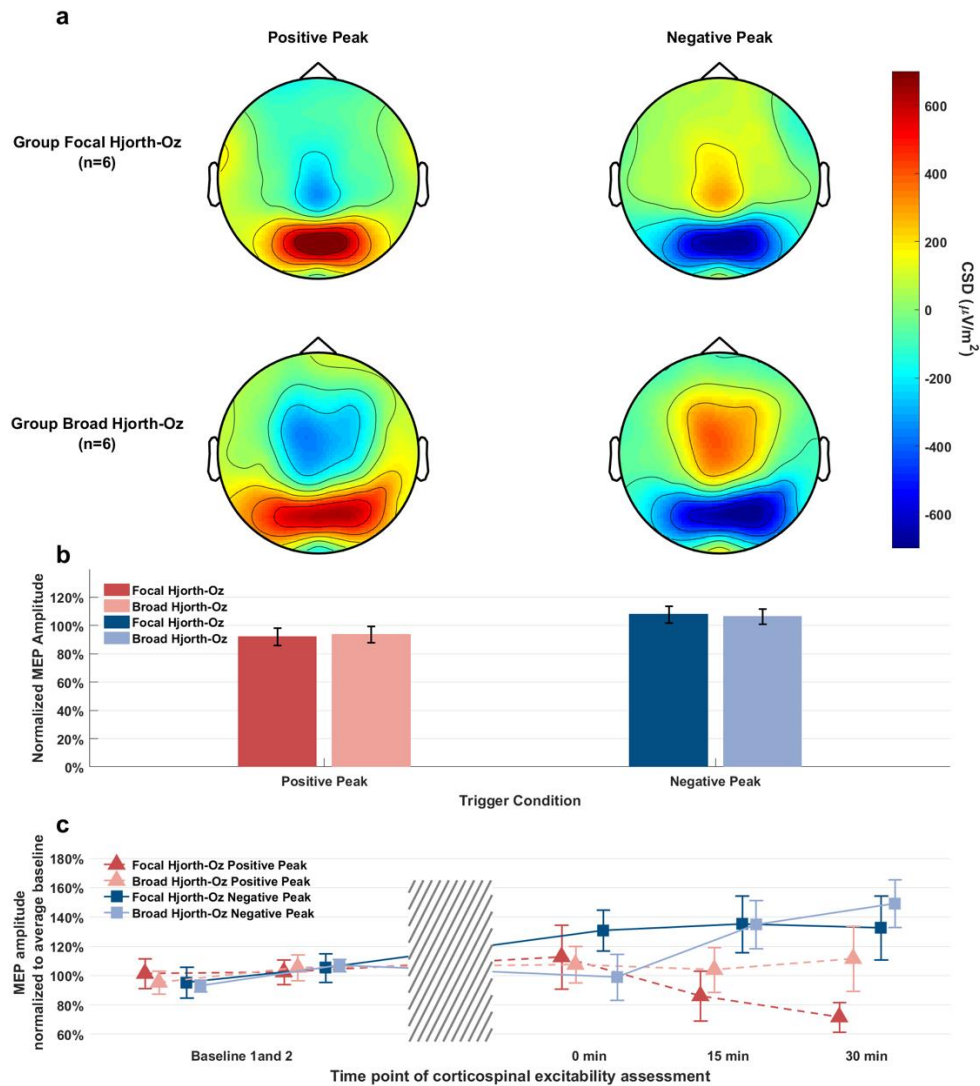
Supplementary Figure 5 | Individual data (subjects S13-S23) of the Hjorth-C3 derived estimation of the sensorimotor μ -rhythm for triggering TMS pulses in Control Experiment 3. (a) EEG power spectrum derived from the CSD C3 signal estimated from the triggered but non-stimulated trials (1 s window, positive peak trigger in red, negative peak trigger in blue). Note high within-subject consistency across the positive peak, random phase and negative peak conditions of alpha-peak power (individual alpha range indicated by vertical dashed lines) given as percentage of total power in the spectrum. (b) Individual current source density (CSD) plots of the triggered non-stimulated positive peak, random phase and negative peak conditions. Amplitudes are individually scaled and centered at $0 \mu V/m^2$, individual maximum negativity (blue) and maximum positivity (red) are indicated by the color bar. (c) Distribution of actual phases determined from real-time triggered non-stimulated epochs of

the Hjorth-C3 positive peak, random phase, and negative peak conditions, shaded red, grey and blue, respectively. Radius axis of the rose plots is 15% for the inner and 30% for the outer ring in all subjects. **(d)** Average amplitude ± 0.3 s around the time of the real-time trigger (time = 0) for positive peak (red), random phase (grey) and negative peak (blue) conditions, showing the average raw Hjorth-C3 signal, and after FIR 8-12 Hz bandpass filtering. Note that at least 2 cycles of the μ -oscillation can be detected in the pre-trigger period in all of the subjects. **(e)** Individual mean (± 1 s.d.) absolute MEP amplitudes (in mV) in the positive peak (in red font), random phase (grey) and negative peak condition (blue). Data correspond to the normalized to the individual mean MEP data in Fig. 6e.

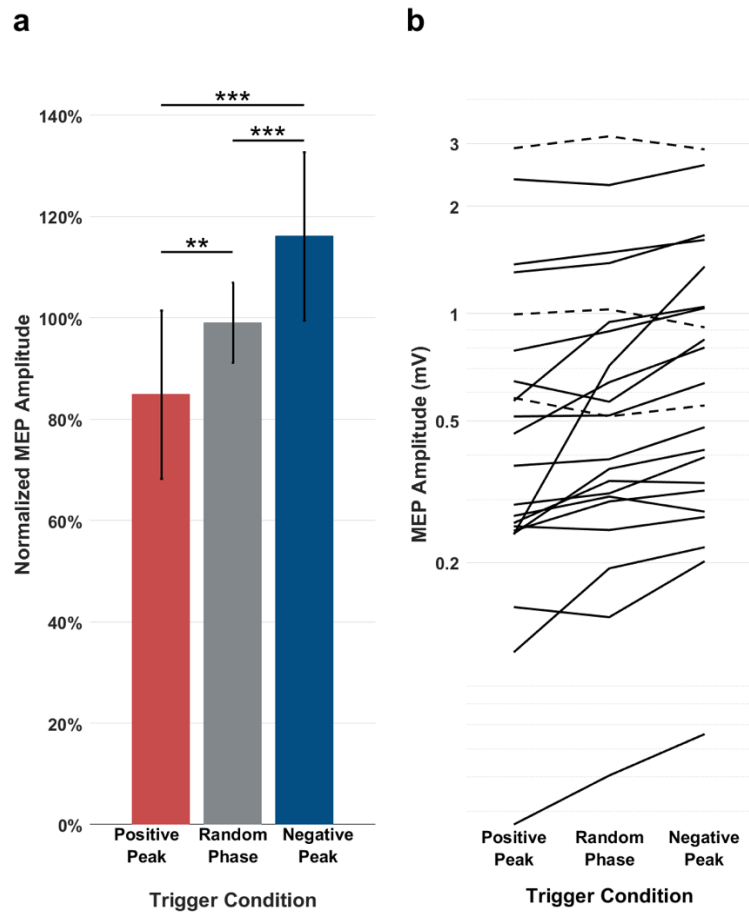


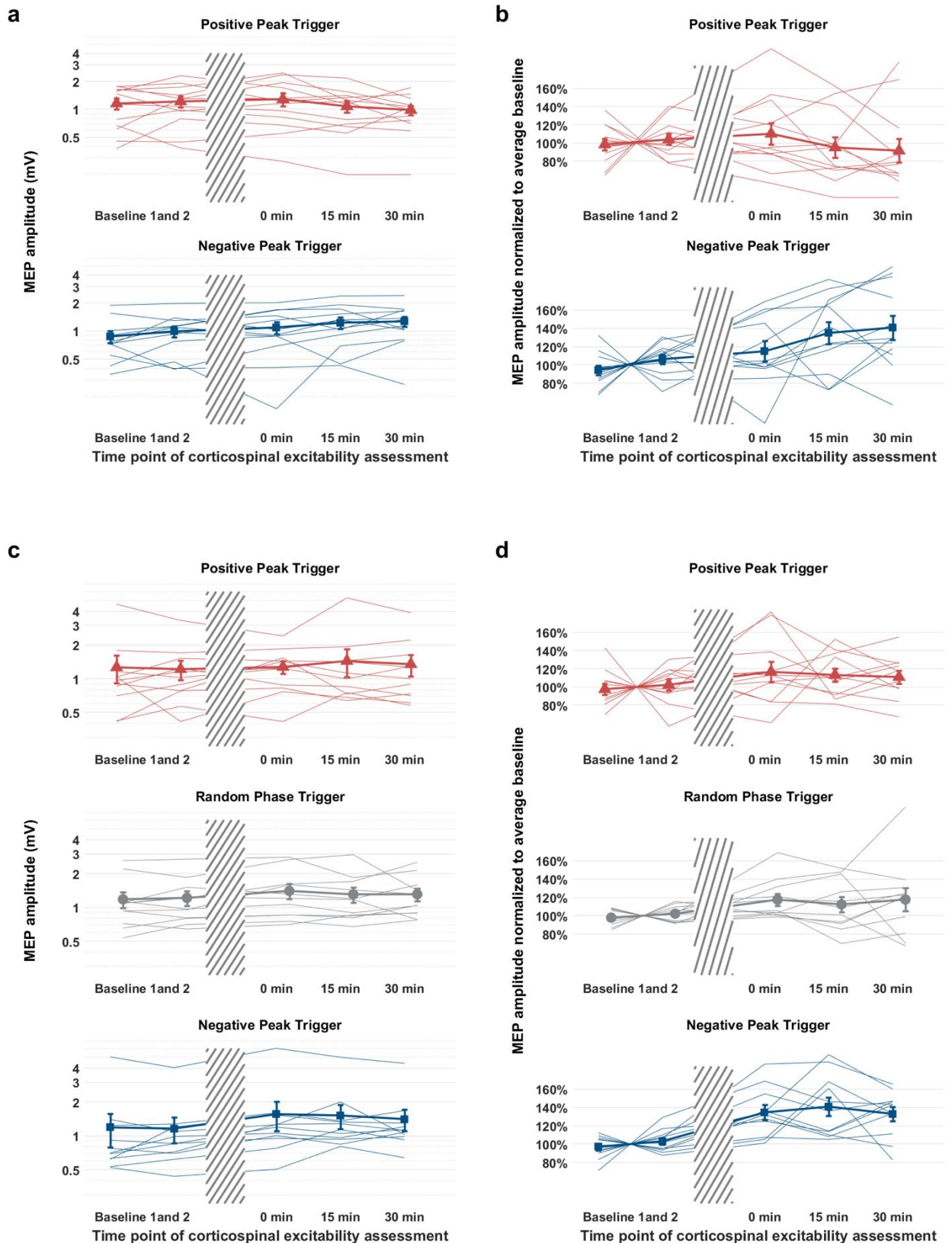
Supplementary Figure 6 | Relation of pre-stimulus μ -power and MEP amplitude in Control Experiment 3.

Spectral power was estimated from the 500 ms window of EEG data preceding TMS by performing FFT on the Hjorth-C3 EEG signal overlying left sensorimotor cortex. **(a)** Group data normalized to the mean MEP for each subject and condition (y-axis); pre-stimulus μ -power is given in μV^2 (logarithmized x-axis). Left: Hjorth-C3 positive peak condition, middle: random phase condition; right: Hjorth-C3 negative peak condition. Linear regression analysis indicated that <2.5% of the variability of MEP amplitude is explained by pre-stimulus μ -power. **(b)** Individual scatter plots of pre-stimulus power (in μV^2) vs. MEP amplitude (in mV) for each subject (S13-S23) in the Hjorth-C3 positive peak (red), random phase (grey) and Hjorth-C3 negative peak condition (blue). All data were normally distributed. Note that even at individual level pre-stimulus μ -power never explained >18% of MEP amplitude variability.

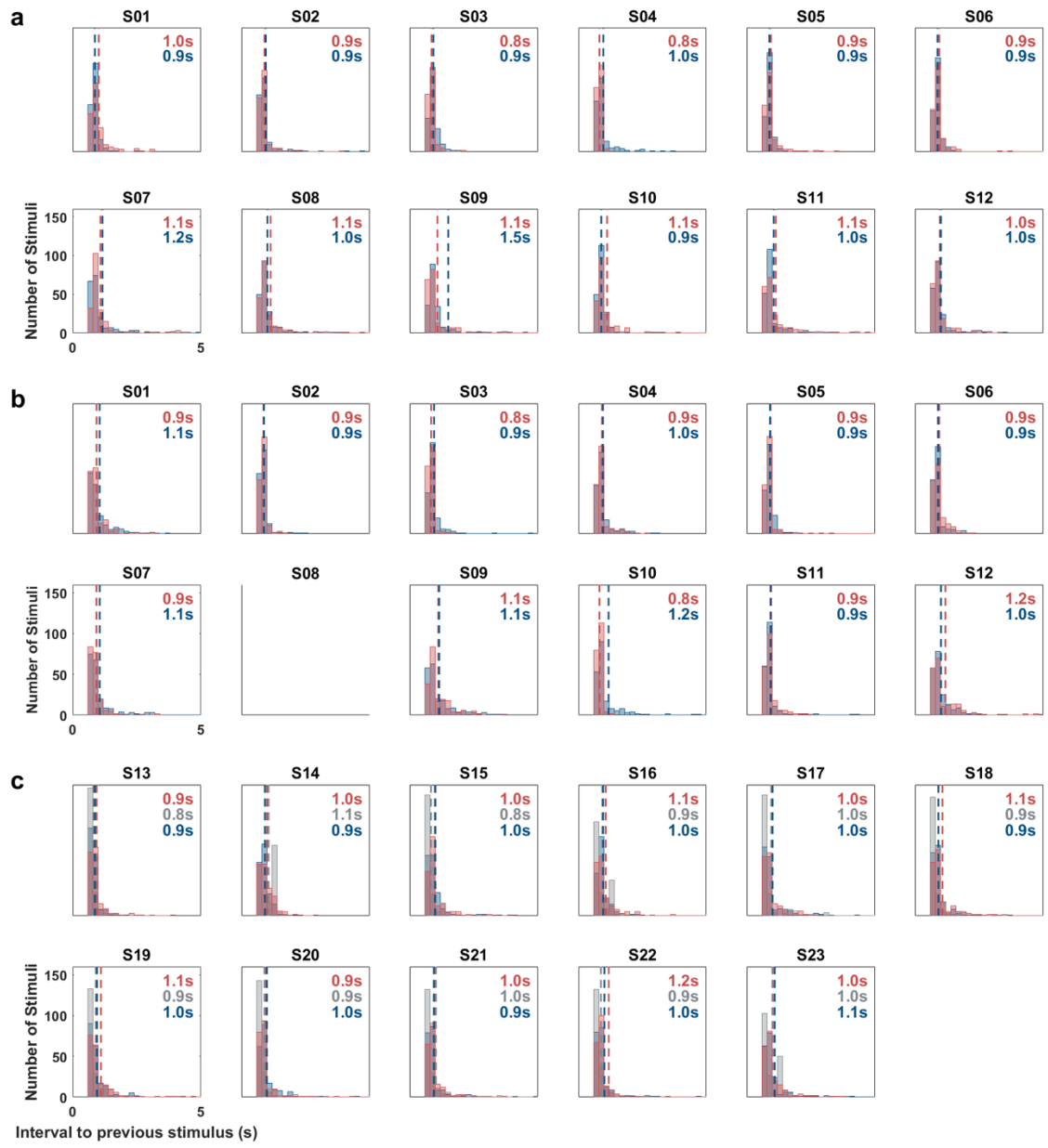


Supplementary Figure 7 | Subgroup analysis by focality of the Oz-Hjorth 8-12 Hz signal. A fixed 5-point Hjorth-Laplace montage was used to isolate local oscillations in the hand knob area of motor cortex being stimulated by TMS (centered on C3, Main Experiment). Since the Hjorth-C3 EEG signals was not completely uncorrelated from occipital alpha-oscillations in the Hjorth-Oz montage (cf. Fig. 5b), a supplementary analysis was performed to assess whether the degree of contamination of the Hjorth-C3 signal from occipital alpha affected the results. The 12 subjects included in Main Experiment were divided in two subgroups according to the focality of their occipital 8-12 Hz signal: a 5 minute eyes open resting-state EEG recording acquired immediately before the experimental session was used for post-hoc phase-detection of the zero phase 8-12 Hz filtered signal, detecting positive and negative peaks of the Hjorth-Oz filtered signal, 150 markers per condition, with a minimum interval of 1 s between markers; the average signal in the ± 20 ms window around the positive and negative peak markers was then used to generate current scalp density (CSD) surface topographies for each subject using the Fieldtrip toolbox spline method. Subjects were then grouped into either the focal or the broad signal subgroup by visual inspection of the topographies. **(a)** Average CSD topographies in the focal and broad Hjorth-Oz signal subgroups for the ± 20 ms period surrounding the positive and negative Hjorth-Oz peak. **(b)** Normalized to individual mean MEP amplitude data, showing no significant effect of Hjorth-Oz subgroup (dark colors: focal, light colors: broad Hjorth-Oz signal) on the corticospinal excitability difference between Hjorth-C3 positive peak (red) vs. negative peak (blue) conditions. **(c)** Time course of mean normalized to average baseline MEP amplitude ± 1 s.e.m., with rTMS (hashed bar) triggered in separate sessions by the Hjorth-C3 positive peak (red triangles) or negative peak (blue squares) of ongoing μ -rhythm, showing no effect by Hjorth-Oz focality subgroups (dark colors: focal, light colors: broad Hjorth-Oz signal) on Hjorth-C3 phase-dependent corticospinal excitability.

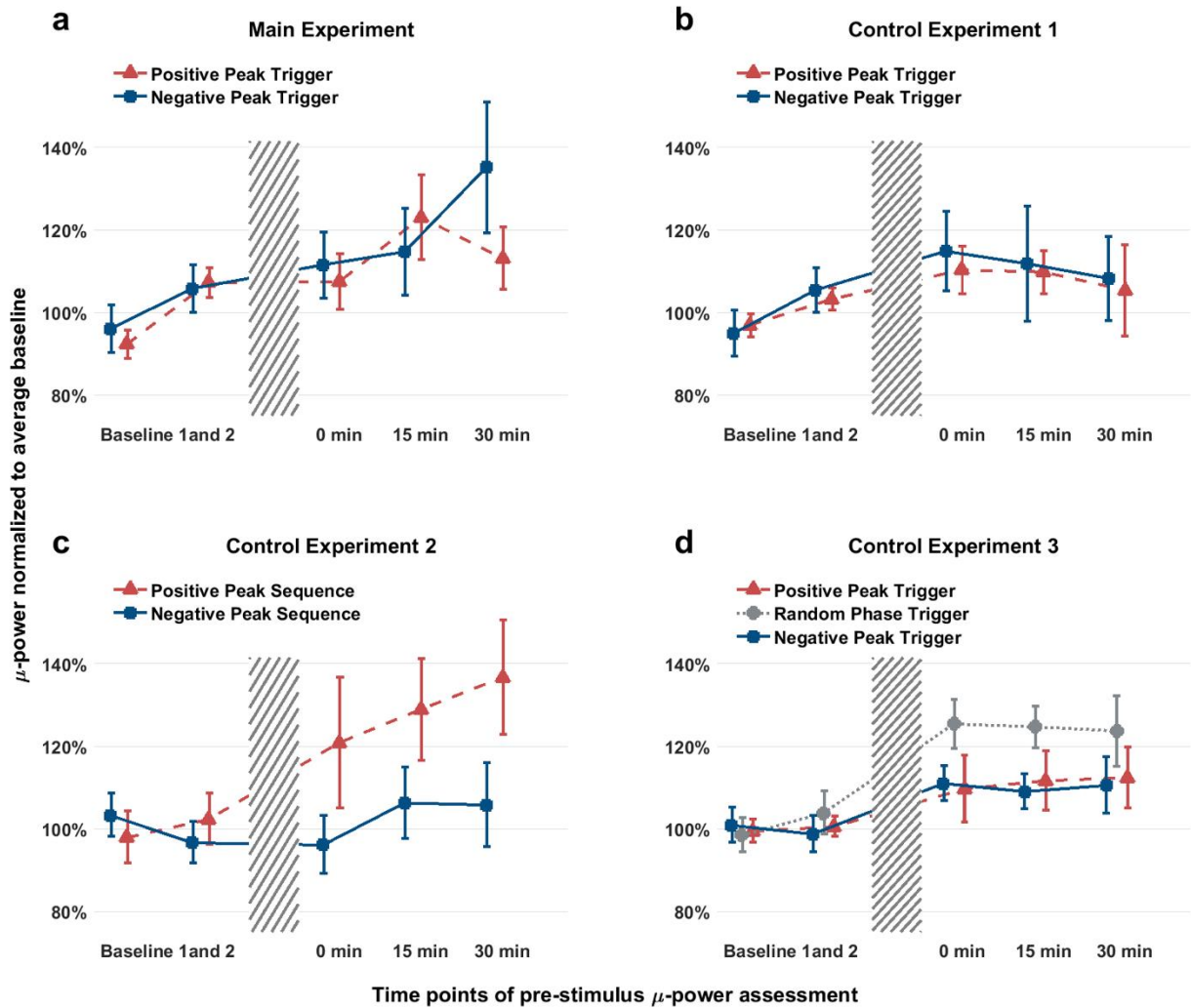




Supplementary Figure 9 | Single subject data of EEG-triggered rTMS-induced plasticity. Absolute MEP amplitudes (in mV, panels **a**, **c**, y-axes logarithmized) and MEP amplitudes normalized to average baseline (panels **b**, **d**) are shown for each individual subject (thin lines) as well as the grand averages (thick line, with error bars indicating ± 1 s.e.m.), before and after the rTMS intervention (shaded area, conditions indicated at the top of each panel). (**a**, **b**) Data from Main Experiment, (**c**, **d**) Data from Control Experiment 3. Refer to the results section of the main text for statistical analyses.




Supplementary Figure 10 | RTMS pulse train stochastics in the plasticity experiments. The distribution of inter-triplet-intervals is plotted for each subject for the Hjorth-C3 positive peak condition (red), negative peak condition (blue), and random phase condition (grey, only applicable for the Control Experiment 3 in **c**). (**a-c**) Data of the Main Experiment, Control Experiment 1 and Control Experiment 3, respectively. Mean inter-triplet-intervals are given (in s) for each subject in the inset.



Supplementary Figure 11 | Pre-stimulus power of the sensorimotor μ -rhythm before and after the EEG-triggered rTMS intervention. This supplementary analysis was performed to assess whether power of the sensorimotor μ -rhythm was also differentially modulated by rTMS intervention. Power spectral density (PSD) was estimated using the Yule-Walker Method to optimally fit an autoregressive model of order 1250 to the 500ms window (containing 2500 samples at sample frequency 5 kHz) preceding each test-pulse within each of the five blocks of 100 test pulses (baselines 1 and 2, and 0, 15 and 30 min post-rTMS). Data are means \pm 1 s.e.m. normalized to average baseline, with rTMS (hashed bar, 200 x 100-Hz-triplets, intensity 80% of MEP threshold) triggered in separate experimental conditions as indicated at the top of each panel (for details, see main text and methods). **(a)** Main Experiment (n=12). **(b)** Control Experiment 1 (n=11). **(c)** Control Experiment 2 (n=8). **(d)** Control Experiment 3 (n=11). Note, that there was no significant effect of rTMS on μ -power in any of the conditions.

2.2 Phase of sensorimotor μ -oscillation modulates cortical responses to TMS of the human motor cortex

Phase of sensorimotor μ -oscillation modulates cortical responses to transcranial magnetic stimulation of the human motor cortex

Debora Desideri, Christoph Zrenner, Ulf Ziemann  and Paolo Belardinelli

Department of Neurology & Stroke, and Hertie Institute for Clinical Brain Research, University of Tübingen, Hoppe-Seyler-Str. 3, 72076 Tübingen, Germany

Edited by: Janet Taylor & Richard Carson

Key points

- Oscillatory brain activity coordinates the response of cortical neurons to synaptic inputs in a phase-dependent manner.
- Larger motor-evoked responses are obtained in a hand muscle when transcranial magnetic stimulation (TMS) is synchronized to the phase of the sensorimotor μ -rhythm.
- In this study we further showed that TMS applied at the negative *vs.* positive peak of the μ -rhythm is associated with higher absolute amplitude of the evoked EEG potential at 100 ms after stimulation.
- This demonstrates that cortical responses are sensitive to excitability fluctuation with brain oscillations
- Our results indicate that brain state-dependent stimulation is a new useful technique for the investigation of stimulus-related cortical dynamics.

Abstract Oscillatory brain activity coordinates the response of cortical neurons to synaptic inputs in a phase-dependent manner. Transcranial magnetic stimulation (TMS) of the human primary motor cortex elicits larger motor-evoked potentials (MEPs) when applied at the negative *vs.* positive peak of the sensorimotor μ -rhythm recorded with EEG, demonstrating that this phase represents a state of higher excitability of the cortico-spinal system. Here, we investigated the influence of the phase of the μ -rhythm on cortical responses to TMS as measured by EEG. We tested different stimulation intensities above and below resting motor threshold (RMT), and a realistic sham TMS condition. TMS at 110% RMT applied at the negative *vs.* positive peak of the μ -rhythm was associated with higher absolute amplitudes of TMS-evoked potentials at 70 ms (P70) and 100 ms (N100). Enhancement of the N100 was confirmed with negative peak-triggered 90% RMT TMS, while phase of the μ -rhythm did not influence evoked responses elicited by sham TMS. These findings extend the idea that TMS applied at the negative *vs.* positive peak of

Debora Desideri is a PhD student at the Department of Neurology & Stroke, University Hospital of Tübingen, and Hertie Institute for Clinical Brain Research in Tübingen. Her research combines non-invasive brain stimulation with EEG recordings to achieve a brain state-dependent stimulation of the human motor cortex. Her PhD focuses on the role of oscillatory brain activity originating in the human sensorimotor cortex in modulating EMG and EEG responses to brain stimulation.



the endogenous μ -oscillation recruits a larger portion of neurons as a function of stimulation intensity. This further corroborates that brain oscillations determine fluctuations in cortical excitability and establishes phase-triggered EEG-TMS as a sensitive tool to investigate the effects of brain oscillations on stimulus-related cortical dynamics.

(Received 18 July 2019; accepted after revision 17 September 2019; first published online 19 September 2019)

Corresponding author Prof. U. Ziemann: Department of Neurology & Stroke, and Hertie Institute for Clinical Brain Research, University of Tübingen, Hoppe-Seyler-Str. 3, 72076 Tübingen, Germany.

Email: ulf.ziemann@uni-tuebingen.de

Introduction

EEG allows non-invasive access to the electrical activity of cortical neurons, which is mostly expressed in the form of oscillatory waves (Buzsáki, 2006). These brain oscillations are thought to functionally coordinate the response of cortical neurons to synaptic inputs, therefore representing fluctuations in cortical excitability (Buzsáki & Draguhn, 2004). Transcranial magnetic stimulation (TMS) is a non-invasive technique that can be used to directly probe human cortical excitability *in vivo* (Hallett, 2007). When applied to the primary motor cortex (M1), TMS elicits a response in muscles, the motor-evoked potential (MEP). MEP amplitude is considered a measure of corticospinal system excitability (Hallett, 2007). In a previous study, we used the real-time estimated phase of the sensorimotor μ -oscillation to trigger TMS over the left M1 at rest, and demonstrated that MEP amplitude is larger at the negative peak *vs.* positive peak of the sensorimotor μ -oscillation (Zrenner *et al.* 2018). This confirms and extends results of previous animal and human research (Hari, 2006; Jensen & Mazaheri, 2010; Haegens *et al.* 2011), and is in line with the concept that the negative peak of the μ -oscillation represents a state in which the dendritic trees of pyramidal neurons are closer to firing threshold and, therefore, are more likely to generate action potentials in response to a TMS pulse (Buzsáki *et al.* 2012; Zrenner *et al.* 2018). In the EEG, TMS elicits a sequence of TMS-evoked cortical potentials (TEPs), usually up to 300 ms after the TMS pulse (Ilmoniemi *et al.* 1997; Paus *et al.* 2001; Bonato *et al.* 2006), as well as a modulation of spontaneous oscillatory activity (Fuggetta *et al.* 2005; Rosanova *et al.* 2009; Fecchio *et al.* 2017; Premoli *et al.* 2017). Previous research has shown that the current brain state influences amplitude and spatio-temporal spread of EEG responses following TMS (Massimini *et al.* 2005; Bergmann *et al.* 2012). TEPs and oscillatory activity in response to TMS over M1 are consistently larger during the up-state *vs.* down-state of slow-wave sleep oscillations (Bergmann *et al.* 2012). Variations in the global mean field amplitude, which is a measure of global brain reactivity, are predicted by ongoing beta (15–25 Hz) phase when TMS is applied over the superior parietal lobule during a short-term memory task (Kundu *et al.* 2014). These results suggest that oscillatory phase influences cortical

responses to TMS. In this background, we expected the phase of the sensorimotor μ -oscillation to modulate EEG responses to TMS. More specifically, we expected TEP amplitudes and post-TMS oscillatory activity to be larger when TMS is applied at the negative *vs.* positive peak of the sensorimotor μ -oscillation, as the negative peak represents a motor high-excitability state.

To test this hypothesis, we analysed EEG data obtained upon application of μ -phase-triggered TMS at different stimulation intensities above and below resting motor threshold (RMT), and a realistic sham TMS condition. The inclusion of a subthreshold stimulation intensity allowed us to disentangle between phase-dependent modulation of brain responses evoked by TMS *vs.* sensory re-afferent feedback caused by MEPs. The realistic sham TMS condition allowed us to exclude a significant contribution of the auditory and scalp somatosensory inputs associated with TMS to the μ -phase-dependent modulation of direct brain responses evoked by TMS.

Methods

Ethical approval

The study protocol was approved by the local ethics committee of the medical faculty of the University of Tübingen (protocol 716/2014BO2). Experiments were conducted in accordance with the *Declaration of Helsinki*, except for registration in a database, and with the current TMS safety guidelines (Rossi *et al.* 2009). Written informed consent was obtained for all participants.

Subjects

Twelve right-handed volunteers (four males, age range 22–51 years, mean age \pm SD 27.5 \pm 7.7 years, Edinburgh Inventory handedness laterality score 75 \pm 23) free of medications and without a history of neurological or psychiatric disorders took part in the study. Subjects were tested with a stimulation intensity (SI) of 110% RMT, 90% RMT and with realistic sham TMS (see below, *Experimental design*). All subjects fulfilled a power criterion in the μ -band (8–12 Hz) of > 25% of the power in the 1–80 Hz power spectrum of the current scalp density

signal of the C3 EEG electrode when at rest and with eyes open. This ensured a sufficient signal-to-noise ratio for reliable estimation of the instantaneous phase of the sensorimotor μ -oscillation in real time (Zrenner *et al.* 2018). Approximately 40% of the screened individuals met the μ -power inclusion criterion.

Experimental set-up and procedure

Participants were seated in a comfortable armchair with their hands relaxed and fixating on a cross in front of them while TMS pulses were delivered to the left M1. A high-frequency magnetic stimulator (Research 100, MAG & More, Munich, Germany) was used to deliver single biphasic TMS pulses (single cosine, 160 μ s period) through a passively cooled TMS double coil (PMD70-pCool, 70 mm winding diameter, MAG & More). The participant's head was immobilized by a vacuum pillow (Vacuform, B.u.W. Schmidt GmbH, Garbsen, Germany) and a fixation arm (Magic Arm, Lino Manfrotto + Co. S.p.A., Cassola, Italy) fixated to a metallic frame was used to hold the TMS coil. Realistic sham TMS was achieved using two identical TMS coils and an electrical stimulator. The first coil was placed on the participant's head and the second one was held in the air next to the first. Only the second coil was connected to the TMS stimulator and was used to produce the typical TMS clicks at SI 90% RMT. To mimic the scalp sensation associated with TMS stimulation, electrical stimulation of the scalp with 200 μ s pulse duration, 200 V compliance voltage and 2.50 mA output current was delivered through two round electrodes (diameter 1 cm) integrated in the EEG cap. The cathode was placed between Cz and CP1 and the anode between FC5 and C3, and connected to a constant-current high-voltage electrical stimulator (Constant current stimulator DS7A, Digitimer Ltd, Welwyn Garden City, UK). Impedance between the electrodes and the scalp was improved with a highly conductive gel (SignaGel, Parker Laboratories, Inc., Fairfield, NJ, USA). This combination of electrode configuration and stimulation parameters was chosen as it was shown to achieve a scalp sensation comparable to real TMS at 90% RMT. MEPs were recorded from the right abductor pollicis brevis (APB) muscle through surface EMG (5 kHz sampling rate, 0.16 Hz to 1.25 kHz bandpass filter) using adhesive hydrogel electrodes (Kendall, Covidien, Dublin, Ireland) in a bipolar belly-tendon montage. RMT was determined by adjusting the stimulation intensity in steps of 1% of the maximum stimulator output and was defined, using the standard relative frequency method (Rossini *et al.* 2015), as the minimum stimulation intensity that produced MEPs > 50 μ V in the target muscle in at least 5/10 consecutive trials. The motor 'hotspot' was defined as the coil position

eliciting, at a slightly suprathreshold stimulation intensity, maximum MEP amplitudes (Rossini *et al.* 2015). Coil orientation was orthogonal to the central sulcus, so that the electric field induced in the brain by the second phase of the biphasic pulse was lateral–posterior to medial–anterior (Rossini *et al.* 2015). Coil position was kept constant relative to the participant's head using a stereoscopic neuronavigation system (Localite GmbH, Sankt Augustin, Germany). The EEG signal was recorded from 64 channels arranged in the International 10–20 montage (Seeck *et al.* 2017) in a TMS-compatible Ag/AgCl sintered ring electrode cap (EasyCap GmbH, Woerthsee-Ettersschlag, Germany), with FCz as the reference electrode and PPO1h as the ground electrode. The impedance at the skin–EEG electrodes interface was kept < 5 k Ω . A 24-bit 80-channel biosignal amplifier was used for EEG and EMG recordings (NeurOne, Bittium Biosignals Ltd, Kuopio, Finland) in the real-time 'Digital Out' mode and data were acquired in DC mode (1.25 kHz low-pass anti-aliasing filter) with a sample rate of 5 kHz and a head-stage sample rate of 80 kHz. A real-time system implemented as a Simulink Real-Time model (R2015a; Mathworks, Natick, MA, USA) and executed on a dedicated xPC Target PC running the Simulink Real-Time operating system (DFI-ACP CL630-CRM mainboard) was used for real-time analysis of the EEG signal and for triggering TMS pulses according to the instantaneous phase of oscillatory EEG activity (for details, see Zrenner *et al.* 2018). White noise at individually adjusted loudness was applied through earphones to mask the TMS click and minimize TMS-evoked auditory potentials (Massimini *et al.* 2005; Casarotto *et al.* 2010; Ilmoniemi & Kicic, 2010).

Experimental design

The sensorimotor μ -oscillation originating in the left sensorimotor cortex was isolated at sensor level with a spatial filter centred on the electrode C3 and using the four adjacent electrodes FC3, C1, CP3 and C5 (Hjorth, 1975) and its instantaneous phase was estimated in real time (for details, see Zrenner *et al.* 2018). The experiment started with 5 min of eyes open resting-state EEG. Then, 110% RMT SI, 90% RMT SI and sham TMS were tested in three different blocks in the same session in a blinded randomized crossover design. Blocks were separated by pauses of 5–10 min. To assess success of the blinding procedure, at the end of the session subjects filled in a questionnaire in which they reported how they perceived the three experimental blocks. In each block, triggers were generated by the positive peak, negative peak and random phase of the sensorimotor μ -oscillation. A total of 900 triggers were generated in each block, corresponding to 150 stimulated trials and 150 non-stimulated trials per μ -phase condition, in randomized order and with a

jittered minimum intertrial interval of 2 s. A μ -power threshold was used to ensure that the phase estimation was performed on physiological μ -oscillation and not filtered noise. The μ -power threshold was set manually at the beginning of the experiment and, if necessary, was adjusted during the experiment to keep the intertrial interval around 2–4 s.

Data analysis

EEG and EMG data processing and analysis were performed using customized analysis scripts on MATLAB R2016a and the Fieldtrip open source MATLAB toolbox (Oostenveld *et al.* 2011). Data were preprocessed without knowledge of the experimental condition.

EEG data preprocessing. Data were segmented in epochs from 0.5 s before to 1 s after the trigger markers. Data from 1 ms before to 15 ms after the marker, where high-amplitude TMS artifacts occur, were removed and cubic interpolated. For the sham TMS block, data up to 40 ms needed to be removed and interpolated, as the electrical stimulation produced a longer lasting artifact. EEG data were then centred and visually inspected. Epochs containing major artifacts were removed as well as channels that showed prominent noise in most of the epochs (percentage of removed epochs: $3.9 \pm 2.4\%$, number of removed channels: 2.7 ± 0.9 , results are reported as mean \pm SD). Independent component analysis (ICA) based on the FastICA algorithm (Hyvärinen, 1999; Hyvärinen *et al.* 2001) was applied to the data. Data underwent ICA twice, in a two-step procedure as proposed by Rogasch *et al.* (2017). In both steps, ICA components were visually inspected and removed based on their topography, single-trial time course, average time course and power spectrum. In the first step, only components representing high-amplitude TMS-related artifacts were removed (mean \pm SD 7.4 ± 2.1). Then, ICA was again applied to the data upon filtering with a 1–80 Hz bandpass filter (zero-phase Butterworth, third order) and a 49–51 Hz notch filter (zero-phase Butterworth, third order) and down-sampling to 1000 Hz. Components representing biological (eye blinks and movements, persistent muscle activity) or small-amplitude TMS-related artifacts were removed (mean \pm SD 23.9 ± 8.9). Channels discarded during visual inspection of the data were then spline-interpolated using the signal of the neighbouring channels (Perrin *et al.* 1989) and data were re-referenced to the average reference signal.

EMG data preprocessing. For the 110% RMT block, peak-to-peak MEP amplitudes were automatically

determined in the epochs corresponding to a TMS marker in the 20–40 ms after the TMS pulse.

TMS-evoked EEG potentials. Stimulated EEG epochs retained after data cleaning were lowpass filtered (45 Hz, zero-phase Butterworth, third order) and averaged by condition.

TMS-induced EEG oscillations. TMS also produces responses that are not time-locked to the onset of the pulse, for example changes in spontaneous oscillatory activity (Fuggetta *et al.* 2005; Rosanova *et al.* 2009; Fecchio *et al.* 2017; Premoli *et al.* 2017). The non-time-locked, i.e. induced, response can be isolated in the time domain by a channel-wise subtraction of the evoked response from each single trial (Donner & Siegel, 2011; Premoli *et al.* 2017) and be uncovered by time–frequency representations (TFRs). Prior to time–frequency analysis, mean value and linear trends were been removed from the data. Subsequently, we calculated the TFRs convolving single trials with complex Morlet wavelets (Tallon-Baudry & Bertrand, 1999). We analysed the frequency range from 6 to 45 Hz in steps of 1 Hz, and the centre of the wavelet was shifted in steps of 10 ms in the time window –500 ms to 1000 ms relative to TMS application, with the length of the wavelet increased linearly from two cycles at 6 Hz to nine cycles at 45 Hz (Busch & VanRullen, 2010). The result of the wavelet transformation is a complex time series for each frequency in the examined frequency range. We then obtained the TFRs of power by taking the squared absolute values of the complex time series. We then normalized the single-trial TFRs with a z-transformation based on the mean and standard deviation of the full-length trial as described by Grandchamp & Delorme (2011). This full-length single-trial z-transformation calls for a pre-stimulus baseline correction, i.e. subtraction of the mean value (over time) of the baseline period (from 300 to 100 ms before TMS), to ensure that the average pre-stimulus values do not differ from zero and that z-values can be interpreted as a modulation of the pre-stimulus oscillatory activity. Finally, for each subject and each experimental condition we averaged the TFRs across trials, and trimmed the average TFRs to remove the time points where no time–frequency values could be calculated (from –500 to –333 ms and from 833 to 1000 ms with respect to the TMS marker in the data, corresponding to one cycle of the 6 Hz oscillation at the beginning and end of the epoch).

Caveats for the analysis of μ -phase-triggered TMS-evoked EEG potentials. The assumption underlying the averaging procedure used to obtain TEPs is that the response evoked by a single stimulus sums linearly to the ‘background’ ongoing brain activity: in the time-locked

average the background activity is cancelled out, while the evoked response survives (Başar & Dumermuth, 1982; Luck, 2005; Nunez & Srinivasan, 2006). In our dataset, TMS pulses are consistently delivered only at predetermined phases of the μ -oscillation. Consequently, the time-locked μ -oscillations in the negative peak and positive peak conditions will also survive the averaging procedure together with the TMS-evoked responses. In our experimental design, we have randomly interleaved non-stimulated trials to use them to correct for the time-locked μ -oscillations by applying a channel-wise subtraction of the average signal in the non-stimulated trials from that in the stimulated trials, as in Kruglikov & Schiff (2003) and Bergmann *et al.* (2012). However, for correctness of this procedure the following preconditions had to be met: (1) preservation of the phase of the ongoing μ -oscillation after the TMS pulse, i.e. no occurrence of phase reset; and (2) matching of the average amplitude of the μ -oscillations in the non-stimulated trials with that in the stimulated trials (Ritter & Becker, 2009).

To assess the occurrence of phase reset, a feasible measure is the phase preservation index (PPI; Mazaheri & Jensen, 2006). The PPI quantifies the stability of the phase of an oscillation over time with respect to a reference phase: if the phase of an oscillation is reset, the difference between the pre- and the post-stimulus phase should be random across trials, meaning that the pre-stimulus phase and the post-stimulus phase are not related to each other. The PPI is defined as:

$$PPI(c, f, t) = \frac{1}{n} \left| \sum_{k=1}^n e^{i(\varphi_k(c, f, t_{ref}) - \varphi_k(c, f, t))} \right|$$

where c denotes a channel, f and t denote a time–frequency point, n is the number of trials, $\varphi_k(c, f, t)$ is the phase of frequency f at time t for trial k at channel c and t_{ref} denotes a reference time point before the stimulus. PPI is a number between 0 and 1, with a PPI of 0 meaning no relationship between pre- and post-stimulus phases and a PPI of 1 meaning phase preservation as a function of time over trials.

Because in the positive and negative peak-triggered trials the phase before the stimulus is not random, the PPI of these trials would result in a high degree of phase stability in the case of both reset and preservation of the μ -oscillation phase. Therefore, we have calculated the PPI for the random phase TMS trials. The results of the phase reset analysis applied to the random phase TMS trials are transferable to the μ -phase-triggered trials, as they have been acquired in the same experimental conditions.

The PPI was calculated for each EEG channel and subject at the individual μ -oscillation frequency, defined as the peak of the power spectrum in the 8–12 Hz frequency band derived from the current scalp density signal of the C3 electrode in the non-stimulated trials. A Morlet

wavelet transformation was applied to the EEG signal of the stimulated trials without prior subtraction of the ‘evoked’ component (see *TMS-induced EEG oscillations* for technical details of the Morlet wavelet) to extract the phase for the individual μ -frequency used for calculation of the PPI. The reference time t_{ref} for PPI calculation was set at 200 ms before TMS. This time point is close enough to the stimulation onset to avoid spurious results due to the natural decay of the PPI over time, and sufficiently distant from the stimulation to avoid any bias in the phase estimation related to interpolation of data around the TMS pulse. PPI was calculated every 100 ms from the reference time to 800 ms after the TMS pulse.

Regarding the match of μ -oscillation amplitude between non-stimulated and stimulated trials, we know that oscillatory power (which is an indirect measure of the amplitude of brain oscillations) is modulated by TMS (Fuggetta *et al.* 2005; Rosanova *et al.* 2009; Fecchio *et al.* 2017) and that TEPs obtained after M1 stimulation have a strong component in the 8–12 Hz frequency range (Rosanova *et al.* 2009; Fecchio *et al.* 2017). As the μ -oscillations and the TMS-evoked potentials are both time-locked to the TMS pulse, it is not possible to isolate one from another in the post-TMS period. Therefore, to the best of our knowledge, it is not possible to control for this confounder.

Statistics

TMS-evoked EEG potentials. For the real TMS blocks, six non-overlapping time windows of interest (TOIs) were *a priori* defined based on the group average TEPs across subjects and conditions. TOIs were centred around the latencies of the typical M1 TEP peaks P25, N45, P70, N100, P180 and N280 (Paus *et al.* 2001; Komssi *et al.* 2004; Bonato *et al.* 2006; Van Der Werf & Paus, 2006; Farzan *et al.* 2013; Veniero *et al.* 2013; Premoli *et al.* 2014aa; Petrichella *et al.* 2017). Specifically, the boundaries of the TOIs were set at 18–39, 40–53, 55–72, 89–129, 151–241 and 260–325 ms after the TMS pulse. For the sham TMS block, three TOIs were identified, with boundaries of 40–57 ms (P50), 89–129 ms (N100), 151–241 ms (P180) and 260–325 ms (N280). For each experimental block, significant differences between evoked responses were evaluated for each individual TOI using channel-wise paired-sample two-tailed t tests. To control for the family-wise error rate (FWER), we used a cluster-based permutation approach (Maris & Oostenveld, 2007) as implemented in Fieldtrip. This approach tests the null hypothesis that the data in the experimental conditions are drawn from the same probability distribution and clusters the t values resulting from the paired-sample t tests that exceed an *a priori* defined threshold of $P < 0.05$ based on neighbouring channels and time points.

Two was the minimum number of channels below the significance threshold to form a cluster. The t statistics at the cluster level is then computed summing the t values within each cluster and comparing the maximum of the obtained t values. A reference distribution of the maximum of the cluster t values is obtained by re-applying the same procedure on the data randomized across the two experimental conditions. We used 1500 randomizations to obtain the reference distribution and rejected the null hypothesis with $P < 0.05$ if less than 5% of the permutations used to construct the reference distribution yielded a maximum cluster-level t value larger than that observed in the original data.

Additionally, we investigated the effect of μ -phase on the P25–N45 complex. The P25–N45 complex was defined by first computing for each subject the voltage distribution on the scalp in the TOI for the P25 and N45 TEP components, respectively. This was done separately for the negative and positive μ -peak condition. The channel-wise difference between the P25 and N45 voltage distributions on the scalp was then calculated, resulting in the amplitude of the P25–N45 complex at each EEG channel, for each subject and each μ -phase condition. The above described cluster-based statistical analysis was applied to compare the amplitude of the P25–N45 complex in the negative vs. positive μ -phase condition. In this case, the average across time points was not performed, as the average in the time windows of interest was performed in the first step for computation of the amplitude of the P25–N45 complex. This analysis was done separately for the 110% RMT and the 90% RMT blocks. For the sham TMS condition no P25 and N45 are defined (see definition of TOIs above). Therefore, this analysis could not be performed for the sham TMS block.

For the TEP components that resulted in a significant difference between the negative and positive peak conditions, we computed Cohen's d and the minimum detectable change (MDC) assuming 0.80 power ($1 - \beta$). Given the high dimensionality of our data, we defined the amplitude of the TEPs of interest as the average amplitude across channels for all the identified clusters with $P < 0.05$.

Cohen's d was computed with the formula for paired samples:

$$d = \frac{(\text{mean}_{x1} - \text{mean}_{x2})}{\sqrt{\frac{(\text{std}_{x1}^2 + \text{std}_{x2}^2)}{2}}}$$

where $x1$ and $x2$ are the vectors of TEP amplitudes for the negative and positive peak conditions, respectively.

MDC was computed as follows:

$$\text{MDC} = (z_{1-\beta} + z_{\alpha/2}) * \sqrt{\frac{2 * \text{var}_{x1x2}}{n}}$$

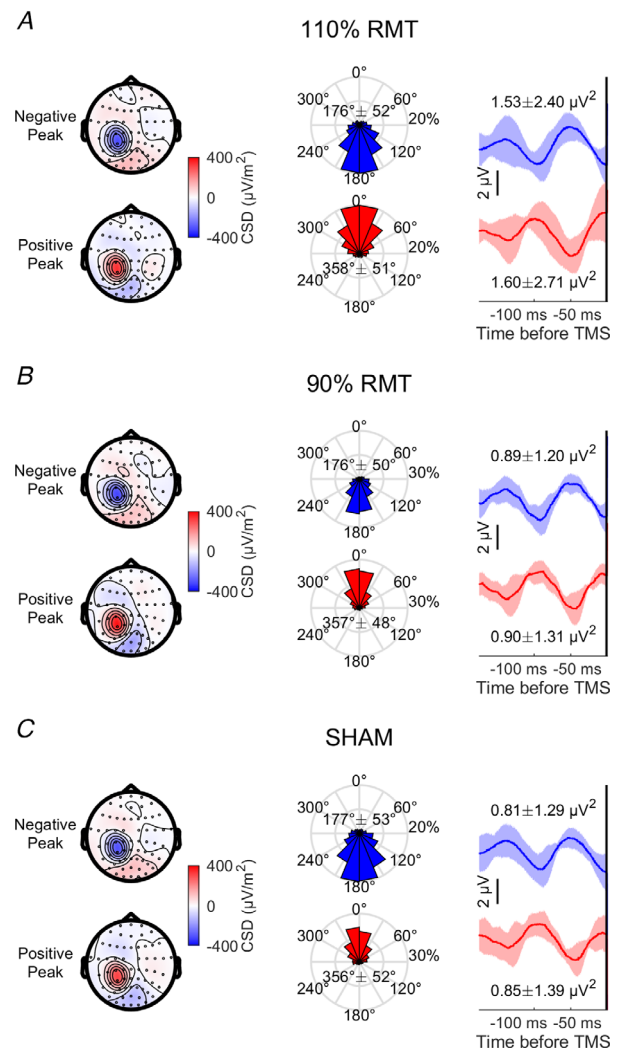


Figure 1. Accuracy of μ -phase targeting

A, 110% RMT TMS. Left: group mean current scalp density (CSD) plots for the negative (top) and positive (bottom) peak conditions for the time points ± 20 ms around the trigger for non-stimulated trials; amplitudes (in $\mu\text{V}/\text{m}^2$) are indicated by the colour bar. The clear negative and positive distributions in the channels located over the left motor cortex indicate spatial specificity of the spatial filter used to isolate the μ -oscillation. Middle: distribution of estimated phase angles at the time of the trigger in triggered non-stimulated trials for the negative (blue) and positive (red) peak conditions. Phase angles are binned (width, 22.5°) and frequencies are indicated in percentage for the outer ring. Angular means ± 1 SD are indicated in the phase distribution plots. *Post hoc* phase estimation in the non-stimulated trials was performed filtering the spatially filtered μ -oscillation in the individual μ -band (individual μ -oscillation frequency ± 2 Hz) and taking the phase at the time of the trigger of the analytical signal obtained with Hilbert transform. Right: grand averages across all trials and subjects of raw sensorimotor μ -oscillations for the negative (blue) and positive (red) peak conditions preceding the TMS pulse at 0 ms. Shadings represent ± 1 SD. Group means (\pm SD) of the pre-stimulus μ -power for the negative and peak conditions are reported above (negative) and below (positive) the relative μ -oscillation traces. A paired t test performed on μ -power log-transformed data resulted in $P > 0.05$. B and C, the same as A but for the 90% RMT and realistic sham TMS. [Colour figure can be viewed at wileyonlinelibrary.com]

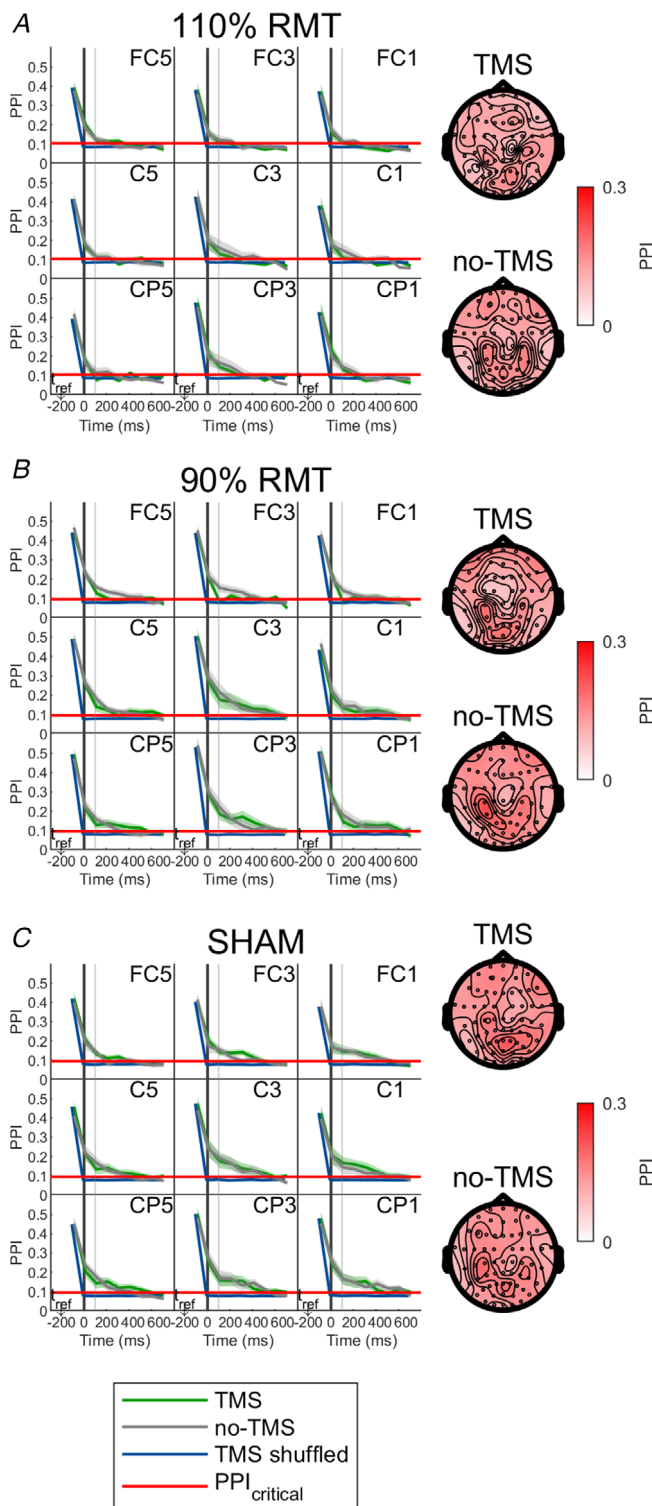


Figure 2. Measure of phase reset of the ongoing μ -oscillation
A, left: PPI of the μ -oscillation in the random phase block for 110% RMT TMS on nine EEG channels located over the left sensorimotor cortex (green traces). The PPI across time is averaged over 12 subjects for the individual μ -frequency. Shades indicate ± 1 SEM. The reference time is set at -200 ms. PPI values below the red line are considered statistically significant ($P < 0.01$). The dark blue traces indicate the PPI for trials shuffled in time (temporally uncorrelated).

where $z_{1-\beta} = 0.84$ for a power of 0.80 and $z_{\alpha/2} = 1.96$ for $\alpha = 0.05$, n is the sample size (12) and $\text{var}_{x_1x_2}$ is the pooled variance of the negative and positive peak conditions calculated as:

$$\text{var}_{x_1x_2} = \frac{(\text{std}_{x_1}^2 + \text{std}_{x_2}^2)}{2}$$

TMS-induced EEG oscillations. The alpha (8–12 Hz) and beta (13–30 Hz) frequency bands were considered for statistical comparisons, as they constitute the dominant oscillations in the sensorimotor cortex (Neuper *et al.* 2005). Based on the group average TFRs across conditions and channels, we *a priori* defined two TOIs enclosing the two most prominent TMS-related power modulations over time, namely an early increase followed by a late decrease in the oscillatory power of the alpha and beta frequency bands (Fecchio *et al.* 2017; Premoli *et al.* 2017). The boundaries were 50–200 ms (80–200 ms for the sham TMS block) and 200–600 ms for the early and late TOI, respectively. For each experimental block, significant differences between TMS-induced oscillations were evaluated for the alpha and beta frequency bands in each individual TOI using channel-wise paired-sample two-tailed *t* tests and the cluster-based permutation approach (Maris & Oostenveld, 2007) described above.

MEPs. For the 110% RMT block, the effect of μ -phase on MEP amplitude was tested using a Kruskal–Wallis test, as the data were non-normally distributed.

Perception of real vs. sham TMS stimulation. A chi-squared test of independence was performed comparing the conditions applied in each block with the relative conditions perceived by the participants.

PPI. The statistical significance of the PPI can be assessed with Rayleigh’s test for circular uniformity (Fisher, 1993; Zar, 1999). First, the PPI of each subject is *z*-transformed according to the formula $Z = n\text{PPI}^2$, where n is the number of trials used to compute the PPI. For $n > 60$ (Fisher, 1993)

The PPI decays slowly, showing that the post-stimulus phases are preserved with respect to the pre-stimulus phase, up to 100 ms after TMS. The grey traces indicate the PPI for non-stimulated trials. The PPI values between the stimulated and TMS-free trials were not significantly different across time (100–700 ms, all $P > 0.7$). Right: the topographies of the PPI at 100 ms (indicated by the light grey shaded vertical lines in the time plots) for the stimulated (TMS) and non-stimulated (no-TMS) trials. In all cases, PPI values stayed above the critical PPI value up to 100 ms after stimulation. The PPI values between the stimulated and non-stimulated trials were not significantly different across time (100–700 ms, all $P > 0.1$ for 90% RMT, and all $P > 0.3$ for SHAM). [Colour figure can be viewed at wileyonlinelibrary.com]

the critical PPI value given a significance threshold can be computed as:

$$PPI_{critical} = \sqrt{\frac{-\ln(p) \times \sqrt{S}}{N}}$$

where p is a given P value, S is the number of subjects and N is the total number of trials across subjects. Under the null hypothesis that the phase differences across trials are randomly distributed, i.e. there is no relationship between pre- and post-stimulus phases, a post-stimulus PPI smaller than $PPI_{critical}$ can be interpreted as indicating the occurrence of phase reset of the μ -oscillation. With

12 subjects and a P value of 0.01, $PPI_{critical}$ was 0.105 for the 110% RMT block, 0.096 for the 90% RMT block and 0.095 for the sham TMS block. Moreover, we estimated the PPI trend for data with no relationship between pre- and post-stimulus phase, i.e. phase reset, shuffling the post-stimulus data in time 100 times (Mazaheri & Jensen, 2006). Finally, we compared the PPI in the random phase block to that in non-stimulated trials. To this end, we used the non-stimulated random phase-triggered trials. Significant differences between post-TMS PPI and the corresponding resting-state PPI were assessed using channel-wise paired-sample two-tailed t tests and the cluster-based permutation approach (Maris & Oostenveld,

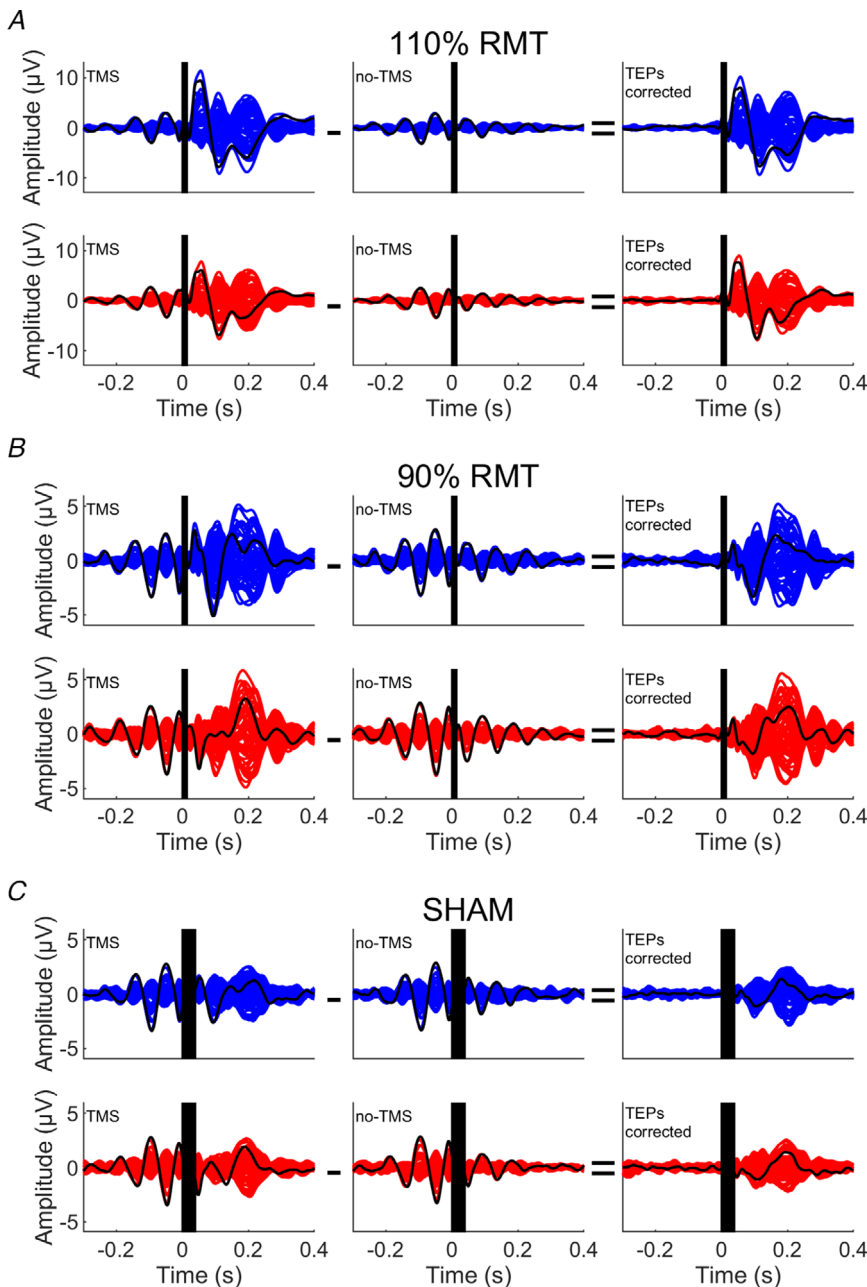


Figure 3. Subtraction procedure for correction of TEPs

A, group average of single-channel EEG signals (blue, negative peak triggered; red, positive peak triggered) time-locked to the trigger (time = 0 s) for the 110% RMT TMS. C3, the EEG channel closer to the stimulation site, is highlighted in black. Left panels: stimulated (TMS) conditions, middle panels: non-stimulated (no-TMS) conditions, right panels: subtraction of the no-TMS from the TMS conditions (TEPs corrected). The subtraction was performed at the single subject level. Time windows highlighted in black indicate signal affected by TMS-related artifacts that were removed and interpolated. Data are shown as an average. B and C, the same procedure for the 90% RMT and realistic sham TMS. Physiological shifts in μ -oscillation frequency across different trials and individuals are responsible for the declining oscillation amplitudes in the post-trigger time period. [Colour figure can be viewed at wileyonlinelibrary.com]

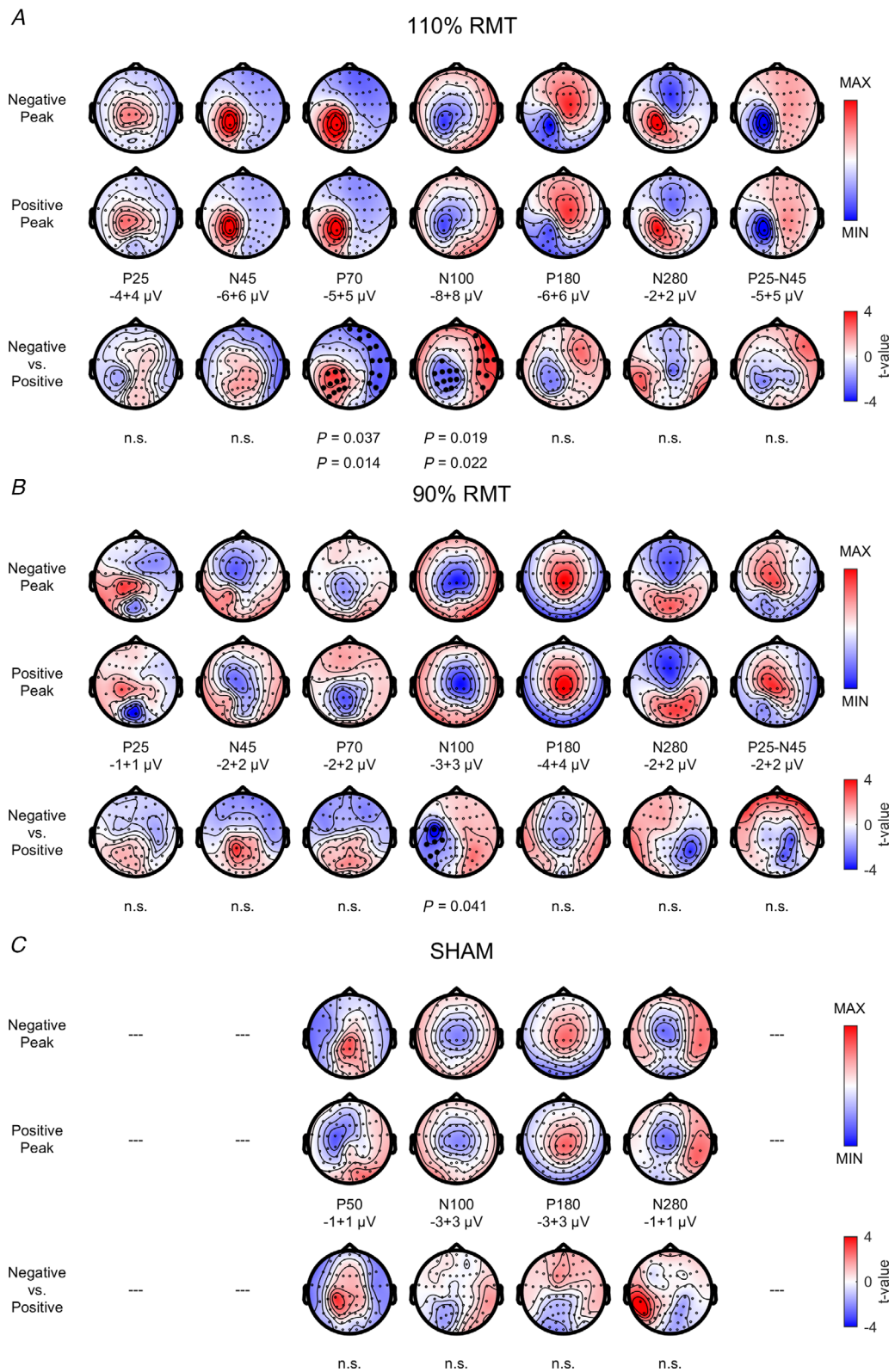


Figure 4. Topographical plots of average TEPs and results of TEPs statistics
 A, the first two rows show the topographical distributions of evoked EEG responses resulting from the average across all subjects and all trials of the negative and positive peak conditions for the 110% RMT TMS. TEP peaks are named according to their approximate latency after TMS application and the topographical plots are obtained by averaging the EEG signal in the relative *a priori* defined time windows (P25: 18–39 ms, N45: 40–53 ms, P70:

Table 1. Cohen's *d* and minimum detectable change for TEP modulated by pre-stimulus μ -phase

	Negative peak, mean \pm 1 SD (μ V)	Positive peak, mean \pm 1 SD (μ V)	Cohen's <i>d</i> (observed)	MDC (μ V)
110% RMT, N100 positive cluster	2.92° \pm 2.14	2.14° \pm 2.17	0.37	2.46
110% RMT, N100 negative cluster	-4.43° \pm 3.16	-3.83° \pm 3.05	-0.19	3.55
110% RMT, P70 positive cluster	5.42° \pm 5.60	4.06° \pm 4.55	0.27	5.83
110% RMT, P70 negative cluster	-2.55° \pm 3.16	-1.73° \pm 2.52	-0.29	3.27
90% RMT, N100 negative cluster	-0.04° \pm 0.82	0.60° \pm 0.73	-0.82	0.89

For the P70 and N100 for the 110% RMT dataset and N100 for the 90% RMT dataset, Cohen's *d* and the minimum detectable change (MDC) assuming 0.80 power ($1 - \beta$) and given the study sample size ($n = 12$) and the *a priori* defined statistical threshold ($\alpha = 0.05$). The first and second columns report the group average ($\pm 1SD$) of the EEG signal over the time window of interest and the EEG channels belonging to the identified cluster with $P < 0.05$.

2007) described above. In this case, the minimum number of channels below the significance threshold to form a cluster was set to 1. The MATLAB code used for PPI calculation and statistics can be downloaded from the following link: <https://github.com/bnplab/desideri> 2019.

Results

Negative and positive peak of the μ -rhythm were successfully targeted (110% RMT: 176° \pm 52° and 358° \pm 51°, 90% RMT: 176° \pm 5° and 357° \pm 48°, SHAM: 177° \pm 53° and 356° \pm 52°). Paired *t* tests between positive and negative peak trials performed on log-transformed pre-stimulus μ -power data resulted in $P > 0.05$ for all the experimental conditions (Fig. 1).

The mean (± 1 SD) intertrial interval (ITI, time between one trigger and the next) was 2.54° \pm 0.22, 2.55° \pm 0.21 and 2.63° \pm 0.29 s for the 110% RMT, 90% RMT and SHAM block respectively. The Kruskal–Wallis test between the ITI showed no significant effect of block ($\chi^2_2 = 0.46$, $P = 0.79$). The mean (± 1 SD) interstimulus interval (ISI, time between one trigger resulting in a stimulus and the next) was 5.08° \pm 0.42, 5.10° \pm 0.43 and 5.23° \pm 0.60 s for the 110% RMT, 90% RMT and SHAM block, respectively. The Kruskal–Wallis test between the ISI showed no significant effect of block ($\chi^2_2 = 0.52$, $P = 0.77$). The reported ISI corresponds to a mean (± 1 SD) frequency of stimulation of 0.20° \pm 0.02, 0.20° \pm 0.01 and 0.19° \pm 0.02 Hz.

Perception of real vs. sham TMS stimulation

The chi-squared test of independence resulted in a significant interaction between real condition and condition perceived by the participants ($\chi^2_4 = 40$, $P < 0.0001$), suggesting that subjects were able to distinguish between the conditions applied. This was because all subjects could correctly identify the 110% RMT condition associated with muscle twitches. In the 90% RMT and SHAM conditions, 8/12 participants (66.6%) reported a perceived condition corresponding to the real condition. When only 90% RMT and SHAM were analysed, no statistical relationship between the real and perceived conditions was observed, as the null hypothesis could not be rejected ($\chi^2_2 = 2.66$, $P = 0.10$). This suggests that participants could not reliably distinguish realistic sham TMS from subthreshold real TMS.

Phase preservation index (PPI)

Figure 2 shows the group average of the PPI trend over time (green curves) for nine representative channels located over the left-hemispheric sensorimotor area and the topographies of PPI at 100 ms after TMS for the 110% RMT, 90% RMT and sham TMS blocks. For all blocks, at this time point, the PPI remained above the critical threshold. In addition, it decays slower than the PPI for the data shuffled in time (dark blue curves), crossing the PPI_{critical} threshold (red line) only after 200 ms on 17/64

55–72 ms, N100: 89–129 ms, P180: 151–241 ms, N280: 260–325 ms). The rightmost topographical distribution represents the amplitude of the P25–N45 complex. The maximum and minimum voltages are reported (μ V) below the relative topographies. The lowest row shows the topographical *t* statistics maps resulting from the cluster-based statistical comparison between the negative and positive peak conditions. Significant clusters (electrodes) are highlighted by black dots and *P* values are reported below each plot. When two *P* values are reported, the top one is related to the positive cluster (*t* values > 0 , red) and the bottom one is related to the negative cluster (*t* values < 0 , blue). If no significant cluster was identified, 'n.s.' (not significant) is reported below the relative topographical *t* statistics map. *B* and *C*, same as *A* but for the 90% RMT and realistic sham TMS, respectively. Time windows for the topographical distributions in *B* are the same as in *A*, whereas in *C* they are: P50: 40–57 ms, N100: 89–129 ms, P180: 151–241 ms, N280: 260–325 ms. No P25–N45 complex is defined for the sham TMS condition. [Colour figure can be viewed at wileyonlinelibrary.com]

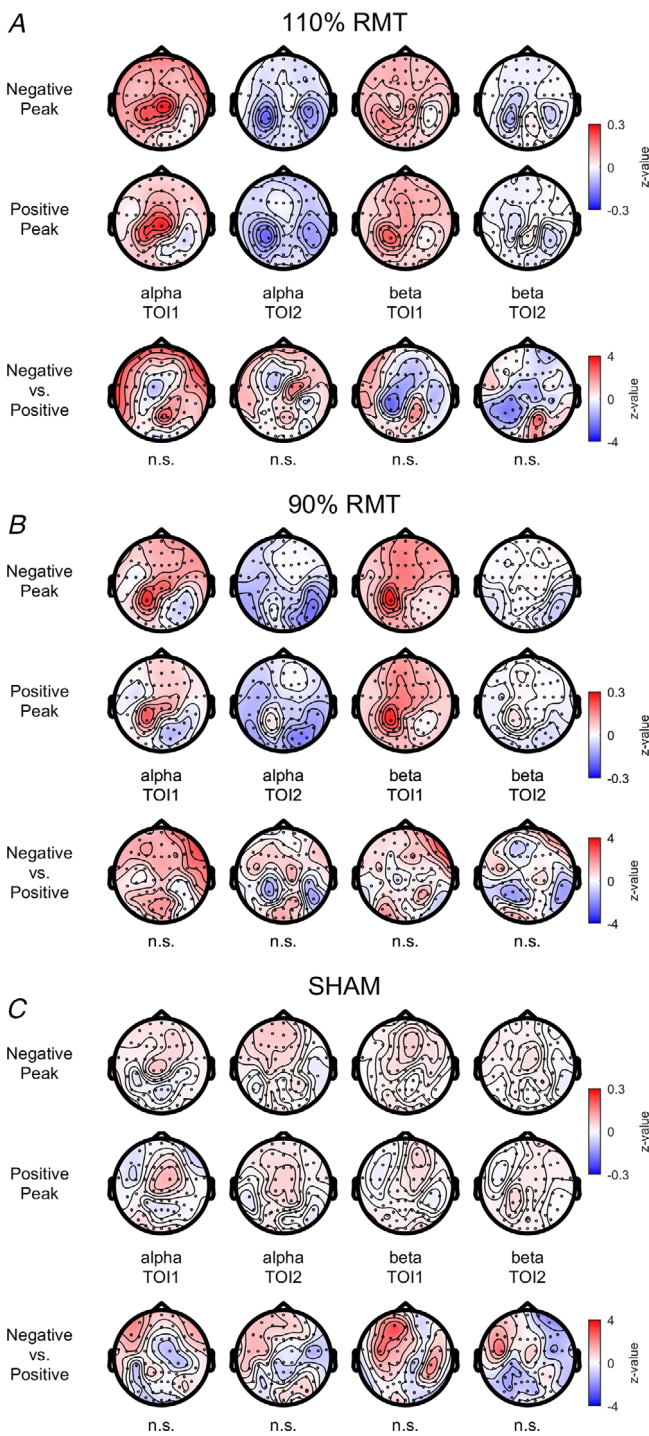


Figure 5. Topographical plots of average TMS-induced EEG oscillations

The upper and middle rows show the topographical plots of the average power for the induced TMS-EEG oscillatory activity in the negative and positive peak conditions for the 110% RMT, 90% RMT and realistic sham TMS for the four *a priori* defined time–frequency regions: alpha (8–12 Hz), beta (13–30 Hz), TOI1 (50–200 ms for 110% RMT and 90% RMT TMS and 80–200 ms for realistic sham TMS) and TOI2 (200–600 ms). For the real TMS conditions, the activation patterns are substantially similar across different stimulation intensities, with (absolute) response amplitude generally

in the 110% RMT block (Fp1, Fpz, Fp2, AF8, F6, F8, FT9, FC4, T7, C2, TP9, TP7, CP5, P7, P5, P3, P8), 7/64 in the 90% RMT block (FC3, FC1, FC2, Cz, T7, TP9, TP7) and 1/64 in the sham TMS block (TP7). This indicates that occurrence of phase reset in the TMS trials can be excluded up to 200 ms, a latency beyond most TEP peaks. Furthermore, most of these channels are not located over the left motor cortex and often did not belong to the significant clusters identified in the TEPs statistics (see below). Importantly, the results of permutation statistics comparing the PPI in TMS trials and the PPI obtained in TMS-free trials (grey curve) did not reach the significance threshold in any channel or time point after stimulation (all $P > 0.7$ for 110% RMT, all $P > 0.1$ for 90% RMT and all $P > 0.3$ for sham TMS). This suggests strongly that the phase of the μ -oscillation is preserved after TMS.

MEPs

In the 110% RMT block, the Kruskal–Wallis test showed a significant effect of trigger condition [$\chi^2_2 = 12.46$, $P = 0.002$; mean MEP amplitude (± 1 SD) $0.59^\circ \pm 0.41$, $0.51^\circ \pm 0.36$ and $0.48^\circ \pm 0.39$ mV for negative peak, random phase and positive peak, respectively] with MEPs in the negative peak condition significantly larger than MEPs in the positive peak ($P = 0.002$) and random phase conditions ($P = 0.023$).

TMS-evoked EEG potentials

As the PPI results (see above) did not support a phase reset of the ongoing μ -oscillations by the TMS pulse, for each subject time-locked μ -oscillations superimposed on the TEPs were removed by a channel-wise subtraction of the average of the non-stimulated trials from the average of the stimulated trials (Fig. 3). The topographies of the real TMS conditions (Fig. 4A, B) were comparable to the typical M1 TEP topographies reported in the literature (Bonato *et al.* 2006; Farzan *et al.* 2013; Rogasch *et al.* 2014; Premoli *et al.* 2014a; Petrichella *et al.* 2017). Comparison of individual TEP peaks in the negative vs. positive peak conditions revealed a significant difference in the P70 (positive cluster $P = 0.037$ and negative cluster $P = 0.014$) and N100 (positive cluster $P = 0.019$ and negative cluster $P = 0.022$) components for the 110% RMT TMS (Fig. 4A) and in the N100 ($P = 0.041$) for the 90% RMT TMS (Fig. 4B), with significant clusters located where these TEPs are usually expressed and modulated (Fig. 4A, B, lowest rows, Premoli *et al.* 2014a,b; Darmani *et al.* 2016).

decreasing with decreasing stimulation intensity. The cluster-based statistical comparison between the negative and positive peak conditions did not result in any significant difference (lowest row in each panel, 'n.s.' = not significant). [Colour figure can be viewed at wileyonlinelibrary.com]

In all cases, TEP components were larger in (absolute) amplitude in the negative peak condition. No comparison reached the threshold of significance for realistic sham TMS (all $P > 0.19$, Fig. 4C). Furthermore, the negative vs. positive peak of the μ -rhythm had no effect on the P25, N45, P180 or N280 components (Fig. 4A, B), and the amplitude of the P25–N45 complex was also not affected by the negative vs. positive μ -phase (Fig. 4A, B).

For the TEP components that resulted in a significant difference between the negative and positive peak conditions (P70 and N100 in the 110% RMT TMS condition, and N100 in the 90% RMT TMS condition), Cohen's d and MDC are reported in Table 1.

TMS-induced EEG oscillations

Our results replicated the typical early power increase followed by a late power decrease in the alpha and beta frequency bands (Fecchio *et al.* 2017; Premoli *et al.* 2017). For the real TMS conditions, the activation patterns of TMS-induced oscillations in the *a priori* defined TOI

for the alpha and beta bands were substantially similar across different stimulation intensities (Fig. 5A, B), with (absolute) response amplitude generally decreasing with decreasing stimulation intensity, in agreement with previous literature (Fuggetta *et al.* 2005). Sham TMS showed no or little power changes with respect to baseline (Fig. 5C), again reproducing previously reported results (Fuggetta *et al.* 2005).

Comparison between negative and positive peak conditions for the two frequency bands and the two TOIs of interest did not reach the significance threshold (all $P > 0.06$) for 110% RMT, 90% RMT and sham TMS (Fig. 5, lowest row).

Discussion

In this TMS-EEG study, we have analysed cortical responses elicited by μ -phase-triggered single-pulse TMS. Different TMS stimulation intensities, i.e. 110% RMT, 90% RMT and a realistic sham TMS, have been used to disentangle modulation of TMS direct responses

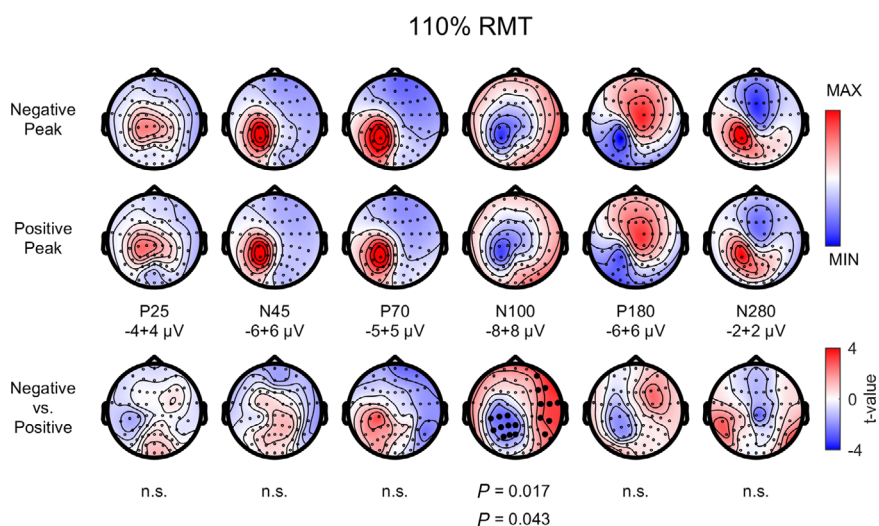


Figure 6. Topographical plots of average TEPs and results of TEP statistics after compensation for the difference in MEPs

The first two rows show the topographical distributions of evoked EEG responses resulting from the average across all subjects and all trials of the negative and positive peak conditions for the 110% RMT TMS after compensation for the difference in MEP amplitude. TEP peaks are named according to their approximate latency after TMS application and the topographical plots are obtained averaging the EEG signal in the relative *a priori* defined time windows (P25: 18–39 ms, N45: 40–53 ms, P70: 55–72 ms, N100: 89–129 ms, P180: 151–241 ms, N280: 260–325 ms). The maximum and minimum voltages are reported (μV) below the relative topographies. The lowest row shows the topographical t statistics maps resulting from the cluster-based statistical comparison between the negative and positive peak conditions. Significant clusters (electrodes) are highlighted by black dots and P values are reported below each plot. When two P values are reported, the top one is related to the positive cluster (t values > 0 , red) and the bottom one is related to the negative cluster (t values < 0 , blue). If no significant cluster was identified, 'n.s.' (not significant) is reported below the relative topographical t statistics map. To compensate for the difference in MEP amplitude between the positive vs. negative peak conditions, for each subject, we created empirical histograms of MEP amplitudes for the μ -rhythm positive and negative peak conditions using the same bin edges. In principle, in each bin there is a different number of trials per condition. When one condition has more trials in one of the bins, epochs are randomly selected to match the number of epochs of the other condition. This process leads to an 'equalization' of the empirical histograms, ensuring the same average MEP amplitude, range of MEP amplitude and same number of trials across μ -rhythm positive and negative peak conditions. [Colour figure can be viewed at wileyonlinelibrary.com]

from modulation of re-afferent signals caused by muscle twitch associated with suprathreshold TMS, and of somatosensory and auditory inputs caused by scalp stimulation and TMS pulse click. In a previous study (Zrenner *et al.* 2018), we had shown that the phase of the endogenous sensorimotor μ -oscillation modulates corticospinal excitability, as measured by MEP amplitude on a hand muscle in response to single-pulse TMS: corticospinal excitability is enhanced at the negative *vs.* positive peak of the μ -oscillation. Here, we expected to observe a similar modulation at the cortical level, reflected by the amplitude of the TMS-evoked EEG potentials and by the power of the TMS-induced EEG oscillations, as previous studies have demonstrated that these responses are modulated by functional and experimental changes in cortical excitability (Massimini *et al.* 2005; Esser *et al.* 2006; Morishima *et al.* 2009; Ferrarelli *et al.* 2010; Premoli *et al.* 2014a, 2017; Darmani *et al.* 2016).

According to our expectations, negative peak-triggered TMS produced larger TEP peak amplitudes in the modulated TEP components. The effect sizes ranged from small to large in different conditions (Table 1). How can we interpret the dependence of TEP amplitude on the phase of the μ -rhythm? Nil findings in the realistic sham TMS excluded that these results were caused by a μ -phase-specific modulation of the somatosensory and auditory inputs. Moreover, a phase-specific modulation of the re-afferent input occurring approximately 40–60 ms after the TMS pulse and reaching the cortex at different phases of the non-reset μ -oscillation cannot explain all the observed findings. 110% RMT TMS led to modulation of the P70 and N100 TEP components. Both these components may be possibly affected by the re-afferent input, but 90% RMT TMS, which is subthreshold for generation of MEPs, still resulted in larger N100 if triggered at the negative peak of the μ -rhythm. Previous studies have reported that P70 may represent a component of the evoked potentials associated with the re-afferent feedback (Paus *et al.* 2001; Rogasch *et al.* 2013). This would also explain the different pattern (i.e. a wide central parietal negativity) of this potential in our subthreshold dataset (90% RMT), where MEPs were not elicited, with respect to those in suprathreshold dataset (110% RMT) and the absence of this potential in the sham TMS condition (Fig. 4). In this context, a larger P70 in the negative *vs.* positive peak-triggered condition may be caused either by μ -phase-dependent modulation of brain responses to the TMS pulse, by μ -phase-dependent modulation of the re-afferent input or by a larger re-afferent potential associated with larger MEPs. Comparison of TEPs in the negative *vs.* positive peak conditions after compensation of the difference in MEP amplitude for the 110% RMT TMS did not result in a μ -phase-specific modulation of P70 (Fig. 6), suggesting that this result may at least partially reflect a contribution

of the re-afferent input. By contrast, N100 probably reflects modulation of direct cortical activations. The N100–P180 complex has been associated with auditory inputs caused by the click of the TMS coil (Nikouline *et al.* 1999). The phase-dependent modulation of the N100 across different TMS intensities but not sham TMS suggests strongly that this TEP reflects predominantly activation of cortex directly by the TMS pulse rather than by auditory input, an idea also supported by other studies (Komssi *et al.* 2004; Bonato *et al.* 2006; Ferreri *et al.* 2011; Gordon *et al.* 2018). GABABergic inhibitory mechanisms seem to underlie the generation of N100 (Nikulin *et al.* 2003; Bender *et al.* 2005; Kičić *et al.* 2008; Bonnard *et al.* 2009; Rogasch & Fitzgerald, 2013; Premoli *et al.* 2014a). TMS applied at the negative peak of the μ -oscillation may lead to recruitment of a larger proportion of inhibitory neurons, which would then result in an enhancement of N100 amplitude.

Despite a growing body of literature investigating TMS-associated cortical responses, the origin of the TEPs is not yet fully understood and it is still not clear how the ongoing brain oscillations may contribute to the generation of these potentials. Our results on TEPs confirm at the cortical level that the negative peak of the μ -oscillation represents a state in which the dendritic trees of pyramidal neurons are closer to firing threshold and, therefore, are more likely to generate action potentials in response to a TMS pulse (Buzsáki *et al.* 2012; Zrenner *et al.* 2018), further stressing the important role of oscillatory phase in the coordination of the response of cortical neurons to synaptic inputs (Buzsáki & Draguhn, 2004; Hari, 2006; Jensen & Mazaheri, 2010; Haegens *et al.* 2011).

While TMS applied at the negative *vs.* positive peak of the ongoing μ -oscillation produced larger TEPs, TMS-induced EEG oscillations were not significantly modulated by the phase of the ongoing μ -oscillation. A TMS-induced early power increase and late power decrease observed after TMS of M1 may be controlled by several inhibitory mechanisms, as they are enhanced by GABA_A and GABA_B receptor agonists (Premoli *et al.* 2017). It has been suggested that induced oscillatory activity captures processes that evolve over hundreds of milliseconds and result from intrinsic network interactions within the brain (Donner & Siegel, 2011). Therefore, the effect of a local excitability state (μ -phase) may only be observed in transient responses phase-locked to stimulus onset (TEPs), while modulation of non-phase-locked induced activity may be observed only when network balances are altered (Premoli *et al.* 2017).

A limitation of the study is that realistic sham TMS was designed to match the 90% RMT condition only. While this led to a successful blinding, as both conditions lack muscle twitches, we cannot completely exclude that the more intense somatosensory and auditory inputs associated with the 110% RMT condition played a role

in some of the obtained results. Another limitation is the pre-selection of participants according to the expressed μ -power. This limitation could be overcome with the use of more sophisticated and individualized spatial filters that will isolate a sufficiently strong μ -oscillation in a larger proportion of participants than the spatial filter used in the present study. At present it remains unclear to what extent the results of this study are generalizable to the population as a whole. The amplitude of both the P25 TEP peak and the P25–N45 complex were not affected by the ongoing μ -phase, although the amplitude of the early EEG response to TMS has been shown to be associated with MEP size (Mäki & Ilmoniemi, 2010). The loss of EEG signal for up to 15 ms after the TMS pulse therefore represents a limitation of our study. We cannot exclude that significant changes in TMS-evoked or induced EEG responses have occurred in this very early time window, especially because excitation of pyramidal neurons projecting to the spinal cord and responsible for the MEP generation occurs in the very first milliseconds after the TMS pulse (Li *et al.* 2017). This limitation could be possibly overcome in future studies using faster sampling rates and more focal coils that minimize the activation of scalp muscles and produce smaller TMS-related artifacts.

To conclude, we have shown here that instantaneous cortical excitability of the motor cortex fluctuates with the phase of the ongoing μ -oscillation. Our findings corroborate that TEPs are a sensitive measure of the excitability state of the cortex and, therefore, are a valuable tool to quantify the responsiveness of brain areas outside the motor cortex with no other objective readout.

References

- Başar E & Dumermuth G (1982). EEG-brain dynamics: relation between EEG and brain evoked potentials. *Comp Program Biomed* **14**, 227–228.
- Bender S, Basseler K, Sebastian I, Resch F, Kammer T, Oelkers-Ax R & Weisbrod M (2005). Electroencephalographic response to transcranial magnetic stimulation in children: evidence for giant inhibitory potentials. *Ann Neurol* **58**, 58–67.
- Bergmann TO, Molle M, Schmidt MA, Lindner C, Marshall L, Born J & Siebner HR (2012). EEG-guided transcranial magnetic stimulation reveals rapid shifts in motor cortical excitability during the human sleep slow oscillation. *J Neurosci* **32**, 243–253.
- Bonato C, Miniussi C & Rossini PM (2006). Transcranial magnetic stimulation and cortical evoked potentials: a TMS/EEG co-registration study. *Clin Neurophysiol* **117**, 1699–1707.
- Bonnard M, Spieser L, Meziane HB, de Graaf JB & Pailhoux J (2009). Prior intention can locally tune inhibitory processes in the primary motor cortex: direct evidence from combined TMS–EEG. *Eur J Neurosci* **30**, 913–923.
- Busch NA & VanRullen R (2010). Spontaneous EEG oscillations reveal periodic sampling of visual attention. *Proc Natl Acad Sci U S A* **107**, 16048–16053.
- Buzsáki G (2006). *Rhythms of the Brain*. Oxford University Press, Oxford.
- Buzsáki G, Anastassiou CA & Koch C (2012). The origin of extracellular fields and currents – EEG, ECoG, LFP and spikes. *Nat Rev Neurosci* **13**, 407–420.
- Buzsáki G & Draguhn A (2004). Neuronal oscillations in cortical networks. *Science* **304**, 1926–1929.
- Casarotto S, Romero Lauro LJ, Bellina V, Casali AG, Rosanova M, Pigorini A, Defendi S, Mariotti M & Massimini M (2010). EEG responses to TMS are sensitive to changes in the perturbation parameters and repeatable over time. *PLoS One* **5**, e10281.
- Darmani G, Zipser CM, Böhmer GM, Deschet K, Müller-Dahlhaus F, Belardinelli P, Schwab M & Ziemann U (2016). Effects of the selective $\alpha 5$ -GABAAR antagonist S44819 on excitability in the human brain: a TMS-EMG and TMS-EEG phase i study. *J Neurosci* **36**, 12312–12320.
- Donner TH & Siegel M (2011). A framework for local cortical oscillation patterns. *Trends Cogn Sci* **15**, 191–199.
- Esser SK, Huber R, Massimini M, Peterson MJ, Ferrarelli F & Tononi G (2006). A direct demonstration of cortical LTP in humans: a combined TMS/EEG study. *Brain Res Bull* **69**, 86–94.
- Farzan F, Barr MS, Hoppenbrouwers SS, Fitzgerald PB, Chen R, Pascual-Leone A & Daskalakis ZJ (2013). The EEG correlates of the TMS-induced EMG silent period in humans. *Neuroimage* **83**, 120–134.
- Fecchio M, Pigorini A, Comanducci A, Sarasso S, Casarotto S, Premoli I, Derchi CC, Mazza A, Russo S, Resta F, Ferrarelli F, Mariotti M, Ziemann U, Massimini M & Rosanova M (2017). The spectral features of EEG responses to transcranial magnetic stimulation of the primary motor cortex depend on the amplitude of the motor evoked potentials. *PLoS One* **12**, e0184910.
- Ferrarelli F, Massimini M, Sarasso S, Casali A, Riedner BA, Angelini G, Tononi G & Pearce RA (2010). Breakdown in cortical effective connectivity during midazolam-induced loss of consciousness. *Proc Natl Acad Sci U S A* **107**, 2681–2686.
- Ferreri F, Pasqualetti P, Maatta S, Ponzo D, Ferrarelli F, Tononi G, Mervaala E, Miniussi C & Rossini PM (2011). Human brain connectivity during single and paired pulse transcranial magnetic stimulation. *Neuroimage* **54**, 90–102.
- Fisher NI (1993). *Statistical Analysis of Circular Data*. Cambridge University Press, Cambridge.
- Fuggetta G, Fiaschi A & Manganotti P (2005). Modulation of cortical oscillatory activities induced by varying single-pulse transcranial magnetic stimulation intensity over the left primary motor area: a combined EEG and TMS study. *Neuroimage* **27**, 896–908.
- Gordon PC, Desideri D, Belardinelli P, Zrenner C & Ziemann U (2018). Comparison of cortical EEG responses to realistic sham versus real TMS of human motor cortex. *Brain Stimul* **11**, 1322–1330.
- Grandchamp R & Delorme A (2011). Single-trial normalization for event-related spectral decomposition reduces sensitivity to noisy trials. *Front Psychol* **2**, 236.

- Haegens S, Nacher V, Luna R, Romo R & Jensen O (2011). α -Oscillations in the monkey sensorimotor network influence discrimination performance by rhythmical inhibition of neuronal spiking. *Proc Natl Acad Sci U S A* **108**, 19377–19382.
- Hallett M (2007). Transcranial magnetic stimulation: a primer. *Neuron* **55**, 187–199.
- Hari R (2006). Action–perception connection and the cortical mu rhythm. *Prog Brain Res* **159**, 253–260.
- Hjorth B (1975). An on-line transformation of EEG scalp potentials into orthogonal source derivations. *Electroencephalogr Clin Neurophysiol* **39**, 526–530.
- Hyvärinen A (1999). Fast and robust fixed-point algorithms for independent component analysis. *IEEE Trans Neural Netw* **10**, 626–634.
- Hyvärinen A, Karhunen J & Oja E (2001). *Independent Component Analysis*. Wiley, Chichester.
- Ilmoniemi RJ & Kicic D (2010). Methodology for combined TMS and EEG. *Brain Topogr* **22**, 233–248.
- Ilmoniemi RJ, Virtanen J, Ruohonen J, Karhu J, Aronen HJ, Naatanen R & Katila T (1997). Neuronal responses to magnetic stimulation reveal cortical reactivity and connectivity. *Neuroreport* **8**, 3537–3540.
- Jensen O & Mazaheri A (2010). Shaping functional architecture by oscillatory alpha activity: gating by inhibition. *Front Hum Neurosci* **4**, 186.
- Kičić D, Lioumis P, Ilmoniemi RJ & Nikulin VV (2008). Bilateral changes in excitability of sensorimotor cortices during unilateral movement: combined electroencephalographic and transcranial magnetic stimulation study. *Neuroscience* **152**, 1119–1129.
- Komssi S, Kahkonen S & Ilmoniemi RJ (2004). The effect of stimulus intensity on brain responses evoked by transcranial magnetic stimulation. *Hum Brain Mapp* **21**, 154–164.
- Kruglikov SY & Schiff SJ (2003). Interplay of electroencephalogram phase and auditory-evoked neural activity. *J Neurosci* **23**, 10122–10127.
- Kundu B, Johnson JS & Postle BR (2014). Prestimulation phase predicts the TMS-evoked response. *J Neurophysiol* **112**, 1885–1893.
- Li B, Virtanen JP, Oeltermann A, Schwarz C, Giese MA, Ziemann U & Benali A (2017). Lifting the veil on the dynamics of neuronal activities evoked by transcranial magnetic stimulation. *Elife* **6**, e30552.
- Luck SJ (2005). *An Introduction to the Event-Related Potential Technique*. MIT Press, Cambridge.
- Mäki H & Ilmoniemi RJ (2010). The relationship between peripheral and early cortical activation induced by transcranial magnetic stimulation. *Neurosci Lett* **478**, 24–28.
- Maris E & Oostenveld R (2007). Nonparametric statistical testing of EEG- and MEG-data. *J Neurosci Methods* **164**, 177–190.
- Massimini M, Ferrarelli F, Huber R, Esser SK, Singh H & Tononi G (2005). Breakdown of cortical effective connectivity during sleep. *Science* **309**, 2228–2232.
- Mazaheri A & Jensen O (2006). Posterior alpha activity is not phase-reset by visual stimuli. *Proc Natl Acad Sci U S A* **103**, 2948–2952.
- Morishima Y, Akaishi R, Yamada Y, Okuda J, Toma K & Sakai K (2009). Task-specific signal transmission from prefrontal cortex in visual selective attention. *Nat Neurosci* **12**, 85–91.
- Neuper C, Grabner RH, Fink A & Neubauer AC (2005). Long-term stability and consistency of EEG event-related (de-)synchronization across different cognitive tasks. *Clin Neurophysiol* **116**, 1681–1694.
- Nikouline V, Ruohonen J & Ilmoniemi RJ (1999). The role of the coil click in TMS assessed with simultaneous EEG. *Clin Neurophysiol* **110**, 1325–1328.
- Nikulin VV, Kičić D, Kahkonen S & Ilmoniemi RJ (2003). Modulation of electroencephalographic responses to transcranial magnetic stimulation: evidence for changes in cortical excitability related to movement. *Eur J Neurosci* **18**, 1206–1212.
- Nunez PL & Srinivasan R (2006). *Electric Fields of the Brain: The Neurophysics of EEG*. Oxford University Press, Oxford.
- Oostenveld R, Fries P, Maris E & Schoffelen JM (2011). FieldTrip: Open source software for advanced analysis of MEG, EEG, and invasive electrophysiological data. *Comput Intell Neurosci* **2011**, 156869.
- Paus T, Sipila PK & Strafella AP (2001). Synchronization of neuronal activity in the human primary motor cortex by transcranial magnetic stimulation: an EEG study. *J Neurophysiol* **86**, 1983–1990.
- Perrin F, Pernier J, Bertrand O & Echallier JF (1989). Spherical splines for scalp potential and current density mapping. *Electroencephalogr Clin Neurophysiol* **72**, 184–187.
- Petrichella S, Johnson N & He B (2017). The influence of corticospinal activity on TMS-evoked activity and connectivity in healthy subjects: a TMS-EEG study. *PLoS One* **12**, e0174879.
- Premoli I, Bergmann TO, Fecchio M, Rosanova M, Biondi A, Belardinelli P & Ziemann U (2017). The impact of GABAergic drugs on TMS-induced brain oscillations in human motor cortex. *Neuroimage* **163**, 1–12.
- Premoli I, Castellanos N, Rivolta D, Belardinelli P, Bajo R, Zipser C, Espenhahn S, Heidegger T, Müller-Dahlhaus F & Ziemann U (2014a). TMS-EEG signatures of GABAergic neurotransmission in the human cortex. *J Neurosci* **34**, 5603–5612.
- Premoli I, Rivolta D, Espenhahn S, Castellanos N, Belardinelli P, Ziemann U & Müller-Dahlhaus F (2014b). Characterization of GABAB-receptor mediated neurotransmission in the human cortex by paired-pulse TMS-EEG. *Neuroimage* **103**, 152–162.
- Ritter P & Becker R (2009). Detecting alpha rhythm phase reset by phase sorting: caveats to consider. *Neuroimage* **47**, 1–4.
- Rogasch NC, Daskalakis ZJ & Fitzgerald PB (2013). Mechanisms underlying long-interval cortical inhibition in the human motor cortex: a TMS-EEG study. *J Neurophysiol* **109**, 89–98.
- Rogasch NC & Fitzgerald PB (2013). Assessing cortical network properties using TMS-EEG. *Hum Brain Mapp* **34**, 1652–1669.
- Rogasch NC, Sullivan C, Thomson RH, Rose NS, Bailey NW, Fitzgerald PB, Farzan F & Hernandez-Pavon JC (2017). Analysing concurrent transcranial magnetic stimulation and electroencephalographic data: a review and introduction to the open-source TESA software. *Neuroimage* **147**, 934–951.

- Rogasch NC, Thomson RH, Farzan F, Fitzgibbon BM, Bailey NW, Hernandez-Pavon JC, Daskalakis ZJ & Fitzgerald PB (2014). Removing artefacts from TMS-EEG recordings using independent component analysis: importance for assessing prefrontal and motor cortex network properties. *Neuroimage* **101**, 425–439.
- Rosanov M, Casali A, Bellina V, Resta F, Mariotti M & Massimini M (2009). Natural frequencies of human corticothalamic circuits. *J Neurosci* **29**, 7679–7685.
- Rossi S, Hallett M, Rossini PM, Pascual-Leone A; Safety of the TMS Consensus Group (2009). Safety, ethical considerations, and application guidelines for the use of transcranial magnetic stimulation in clinical practice and research. *Clin Neurophysiol* **120**, 2008–2039.
- Rossini PM, Burke D, Chen R, Cohen LG, Daskalakis Z, Di Iorio R, Di Lazzaro V, Ferreri F, Fitzgerald PB, George MS, Hallett M, Lefaucheur JP, Langguth B, Matsumoto H, Miniussi C, Nitsche MA, Pascual-Leone A, Paulus W, Rossi S, Rothwell JC, Siebner HR, Ugawa Y, Walsh V & Ziemann U (2015). Non-invasive electrical and magnetic stimulation of the brain, spinal cord, roots and peripheral nerves: basic principles and procedures for routine clinical and research application. An updated report from an I.F.C.N. Committee. *Clin Neurophysiol* **126**, 1071–1107.
- Seeck M, Koessler L, Bast T, Leijten F, Michel C, Baumgartner C, He B & Beniczky S (2017). The standardized EEG electrode array of the IFCN. *Clin Neurophysiol* **128**, 2070–2077.
- Tallon-Baudry C & Bertrand O (1999). Oscillatory gamma activity in humans and its role in object representation. *Trends Cogn Sci* **3**, 151–162.
- Van Der Werf YD & Paus T (2006). The neural response to transcranial magnetic stimulation of the human motor cortex. I. Intracortical and cortico-cortical contributions. *Exp Brain Res* **175**, 231–245.
- Veniero D, Ponzo V & Koch G (2013). Paired associative stimulation enforces the communication between interconnected areas. *J Neurosci* **33**, 13773–13783.
- Zar JH (1999). *Biostatistical Analysis*. Prentice Hall, Upper Saddle River.
- Zrenner C, Desideri D, Belardinelli P & Ziemann U (2018). Real-time EEG-defined excitability states determine efficacy of TMS-induced plasticity in human motor cortex. *Brain Stimul* **11**, 374–389.

Additional information

Conflict of interest

The authors declare no competing financial interest.

Author contributions

This work was carried out at the University of Tübingen. All authors jointly conceived and designed the study. D.D. performed the data collection and analysis, created the figures and drafted the manuscript. P.B., C.Z. and U.Z. revised and approved the final version of the manuscript. All persons designated as authors qualify for authorship, and all those who qualify for authorship are listed.

Funding

This work was supported by DFG grant ZI 542/7-1 to U.Z., Industry-on-Campus Grant IoC 211 to P.B. and D.D., and University of Tübingen Fortune Junior Grant 2287-0-0 to C.Z.

Acknowledgements

We thank Dr Til Ole Bergmann for his comments on the experimental design and the discussions on the data analysis. We also thank Pedro Caldana Gordon for his comments on the figures and on a first version of the manuscript.

Keywords

brain oscillations, cortical excitability, EEG-TMS, motor cortex, TMS-evoked EEG potentials

2.3 Nil effects of μ -rhythm phase- dependent burst-rTMS on cortical excitability in humans: a resting-state EEG and TMS-EEG study

RESEARCH ARTICLE

Nil effects of μ -rhythm phase-dependent burst-rTMS on cortical excitability in humans: A resting-state EEG and TMS-EEG study

Debora Desideri¹, Christoph Zrenner¹, Pedro Caldana Gordon^{1,2}, Ulf Ziemann^{1*}, Paolo Belardinelli¹

1 Department of Neurology & Stroke, and Hertie Institute for Clinical Brain Research, University of Tübingen, Tübingen, Germany, **2** Service of Interdisciplinary Neuromodulation, Laboratory of Neuroscience (LIM27) and National Institute of Biomarkers in Psychiatry (INBioN), Department and Institute of Psychiatry, Hospital das Clínicas HCFMUSP, Faculdade de Medicina, Universidade de São Paulo, São Paulo, Brazil

* ulf.ziemann@uni-tuebingen.de



OPEN ACCESS

Citation: Desideri D, Zrenner C, Gordon PC, Ziemann U, Belardinelli P (2018) Nil effects of μ -rhythm phase-dependent burst-rTMS on cortical excitability in humans: A resting-state EEG and TMS-EEG study. PLoS ONE 13(12): e0208747. <https://doi.org/10.1371/journal.pone.0208747>

Editor: Alessio Avenanti, University of Bologna, ITALY

Received: July 21, 2018

Accepted: November 21, 2018

Published: December 7, 2018

Copyright: © 2018 Desideri et al. This is an open access article distributed under the terms of the [Creative Commons Attribution License](https://creativecommons.org/licenses/by/4.0/), which permits unrestricted use, distribution, and reproduction in any medium, provided the original author and source are credited.

Data Availability Statement: All relevant data are within the paper and its Supporting Information files.

Funding: This study was supported by DFG grant ZI 542/7-1 (to U.Z.), Industry-on-Campus Grant IoC 211 (to P.B., and D.D.), and University of Tübingen Fortüne Junior Grant 2287-0-0 (to C.Z.). The funders had no role in study design, data collection and analysis, decision to publish, or preparation of the manuscript.

Abstract

Repetitive transcranial magnetic stimulation (rTMS) can induce excitability changes of a stimulated brain area through synaptic plasticity mechanisms. High-frequency (100 Hz) triplets of rTMS synchronized to the negative but not the positive peak of the ongoing sensorimotor μ -rhythm isolated with the concurrently acquired electroencephalography (EEG) resulted in a reproducible long-term potentiation like increase of motor evoked potential (MEP) amplitude, an index of corticospinal excitability (Zrenner et al. 2018, *Brain Stimul* 11:374–389). Here, we analyzed the EEG and TMS-EEG data from (Zrenner et al., 2018) to investigate the effects of μ -rhythm-phase-dependent burst-rTMS on EEG-based measures of cortical excitability. We used resting-state EEG to assess μ - and β -power in the motor cortex ipsi- and contralateral to the stimulation, and single-pulse TMS-evoked and induced EEG responses in the stimulated motor cortex. We found that μ -rhythm-phase-dependent burst-rTMS did not significantly change any of these EEG measures, despite the presence of a significant differential and reproducible effect on MEP amplitude. We conclude that EEG measures of cortical excitability do not reflect corticospinal excitability as measured by MEP amplitude. Most likely this is explained by the fact that rTMS induces complex changes at the molecular and synaptic level towards both excitation and inhibition that cannot be differentiated at the macroscopic level by EEG.

Introduction

Repetitive transcranial magnetic stimulation (rTMS) can be used to non-invasively modify excitability and connectivity of stimulated cortical areas [1]. In the motor cortex (M1), excitability changes can be assessed by comparing the responses to single-pulse TMS in a contralateral hand muscle (motor evoked potentials, MEPs) before and after rTMS. However, MEPs represent an indirect measure of cortical and corticospinal excitability. It is believed that rTMS-induced changes in MEP amplitude most likely originate at the level of the motor cortex

Competing interests: The authors have declared that no competing interests exist.

(for review see [2]), therefore rTMS would be expected to produce lasting changes in cortical excitability and connectivity. Electroencephalography (EEG) is used to measure electrical activity of the brain [3] and in combination with TMS (TMS-EEG) provides access to a more direct measure of cortical excitability and connectivity. Cortical responses to TMS are expressed in the EEG in a series of evoked potentials (TEPs) [4–6] as well as in a modulation of spontaneous oscillatory activity [7–10]. Previous studies showed that rTMS induced LTP-/LTD-like plastic changes can be successfully measured with TMS-EEG at a macroscopic scale. For example, Esser and colleagues [11] reported an increase both in MEP size and in the global mean field power (a compressed representation of the total TMS-evoked response) in the area of premotor cortex after 5 Hz rTMS of the left M1. Also, in [12], 1 Hz rTMS decreased MEPs and produced a significant increase in the TEP components peaking at around 60 ms and 100 ms after TMS. High-frequency rTMS of the left M1 has also been found to affect oscillatory activity in the α and β bands, both at the stimulation site and in interconnected cortical areas [13, 14]. In a previous study of our group [15], we have shown that the negative vs. positive peak of the ongoing sensorimotor oscillation in the 8–12 Hz frequency band (μ -oscillation) represents a state of higher excitability of the motor system, where the dendritic trees of pyramidal neurons receive mainly excitatory inputs and are closer to firing threshold. Results of *in vitro* studies [16–19] showed that the direction of synaptic plasticity critically depends on the coupling between stimulus and the state of neuronal population receiving it. On this basis, we have investigated the after-effects of high-frequency (100 Hz) triplets of rTMS delivered to M1, synchronized to the instantaneous phase of the ongoing sensorimotor oscillation in the 8–12 Hz frequency band (μ -oscillation) and demonstrated that when rTMS is applied at the negative peak of the μ -oscillation MEP size increases for more than 30 minutes after the intervention, compatible with long-term potentiation (LTP)-like plasticity, while no significant changes in MEP size are observed when rTMS is applied at the positive peak of the μ -oscillation [15]. In this study, we sought to investigate whether μ -rhythm phase-dependent rTMS produces similar changes in cortical excitability that are expressed in the spontaneous oscillatory activity of M1 ipsi- and contralateral to the stimulation in the resting-state EEG, and/or in the TEPs and in the oscillations induced by TMS over the stimulated M1. Oscillatory activity, both spontaneous and induced by TMS, has been analyzed in the μ - and β -bands, as these are the typical and dominant oscillations in the sensorimotor system [20].

Materials and methods

The EEG data used in this study have been collected in [15].

Subjects

The study protocol was approved by the local ethics committee of the medical faculty of the University of Tübingen (protocol 716/2014BO2). Experiments were conducted in accordance with the declaration of Helsinki and the current TMS safety guidelines [21]. Two groups of volunteers free of medications and without history of neurological or psychiatric disorders took part in the study, after giving written informed consent. Twelve right-handed male participants (age range 20–48 years, mean age \pm s.d. 26.5 \pm 7.5 years, Edinburgh Handedness inventory laterality score 62 \pm 21) were tested in the first series of experiments, while eleven right-handed participants (9 females, age range 21–32 years, mean age \pm s.d. 25.4 \pm 3.7 years, Edinburgh Handedness inventory laterality score 91 \pm 13) were tested in the second series of experiments (see below *Experimental design* and Fig 1). All included subjects exhibited a spectral power in the μ -band (8–12 Hz) > 25% of the power in the 1–80 Hz power spectrum of the current scalp density (CSD) signal of the C3 EEG electrode. This ensured a sufficient signal-to-noise ratio

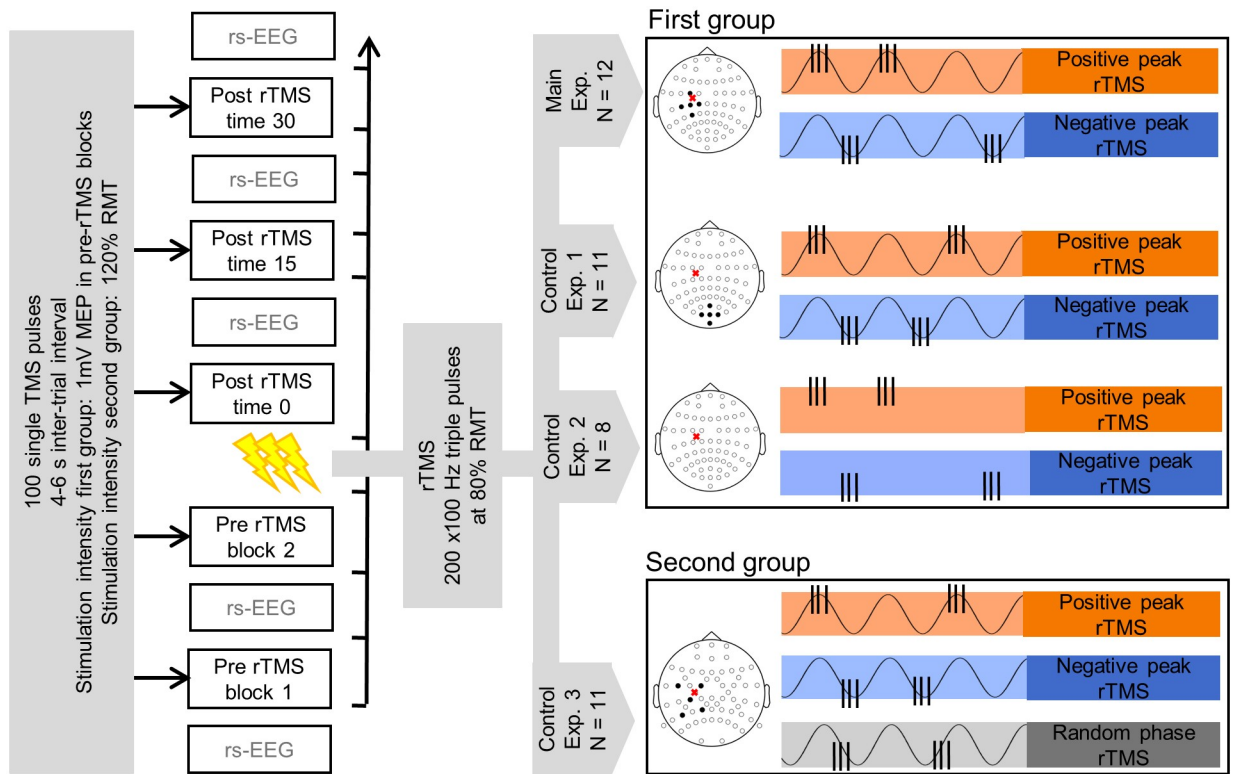


Fig 1. Experimental design and sessions. Left side: blocks of 100 single TMS pulses were used to test effects of different rTMS interventions on cortical and corticospinal measurements. Two pre-rTMS test blocks were acquired 15 minutes apart and three test blocks were acquired at 0, 15 and 30 minutes after rTMS. Resting state EEG periods of ca. 4–5 minutes preceded the test blocks before rTMS and followed them after rTMS. The rTMS intervention consisted of 200 bursts of triple pulses TMS with an inter-pulse interval of 10 ms (100 Hz triplets) delivered at 80% RMT. The mean triplet repetition rate \pm 1 s.d. was 1.01 ± 0.12 Hz and 1.04 ± 0.08 Hz for the first and second group of participants, respectively. Right side: sessions differed from one another in the brain state used to trigger the rTMS triplets. TMS was applied to the left motor cortex, as indicated by the red cross in the schematic picture of the participants' head. Circles represent the positions of the EEG electrodes, filled black circles highlight the EEG electrodes used to isolate the brain signal of interest to trigger rTMS. In the first group of participants, rTMS was triggered by the phase (positive or negative peak) of the left sensorimotor μ -rhythm (Main Experiment, 12 subjects), by the phase (positive or negative peak) of the endogenous occipital α -oscillation (Control Experiment 1, 11 subjects) or by the identical rTMS sequence of the Main Experiment (Control Experiment 2, 8 subjects). In the second group of participants, rTMS was triggered by the phase (positive peak, negative peak or random) of the left sensorimotor μ -rhythm (Control Experiment 3, 11 subjects). The order of the sessions was pseudo-randomized for the first group of participants (with Control Experiment 2 sessions always following Main Experiment sessions) and fully randomized for the second group of participants. For a given participant, consecutive sessions were performed at least 3 days apart.

<https://doi.org/10.1371/journal.pone.0208747.g001>

for a reliable real-time estimation of the instantaneous phase of the sensorimotor μ -oscillation [15]. Moreover, resting motor threshold (RMT) of the right abductor pollicis brevis (APB) or the first dorsal interosseous (FDI) muscle had to be $\leq 60\%$ and $\leq 67.5\%$ of maximum stimulator output for the first and second group, respectively. This guaranteed that for each participant 80% RMT did not exceed the maximum intensity at which the stimulators used in the two series of experiments (see below *Experimental set-up & procedure*) could generate 100 Hz rTMS pulses (48% and 54%, respectively). When RMT was comparable for APB and FDI, APB was used as target muscle, otherwise the muscle with lower RMT was chosen to increase the chance of a subject being included in the study. APB was the target muscle for 3/12 subjects in the first group and for 6/11 subjects in the second group. For each subject, the target muscle was kept consistent across different experimental sessions.

Experimental set-up & procedure

Participants were seated in an armchair with their hands relaxed and looking at a fixation cross while TMS pulses were delivered to the left M1. In the first series of experiments the set-up consisted of an air cooled TMS coil (Magstim 70 mm Double Air Film Coil, Magstim, Ltd, UK) connected to a high-frequency magnetic stimulator (Magstim Super Rapid Plus, Magstim Ltd, UK) delivering biphasic single cosine cycle pulses with 400 μ s period. In the second series of experiments a passively cooled TMS double coil (PMD70-pCool, 70 mm winding diameter, MAG & More, Germany) connected to a high frequency magnetic stimulator (research 100, MAG & More, Germany) delivering biphasic single cosine cycle pulses with 160 μ s period was used instead. Motor evoked potentials (MEPs) were recorded from the right APB and FDI muscles in a bipolar belly-tendon montage through electromyography (EMG, 5 kHz sampling rate, 0.16 Hz -1.25 kHz bandpass filter) adhesive hydrogel electrodes (Kendall, Covidien). RMT was defined according to the standard relative frequency method [22] as the minimum stimulation intensity that produced MEPs $> 50 \mu$ V in the target muscle in 5/10 consecutive trials. The motor "hotspot" was defined as the coil position and orientation eliciting maximum MEP amplitudes, using a slightly suprathreshold stimulation intensity [22]. The stimulating coil was oriented orthogonally to the central sulcus, so that the second phase of the biphasic pulse induced a lateral-posterior to medial-anterior electric field in the brain. Coil position was kept constant relative to the participant's head using a stereoscopic neuronavigation system (Localite GmbH, Sankt Augustin, Germany). The EEG signal was recorded from 64 channels inserted in a TMS compatible Ag/AgCl sintered ring electrode cap (EasyCap GmbH, Germany). In the first series of experiments, the EEG channels were arranged according to the International 10–20 system and FCz and AFz were used as reference and ground electrode, respectively. In the second series of experiments, a customized layout based on the International 10–20 system, but with higher electrode density over sensorimotor cortex was used and FCz and PPO1h were taken as reference and ground electrode, respectively. The impedance at the interface skin-EEG electrodes was $< 5 \text{ k}\Omega$ throughout. A 24-bit 80-channel biosignal amplifier was used for EEG and EMG recordings (NeurOne Tesla with Analog Real-time Out Option, Bittium Biosignals Ltd., Finland). Data were acquired at 5 kHz sampling rate in AC mode for the first series of experiments (band pass filter 0.16 Hz—1.25 kHz) and in DC mode for the second series of experiments (1.25 kHz low-pass anti-aliasing filter) with a head-stage sample rate of 80 kHz. A real-time system implemented as a Simulink Real-Time model (Mathworks Ltd, USA, R2015a), executed on a dedicated xPC Target PC running the Simulink Real-Time operating system (DFI-ACP CL630-CRM mainboard) was used for a real-time analysis of the EEG signal and for triggering rTMS bursts according to the instantaneous phase of oscillatory EEG activity (for details [15]). White noise at individually adjusted loudness was applied through ear phones to mask the TMS click and minimize TMS-evoked auditory potentials [23, 24].

Experimental design

The experimental design is schematically represented in Fig 1. Each experimental session consisted of 2 pre-rTMS and 3 post-rTMS blocks of 100 suprathreshold single-pulse TMS trials and of 2 pre-rTMS and 3 post-rTMS periods of approximately 4–5 minutes resting-state EEG (rsEEG) recording with eyes open. The 2 pre-rTMS blocks started 15 minutes apart, as well as the 3 post-rTMS blocks, while the last pre- and first post-rTMS blocks were separated only by the duration of the rTMS intervention. The rsEEG recordings preceded the single-pulse TMS blocks in the pre-rTMS and followed them in the post-rTMS measurements. The rTMS

intervention consisted of 200 bursts of 100 Hz TMS bursts delivered at 80% RMT. In each session, triplets were triggered by a different pre-defined brain state.

In the first series of experiments the following brain states were used to trigger the rTMS triplets: positive peak or negative peak of the local μ -rhythm (Main Experiment), positive peak or negative peak of distal occipital α -rhythm (Control Experiment 1), replay of positive peak or negative peak μ -rhythm rTMS sequence from Main Experiment independent of ongoing μ -rhythm (Control Experiment 2). Local μ -rhythm originating in the left sensorimotor cortex was isolated at sensor level with a spatial filter [25] centered on the electrode C3 and using the four adjacent electrodes FC3, C1, CP3, C5. A similar filter centered on the electrode Oz and using the neighbor electrodes POz, O1, O2, Iz was used to isolate the occipital α -rhythm. The Main Experiment investigated the effects of sensorimotor μ -phase on corticospinal plasticity. Control Experiment 1 served to demonstrate that the phase-dependent effects on corticospinal plasticity observed in the Main Experiment were produced only when a locally generated oscillation is used to trigger the rTMS triplets. Control Experiment 2 was used to show that the results in the Main Experiment depended on the synchronization between stimulus and brain state and were not caused by the temporal properties of the rTMS sequence.

In the second series of experiment the following brain states were used to trigger the rTMS triplets: positive peak, negative peak or random phase of the local μ -rhythm (Control Experiment 3). Local μ -rhythm was isolated with a slightly different spatial filter centered on the electrode C3 and using the neighbor electrodes FC1, FC5, CP1, CP5. This different spatial filter was used to be able to record oscillatory activity also from an off-center EEG source of the μ -rhythm. Control Experiment 3 was designed to validate, generalize and extend the results of the Main Experiment.

In the brain state-triggered sessions a power threshold was used to ensure that triplets were triggered by physiological signal instead of filtered noise. The power threshold was set manually and chosen to ensure an average inter-burst interval of approximately 1 s [15]. The mean triplet repetition rate \pm 1 s.d. was 1.01 ± 0.12 Hz and 1.04 ± 0.08 Hz for the first and second group of participants, respectively. For a given participant, consecutive sessions were performed at least 3 days apart and the order of the sessions was pseudo-randomized for the first group (with Control Experiment 2 sessions always following Main Experiment sessions) and fully randomized for the second group of participants.

Data analysis

Data processing and analysis were performed using customized analysis scripts on MATLAB R2018a and the Fieldtrip open source MATLAB toolbox [26].

Resting-state EEG. The rsEEG periods were segmented in epochs of 2 s, down-sampled to 500 Hz and filtered with a 1–80 Hz bandpass filter (zero-phase Butterworth, 3rd order) and a 49–51 Hz notch filter (zero-phase Butterworth, 3rd order). Epochs containing major artifacts as well as noisy EEG channels were removed upon visual inspection (percentage of removed epochs: $9.7 \pm 5.9\%$, number of removed channels: 2 ± 2 , mean \pm s.d.). Then, independent component analysis (ICA) based on FastICA algorithm [27, 28] was applied to the data. ICA components representing biological (eye blinks and movements, persistent muscle activity) or electrical artifacts were removed based on their topography, single-trial time-course and power spectrum (mean \pm s.d. 22 ± 6). Discarded channels were spline-interpolated using the signal of the neighbor channels [29]. CSD signals [29] of the EEG channels C3 and C4, chosen as representative of the left and right sensorimotor cortices, respectively, were computed and their power spectra were estimated based on the fast Fourier transform (FFT) algorithm. For each subject and channel, individual μ - and β -bands were defined as 2 Hz wide bands centered

at the maximum peak in the 5–15 Hz and 15–30 Hz ranges of the average power spectrum, respectively. Finally, for each subject, rsEEG period and session, C3 and C4 μ - and β -powers were defined as the power in the individual C3 and C4 μ - and β -bands and used for statistical analysis (see below, *Statistics*).

TMS-EEG evoked potentials. The single-pulse TMS trials were segmented in epochs from 0.5 s before the TMS marker to 1 s after the TMS marker. Data from 1 ms before to 15 ms after the marker, where high amplitude TMS artifacts occur, were removed and cubic interpolated. Epochs were then centered and visually inspected (percentage of removed epochs: $4.0 \pm 3.4\%$, number of removed channels: 3 ± 2 , mean \pm s.d.). Then, the same ICA used for the rsEEG data was applied to the TMS-EEG data. Data underwent ICA twice, in a two-step procedure as proposed in [30]. In the first step, only components representing high-amplitude TMS-related artifacts were removed (mean \pm s.d. 7 ± 4). Then, data were filtered with a 1–80 Hz bandpass filter (zero-phase Butterworth, 3rd order) and a 49–51 Hz notch filter (zero-phase Butterworth, 3rd order), down-sampled to 1000 Hz and ICA was again applied to the data. Components representing biological (eye blinks and movements, persistent muscle activity), electrical or smaller amplitude TMS-related artifacts were removed (mean \pm s.d. 22 ± 6). Then, channels discarded during the visual inspection of the data were spline-interpolated [29] and data were re-referenced to the average reference signal. Epochs were lowpass filtered (45 Hz, zero-phase Butterworth, 3rd order) and averaged per block. Five non-overlapping time windows of interest (TOIs) were *a priori* defined based on the group average TEPs across subjects, blocks and sessions. The pre-selected TOIs were approximately centered around the latencies of the typical motor cortex TEP peaks P25, N45, P70, N100 and P180 [4, 6, 31]. Specifically, beginning and end of the TOIs were set at 22–39 ms, 40–53 ms, 53–70 ms, 77–131 ms, 151–240 ms after the TMS pulse, respectively, for the first group of subjects, and at 22–39 ms, 40–56 ms, 56–79 ms, 80–134 ms, 145–231 ms for the second group of subjects. Moreover, for each TOI, eight channels of interest were defined as the channels with maximum voltage for P25, P70 and P180 and the channels with minimum voltage for N45 and N100 (first group: P25 – Cz, FC1, C1, C2, FC2, CP2, CPz, CP1, N45 – F2, FC2, F4, AF4, C2, FC4, Fp2, F6, P70 – CP3, C5, C3, P5, P1, CP5, P3, CP1, N100 – C1, C3, CP3, FC1, CP1, FC3, Cz, C5, P180 – Fz, F2, FC2, F4, FC4, AF4, C4, FC6; second group: P25 – Cz, C1, CCP1h, CCP2h, C2, FCC3h, FC1, FC2, N45 – FFC6h, FT8, C6, F6, FC4, FC6, AF4, F8, P70 – CP3, CCP5h, P5, P1, P3, CP5, C3, CP1, N100 – C1, FCC3h, C3, Cz, FC1, CCP1h, CP1, CP3, P180 – FC2, FFC2h, FCC4h, C2, FFC1h, Cz, Fz, F2). Selected TOIs and channels for each TOI can be seen in Fig 2. Information about TMS-evoked cortical activation was then compressed computing the local mean field power (LMFP, [12, 32–34]) over the selected channels in the corresponding TOI. For each TOI, subject, test block and session the area under the obtained LMFP was used for statistical analysis (see below, *Statistics*).

TMS-EEG induced oscillations. A time-frequency representations (TFRs) of the TMS-EEG data can uncover responses to TMS that are not time-locked to the onset of the pulse and are expressed as changes in spontaneous oscillatory activity [7–10, 35]. We have focused on the CSD signal of the C3 channel and have isolated the non-time-locked, i.e. induced, activity, in the time-domain by subtracting the average evoked response from each single trial [10, 35, 36]. Subsequently, we have calculated the TFRs convolving single trials with complex Morlet wavelets [37] in the frequency range from 6 to 45 Hz in steps of 1 Hz and shifting the center of the wavelet in steps of 10 ms in the time window -500 ms to 1000 ms relative to TMS application. The length of the wavelets linearly increased from 2 cycles at 6 Hz to 9 cycles at 45 Hz [35, 38]. TFRs of power were obtained taking the squared absolute values of the complex time series resulting from the wavelet transformation. These were then trial-wise z-transformed based on the mean and standard deviation of the full-length trial as described in

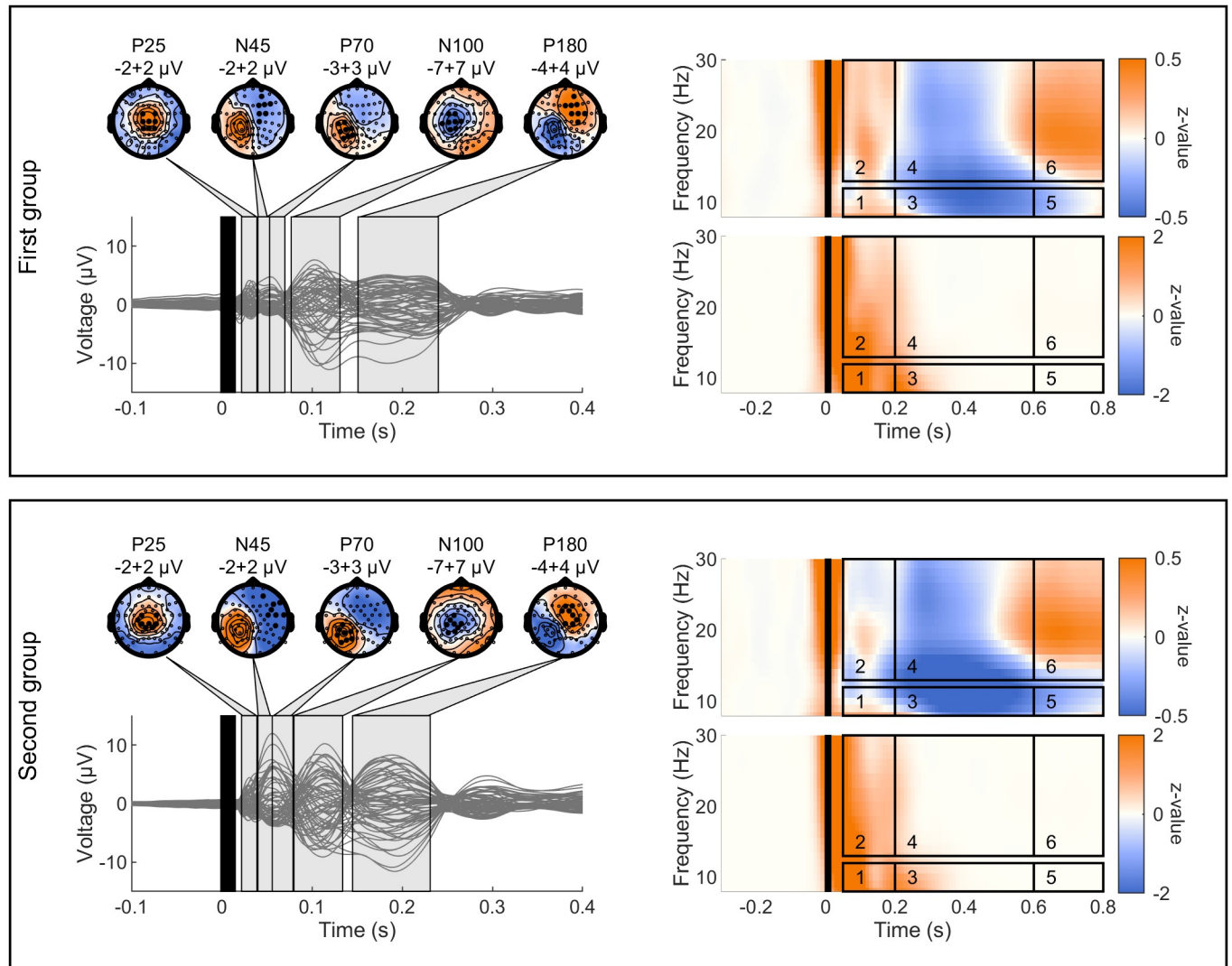


Fig 2. Selection of TEPs TOIs and channels and induced and evoked oscillations ROIs. On the left, single EEG channel traces and topographical plots resulting from the average across all subjects, test blocks and sessions for the first (top) and second (bottom) group of subjects. TEPs peaks are named according to their approximate latency after TMS application. Topographical distributions are obtained averaging the signal in the grey-shaded time windows. The maximum and minimum voltages are reported in μV below the relative topographies. Black filled dots in the topographies indicate the channels where the corresponding TEP peak was maximally expressed and that were used for calculation of LMFP in the relative TOI. On the right side, TFRs of induced (upper part) and evoked (lower part) oscillations on channel C3 averaged across all subjects, test blocks and sessions for the first (top) and second (bottom) group of subjects. Time-frequency ROIs used for the analysis are enclosed by the black rectangles. In all plots, time windows highlighted in black indicate signal affected by TMS-related artifacts that was removed and interpolated.

<https://doi.org/10.1371/journal.pone.0208747.g002>

[39] and baseline corrected subtracting the mean value (over time) of the baseline period (from 300 ms to 100 ms before TMS), to ensure that the average pre-TMS values did not differ from zero and that z-values could be interpreted as a modulation of the pre-TMS oscillatory activity. Finally, TFRs were averaged per block and trimmed to remove the time points where no time-frequency values could be calculated (from -500 to -333 ms and from 833 to 1000 ms with respect to the TMS marker in the data, corresponding to 1 cycle of the 6 Hz oscillation at the beginning and end of the epoch). Based on previous literature [10, 40], six non-overlapping time-frequency regions of interest (ROIs) were *a priori* defined (Fig 2). For each subject, block

and session, time-frequency values were averaged in the pre-defined ROIs (ROI1–8–12 Hz, 50–200 ms, ROI2–13–30 Hz, 50–200 ms, ROI3–8–12 Hz, 200–600 ms, ROI4–13–30 Hz, 200–600 ms, ROI5–8–12 Hz, 600–800 ms, ROI6–13–30 Hz, 600–800 ms) and used for statistical analysis (see below, *Statistics*).

TMS-EEG evoked oscillations: Local TMS-EEG evoked oscillatory activity [6, 7, 41, 42] was obtained averaging across trials the CSD signal of the C3 channel in each block and calculating the TFRs thereof with complex Morlet wavelets as described in the previous paragraph. For each subject, block and session, time-frequency values were averaged in the same six pre-defined ROIs of the induced activity (Fig 2) and used for statistical analysis (see below, *Statistics*).

Statistics. For each group of participants and for each investigated parameter, repeated measures analyses of variance (rmANOVAs) were run on the raw, i.e. not normalized, pre-rTMS data to demonstrate that there was no effect of TIME (2 levels, i.e. block 1 and block 2), SESSION (6 levels for first group of participants, 3 levels for second group of participants) or the interaction SESSION*TIME. For this analysis, the rsEEG data and LMFP data were ln-transformed to ensure normality. Then for each experiment, i.e. Main Experiment, Control Experiment 1, Control Experiment 2 and Control Experiment 3, and for each investigated parameter, rmANOVAs with the within-subject effects of PHASE (2 levels, i.e. positive and negative peak, for Main Experiment, Control Experiment 1 and Control Experiment 2, 3 levels, i.e. positive peak, negative peak and random phase, for Control experiment 3) and TIME (3 levels, i.e. time 0, time 15, time 30), were performed on normalized data. For the normalization, the rsEEG and LMFP data were divided by the average of the pre-rTMS blocks, while the average of the pre-rTMS blocks was subtracted from the TFRs data. Sphericity in all rmANOVAs was tested using Mauchly's test and, whenever it was violated, the Greenhouse-Geisser correction was applied. Post-hoc paired two-tailed t-tests were applied in case of a significant main effects or interactions. For all tests, the Lilliefors test was used to verify normal distribution. The significance level was $p < 0.05$. Bonferroni's correction was used for all *post hoc* analyses following rmANOVA to correct for multiple comparisons.

Results

Effect of rTMS on resting-state EEG μ - and β -power

Fig 3 shows the normalized μ - and β -power on C3 and C4 in the rsEEG periods for all the experimental sessions. C3 μ -power showed a significant effect of TIME in Control Exp. 2 ($F_{2,14} = 4.825$, $p = 0.025$), while C3 β -power showed a significant interaction PHASE*TIME in Control Exp. 2 ($F_{2,14} = 5.601$, $p = 0.029$). In both cases, all *post hoc* pairwise comparisons were not significant (all $p > 0.05$).

Effect of rTMS on TEP LMFPs

Fig 4 shows the normalized LMFP of the different TEP components for all the experimental sessions. In the Main Experiment, LMFP data showed a significant interaction PHASE*TIME for the P180 TEP component ($F_{2,22} = 8.734$, $p = 0.006$). *Post hoc* pairwise comparisons demonstrated a decrease of the P180 LMFP 30 min after rTMS in the negative peak condition ($p = 0.027$) compared to the average pre-rTMS value. In Control Experiment 1, there was a significant effect of PHASE for the N100 TEP ($F_{1,10} = 8.649$, $p = 0.015$). Pairwise comparisons revealed an increased N100 LMFP in the positive peak vs. negative peak condition ($p = 0.045$).

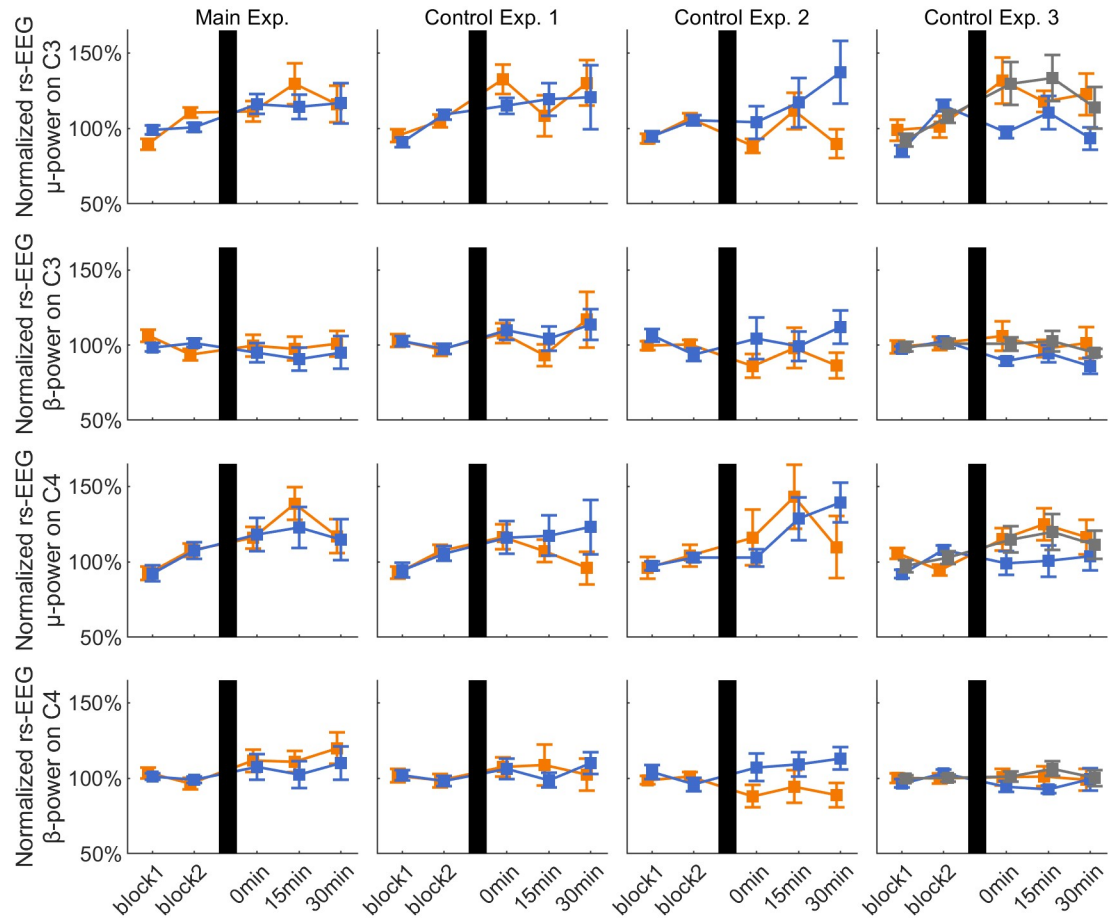


Fig 3. Resting-state EEG μ - and β -power on C3 and C4. Time course of group average \pm 1 s.e.m. resting-state EEG μ - and β -power on channels C3 (upper rows) and C4 (lower rows), for the positive (orange lines), negative (blue lines) and random (gray lines) phase triggered conditions in each experiment. Data are normalized to the average of the pre-rTMS blocks. In all plots, vertical black bars indicate the rTMS intervention.

<https://doi.org/10.1371/journal.pone.0208747.g003>

Effect of rTMS on local TMS-induced oscillations

Fig 5 shows the normalized TMS-induced oscillations on C3 in the six *a priori* defined ROIs for all the experimental sessions. TFRs data showed a significant effect of PHASE for ROI 3 ($F_{2,20} = 3.565$, $p = 0.047$) in Control Experiment 3 and a significant effect of TIME for ROI 3 ($F_{2,14} = 4.844$, $p = 0.0275$) and ROI 5 ($F_{2,14} = 5.167$, $p = 0.021$) and ROI 6 ($F_{2,14} = 4.509$, $p = 0.031$) in Control Experiment 2. Post hoc pairwise comparisons were all non-significant after Bonferroni correction (all $p > 0.05$).

Effect of rTMS on local TMS-evoked oscillations. Fig 6 shows the normalized TMS-evoked oscillations on C3 in the six *a priori* defined ROIs for all the experimental sessions. TFRs data showed no significant main effect of PHASE, TIME or of the interaction PHASE*TIME in any of the ROIs (all $p > 0.05$).

Discussion

We have investigated here the effects of μ -rhythm phase-dependent rTMS on several EEG measures of cortical excitability, i.e. resting-state EEG μ - and β -power, TEP LMFs and TMS-

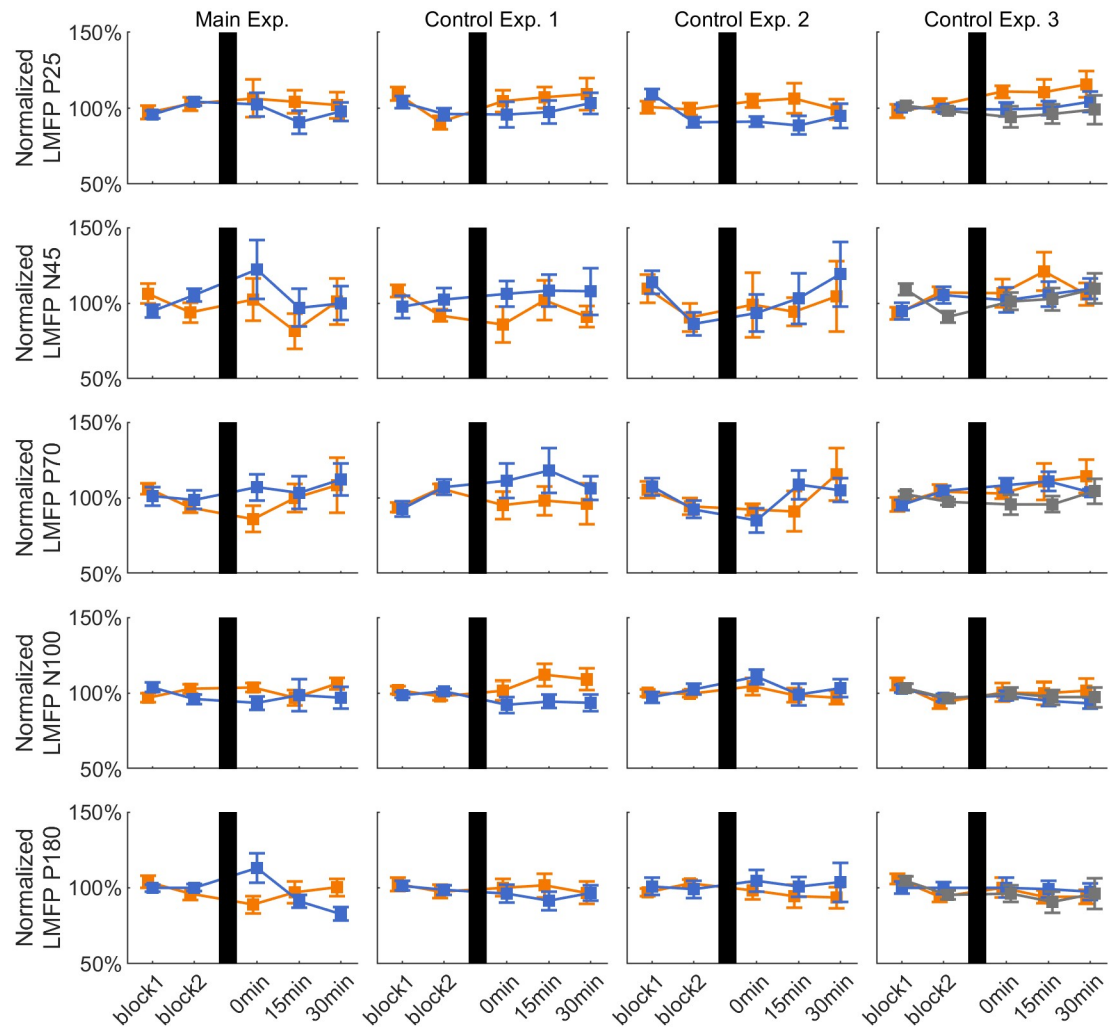


Fig 4. LMFP of TEPs. Time course of group average \pm 1 s.e.m. of LMFP of TEP components (P25, N45, P70, N100, P180) for the positive (orange lines), negative (blue lines) and random (gray lines) phase triggered conditions in each experiment. Data are normalized to the average of the pre-rTMS blocks. In all plots, vertical black bars indicate the rTMS intervention.

<https://doi.org/10.1371/journal.pone.0208747.g004>

induced and -evoked oscillatory activity. In line with previous results from our group on corticospinal plasticity [15], we expected LTP-like changes of these parameters when rTMS was applied at the negative peak of the local μ -oscillation, but none of the EEG measures was consistently and differentially modulated by rTMS when triggered on the negative vs. positive peak of the μ -rhythm. At a first glance, our results may seem counterintuitive, as a clear and reproducible change in MEP size, i.e. the long-term increase with synchronization of rTMS to the negative peak of the μ -rhythm, was not paralleled by similar changes in the investigated EEG measures. There is sufficient evidence that high-frequency rTMS-induced long-term increases in MEP amplitude occur at the level of cortex, as demonstrated, for example, by a reduced paired-pulse inhibition [43] and an increased regional cerebral metabolic rate of glucose [44] in the stimulated motor cortex. This notion is also supported by studies in animals showing that rTMS can modulate protein expression [45, 46], neurotransmitter and neuromodulator release and turnover [47, 48], as well as neuronal spiking [46]. However, several

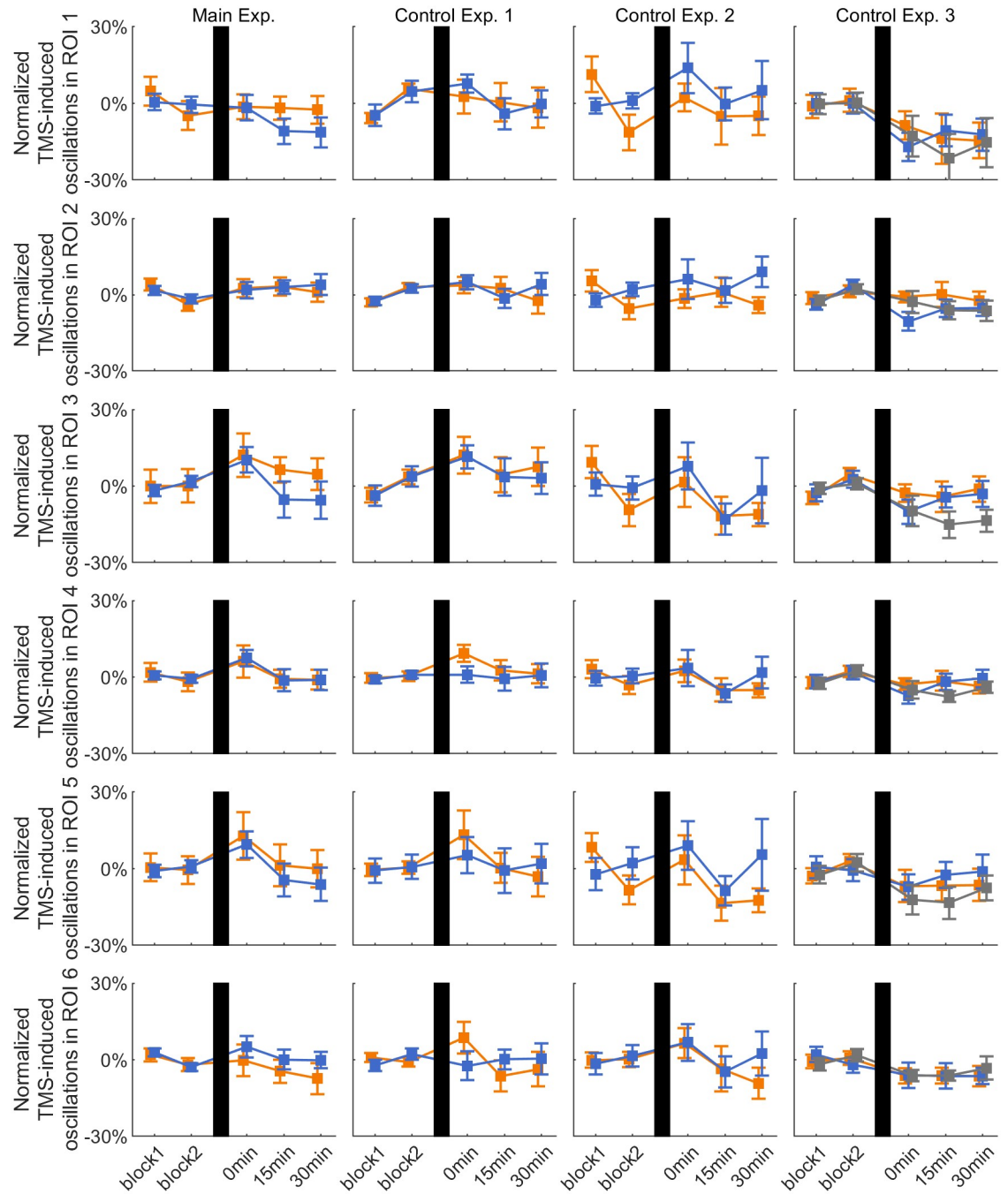


Fig 5. TMS-induced oscillations on C3. Time course of group average ± 1 s.e.m. of TMS-induced oscillations on channel C3 in the six *a priori* defined ROIs for the positive (orange lines), negative (blue lines) and random (gray lines) phase triggered conditions in each experiment. Data are normalized to the average of the pre-rTMS blocks. In all plots, vertical black bars indicate the rTMS intervention.

<https://doi.org/10.1371/journal.pone.0208747.g005>

TMS-EEG studies that investigated the aftereffects of rTMS on EEG measures have already reported substantial discrepancies between EEG-based measures of cortical excitability and MEP amplitude as an index of corticospinal excitability. Van der Werf and Paus [42] applied low-frequency subthreshold rTMS, known to induce depression of MEPs, to the left M1 and

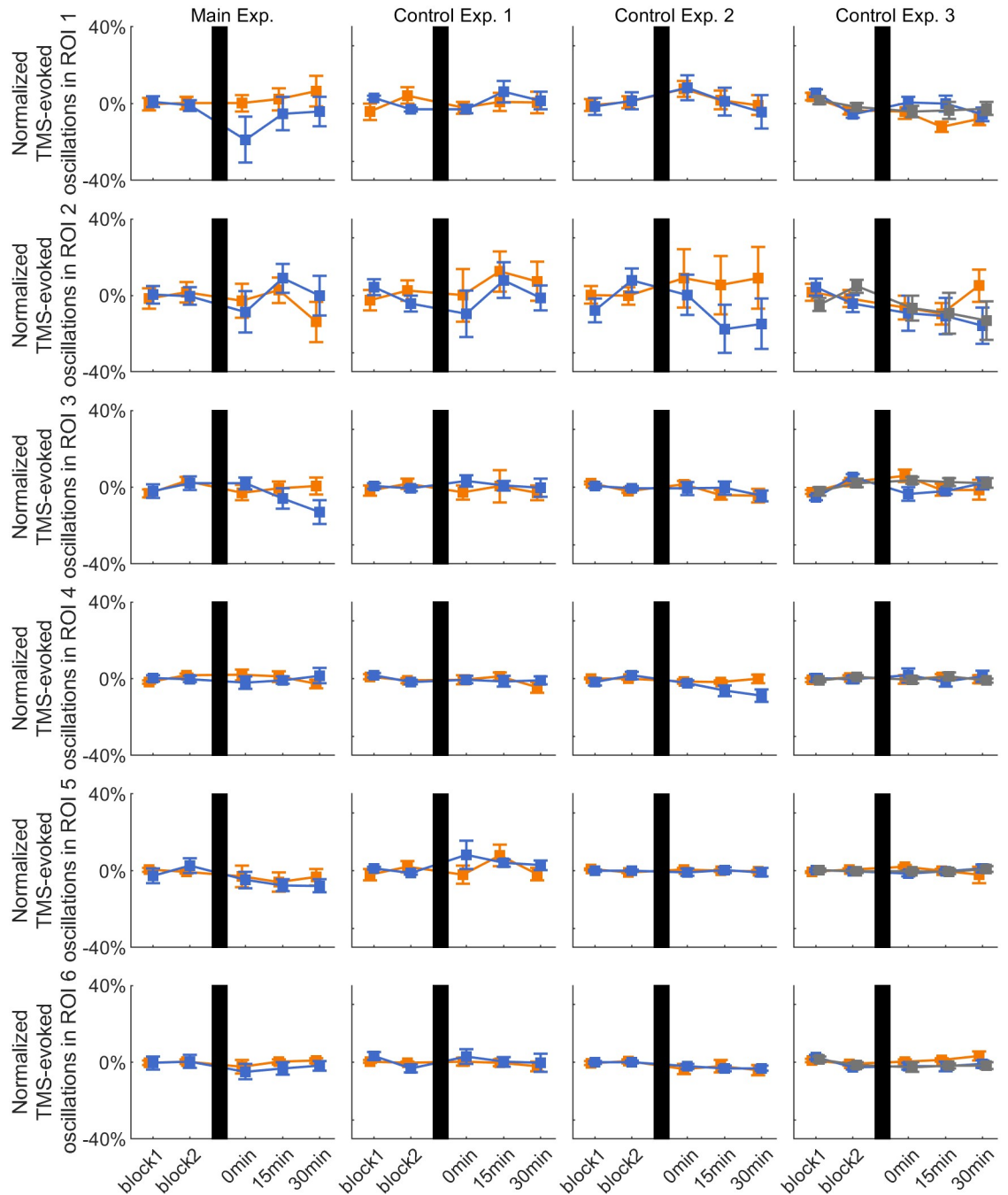


Fig 6. TMS-evoked oscillations on C3. Time course of group average \pm 1 s.e.m. of TMS-evoked oscillations on channel C3 in the six *a priori* defined ROIs for the positive (orange lines), negative (blue lines) and random (gray lines) phase triggered conditions in each experiment. Data are normalized to the average of the pre-rTMS blocks. In all plots, vertical black bars indicate the rTMS intervention.

<https://doi.org/10.1371/journal.pone.0208747.g006>

did not observe lasting changes in MEP size with respect to the pre-rTMS baseline, while reporting an early reduction followed by a later increase of the amplitude of the N45 TEP component. Similarly, inconsistent results have been obtained after continuous theta burst stimulation (cTBS, [49]). McAllister and colleagues [50] analyzed resting-state EEG over the left M1

before and after cTBS and found that spectral power in the δ , θ , α or β did not predict the MEP reduction after cTBS. Moreover, resting-state EEG power was unaffected by cTBS. Similarly, Vernet and colleagues [51], while reporting that changes in MEP size could be explained by a combination of different TEP peaks at group level, did not report a modulation of specific TEP peaks after cTBS. Another recent cTBS study on motor cortex reported unchanged MEP amplitude and unchanged LMFP over the stimulation site, but decreased δ power in resting-state EEG as well as decreased δ , θ and γ TMS-EEG oscillatory activity after the intervention [52]. Another study [53] did not find any change in TEPs in the presence of a significant increase in MEP size after intermittent theta burst stimulation (iTBS,[49]). Altogether, rTMS interventions thought to induce LTD- or LTP-like changes in corticospinal excitability produced inconsistent effects on all tested readouts, i.e. MEP and EEG measures. In summary, our nil findings are in line with these conflicting results. A possible explanation for these discordant results is that rTMS induces complex changes in molecular and synaptic mechanisms of the cortex that involve both inhibitory and facilitatory effects [54–58]. Since EEG can infer events only on a macroscopic scale and does not discriminate between excitatory and inhibitory processes, rTMS-induced changes in cortical dynamics may remain undetected by the EEG measures used in this study. Moreover, the relationship between MEPs and resting-state or TMS-evoked or induced EEG responses may be not linear, as already suggested by a lack of correlation between these measures in previous studies [12, 50, 52, 59].

A limitation of the present study is the use of suprathreshold TMS intensity in the test blocks pre- and post-rTMS. While this allowed to observe lasting excitability changes on MEPs [15], the associated changes in re-afferent input from the induced muscle twitch could contribute to the modulation of TMS cortical responses. However, the re-afferent input probably did not play a significant role in the reported results, as the investigated EEG measures remained largely unchanged with respect to the pre-rTMS values despite the increase in MEP amplitude. Another limitation is the loss of the EEG signal for up to 15 ms after the TMS pulse. We cannot exclude that significant changes in TMS-evoked or induced EEG responses have occurred in this very early time window, especially because excitation of pyramidal neurons projecting to the spinal cord and responsible for the MEP generation occurs in the very first milliseconds after the TMS pulse [60]. This limitation could be possibly overcome in future studies using faster sampling rates and more focal coils that minimize the activation of scalp muscles and produce smaller TMS related artifacts. Finally, another possible limitation of the study is the use of a data cleaning procedure based on ICA. While ICA is often used and necessary in the analysis of TMS-EEG data [12, 35, 52, 61, 62], it cannot be excluded that the removal of a large number of components partially affected the obtained results.

To conclude, while information over local neuronal excitability state at the time of rTMS has proved to lead to a more controlled efficacy of corticospinal plasticity induction as measured by a LTP-like increase in MEP size (in 91.3% of subjects vs. 52–61% in previous conventional rTMS protocols that did not employ EEG information about ongoing brain state, [15]), we did not observe any consistent modulation of EEG measures and no differential effect dependent on the phase of the ongoing μ -rhythm. The most likely explanation for this nil finding is that resting-state EEG, and TMS-evoked and induced EEG responses do not reflect excitability of corticospinal circuitry.

Acknowledgments

We thank Dr. Til Ole Bergmann for his comments on the experimental design and data analysis.

Author Contributions

Conceptualization: Christoph Zrenner, Ulf Ziemann.

Data curation: Debora Desideri, Paolo Belardinelli.

Formal analysis: Debora Desideri, Pedro Caldana Gordon.

Funding acquisition: Christoph Zrenner, Ulf Ziemann.

Methodology: Christoph Zrenner.

Project administration: Christoph Zrenner.

Software: Christoph Zrenner.

Supervision: Ulf Ziemann.

Writing – original draft: Debora Desideri.

Writing – review & editing: Christoph Zrenner, Pedro Caldana Gordon, Ulf Ziemann, Paolo Belardinelli.

References

- Ridding MC, Rothwell JC. Is there a future for therapeutic use of transcranial magnetic stimulation? *Nat Rev Neurosci*. 2007; 8(7):559–67. Epub 2007/06/15. <https://doi.org/10.1038/nrn2169> PMID: 17565358.
- Ziemann U, Paulus W, Nitsche MA, Pascual-Leone A, Byblow WD, Berardelli A, et al. Consensus: Motor cortex plasticity protocols. *Brain Stimul*. 2008; 1(3):164–82. Epub 2008/07/01. <https://doi.org/10.1016/j.brs.2008.06.006> PMID: 20633383.
- Niedermeyer E, Lopes da Silva FH. *Electroencephalography: basic principles, clinical applications, and related fields*. 5th ed. Philadelphia; London: Lippincott Williams & Wilkins; 2005. xiii, 1309 p., 4 p. of plates p.
- Bonato C, Miniussi C, Rossini PM. Transcranial magnetic stimulation and cortical evoked potentials: a TMS/EEG co-registration study. *Clin Neurophysiol*. 2006; 117(8):1699–707. Epub 2006/06/27. <https://doi.org/10.1016/j.clinph.2006.05.006> PMID: 16797232.
- Ilmoniemi RJ, Virtanen J, Ruohonen J, Karhu J, Aronen HJ, Naatanen R, et al. Neuronal responses to magnetic stimulation reveal cortical reactivity and connectivity. *Neuroreport*. 1997; 8(16):3537–40. Epub 1998/01/14. PMID: 9427322.
- Paus T, Sipila PK, Strafella AP. Synchronization of neuronal activity in the human primary motor cortex by transcranial magnetic stimulation: an EEG study. *J Neurophysiol*. 2001; 86(4):1983–90. Epub 2001/10/16. <https://doi.org/10.1152/jn.2001.86.4.1983> PMID: 11600655.
- Fuggetta G, Fiaschi A, Manganotti P. Modulation of cortical oscillatory activities induced by varying single-pulse transcranial magnetic stimulation intensity over the left primary motor area: a combined EEG and TMS study. *Neuroimage*. 2005; 27(4):896–908. Epub 2005/08/02. <https://doi.org/10.1016/j.neuroimage.2005.05.013> PMID: 16054397.
- Rosanova M, Casali A, Bellina V, Resta F, Mariotti M, Massimini M. Natural frequencies of human corticothalamic circuits. *J Neurosci*. 2009; 29(24):7679–85. Epub 2009/06/19. <https://doi.org/10.1523/JNEUROSCI.0445-09.2009> PMID: 19535579.
- Fecchio M, Pigorini A, Comanducci A, Sarasso S, Casarotto S, Premoli I, et al. The spectral features of EEG responses to transcranial magnetic stimulation of the primary motor cortex depend on the amplitude of the motor evoked potentials. *PLoS One*. 2017; 12(9):e0184910. Epub 2017/09/15. <https://doi.org/10.1371/journal.pone.0184910> PMID: 28910407.
- Premoli I, Bergmann TO, Fecchio M, Rosanova M, Biondi A, Belardinelli P, et al. The impact of GABAergic drugs on TMS-induced brain oscillations in human motor cortex. *Neuroimage*. 2017; 163:1–12. Epub 2017/09/18. <https://doi.org/10.1016/j.neuroimage.2017.09.023> PMID: 28917695.
- Esser SK, Huber R, Massimini M, Peterson MJ, Ferrarelli F, Tononi G. A direct demonstration of cortical LTP in humans: a combined TMS/EEG study. *Brain Res Bull*. 2006; 69(1):86–94. Epub 2006/02/09. <https://doi.org/10.1016/j.brainresbull.2005.11.003> PMID: 16464689.
- Casula EP, Tarantino V, Basso D, Arcara G, Marino G, Toffolo GM, et al. Low-frequency rTMS inhibitory effects in the primary motor cortex: Insights from TMS-evoked potentials. *Neuroimage*. 2014; 98:225–32. Epub 2014/05/06. <https://doi.org/10.1016/j.neuroimage.2014.04.065> PMID: 24793831.

13. Veniero D, Brignani D, Thut G, Miniussi C. Alpha-generation as basic response-signature to transcranial magnetic stimulation (TMS) targeting the human resting motor cortex: a TMS/EEG co-registration study. *Psychophysiology*. 2011; 48(10):1381–9. Epub 2011/05/06. <https://doi.org/10.1111/j.1469-8986.2011.01218.x> PMID: 21542853.
14. Fuggetta G, Pavone EF, Fiaschi A, Manganotti P. Acute modulation of cortical oscillatory activities during short trains of high-frequency repetitive transcranial magnetic stimulation of the human motor cortex: a combined EEG and TMS study. *Hum Brain Mapp*. 2008; 29(1):1–13. Epub 2007/02/24. <https://doi.org/10.1002/hbm.20371> PMID: 17318833.
15. Zrenner C, Desideri D, Belardinelli P, Ziemann U. Real-time EEG-defined excitability states determine efficacy of TMS-induced plasticity in human motor cortex. *Brain Stimul*. 2018; 11(2):374–89. Epub 2017/12/02. <https://doi.org/10.1016/j.brs.2017.11.016> PMID: 29191438.
16. Huerta PT, Lisman JE. Heightened synaptic plasticity of hippocampal CA1 neurons during a cholinergically induced rhythmic state. *Nature*. 1993; 364(6439):723–5. Epub 1993/08/19. <https://doi.org/10.1038/364723a0> PMID: 8355787.
17. Huerta PT, Lisman JE. Bidirectional synaptic plasticity induced by a single burst during cholinergic theta oscillation in CA1 in vitro. *Neuron*. 1995; 15(5):1053–63. Epub 1995/11/01. PMID: 7576649.
18. Artola A, Brocher S, Singer W. Different voltage-dependent thresholds for inducing long-term depression and long-term potentiation in slices of rat visual cortex. *Nature*. 1990; 347(6288):69–72. Epub 1990/09/06. <https://doi.org/10.1038/347069a0> PMID: 1975639.
19. Sjöström PJ, Häusser M. A cooperative switch determines the sign of synaptic plasticity in distal dendrites of neocortical pyramidal neurons. *Neuron*. 2006; 51(2):227–38. Epub 2006/07/19. <https://doi.org/10.1016/j.neuron.2006.06.017> PMID: 16846857.
20. Neuper C, Grabner RH, Fink A, Neubauer AC. Long-term stability and consistency of EEG event-related (de-)synchronization across different cognitive tasks. *Clin Neurophysiol*. 2005; 116(7):1681–94. Epub 2005/06/01. <https://doi.org/10.1016/j.clinph.2005.03.013> PMID: 15922658.
21. Rossi S, Hallett M, Rossini PM, Pascual-Leone A. Safety of TMS. Safety, ethical considerations, and application guidelines for the use of transcranial magnetic stimulation in clinical practice and research. *Clin Neurophysiol*. 2009; 120(12):2008–39. Epub 2009/10/17. <https://doi.org/10.1016/j.clinph.2009.08.016> PMID: 19833552.
22. Rossini PM, Burke D, Chen R, Cohen LG, Daskalakis Z, Di Iorio R, et al. Non-invasive electrical and magnetic stimulation of the brain, spinal cord, roots and peripheral nerves: Basic principles and procedures for routine clinical and research application. An updated report from an I.F.C.N. Committee. *Clin Neurophysiol*. 2015; 126(6):1071–107. Epub 2015/03/24. <https://doi.org/10.1016/j.clinph.2015.02.001> PMID: 25797650.
23. Casarotto S, Romero Lauro LJ, Bellina V, Casali AG, Rosanova M, Pigorini A, et al. EEG responses to TMS are sensitive to changes in the perturbation parameters and repeatable over time. *PLoS One*. 2010; 5(4):e10281. Epub 2010/04/28. <https://doi.org/10.1371/journal.pone.0010281> PMID: 20421968.
24. Massimini M, Ferrarelli F, Huber R, Esser SK, Singh H, Tononi G. Breakdown of cortical effective connectivity during sleep. *Science*. 2005; 309(5744):2228–32. Epub 2005/10/01. <https://doi.org/10.1126/science.1117256> PMID: 16195466.
25. Hjorth B. An on-line transformation of EEG scalp potentials into orthogonal source derivations. *Electroencephalogr Clin Neurophysiol*. 1975; 39(5):526–30. Epub 1975/11/01. PMID: 52448.
26. Oostenveld R, Fries P, Maris E, Schoffelen JM. FieldTrip: Open source software for advanced analysis of MEG, EEG, and invasive electrophysiological data. *Comput Intell Neurosci*. 2011; 2011:156869. Epub 2011/01/22. <https://doi.org/10.1155/2011/156869> PMID: 21253357.
27. Hyvärinen A. Fast and robust fixed-point algorithms for independent component analysis. *IEEE Trans Neural Netw*. 1999; 10(3):626–34. Epub 2008/02/07. <https://doi.org/10.1109/72.761722> PMID: 18252563.
28. Hyvärinen A, Karhunen J, Oja E. Independent component analysis. New York: Chichester: Wiley; 2001. xxi, 481 p. p.
29. Perrin F, Pernier J, Bertrand O, Echallier JF. Spherical splines for scalp potential and current density mapping. *Electroencephalogr Clin Neurophysiol*. 1989; 72(2):184–7. Epub 1989/02/01. PMID: 2464490.
30. Rogasch NC, Sullivan C, Thomson RH, Rose NS, Bailey NW, Fitzgerald PB, et al. Analysing concurrent transcranial magnetic stimulation and electroencephalographic data: A review and introduction to the open-source TESA software. *Neuroimage*. 2017; 147:934–51. Epub 2016/10/25. <https://doi.org/10.1016/j.neuroimage.2016.10.031> PMID: 27771347.
31. Premoli I, Castellanos N, Rivolta D, Belardinelli P, Bajo R, Zipser C, et al. TMS-EEG signatures of GABAergic neurotransmission in the human cortex. *J Neurosci*. 2014; 34(16):5603–12. Epub 2014/04/18. <https://doi.org/10.1523/JNEUROSCI.5089-13.2014> PMID: 24741050.

32. Lehmann D, Skrandies W. Reference-free identification of components of checkerboard-evoked multi-channel potential fields. *Electroencephalogr Clin Neurophysiol*. 1980; 48(6):609–21. Epub 1980/06/01. PMID: [6155251](#).
33. Pellicciari MC, Brignani D, Miniussi C. Excitability modulation of the motor system induced by transcranial direct current stimulation: a multimodal approach. *Neuroimage*. 2013; 83:569–80. Epub 2013/07/13. <https://doi.org/10.1016/j.neuroimage.2013.06.076> PMID: [23845429](#).
34. Casarotto S, Canali P, Rosanova M, Pigorini A, Fecchio M, Mariotti M, et al. Assessing the effects of electroconvulsive therapy on cortical excitability by means of transcranial magnetic stimulation and electroencephalography. *Brain Topogr*. 2013; 26(2):326–37. Epub 2012/10/12. <https://doi.org/10.1007/s10548-012-0256-8> PMID: [23053600](#).
35. Gordon PC, Zrenner C, Desideri D, Belardinelli P, Zrenner B, Brunoni AR, et al. Modulation of cortical responses by transcranial direct current stimulation of dorsolateral prefrontal cortex: A resting-state EEG and TMS-EEG study. *Brain Stimul*. 2018. Epub 2018/06/21. <https://doi.org/10.1016/j.brs.2018.06.004> PMID: [29921529](#).
36. Donner TH, Siegel M. A framework for local cortical oscillation patterns. *Trends Cogn Sci*. 2011; 15(5):191–9. Epub 2011/04/13. <https://doi.org/10.1016/j.tics.2011.03.007> PMID: [21481630](#).
37. Tallon-Baudry C, Bertrand O. Oscillatory gamma activity in humans and its role in object representation. *Trends Cogn Sci*. 1999; 3(4):151–62. Epub 1999/05/14. PMID: [10322469](#).
38. Busch NA, VanRullen R. Spontaneous EEG oscillations reveal periodic sampling of visual attention. *Proc Natl Acad Sci U S A*. 2010; 107(37):16048–53. Epub 2010/09/02. <https://doi.org/10.1073/pnas.1004801107> PMID: [20805482](#).
39. Grandchamp R, Delorme A. Single-trial normalization for event-related spectral decomposition reduces sensitivity to noisy trials. *Front Psychol*. 2011; 2:236. Epub 2011/10/14. <https://doi.org/10.3389/fpsyg.2011.00236> PMID: [21994498](#).
40. Gordon PC, Desideri D, Belardinelli P, Zrenner C, Ziemann U. Comparison of cortical EEG responses to realistic sham versus real TMS of human motor cortex. *Brain Stimul*. 2018. Epub 2018/08/26. <https://doi.org/10.1016/j.brs.2018.08.003> PMID: [30143417](#).
41. Brignani D, Manganotti P, Rossini PM, Miniussi C. Modulation of cortical oscillatory activity during transcranial magnetic stimulation. *Hum Brain Mapp*. 2008; 29(5):603–12. Epub 2007/06/09. <https://doi.org/10.1002/hbm.20423> PMID: [17557296](#).
42. Van Der Werf YD, Paus T. The neural response to transcranial magnetic stimulation of the human motor cortex. I. Intracortical and cortico-cortical contributions. *Exp Brain Res*. 2006; 175(2):231–45. Epub 2006/06/20. <https://doi.org/10.1007/s00221-006-0551-2> PMID: [16783559](#).
43. Peinemann A, Lehner C, Mentschel C, Munchau A, Conrad B, Siebner HR. Subthreshold 5-Hz repetitive transcranial magnetic stimulation of the human primary motor cortex reduces intracortical paired-pulse inhibition. *Neurosci Lett*. 2000; 296(1):21–4. Epub 2000/12/02. PMID: [11099824](#).
44. Siebner HR, Peller M, Willoch F, Minoshima S, Boecker H, Auer C, et al. Lasting cortical activation after repetitive TMS of the motor cortex: a glucose metabolic study. *Neurology*. 2000; 54(4):956–63. Epub 2000/02/26. PMID: [10690992](#).
45. Fujiki M, Steward O. High frequency transcranial magnetic stimulation mimics the effects of ECS in upregulating astroglial gene expression in the murine CNS. *Brain Res Mol Brain Res*. 1997; 44(2):301–8. Epub 1997/03/01. PMID: [9073172](#).
46. Benali A, Trippe J, Weiler E, Mix A, Petrasch-Parwez E, Girzalsky W, et al. Theta-burst transcranial magnetic stimulation alters cortical inhibition. *J Neurosci*. 2011; 31(4):1193–203. Epub 2011/01/29. <https://doi.org/10.1523/JNEUROSCI.1379-10.2011> PMID: [21273404](#).
47. Ben-Shachar D, Belmaker RH, Grisaru N, Klein E. Transcranial magnetic stimulation induces alterations in brain monoamines. *J Neural Transm (Vienna)*. 1997; 104(2–3):191–7. Epub 1997/01/01. <https://doi.org/10.1007/BF01273180> PMID: [9203081](#).
48. Keck ME, Sillaber I, Ebner K, Welt T, Toschi N, Kaehler ST, et al. Acute transcranial magnetic stimulation of frontal brain regions selectively modulates the release of vasopressin, biogenic amines and amino acids in the rat brain. *Eur J Neurosci*. 2000; 12(10):3713–20. Epub 2000/10/13. PMID: [11029641](#).
49. Huang YZ, Edwards MJ, Rounis E, Bhatia KP, Rothwell JC. Theta burst stimulation of the human motor cortex. *Neuron*. 2005; 45(2):201–6. Epub 2005/01/25. <https://doi.org/10.1016/j.neuron.2004.12.033> PMID: [15664172](#).
50. McAllister SM, Rothwell JC, Ridding MC. Cortical oscillatory activity and the induction of plasticity in the human motor cortex. *Eur J Neurosci*. 2011; 33(10):1916–24. Epub 2011/04/15. <https://doi.org/10.1111/j.1460-9568.2011.07673.x> PMID: [21488985](#).

51. Vernet M, Bashir S, Yoo WK, Perez JM, Najib U, Pascual-Leone A. Insights on the neural basis of motor plasticity induced by theta burst stimulation from TMS-EEG. *Eur J Neurosci*. 2013; 37(4):598–606. Epub 2012/11/30. <https://doi.org/10.1111/ejn.12069> PMID: 23190020.
52. Rocchi L, Ibanez J, Benussi A, Hannah R, Rawji V, Casula E, et al. Variability and Predictors of Response to Continuous Theta Burst Stimulation: A TMS-EEG Study. *Front Neurosci*. 2018; 12:400. Epub 2018/06/28. <https://doi.org/10.3389/fnins.2018.00400> PMID: 29946234.
53. Gedankien T, Fried PJ, Pascual-Leone A, Shafi MM. Intermittent theta-burst stimulation induces correlated changes in cortical and corticospinal excitability in healthy older subjects. *Clin Neurophysiol*. 2017; 128(12):2419–27. Epub 2017/11/03. <https://doi.org/10.1016/j.clinph.2017.08.034> PMID: 29096215.
54. Funke K, Benali A. Modulation of cortical inhibition by rTMS—findings obtained from animal models. *J Physiol*. 2011; 589(Pt 18):4423–35. Epub 2011/07/20. <https://doi.org/10.1113/jphysiol.2011.206573> PMID: 21768267.
55. Labedi A, Benali A, Mix A, Neubacher U, Funke K. Modulation of inhibitory activity markers by intermittent theta-burst stimulation in rat cortex is NMDA-receptor dependent. *Brain Stimul*. 2014; 7(3):394–400. Epub 2014/03/25. <https://doi.org/10.1016/j.brs.2014.02.010> PMID: 24656783.
56. Lenz M, Galanis C, Muller-Dahlhaus F, Opitz A, Wierenga CJ, Szabo G, et al. Repetitive magnetic stimulation induces plasticity of inhibitory synapses. *Nat Commun*. 2016; 7:10020. Epub 2016/01/09. <https://doi.org/10.1038/ncomms10020> PMID: 26743822.
57. Vlachos A, Muller-Dahlhaus F, Rosskopp J, Lenz M, Ziemann U, Deller T. Repetitive magnetic stimulation induces functional and structural plasticity of excitatory postsynapses in mouse organotypic hippocampal slice cultures. *J Neurosci*. 2012; 32(48):17514–23. Epub 2012/12/01. <https://doi.org/10.1523/JNEUROSCI.0409-12.2012> PMID: 23197741.
58. Trippe J, Mix A, Aydin-Abidin S, Funke K, Benali A. Theta burst and conventional low-frequency rTMS differentially affect GABAergic neurotransmission in the rat cortex. *Exp Brain Res*. 2009; 199(3–4):411–21. Epub 2009/08/25. <https://doi.org/10.1007/s00221-009-1961-8> PMID: 19701632.
59. Noh NA, Fuggetta G, Manganotti P, Fiaschi A. Long lasting modulation of cortical oscillations after continuous theta burst transcranial magnetic stimulation. *PLoS One*. 2012; 7(4):e35080. Epub 2012/04/13. <https://doi.org/10.1371/journal.pone.0035080> PMID: 22496893.
60. Li B, Virtanen JP, Oeltermann A, Schwarz C, Giese MA, Ziemann U, et al. Lifting the veil on the dynamics of neuronal activities evoked by transcranial magnetic stimulation. *Elife*. 2017; 6. Epub 2017/11/23. <https://doi.org/10.7554/eLife.30552> PMID: 29165241.
61. Rogasch NC, Thomson RH, Farzan F, Fitzgibbon BM, Bailey NW, Hernandez-Pavon JC, et al. Removing artefacts from TMS-EEG recordings using independent component analysis: importance for assessing prefrontal and motor cortex network properties. *Neuroimage*. 2014; 101:425–39. Epub 2014/07/30. <https://doi.org/10.1016/j.neuroimage.2014.07.037> PMID: 25067813.
62. Chung SW, Lewis BP, Rogasch NC, Saeki T, Thomson RH, Hoy KE, et al. Demonstration of short-term plasticity in the dorsolateral prefrontal cortex with theta burst stimulation: A TMS-EEG study. *Clin Neurophysiol*. 2017; 128(7):1117–26. Epub 2017/05/17. <https://doi.org/10.1016/j.clinph.2017.04.005> PMID: 28511124.

2.4 Comparison of cortical EEG responses to realistic sham versus real TMS of human motor cortex



Comparison of cortical EEG responses to realistic sham versus real TMS of human motor cortex

Pedro Caldana Gordon ², Debora Desideri ², Paolo Belardinelli, Christoph Zrenner ¹, Ulf Ziemann ^{*,1}

Department of Neurology & Stroke, and Hertie Institute for Clinical Brain Research, University of Tübingen, Germany

ARTICLE INFO

Article history:

Received 20 June 2018

Received in revised form

1 August 2018

Accepted 13 August 2018

Available online 16 August 2018

Keywords:

Transcranial magnetic stimulation

Sham TMS

Control condition

Motor cortex

Electroencephalography

Evoked potential

ABSTRACT

Background: The analysis of cortical responses to transcranial magnetic stimulation (TMS) recorded by electroencephalography (EEG) has been successfully applied to study human cortical physiology. However, in addition to the (desired) activation of cortical neurons and fibers, TMS also causes (undesired) indirect brain responses through auditory and somatosensory stimulation, which may contribute significantly to the overall EEG signal and mask the effects of intervention on direct cortical responses. **Objectives:** To test differences in EEG responses to real TMS at intensities above and below resting motor threshold (RMT) and a realistic sham stimulation.

Methods: 12 healthy subjects participated in one session in which single-pulse TMS was applied to the left motor cortex in 3 different blocks, 150 pulses per block: 110%RMT, 90%RMT and realistic sham stimulation. Cortical responses were collected by a 64 electrode EEG system. TMS evoked potentials (TEPs) and TMS induced oscillations were analyzed.

Methods: 12 healthy subjects participated in one session in which single-pulse TMS was applied to the left motor cortex in 3 different blocks, 150 pulses per block: 110%RMT, 90%RMT and realistic sham stimulation. Cortical responses were collected by a 64-channel EEG system. TMS evoked potentials (TEPs) and TMS induced oscillations were analyzed.

Results: TEPs from all conditions differed significantly, with TEPs from 110%RMT showing overall highest amplitudes and realistic sham lowest amplitudes. Sham stimulation had only minor effects on induced cortical oscillations compared to pre-stimulus baseline, TMS at 90%RMT resulted in a significant increase (50–200 m s) followed by a decrease (200–500 m s) in power of alpha and beta oscillations; TMS at 110% RMT led to an additional increase in beta power at late latencies (650–800 m s).

Conclusions: Real TMS of motor cortex results in cortical responses significantly different from realistic sham. These differences very likely reflect to a significant extent direct activation of neurons, rather than sensory evoked activity.

© 2018 Elsevier Inc. All rights reserved.

1. Introduction

The combination of electroencephalography (EEG) with transcranial magnetic stimulation (TMS) has enabled important advances in investigating cortical physiology through analysis of electrophysiological responses recorded from the brain [1,2]. Conventionally, motor cortex was targeted by TMS due to the availability of motor evoked potentials (MEPs) recorded through

electromyography (EMG) from hand muscles as an indirect measure of corticospinal excitability [3]. TMS evoked EEG potentials (TEPs) serve as a more direct measure of cortical excitability and connectivity that enables analysis of spatiotemporal cortical response profiles, e.g., before and after brain stimulation or pharmacological interventions [4,5]. For TMS target sites other than motor cortex, TEPs gain additional importance, as there are no other straightforward electrophysiological outcome measures available [1].

The technical challenges regarding the design of EEG amplifiers for compatibility with TMS have largely been solved, and it is now possible to analyze neural responses a few milliseconds after the TMS pulse [2,6]. Nevertheless, interpretation of the EEG response to

* Corresponding author. Hoppe-Seyler-Straße 3, 72076, Tübingen, Germany.

E-mail address: ulf.ziemann@uni-tuebingen.de (U. Ziemann).

¹ These authors share senior authorship.

² These authors contributed equally to this work.

TMS regarding its origin remains difficult, since this response is a combination of the experimentally desired (i.e., TMS evoked) activation of the brain, and experimentally undesired responses, such as indirect brain activation due to somatosensory and auditory inputs, that are inevitably caused by excitation of trigeminal nerve endings in the scalp and the TMS click sound, as well as non-neural signals, such as scalp muscle activation. The click sound generated by the coil during each TMS pulse results in a prominent auditory evoked potential (AEP), which contaminates the EEG signal of interest [7,8], but can be partially mitigated using masking noise [9]. Similarly, somatosensory input due to vibration of the stimulating coil during the TMS pulse, as well as direct activation of peripheral sensory nerves in the scalp, result in somatosensory evoked potentials (SEP) in the EEG signal [10]. The use of a spacer between the coil and the scalp has been proposed to reduce sensory activation [11,12]. Despite these efforts, there is still concern that remaining signals from these auditory and somatosensory inputs still act as significant confounders in the analysis of TMS-EEG [11].

Consequently, incorporation of a sham stimulation condition has been advocated in TMS-EEG research, to ensure that observed effects cannot be attributed to experimentally undesired responses. However, it is not trivial to design a proper TMS sham condition that does not produce effective direct cortical stimulation but is otherwise equivalent to real TMS in all its indirect effects [13]. Realistic sham procedures that incorporate both an auditory click, as well as a weak electrical stimulation to reproduce the skin sensation and scalp muscle activation near the TMS target, have been proposed as a possible solution, although so far only few studies have adopted this approach [13,14]. Another issue, specifically concerning TMS of motor cortex, is the re-afferent feedback from the evoked muscle twitch with suprathreshold TMS intensities, which contributes to TEPs [10,15] and to the spectral pattern of TMS induced cortical oscillations [16–18], adding to the contamination of the direct cortical response signal.

In this study, we aim to disentangle these phenomena by comparing EEG responses generated by real TMS of the motor cortex vs. a realistic sham stimulation. Specifically, we compared EEG responses to TMS with an intensity above motor threshold (eliciting MEP), TMS with an intensity below motor threshold (without eliciting MEP), and realistic sham stimulation. We expected to find differential EEG responses between these conditions, which would allow identification of brain responses caused by direct activation by TMS rather than indirect activation by somatosensory or auditory inputs or re-afferent feedback.

2. Methods

2.1. Subjects

The sample for the present study was drawn from a previous experiment (Desideri et al., under review). Subjects included 12 healthy right-handed individuals (4 males, age range 22–51 years, mean age \pm s.d. 27.5 ± 7.7 years, Edinburgh Handedness inventory laterality score 75 ± 23). Experiments were conducted in accordance with the Declaration of Helsinki and within the current TMS safety guidelines of the International Federation of Clinical Neurophysiology [19]. All subjects provided written informed consent prior to participation, and the study was approved by the ethics committee of the medical faculty of the University of Tübingen (protocol 716/2014B02).

2.2. Experimental design

The experiment involved a single session, with the application of single-pulse TMS to the hand area of the left primary motor

cortex. Stimulation was divided into 3 separate blocks: 1. Real TMS with stimulation intensity of 110%RMT; 2. Real TMS with intensity of 90%RMT; and 3. Realistic SHAM stimulation. The order of the blocks was randomized across subjects, who were blinded to the nature of the stimulation applied in each block. To test the quality of blinding, subjects filled a questionnaire at the end of the experimental session, designed to report the order in which each condition (110%RMT, 90%RMT or SHAM) was applied according to their impression.

2.3. Experimental set-up & procedure

Participants were seated in a comfortable armchair with their hands relaxed and were required to watch a fixation cross 1 m in front of them. The experiment involved a figure-of-eight TMS coil (PMD70-pCool, 70 mm winding diameter, Research 100, MAG & More, Germany), which delivered single pulses with a biphasic waveform (single cosine, 160 μ s period). The coil orientation was 45° with respect to the midline, resulting in the major component of the electric field induced in the brain underneath the coil pointing from lateral-posterior to medial-anterior. MEPs were recorded from the right abductor pollicis brevis muscle in a bipolar belly-tendon montage through surface electromyography (EMG, 5 kHz sampling rate, 0.16 Hz – 1.25 kHz bandpass filter) using adhesive hydrogel electrodes (Kendall, Covidien). The motor “hot-spot” was defined as the coil position and orientation eliciting, at a slightly suprathreshold stimulation intensity, maximum MEP amplitudes [20]. The RMT was determined as the minimum stimulation intensity that produced MEPs $>50 \mu$ V in the target muscle in more than 50% of the trials [20]. Coil position angulation and orientation were kept constant relative to the participant’s head using a stereoscopic neuronavigation system based on a standard Montreal Neurological Institute (MNI) brain anatomy (Localite GmbH, Sankt Augustin, Germany).

EEG signal was recorded from 64 channels arranged in the International 10–20 montage [21] in a TMS compatible Ag/AgCl sintered ring electrode cap (EasyCap GmbH, Germany). Data were acquired in DC mode (5 kHz sampling rate, 1.25 kHz low-pass anti-aliasing filter). The impedance at the interface between skin and all EEG electrodes was $<5 \text{ k}\Omega$ throughout the experiment. A 24-bit 80-channel biosignal amplifier was used for EEG and EMG recordings (NeuroOne Tesla with Analog Real-time Out Option, Bittium Biosignals Ltd., Finland). To minimize TMS-evoked auditory potentials, white noise was applied to the subjects through earphones, with attached plugs that attenuate external noise [6,9]. The loudness of the white noise was individually adjusted to optimally mask the TMS click.

In the SHAM block, the original coil was disconnected from the TMS stimulator, while still positioned over the subject’s scalp on the “hotspot” target. A second identical coil was then connected to the TMS stimulator, which was used to produce the typical TMS click at a stimulation intensity of 90%RMT. The second coil was positioned next to the first coil in the air and held by a fixation arm, but kept at a distance of 20 cm away from the scalp, which models showed to produce only a negligible electric field in the cortex, thus avoiding undesired neuronal stimulation [22]. To simulate the scalp sensation associated with TMS, electrical stimulation of the scalp with 200 μ s pulse duration, 200 V compliance voltage and 2.50 mA output current was delivered through two round electrodes (diameter 1 cm) integrated in the EEG cap, covered in conductive gel, with the cathode placed between Cz and CP1, corresponding to the position of the electrode CCP1h in the high-density 5% EEG montage, and the anode placed between FC5 and C3, corresponding to the position of the electrode FCC5h, and connected to a constant

current high voltage electrical stimulator (Constant current stimulator DS7A, Digitimer Ltd, UK).

In the original experiment (Desideri et al., under review), TMS triggers in each block were generated randomly at the positive peak, negative peak or at random phase of the ongoing sensorimotor μ -oscillation (for details, see Ref. [23]). For the purposes of the present study, only the trials with TMS triggered at random phase were used, to avoid possible confounding factors on the EEG response from stimulation at specified brain states [24] (Desideri et al., under review). TMS triggers were applied with a jittered minimum inter-trial interval of 2 s.

2.4. Data analysis

EEG and EMG data processing and analysis were performed using customized analysis scripts on MATLAB R2017b and the Fieldtrip open source MATLAB toolbox [25]. The continuously recorded EEG signal was segmented with respect to the trigger markers in the data. The epochs were defined from 500 ms before the marker to 1 s after the marker. Additionally, trials from the 90% RMT dataset which elicited any MEP with a peak-to-peak amplitude of $>25 \mu\text{V}$ within 20–40 ms after TMS were excluded, to ensure that the data in the 90%RMT condition exclusive contained trials without MEPs.

EEG data preprocessing: For the 110%RMT and 90%RMT datasets, data from 1 ms before to 15 ms after the marker, where high amplitude TMS artifacts occur, were removed and cubic interpolated. For the SHAM dataset, data from 1 ms before to 40 ms after the marker needed to be removed and interpolated, as the electrical stimulation and scalp muscle activation produced longer lasting artifacts. EEG data were then visually inspected. Epochs containing major artifacts were removed as well as channels that showed prominent noise in most of the epochs. Independent component analysis (ICA) based on FastICA algorithm with a symmetric approach and the “gauss” contrast function for finding the weight matrix [26] was applied. These specifications have been recommended for the processing of TMS-EEG data [27]. Data were submitted to a two-step ICA procedure, in which ICA components were visually inspected and removed based on their topography, single-trial time-course, average time-course and power spectrum [28]. In the first step, only components representing high amplitude TMS-related artifacts were removed. Then, data were filtered with a 1–80 Hz bandpass filter (zero-phase Butterworth, 3rd order) and a 49–51 Hz notch filter (zero-phase Butterworth, 3rd order) and down-sampled to 1000 Hz. Afterwards, ICA was again applied to the data, and components representing eye blinks and movements, persistent muscle activity or smaller amplitude TMS-related artifacts were removed. Finally, channels discarded during the visual inspection of the data were spline-interpolated using signal of the neighbor channels and data were re-referenced to the average reference signal [29].

TMS-EEG evoked potentials (TEPs): For the TEP analysis, the EEG trial epochs of a given block were lowpass filtered (45 Hz, zero-phase Butterworth, 3rd order) and averaged. We included the following 5 TEPs (with post-TMS time windows of interest) into further statistical analyses, as they correspond to those most reproducible according to the literature [5,30]: P25 (20–30 ms), N45 (35–60 ms), P70 (60–80 ms), N100 (85–140 ms), P180 (150–230 ms).

TMS-EEG oscillatory response: Aside from the TEPs, TMS induces oscillations which are not necessarily time-locked to the TMS pulse, i.e., changes in spontaneous oscillatory activity [16,17]. To obtain the induced response, first, we isolated the induced activity in the time-domain by a channel-wise subtraction of the evoked response from each single trial [18,31] for the epochs retained after data

cleaning and after re-afferent feedback compensation (see below). Subsequently, we calculated the time-frequency representations (TFRs) convolving single trials with complex Morlet wavelets [32]. We have analyzed the frequency range from 6 - 45 Hz in steps of 1 Hz and the center of the wavelet was shifted in steps of 10 ms in the time window $-500 \text{ ms} - 1000 \text{ ms}$ relative to the TMS pulse. The length of the wavelet linearly increased from 2 cycles at 6 Hz to 9 cycles at 45 Hz. The result of the wavelet transformation is a complex time series for each frequency in the examined frequency range. We then obtained the TFRs of power taking the squared absolute values of the complex time series. This was followed by the individual trial normalization for each frequency, based on a z-transformation that used the trial's respective mean and standard deviation for the power of each frequency from the full trial length. This normalization procedure transforms all power data to the same scale, allowing comparison across participants, trials and electrodes [18,33]. This full-length single-trial z-transformation calls for a pre-stimulus baseline correction, i.e., subtraction of mean value (over time) of the baseline period (from 300 ms - 100 ms before TMS), to ensure that the average pre-stimulus values do not differ from zero and that z-values can be interpreted as a modulation of the pre-stimulus oscillatory activity. Finally, for each subject and each experimental condition (110%RMT, 90%RMT, SHAM) we averaged the TFRs across trials.

2.5. Statistical analysis

All statistical analyses were performed on the MATLAB platform (R2017b, The Mathworks, USA). Responses in the blinding questionnaire were compared to the actual blocks using chi-square test of independence.

EEG data were analyzed, using all channels, by means of non-parametric cluster-based permutation statistics to control for the family-wise error rate [34]. Clusters were defined as ≥ 2 neighboring electrodes with a p-value < 0.05 . Monte Carlo p-values were subsequently calculated by means of a two-tailed test (i.e., significance level $p < 0.025$), using 1000 iterations for TEPs, and 2000 iterations for induced oscillations.

Significant differences between TEPs in the 3 experimental conditions (110%RMT, 90%RMT, SHAM) were evaluated by means of four analyses of variance (ANOVAs), one for each TEP of interest (N45, P70, N100, P180). The amplitude of the signal was averaged across the respective time windows of interest, and channels were permuted in the cluster based analysis. TEPs that presented clusters with $p < 0.05$ in the ANOVA were further analyzed in post hoc pairwise comparisons, performed by t-tests using the same cluster based methods approach. For the P25 TEP, only the 110%RMT and 90%RMT conditions were compared because within this early period data analysis in the SHAM condition was compromised by the stimulus artifact. We disregarded a comparative analysis between 110%RMT and SHAM, as it would not be possible to attribute any of the observed differences between these two conditions to the TMS brain activation or to differences in somatosensory activation.

The same statistical procedures were repeated in an additional analysis, following normalization of the signal's amplitude. This involved subtraction of the signal's amplitude of each trial by the average of the whole trial's amplitude and dividing the result by the standard deviation of the whole trial's amplitude, obtaining a z-score. By normalizing the amplitudes across interventions, results obtained from the statistical cluster-based analyses would reflect primarily differences in the signal's spatial distribution between conditions.

Induced Oscillations were also analyzed with a cluster-based ANOVA to compare the 3 experimental conditions (110%RMT, 90%

RMT, SHAM). Here, both the space (channels) and time dimensions were permuted in the cluster-based method, within a period 40–800 ms after the TMS pulse. This method was preferred instead of a predetermined set of time windows, given the absence of a consensus for time windows of interest to be used in the TMS induced oscillation analysis. Also, the present cluster-based statistics approach is appropriate for exploratory analyses, as it minimizes false-positives involved in testing multiple time-points [34]. Four ANOVAs were performed, one for each of the 4 frequency bands of interest: alpha (8–12 Hz), beta-1 (13–19 Hz), beta-2 (20–29 Hz), and gamma (30–45 Hz). Time-frequency points that presented clusters with $p < 0.05$ in the ANOVA were proceeded to the pairwise post hoc comparison with cluster-based t-tests.

3. Results

3.1. Blinding

The analysis of the blinding questionnaire suggests that the subjects were able to distinguish between the conditions applied, $\chi^2 = 40$ ($df = 4$, $N = 12$); $p < 0.001$ (Table 1). This was because all subjects could correctly identify the 110%RMT condition associated with muscle twitches. Comparing solely the 90%RMT and SHAM conditions, no statistical relation between the conditions and the subjects' responses was observed, as the null hypothesis could not be excluded: $\chi^2 = 2.66$ ($df = 1$, $N = 12$), $p = 0.102$. This suggests that subjects could not reliably distinguish realistic sham TMS from sub-threshold real TMS.

3.1.1. TMS evoked potentials (TEPs)

The average percentage (± 1 s.d.) of excluded trials during data processing was $3.9 \pm 2.4\%$ (110%RMT), $3.3 \pm 2.1\%$ (90%RMT) and $2.8 \pm 1.7\%$ (SHAM). The average number of components excluded in the first-step ICA were, respectively: 7.4 ± 2.1 , 7.0 ± 2.4 and 4.7 ± 1.6 , and the average number of components excluded in the second-step ICA were, respectively: 23.9 ± 8.9 , 24.5 ± 6.4 , and 26.5 ± 4.7 .

Stimulation (110%RMT, 90%RMT and SHAM) over the left motor cortex resulted in a series of deflections of the EEG signal, that differed among each other already at visual inspection (Fig. 1). Cluster-based ANOVA showed that the signals from all TEPs were statistically different, both for the sensor-level absolute amplitudes (in μV , Fig. 1, top panels) and the z-transformed normalized amplitudes (Fig. 1, bottom panels).

Pairwise comparisons showed that 110%RMT trials presented a significantly higher amplitude of TEPs (P25, N45, P70 N100 and P180) compared to 90%RMT. The difference was expressed mostly in channels located in proximity of the stimulation site (Fig. 2, upper panels). The 90%RMT trials presented a significantly higher amplitude of N45, N100 and P180 but not P70 when compared to SHAM. All differences were in clusters centered around the vertex (Fig. 2, upper panels). Following the normalization of signal amplitude, differences between conditions 110%RMT and 90%RMT remained significant (Fig. 2, lower panels). In contrast, the

difference in N100 between 90%RMT and SHAM was no longer significant, while the differences in N45 and P180 remained, and a new significant difference was observed in P70 (Fig. 2, lower panels).

3.1.2. TMS induced oscillations

Stimulation (110%RMT, 90%RMT and SHAM) over the left motor cortex resulted in a series of changes in the power of ongoing oscillatory activity (Fig. 3). A comparison between all interventions revealed a statistical difference in the oscillatory frequencies corresponding to the alpha (α), low-beta (β_1) and high-beta (β_2) bands. The differences occurred in 3 separate post-TMS pulse periods: an early response with increased power (around 50–200 ms), followed by a depression (around 250–500 ms), and a late response with increased power (after 650 ms), with respect to the baseline period.

A pairwise comparison indicated higher increase in power of cortical oscillations in the frequency bands α , β_1 and β_2 , around 50–200 ms, in the condition 90%RMT, compared to SHAM, in a cluster of channels comprising the stimulated area and the contralateral hemisphere, followed by a larger decrease in power of the oscillations in the frequency bands α and β_1 , around 250–500 ms, in a cluster of channels comprising mostly the stimulated area (Fig. 4). The pairwise comparison between 110% RMT and SHAM indicated a similar pattern of differences. A larger increase in power of the oscillations in the frequency bands β_1 and β_2 was observed around 650–800 ms in the 110%RMT condition compared to both 90%RMT and SHAM (Fig. 4).

4. Discussion

The objective in this study was to compare EEG responses generated by TMS of the motor cortex at supra- and sub-threshold intensities and by realistic sham stimulation. We found that TMS evoked and induced EEG responses present distinct patterns when generated by single-pulse TMS above RMT, below RMT or a realistic sham stimulation.

Motor cortex TMS at 90%RMT effectively activates the brain, as has been demonstrated by inhibition of ongoing motor activity [35], generation of intracortical inhibition and facilitation in paired-pulse TMS protocols [36], or elicitation of corticospinal volleys in epidural spinal recordings [37]. Therefore, the 90%RMT and SHAM conditions should differ only with regard to effective (but sub-threshold for generation of MEPs) cortical stimulation by TMS, while indirect sources of brain activation by auditory input caused by the TMS click and somatosensory inputs caused by excitation of scalp nerve endings should be similar. Nevertheless, the N45, N100 and P180 TEP amplitudes were significantly larger in the 90%RMT than SHAM condition. TEPs evoked by the 90%RMT condition followed the pattern described in previous reports of motor cortex stimulation below RMT [15,38], and these TEPs remained even after subtracting the responses caused by the realistic SHAM (Fig. 2). It is very likely that this difference between TMS 90%RMT and sham is mostly caused by direct cortical activation by the TMS pulse. The analysis of the signal after amplitude normalization suggested also a significant difference in the spatial distribution of TEPs between 90%RMT and SHAM conditions, except for the N100. The realistic sham stimulation evoked cortical responses with a negative peak at around 100 ms after stimulation, followed by a positive peak at around 200 ms (Fig. 1), as expected from sensory and auditory evoked cortical activity generated by TMS [7,10,39]. Given the presence of auditory click and scalp sensation in all conditions in the present study, it is expected that their cortical responses would share this feature. It is possible that the spatial difference of the N100 between 110%RMT and 90%RMT was due to the re-afferent

Table 1
Contingency table of the number of subjects' responses to the blinding questionnaire versus the actual session the subjects received.

Session applied	Responses to the blinding questionnaires			Total number of sessions
	110%RMT	90%RMT	SHAM	
110%RMT	12 (100%)	0 (0%)	0 (0%)	12
90%RMT	0 (0%)	8 (66.6%)	4 (33.3%)	12
SHAM	0 (0%)	4 (33.3%)	8 (66.6%)	12

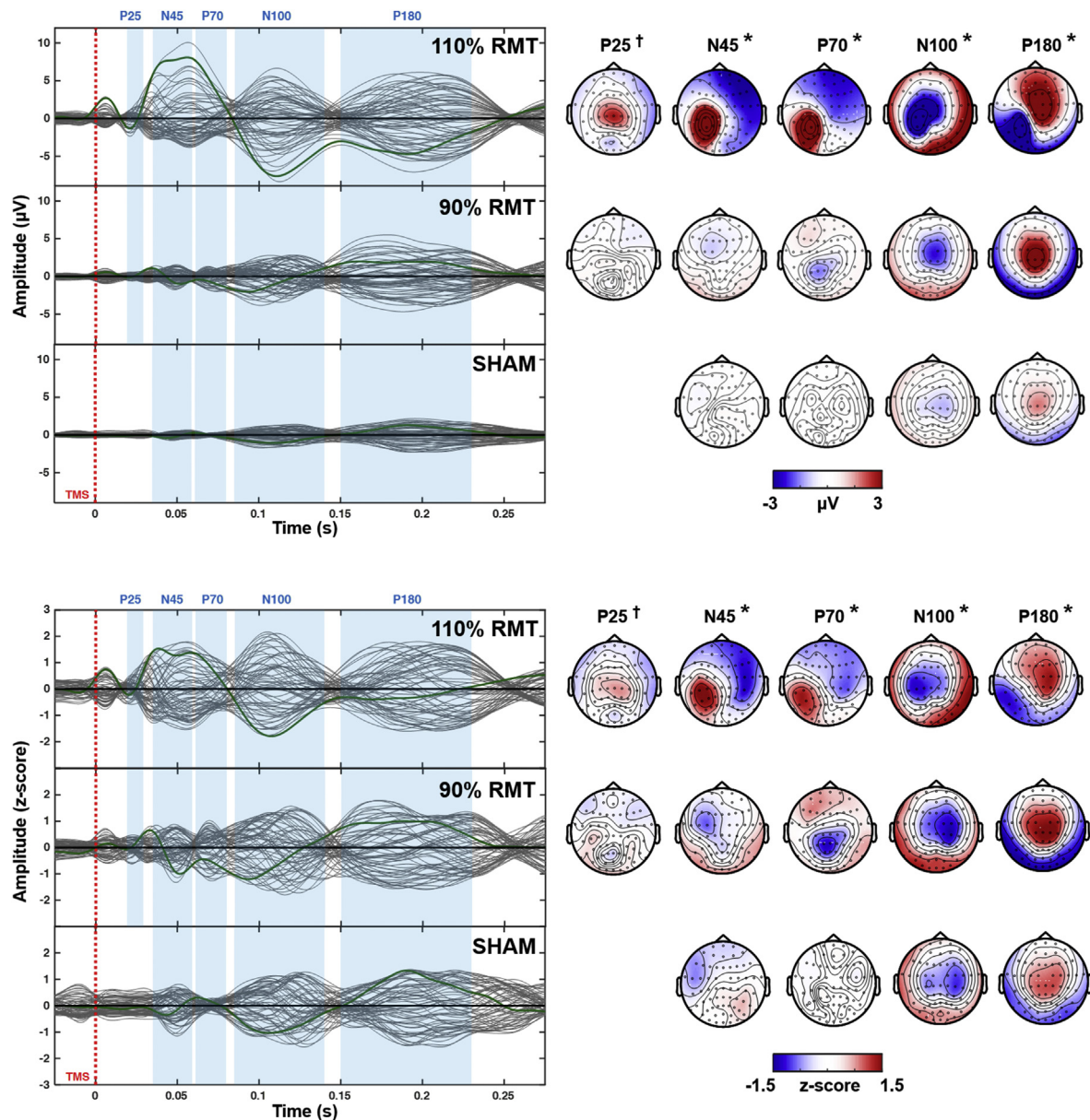


Fig. 1. The top panel shows the EEG sensor amplitude using an average reference montage (μV); the bottom panel shows the normalized amplitudes (z-score). Left: Butterfly plot of the grand average across all subjects ($n = 12$) and trials of each condition (110%RMT, 90%RMT and SHAM). The green curve is the signal recorded from electrode C3 underneath the stimulating coil over left motor cortex. Red dotted line indicates the TMS pulse. Shaded areas represent the latencies of typical TEPs observed after TMS of motor cortex (P25, N45, P70, N100 and P180). Right: Spatial distribution of voltage over the scalp averaged across the latency of each TEP. TEPs that presented statistical significance in the cluster-based ANOVA are marked with * ($p < 0.001$), and statistical significance in the cluster based t -test are marked with † ($p < 0.010$). (For interpretation of the references to colour in this figure legend, the reader is referred to the Web version of this article.)

input from the motor evoked potential in the 110%RMT condition, skewing the voltage distribution of the cortical evoked potential towards the sensorimotor cortex of the stimulated hemisphere.

Moreover, sham stimulation had only minor effects over induced oscillations, especially when compared to the effects of 110%RMT and 90%RMT stimulation (Fig. 3). Specifically, the 90%RMT resulted in increased power of oscillations in the alpha and beta frequencies in an early period, followed by decreased power of alpha and beta-1 frequencies in a later period, as described in previous studies [17,18]. These observations provide further evidence that these patterns originated by direct cortical stimulation by the TMS pulse, rather than by auditory or somatosensory evoked activity.

Significant differences were also found comparing supra-threshold TMS (110%RMT) with subthreshold TMS (90%RMT). Stimuli applied at intensities above RMT by definition elicit a motor response, which in turn leads to a re-afferent somatosensory evoked potential [40]. Motor re-afference from MEPs has been shown to interfere with the signal from TEPs, from approximately 40 ms after TMS pulse on, corresponding to the cumulative latencies of the MEP and somatosensory evoked potentials [6,10]. When stimulating the motor cortex at 100%RMT, one previous study found an increased amplitude of TEPs at latencies around 60 ms in the temporoparietal region in trials that elicited MEPs compared to those that did not, suggesting that this difference is probably caused by the re-afferent feedback from MEPs [38]. A

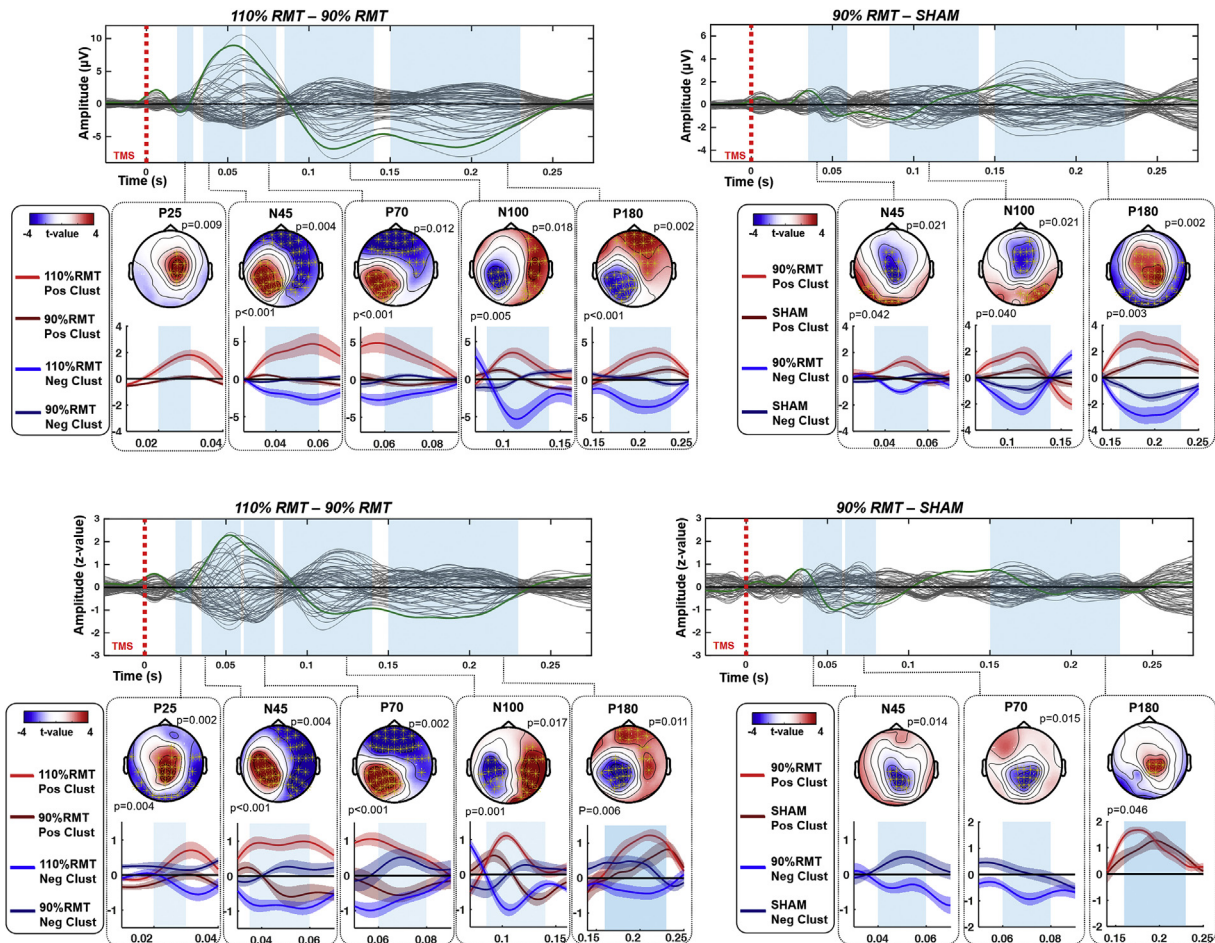


Fig. 2. The upper panels show the EEG sensor amplitude using an average reference montage (μV); the bottom panels show the normalized amplitudes (z-score). Top: Butterfly plots of the difference between interventions. The green curve represents electrode C3. Red dotted lines indicate the TMS pulse. Cyan areas represent the latencies of typical TEPs observed after TMS of motor cortex (P25, N45, P70, N100 and P180) which presented statistical significance in the ANOVA ($p < 0.001$). Mid: Topographical plots of the statistical differences (t-values) of TEP amplitudes indicated by the bold black line on the butterfly plots, channels highlighted (*) belong to clusters in which statistical significance was expressed. Red indicating more positive amplitude in the first condition, and blue indicating more negative amplitudes. P-values of the statistical tests are displayed next to the respective cluster. Bottom: Time courses of the average of the voltages from the EEG channels that comprised the significant electrode clusters, depicted in the above topographical plot (Pos Clust: Positive clusters; Neg Clust: Negative cluster), areas in cyan correspond to latencies of typical TEPs described above, shadows around the average curves correspond to ± 1 SEM. (For interpretation of the references to colour in this figure legend, the reader is referred to the Web version of this article.)

similar result was also observed in our study (Fig. 2). However, intensity of motor cortex stimulation per se has also been correlated to TEP amplitudes, regardless of the presence of MEPs [15]. It is likely that stimuli with higher intensities are able to depolarize neurons in a larger and deeper cortical area, thus leading to higher TEP amplitudes. Also, a study using functional magnetic resonance imaging and suprathreshold TMS suggested that the activation in motor cortical areas due to the re-afference potential does only explain 10–20% of the activation while 80–90% are attributable to direct brain activation by suprathreshold TMS [41]. Activation of motor output neurons by 110%RMT TMS, including connection of these neurons to the contralateral motor cortex through inter-hemispheric connections, might have been responsible for higher amplitudes found in the P25 around the contralateral motor cortex with 110%RMT TMS compared to 90%RMT (Fig. 2) [42]. Moreover, due to its short latency, it is unlikely that the amplitude of this TEP was influenced by re-afference or any other sensory evoked activity [6].

Changes in cortical oscillations following TMS have also been previously explored, with increase in power of alpha and beta frequency bands in the period 50–200 ms after TMS [10,16], with larger changes with increasing TMS intensities, and no change

following sham stimulation [16]. Later studies identified a decrease in power in these frequency bands in a later period 200–500 ms after TMS pulse [17,18]. The latency of this alpha and beta power decrease (event related desynchronization, ERD) may suggest a correspondence to sensory evoked activity [43], such as the motor re-afference [40]. In this line, it was demonstrated in one previous study that the decrease in power of the ERD (200–350 ms after the TMS pulse, alpha and beta frequency bands) was larger in ~110% RMT trials that elicited high amplitude MEPs, compared to trials with low amplitude MEPs, supporting that re-afference signals from the muscle twitch contributed to the ERD [17]. In contrast, we observed no significant difference in alpha/beta ERD between the 110%RMT and 90%RMT condition, but ERD was absent in the SHAM condition (Fig. 4). Another possibility is that alpha/beta ERD over sensorimotor cortices elicited by TMS may simply reflect overall cortical activation, which would include cortico-cortical and cortico-subcortical circuits directly activated by TMS and, to a lesser extent, the re-afferent feedback from the MEPs [18]. Accordingly, one study demonstrated that patients with severe disorders of consciousness, unlike healthy controls, failed to present TMS induced alpha and beta desynchronization [44], likely representing a consequence of the breakdown of cortico-cortical neuronal

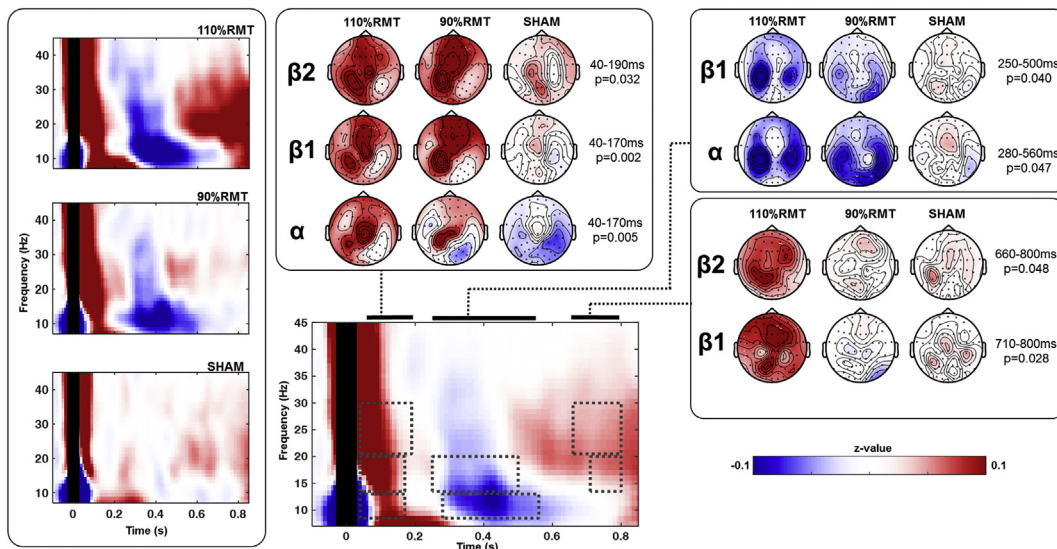


Fig. 3. Left: Time-frequency plots of the induced oscillations from the average across subjects and all EEG channels of each condition (110%RMT, 90%RMT and SHAM). Black area around time = 0 corresponds to the TMS artifact. Middle-Top: Topographical maps indicate the distribution of the standardized power (z-value) of the TMS induced oscillations from each condition, within the time-frequencies where the cluster-based ANOVA detected a statistical difference: Frequency indicated to the left of the plots (α , $\beta 1$, $\beta 2$), post-trigger period and p-value of the ANOVA indicated to the right of the plots. Middle-Bottom: Time-frequency plot of the average across all subjects, conditions and EEG channels, dotted rectangles indicate the time-frequencies where the cluster-based ANOVA detected a statistical difference between conditions (respective p-values to the right of the topographical plots). Topographical plots indicate the distribution of the standardized power (z-value) of the TMS induced oscillations from each condition, within the time-frequencies where the cluster-based ANOVA detected a statistical difference: Frequency indicated to the left of the plots (α , $\beta 1$, $\beta 2$), post-trigger period and p-value of the ANOVA indicated to the right of the plots.

processing in this condition [45,46]. Induced oscillations in the 110%RMT condition presented a significantly larger power increase in the beta band (event related synchronization/ERS) in a late time window (650–800 m s) compared to 90%RMT, suggesting that this phenomenon might correspond specifically to the motor re-ference. Late beta ERS (after approximately 1 s) has been shown to correlate to somatosensory re-ference, as both intentional finger movements and peripheral nerve stimulation without motor response were able to generate beta ERS [40,47]. Also, post-movement beta rebound in latencies beyond 500 m s was found to be increased following executed movements, compared to

movement planning, suggesting a role of re-ference in this phenomenon [48].

The present study has some limitations. As mentioned, the signal at latencies up to 40 m s in the sham condition was lost due to artifacts. Analysis of these data could have added to the understanding of the contribution of downstream activity from the motor cortex to the early TEPs. Latencies beyond 40 m s in conditions using suprathreshold TMS are always subject to interference from re-fferent signals, thus limiting the comparison of the effects between different TMS intensities. A future study might overcome this limitation by pairing TMS with peripheral stimulation in all

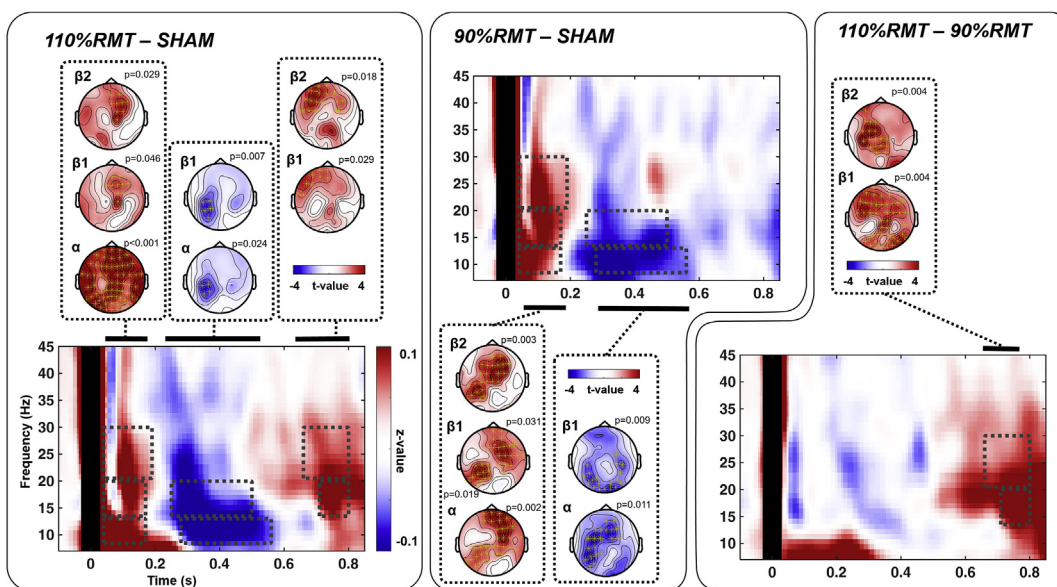


Fig. 4. Time-frequency plots of the difference of the induced oscillations between conditions, from the averages across all subjects ($n = 12$). Dotted rectangles indicate the time-frequencies where the pairwise cluster-based t-tests detected a significant difference between interventions (p-values indicated next to respective topographical plots). Topographical plots indicate significant differences from the pairwise cluster based t-tests, with clusters of channels indicated by (*). The frequency bands are indicated to the left of the plots (α , $\beta 1$, $\beta 2$), p-value of the t-tests are indicated to the right of the plots.

intensities, and subtracting the evoked potential from peripheral stimulation from the TEPs; or by blocking peripheral nerve conduction with local anesthetic nerve block [49]. It would also be of interest to investigate the comparison between different TMS intensities and realistic sham in other cortical areas. A recent preliminary report suggests that effective TMS evoked potentials in other brain regions, namely the frontal and parietal cortex, share many similar features with the responses from sham stimulation [50]. Future studies would be valuable to further confirm these observations to provide guidance for a more accurate extraction of signals that reflect direct cortical activation using TMS-EEG. In summary, our data demonstrate that real TMS of motor cortex results in EEG responses that reflect to a significant extent activation of the brain by the TMS pulse rather than by indirect sources of auditory, somatosensory or re-afferent inputs. Our findings are in close agreement with one previous study that demonstrated that TEPs are genuine cortical responses because they were detectable only when preserved cortical tissue was stimulated in patients with traumatic or ischemic brain lesions, in the presence of otherwise intact nerves in the scalp and cranial muscles [51].

5. Conclusion

Realistic sham TMS of the motor cortex elicits evoked and induced EEG potentials that are of significantly lower amplitudes compared to real TMS. These findings reinforce the evidence that most cortical responses observed with TMS-EEG are mostly unrelated to sensory evoked potentials caused by scalp stimulation and/or auditory stimulation from the TMS pulse, provided proper masking noise and ear protection are used. Nevertheless, the presence of a non-zero signal caused by sensory evoked activity might act as a confounder. Therefore, the use of a sham-controlled design is advisable in TMS-EEG experiments to disentangle the signal originated by direct cortical responses to TMS from auditory and somatosensory evoked activity, to ensure that the effects of experimental interventions are specifically attributed to the genuine cortical response to TMS.

Conflicts of interest

The authors declare that the research was conducted in the absence of any competing financial interest.

Acknowledgements

This study was supported by DFG grant ZI 542/7-1 (to U.Z.), Industry-on-Campus Grant IoC 211 (to P.B., and D.D.), and University of Tübingen Fortune Junior Grant 2287-0-0 (to C.Z.).

References

- [1] Rogasch NC, Fitzgerald PB. Assessing cortical network properties using TMS-EEG. *Hum Brain Mapp* 2013;34(7):1652–69.
- [2] Ilmoniemi RJ, Virtanen J, Ruohonen J, Karhu J, Aronen HJ, Naatanen R, et al. Neuronal responses to magnetic stimulation reveal cortical reactivity and connectivity. *Neuroreport* 1997;8(16):3537–40.
- [3] Ferreri F, Rossini PM. TMS and TMS-EEG techniques in the study of the excitability, connectivity, and plasticity of the human motor cortex. *Rev Neurosci* 2013;24(4):431–42.
- [4] Esser SK, Huber R, Massimini M, Peterson MJ, Ferrarelli F, Tononi G. A direct demonstration of cortical LTP in humans: a combined TMS/EEG study. *Brain Res Bull* 2006;69(1):86–94.
- [5] Premoli I, Castellanos N, Rivalta D, Belardinelli P, Bajo R, Zipsper C, et al. TMS-EEG signatures of GABAergic neurotransmission in the human cortex. *J Neurosci* 2014;34(16):5603–12.
- [6] Ilmoniemi RJ, Kicic D. Methodology for combined TMS and EEG. *Brain Topogr* 2010;22(4):233–48.
- [7] Tiitinen H, Virtanen J, Ilmoniemi RJ, Kamppari J, Ollikainen M, Ruohonen J, et al. Separation of contamination caused by coil clicks from responses elicited by transcranial magnetic stimulation. *Clin Neurophysiol* 1999;110(5):982–5.
- [8] Nikouline V, Ruohonen J, Ilmoniemi RJ. The role of the coil click in TMS assessed with simultaneous EEG. *Clin Neurophysiol* 1999;110(8):1325–8.
- [9] Massimini M, Ferrarelli F, Huber R, Esser SK, Singh H, Tononi G. Breakdown of cortical effective connectivity during sleep. *Science* 2005;309(5744):2228–32.
- [10] Paus T, Sipila PK, Strafella AP. Synchronization of neuronal activity in the human primary motor cortex by transcranial magnetic stimulation: an EEG study. *J Neurophysiol* 2001;86(4):1983–90.
- [11] ter Braack EM, de Vos CC, van Putten MJ. Masking the auditory evoked potential in TMS-EEG: a comparison of various methods. *Brain Topogr* 2015;28(3):520–8.
- [12] Ruddy KL, Woolley DG, Mantini D, Balsters JH, Enz N, Wenderoth N. Improving the quality of combined EEG-TMS neural recordings: introducing the coil spacer. *J Neurosci Meth* 2018;294:34–9.
- [13] Duecker F, Sack AT. Rethinking the role of sham TMS. *Front Psychol* 2015;6:210.
- [14] Mennemeier M, Triggs W, Chelette K, Woods A, Kimbrell T, Dornhoffer J. Sham transcranial magnetic stimulation using electrical stimulation of the scalp. *Brain Stimul* 2009;2(3):168–73.
- [15] Komssi S, Kahkonen S, Ilmoniemi RJ. The effect of stimulus intensity on brain responses evoked by transcranial magnetic stimulation. *Hum Brain Mapp* 2004;21(3):154–64.
- [16] Fuggetta G, Fiaschi A, Manganotti P. Modulation of cortical oscillatory activities induced by varying single-pulse transcranial magnetic stimulation intensity over the left primary motor area: a combined EEG and TMS study. *Neuroimage* 2005;27(4):896–908.
- [17] Fecchio M, Pigorini A, Comanducci A, Sarasso S, Casarotto S, Premoli I, et al. The spectral features of EEG responses to transcranial magnetic stimulation of the primary motor cortex depend on the amplitude of the motor evoked potentials. *PLoS One* 2017;12(9), e0184910.
- [18] Premoli I, Bergmann TO, Fecchio M, Rosanova M, Biondi A, Belardinelli P, et al. The impact of GABAergic drugs on TMS-induced brain oscillations in human motor cortex. *Neuroimage* 2017;163:1–12.
- [19] Rossi S, Hallett M, Rossini PM, Pascual-Leone A. Safety of TMS. Safety, ethical considerations, and application guidelines for the use of transcranial magnetic stimulation in clinical practice and research. *Clin Neurophysiol* 2009;120(12):2008–39.
- [20] Rossini PM, Burke D, Chen R, Cohen LG, Daskalakis Z, Di Iorio R, et al. Non-invasive electrical and magnetic stimulation of the brain, spinal cord, roots and peripheral nerves: basic principles and procedures for routine clinical and research application. An updated report from an I.F.C.N. Committee. *Clin Neurophysiol* 2015;126(6):1071–107.
- [21] Seeck M, Koessler L, Bast T, Leijten F, Michel C, Baumgartner C, et al. The standardized EEG electrode array of the IFCN. *Clin Neurophysiol* 2017;128(10):2070–7.
- [22] Philip NS, Carpenter SL, Carpenter LL. Safe use of repetitive transcranial magnetic stimulation in patients with implanted vagus nerve stimulators. *Brain Stimul* 2014;7(4):608–12.
- [23] Zrenner C, Desideri D, Belardinelli P, Ziemann U. Real-time EEG-defined excitability states determine efficacy of TMS-induced plasticity in human motor cortex. *Brain Stimul* 2018;11(2):374–89.
- [24] Bergmann TO, Molle M, Schmidt MA, Lindner C, Marshall L, Born J, et al. EEG-guided transcranial magnetic stimulation reveals rapid shifts in motor cortical excitability during the human sleep slow oscillation. *J Neurosci* 2012;32(1):243–53.
- [25] Oostenveld R, Fries P, Maris E, Schoffelen JM. FieldTrip: open source software for advanced analysis of MEG, EEG, and invasive electrophysiological data. *Comput Intell Neurosci* 2011;2011:156869.
- [26] Hyvärinen A. Fast and robust fixed-point algorithms for independent component analysis. *IEEE Trans Neural Network* 1999;10(3):626–34.
- [27] Korhonen RJ, Hernandez-Pavon JC, Metsomaa J, Mäki H, Ilmoniemi RJ, Sarvas J. Removal of large muscle artifacts from transcranial magnetic stimulation-evoked EEG by independent component analysis. *Med Biol Eng Comput* 2011;49(4):397–407.
- [28] Rogasch NC, Sullivan C, Thomson RH, Rose NS, Bailey NW, Fitzgerald PB, et al. Analysing concurrent transcranial magnetic stimulation and electroencephalographic data: a review and introduction to the open-source TESA software. *Neuroimage* 2017;147:934–51.
- [29] Perrin F, Pernier J, Bertrand O, Echallier JF. Spherical splines for scalp potential and current density mapping. *Electroencephalogr Clin Neurophysiol* 1989;72(2):184–7.
- [30] Lioumis P, Kicic D, Savolainen P, Makela JP, Kahkonen S. Reproducibility of TMS-Evoked EEG responses. *Hum Brain Mapp* 2009;30(4):1387–96.
- [31] Donner TH, Siegel M. A framework for local cortical oscillation patterns. *Trends Cognit Sci* 2011;15(5):191–9.
- [32] Tallon-Baudry C, Bertrand O. Oscillatory gamma activity in humans and its role in object representation. *Trends Cognit Sci* 1999;3(4):151–62.
- [33] Grandchamp R, Delorme A. Single-trial normalization for event-related spectral decomposition reduces sensitivity to noisy trials. *Front Psychol* 2011;2:236.
- [34] Maris E, Oostenveld R. Nonparametric statistical testing of EEG- and MEG-data. *J Neurosci Meth* 2007;164(1):177–90.

- [35] Davey NJ, Romaiguere P, Maskill DW, Ellaway PH. Suppression of voluntary motor activity revealed using transcranial magnetic stimulation of the motor cortex in man. *J Physiol (London)* 1994;477(Pt 2):223–35.
- [36] Ziemann U, Rothwell JC, Ridding MC. Interaction between intracortical inhibition and facilitation in human motor cortex. *J Physiol (London)* 1996;496(Pt 3):873–81.
- [37] Di Lazzaro V, Oliviero A, Profice P, Saturno E, Pilato F, Insola A, et al. Comparison of descending volleys evoked by transcranial magnetic and electric stimulation in conscious humans. *Electroencephalogr Clin Neurophysiol* 1998;109(5):397–401.
- [38] Petrichella S, Johnson N, He B. The influence of corticospinal activity on TMS-evoked activity and connectivity in healthy subjects: a TMS-EEG study. *PLoS One* 2017;12(4), e0174879.
- [39] Herring JD, Thut G, Jensen O, Bergmann TO. Attention modulates TMS-locked alpha oscillations in the visual cortex. *J Neurosci* 2015;35(43):14435–47.
- [40] Pfurtscheller G, Woertz M, Muller G, Wriessnegger S, Pfurtscheller K. Contrasting behavior of beta event-related synchronization and somatosensory evoked potential after median nerve stimulation during finger manipulation in man. *Neurosci Lett* 2002;323(2):113–6.
- [41] Shitara H, Shinozaki T, Takagishi K, Honda M, Hanakawa T. Movement and afferent representations in human motor areas: a simultaneous neuroimaging and transcranial magnetic/peripheral nerve-stimulation study. *Front Hum Neurosci* 2013;7:554.
- [42] Ferrarelli F, Massimini M, Sarasso S, Casali A, Riedner BA, Angelini G, et al. Breakdown in cortical effective connectivity during midazolam-induced loss of consciousness. *Proc Natl Acad Sci U S A* 2010;107(6):2681–6.
- [43] Stancak A. Cortical oscillatory changes occurring during somatosensory and thermal stimulation. *Prog Brain Res* 2006;159:237–52.
- [44] Formaggio E, Cavinato M, Storti SF, Tonin P, Piccione F, Manganotti P. Assessment of event-related EEG power after single-pulse TMS in unresponsive wakefulness syndrome and minimally conscious state patients. *Brain Topogr* 2016;29(2):322–33.
- [45] Rosanova M, Gosseries O, Casarotto S, Boly M, Casali AG, Bruno MA, et al. Recovery of cortical effective connectivity and recovery of consciousness in vegetative patients. *Brain* 2012;135(Pt 4):1308–20.
- [46] Casarotto S, Comanducci A, Rosanova M, Sarasso S, Fecchio M, Napolitani M, et al. Stratification of unresponsive patients by an independently validated index of brain complexity. *Ann Neurol* 2016;80(5):718–29.
- [47] Neuper C, Wortz M, Pfurtscheller G. ERD/ERS patterns reflecting sensorimotor activation and deactivation. *Prog Brain Res* 2006;159:211–22.
- [48] Caetano G, Jousmäki V, Hari R. Actor's and observer's primary motor cortices stabilize similarly after seen or heard motor actions. *Proc Natl Acad Sci U S A* 2007;104(21):9058–62.
- [49] Liepert J, Weiss T, Meissner W, Steinrucke K, Weiller C. Exercise-induced changes of motor excitability with and without sensory block. *Brain Res* 2004;1003(1–2):68–76.
- [50] Conde V, Tomasevic L, Akopian I, Stanek K, Saturnino GB, Thielscher A, et al. The non-transcranial TMS-evoked potential is an inherent source of ambiguity in TMS-EEG studies. *bioRxiv* 2018. <http://dx.doi.org/10.1101/337782>.
- [51] Gosseries O, Sarasso S, Casarotto S, Boly M, Schnakers C, Napolitani M, et al. On the cerebral origin of EEG responses to TMS: insights from severe cortical lesions. *Brain Stimul* 2015;8(1):142–9.

3. Discussion

In this thesis, we established for the first time a set-up that uses the combination of EEG and TMS to process in real-time with millisecond resolution electrical brain activity and to synchronize the stimulation to desired predefined brain states. We used this real-time EEG-triggered TMS set-up to investigate the dependency of corticospinal and cortical excitability and plasticity on the phase of the endogenously generated sensorimotor μ -rhythm. We estimated the instantaneous phase of the μ -oscillations and delivered single TMS pulses or bursts of rTMS to the left M1 of healthy participants when specific phases, i.e. positive and negative peak, occurred. With our experimental work, we also demonstrated that cortical responses to real vs. realistic sham TMS of M1 are characterized by different patterns of spatiotemporal activations.

In this section, the interpretations and implications of the presented results will be discussed in detail and future perspective will be presented.

In our publication “*Real-time EEG-defined excitability states determine efficacy of TMS-induced plasticity in human motor cortex*” (Zrenner et al., 2018), we demonstrated that corticospinal excitability fluctuates with the phase of the ongoing μ -oscillation. In particular, larger MEPs are obtained when TMS is applied at the negative vs. positive peak or random phase of the μ -rhythm. We also showed that 100 Hz TMS triplets repeatedly applied at the negative peak of the μ -rhythm caused an LTP-like increase in MEP size, while no significant change was observed when the same rTMS protocol was applied at the positive peak or at random phase of the μ -rhythm.

In the Introduction section, we have seen that synchronized EPSPs at the apical dendrites of pyramidal neurons that are oriented perpendicularly to the scalp are the major generators of the negative deflections in the surface EEG (Buzsáki et al., 2012; Kirschstein & Köhling, 2009). Pyramidal neurons in dorsal premotor and primary somatosensory cortex are mostly radially oriented. According to realistic models of TMS induced electric field (Bungert et al., 2017; Laakso et al., 2014), when TMS is applied over the M1 hand knob, their apical dendritic trees are transsynaptically excited (Amassian et al., 1987) and activate corticospinal neurons in M1 through cortico-cortical connections (Dum & Strick,

2005). Therefore, it is likely that we observed larger MEPs when single TMS pulses were applied at the negative vs. the positive peak of the sensorimotor μ -rhythm because this negative deflection is generated when the dendritic trees of pyramidal neurons in the dorsal premotor cortex or the primary somatosensory cortex predominantly receive excitatory synaptic inputs and are closer to firing threshold. As a consequence, a TMS pulse applied at the negative vs. positive peak of the μ -oscillation would recruit a higher fraction of these neurons, leading to the activation of more corticospinal neurons and finally larger MEPs.

Similar mechanisms may explain why we observed LTP-like corticospinal plasticity only when rTMS was synchronized to the negative peak and not the positive peak or random phase of the μ -oscillation. Dendritic membrane potentials play a critical role for the effect size and direction of synaptic plasticity in *in vitro* experiments: LTP is obtained when synaptic stimulation is paired with intracellular depolarization, while synaptic stimulation paired with hyperpolarization leads to LTD (Artola et al., 1990; Sjöström & Häusser, 2006).

In “*Phase of sensorimotor μ -oscillation modulates cortical responses to transcranial magnetic stimulation of the human motor cortex*” (Desideri et al., 2019), we showed that the phase of the ongoing μ -oscillation modulates TEPs when TMS is applied at supra- and subthreshold stimulation intensity, but not TMS-induced oscillations. Importantly, μ -phase did not affect TEPs or TMS-induced oscillations in the realistic sham TMS condition, strongly supporting the notion that results in the real TMS conditions were not caused by a μ -phase specific modulation of somatosensory and auditory inputs.

The most relevant result of our study was an enhancement of the TEP component occurring approximately 100 ms after TMS, i.e. N100, when TMS was applied at the negative vs. the positive peak of the μ -oscillation. N100 has often been associated to auditory inputs caused by the click of the TMS coil (Nikouline et al., 1999), however its μ -phase dependency across different TMS intensities but not sham TMS strongly suggests that this TEP reflects predominantly activation of cortex directly by the TMS pulse rather than by auditory inputs, a notion also supported by other studies (Bonato et al., 2006; Ferreri et al., 2011; Gordon et al., 2018; Komssi et al., 2004). The mechanisms

underlying the generation of N100 seem to be related to GABAergic inhibition (Bender et al., 2005; Bonnard et al., 2009; Kičić et al., 2008; Nikulin et al., 2003; Premoli et al., 2014; Rogasch & Fitzgerald, 2013). Therefore, TMS applied at the negative peak of the μ -oscillation may lead to recruitment of a larger proportion of inhibitory neurons which would then result in the enhancement of N100 amplitude.

The lack of μ -phase-dependent modulation of TMS-induced EEG oscillations may be related to the nature of the brain processes reflected by induced oscillatory activity. In fact, induced oscillations result from intrinsic network interactions within the brain that evolve over hundreds of milliseconds (Donner & Siegel, 2011). Therefore, the effect of a local excitability state (μ -phase) may only be observed in transient responses phase-locked to stimulus onset (TEPs), while modulation of non-phase-locked induced activity may be observed only when network balances are altered, like the administration of neuroactive drugs (Premoli et al., 2017).

In brief, our findings not only show that cortical excitability of the motor cortex fluctuates with the phase of the ongoing μ -oscillation, extending the corticospinal results of our previous study (Zrenner et al., 2018) at the cortical level, they also corroborate that TEPs are a sensitive measure of the instantaneous excitability state of the cortex and, therefore, a valuable tool to quantify the responsiveness of brain areas outside motor cortex with no other objective readout.

In a similar way, in our publication "*Nil effects of μ -rhythm phase-dependent burst-rTMS on cortical excitability in humans: a resting-state EEG and TMS-EEG study*" (Desideri et al., 2018), we investigated whether 100 Hz TMS triplets repeatedly applied at the negative vs. positive peak of the ongoing μ -oscillation induced long-lasting changes in cortical excitability that could be measured with resting-state EEG and TMS-EEG evoked and induced responses. Our results showed that none of the EEG-based measurements used to assess cortical excitability could detect any significant and consistent plastic change with respect to the pre-rTMS values, even in presence of a reproducible and significant LTP-like increase in MEP size when rTMS was applied at the negative peak of the μ -oscillation (Zrenner et al., 2018).

There is sufficient evidence that LTP-like effects induced by high-frequency rTMS on MEPs occur at the level of the stimulated motor cortex (Peinemann et al., 2000; Siebner et al., 2000). Studies in animals show that rTMS can modulate protein expression (Benali et al., 2011; Fujiki & Steward, 1997), neurotransmitter and neuromodulator release and turnover (Ben-Shachar et al., 1997; Keck et al., 2000), as well as neuronal spiking (Benali et al., 2011).

However, several TMS-EEG studies that investigated the aftereffects of rTMS on EEG measures have reported substantial discrepancies between EEG-based measures of cortical excitability and MEP amplitude as an index of corticospinal excitability (Gedankien et al., 2017; McAllister et al., 2011; Rocchi et al., 2018; Van Der Werf & Paus, 2006; Vernet et al., 2013), and our nil findings are in line with these conflicting results. A possible explanation for these discordant results is that rTMS-induced changes in cortical dynamics could not be detected by the EEG-based measures used in this study. In fact, rTMS induces complex changes in molecular and synaptic mechanisms of the cortex that involve both inhibitory and facilitatory effects (Funke & Benali, 2011; Labedi et al., 2014; Lenz et al., 2016; Vlachos et al., 2012), while EEG can infer events only on a macroscopic scale and does not discriminate between excitatory and inhibitory processes.

In this thesis, we also showed that TMS-evoked and -induced responses in the motor cortex present clear distinct patterns when generated by TMS pulses above RMT, below RMT and by a realistic sham stimulation. These results were presented in the publication "*Comparison of cortical EEG responses to realistic sham versus real TMS of human motor cortex*" (Gordon et al., 2018). These findings reinforce the evidence that responses to somatosensory and auditory stimulation associated with TMS represent only a minor part of the responses observed in the EEG compared to responses generated through direct cortical activation.

In conclusion, we demonstrated that synchronizing the stimulation to the negative peak of the endogenously generated μ -oscillation is crucial to obtain LTP-like aftereffects and to better control the directionality of the plastic changes obtained with our high-frequency rTMS protocol. In fact, in recent studies using

“excitability enhancing” NIBS protocols without information about the ongoing brain state only 52-61% of the investigated participants showed MEP changes in the expected direction (Hamada et al., 2013; Lopez-Alonso et al., 2014), while in our study 21/23 (91.3%) subjects exhibited an LTP-like increase in MEP amplitude when rTMS was synchronized to the negative peak of the μ -oscillation, demonstrating that taking into account the ongoing brain state leads to a reduction of inter-subject variability of rTMS aftereffects.

These findings could be relevant to enhance therapeutic effects of NIBS treatments of brain network disorders, like stroke, epilepsy, Parkinson’s disease, depression, and schizophrenia. Future studies could investigate the role of other oscillations in the fluctuation of excitability in the motor system. Further research could also address whether synchronization of rTMS interventions to brain states that are defined using different parameters than the phase of the μ -rhythm plays a significant role in the effective induction of LTP-like and LTD-like effects. Moreover, it would be important to assess experimentally whether oscillations in other brain areas of clinical relevance also influence responses to TMS similarly to what we have observed in the motor cortex for the μ -rhythm.

4. Summary

Non-invasive brain stimulation (NIBS) is a promising tool to modulate brain networks. Among NIBS techniques, transcranial magnetic stimulation (TMS) can activate cortical neurons in a spatiotemporal scale of millimeters and milliseconds and it has proved to have potential not only for electrophysiological, cognitive and behavioral research but also for the treatment of neurological and psychiatric disorders. Nevertheless, electrophysiological responses to TMS as well as clinical improvement of TMS treated patients is often characterized by a high variability across sessions and subjects, which limits the application of TMS in clinical settings. A significant part of this variability may be ascribable to the ongoing brain activity at the time of the stimulation.

To experimentally verify the advantage of brain state-dependent TMS, we built a TMS set-up that is able to trigger TMS pulses in real-time on the basis of the ongoing electrical brain activity concurrently registered with electroencephalography (EEG). We used this real-time EEG-triggered TMS set-up to assess dependency of electrophysiological responses to TMS of the left human motor cortex on the phase of the sensorimotor 8 – 12 Hz oscillation, i.e. μ -oscillation, in healthy participants. We synchronized single TMS pulses to the negative peak, positive peak or random phase of the μ -oscillation to assess μ -phase-dependent corticospinal and cortical excitability. Moreover, we repeatedly applied 200 triplets of TMS at 100 Hz, i.e. repetitive TMS (rTMS), either at the negative peak, positive peak or random phase of the μ -oscillation, to assess dependency of rTMS-induced long-lasting changes in corticospinal and cortical excitability on μ -phase. We measured corticospinal excitability with the amplitude of the motor evoked potentials (MEPs) recorded in a muscle of the right hand and cortical excitability with the amplitude of TMS-evoked potentials (TEPs) and the power of TMS-induced oscillations recorded with EEG. Furthermore, we used part of the data acquired for the assessment of μ -phase-dependent cortical excitability to evaluate the differences in cortical responses between real TMS at intensities above and below resting motor threshold (RMT) and a realistic sham stimulation.

Larger MEPs were obtained with single TMS pulses applied at the negative vs. positive peak or random phase of the ongoing μ -oscillation. Moreover, a long-lasting (>30 minutes) increase of MEP amplitude was achieved with negative peak synchronized rTMS, while no significant change with respect to the pre-intervention MEP amplitude was observed after positive peak synchronized or random phase rTMS. Single TMS pulses applied at the negative vs. positive peak of the μ -rhythm produced also enhanced TEPs. In particular, the negative deflection occurring approximately 100 ms after TMS application was consistently larger in the negative vs. positive peak condition both for above and below RMT intensities. Importantly, evoked responses elicited by realistic sham TMS were not modulated by the phase of the μ -oscillation. Negative peak triggered burst-rTMS did not significantly change any of the investigated EEG measures, despite the reported long-lasting significant increase in MEPs. Finally, TMS above and below RTM resulted in TEPs with larger amplitudes and in a significant modulation of the power of induced oscillatory activity compared to evoked potentials and induced oscillations elicited by realistic sham.

In conclusion, we demonstrated that the negative vs. positive peak of the sensorimotor μ -rhythm represents a state of higher excitability of the motor system and that rTMS synchronized to this high excitability state leads to long-term potentiation (LTP)-like effects on more than 90% of the tested participants. These findings support the notion that brain state-dependent TMS can reduce inter-subject variability with respect to “excitability enhancing” NIBS protocols that are blind to the ongoing brain activity (52-61% LTP-like responders). We also showed that TEPs are sensitive to instantaneous excitability fluctuations, while complex molecular and synaptic changes induced at the cortical level by rTMS may not always be detectable at the macroscopic level by EEG. Finally, cortical responses to real TMS of the motor cortex very likely reflect direct activation of neurons, rather than sensory evoked activity.

These findings are relevant for the improvement of NIBS-based therapies of brain network disorders. Future studies are needed to investigate whether oscillations in other brain areas of clinical relevance also influence responses to TMS similarly to what we observed in the motor cortex for the μ -rhythm.

5. Bibliography

- Ai, L., & Ro, T. (2014). The phase of prestimulus alpha oscillations affects tactile perception. *J Neurophysiol*, *111*(6), 1300-1307. doi:10.1152/jn.00125.2013
- Amassian, V. E., Stewart, M., Quirk, G. J., & Rosenthal, J. L. (1987). Physiological basis of motor effects of a transient stimulus to cerebral cortex. *Neurosurgery*, *20*(1), 74-93.
- Arieli, A., Sterkin, A., Grinvald, A., & Aertsen, A. (1996). Dynamics of ongoing activity: explanation of the large variability in evoked cortical responses. *Science*, *273*(5283), 1868-1871.
- Artola, A., Brocher, S., & Singer, W. (1990). Different voltage-dependent thresholds for inducing long-term depression and long-term potentiation in slices of rat visual cortex. *Nature*, *347*(6288), 69-72. doi:10.1038/347069a0
- Bakker, N., Shahab, S., Giacobbe, P., Blumberger, D. M., Daskalakis, Z. J., Kennedy, S. H., & Downar, J. (2015). rTMS of the dorsomedial prefrontal cortex for major depression: safety, tolerability, effectiveness, and outcome predictors for 10 Hz versus intermittent theta-burst stimulation. *Brain Stimul*, *8*(2), 208-215. doi:10.1016/j.brs.2014.11.002
- Barker, A. T., Jalinous, R., & Freeston, I. L. (1985). Non-invasive magnetic stimulation of human motor cortex. *Lancet*, *1*(8437), 1106-1107.
- Ben-Shachar, D., Belmaker, R. H., Grisaru, N., & Klein, E. (1997). Transcranial magnetic stimulation induces alterations in brain monoamines. *J Neural Transm (Vienna)*, *104*(2-3), 191-197. doi:10.1007/BF01273180
- Benali, A., Trippe, J., Weiler, E., Mix, A., Petrasch-Parwez, E., Girzalsky, W., . . . Funke, K. (2011). Theta-burst transcranial magnetic stimulation alters cortical inhibition. *J Neurosci*, *31*(4), 1193-1203. doi:10.1523/JNEUROSCI.1379-10.2011
- Bender, S., Basseler, K., Sebastian, I., Resch, F., Kammer, T., Oelkers-Ax, R., & Weisbrod, M. (2005). Electroencephalographic response to transcranial magnetic stimulation in children: Evidence for giant inhibitory potentials. *Ann Neurol*, *58*(1), 58-67. doi:10.1002/ana.20521
- Berger, B., Minarik, T., Liuzzi, G., Hummel, F. C., & Sauseng, P. (2014). EEG oscillatory phase-dependent markers of corticospinal excitability in the resting brain. *Biomed Res Int*, *2014*, 936096. doi:10.1155/2014/936096
- Berger, H. (1929). Über das Elektrenkephalogramm des Menschen. *Archiv für Psychiatrie und Nervenkrankheiten*, *87*, 527-570.
- Bergmann, T. O., Molle, M., Schmidt, M. A., Lindner, C., Marshall, L., Born, J., & Siebner, H. R. (2012). EEG-guided transcranial magnetic stimulation reveals rapid shifts in motor cortical excitability during the human sleep slow oscillation. *J Neurosci*, *32*(1), 243-253. doi:10.1523/JNEUROSCI.4792-11.2012
- Bonato, C., Miniussi, C., & Rossini, P. M. (2006). Transcranial magnetic stimulation and cortical evoked potentials: a TMS/EEG co-registration study. *Clin Neurophysiol*, *117*(8), 1699-1707. doi:10.1016/j.clinph.2006.05.006
- Bonnard, M., Spieser, L., Meziane, H. B., de Graaf, J. B., & Pailhous, J. (2009). Prior intention can locally tune inhibitory processes in the primary motor cortex: direct evidence from combined TMS-EEG. *Eur J Neurosci*, *30*(5), 913-923. doi:10.1111/j.1460-9568.2009.06864.x
- Bungert, A., Antunes, A., Espenhahn, S., & Thielscher, A. (2017). Where does TMS Stimulate the Motor Cortex? Combining Electrophysiological Measurements and Realistic Field Estimates to Reveal the Affected Cortex Position. *Cereb Cortex*, *27*(11), 5083-5094. doi:10.1093/cercor/bhw292
- Buzsáki, G. (2006). *Rhythms of the brain*. Oxford: Oxford University Press.

- Buzsáki, G., Anastassiou, C. A., & Koch, C. (2012). The origin of extracellular fields and currents—EEG, ECoG, LFP and spikes. *Nat Rev Neurosci*, *13*(6), 407-420. doi:10.1038/nrn3241
- Buzsáki, G., & Draguhn, A. (2004). Neuronal oscillations in cortical networks. *Science*, *304*(5679), 1926-1929. doi:10.1126/science.1099745
- Casula, E. P., Tarantino, V., Basso, D., Arcara, G., Marino, G., Toffolo, G. M., . . . Bisiacchi, P. S. (2014). Low-frequency rTMS inhibitory effects in the primary motor cortex: Insights from TMS-evoked potentials. *Neuroimage*, *98*, 225-232. doi:10.1016/j.neuroimage.2014.04.065
- Chen, R., Classen, J., Gerloff, C., Celnik, P., Wassermann, E. M., Hallett, M., & Cohen, L. G. (1997). Depression of motor cortex excitability by low-frequency transcranial magnetic stimulation. *Neurology*, *48*(5), 1398-1403.
- Chung, S. W., Lewis, B. P., Rogasch, N. C., Saeki, T., Thomson, R. H., Hoy, K. E., . . . Fitzgerald, P. B. (2017). Demonstration of short-term plasticity in the dorsolateral prefrontal cortex with theta burst stimulation: A TMS-EEG study. *Clin Neurophysiol*, *128*(7), 1117-1126. doi:10.1016/j.clinph.2017.04.005
- Daskalakis, Z. J., Christensen, B. K., Fitzgerald, P. B., & Chen, R. (2002). Transcranial magnetic stimulation: a new investigational and treatment tool in psychiatry. *J Neuropsychiatry Clin Neurosci*, *14*(4), 406-415. doi:10.1176/jnp.14.4.406
- Desideri, D., Zrenner, C., Gordon, P. C., Ziemann, U., & Belardinelli, P. (2018). Nil effects of mu-rhythm phase-dependent burst-rTMS on cortical excitability in humans: A resting-state EEG and TMS-EEG study. *PLoS One*, *13*(12), e0208747. doi:10.1371/journal.pone.0208747
- Desideri, D., Zrenner, C., Ziemann, U., & Belardinelli, P. (2019). Phase of sensorimotor mu-oscillation modulates cortical responses to transcranial magnetic stimulation of the human motor cortex. *J Physiol*, *597*(23), 5671-5686. doi:10.1113/JP278638
- Donner, T. H., & Siegel, M. (2011). A framework for local cortical oscillation patterns. *Trends Cogn Sci*, *15*(5), 191-199. doi:10.1016/j.tics.2011.03.007
- Dum, R. P., & Strick, P. L. (2005). Frontal lobe inputs to the digit representations of the motor areas on the lateral surface of the hemisphere. *J Neurosci*, *25*(6), 1375-1386. doi:10.1523/JNEUROSCI.3902-04.2005
- Esser, S. K., Huber, R., Massimini, M., Peterson, M. J., Ferrarelli, F., & Tononi, G. (2006). A direct demonstration of cortical LTP in humans: a combined TMS/EEG study. *Brain Res Bull*, *69*(1), 86-94. doi:10.1016/j.brainresbull.2005.11.003
- Fecchio, M., Pigorini, A., Comanducci, A., Sarasso, S., Casarotto, S., Premoli, I., . . . Rosanova, M. (2017). The spectral features of EEG responses to transcranial magnetic stimulation of the primary motor cortex depend on the amplitude of the motor evoked potentials. *PLoS One*, *12*(9), e0184910. doi:10.1371/journal.pone.0184910
- Ferreri, F., Pasqualetti, P., Maatta, S., Ponzio, D., Ferrarelli, F., Tononi, G., . . . Rossini, P. M. (2011). Human brain connectivity during single and paired pulse transcranial magnetic stimulation. *Neuroimage*, *54*(1), 90-102. doi:10.1016/j.neuroimage.2010.07.056
- Fitzgerald, P. B., Benitez, J., Oxley, T., Daskalakis, J. Z., de Castella, A. R., & Kulkarni, J. (2005). A study of the effects of lorazepam and dextromethorphan on the response to cortical 1 Hz repetitive transcranial magnetic stimulation. *Neuroreport*, *16*(13), 1525-1528.
- Fitzgerald, P. B., Fountain, S., & Daskalakis, Z. J. (2006). A comprehensive review of the effects of rTMS on motor cortical excitability and inhibition. *Clin Neurophysiol*, *117*(12), 2584-2596. doi:10.1016/j.clinph.2006.06.712
- Fregni, F., Boggio, P. S., Valle, A. C., Rocha, R. R., Duarte, J., Ferreira, M. J., . . . Pascual-Leone, A. (2006). A sham-controlled trial of a 5-day course of repetitive transcranial magnetic stimulation of the unaffected hemisphere in stroke patients. *Stroke*, *37*(8), 2115-2122. doi:10.1161/01.STR.0000231390.58967.6b

- Fuggetta, G., Fiaschi, A., & Manganotti, P. (2005). Modulation of cortical oscillatory activities induced by varying single-pulse transcranial magnetic stimulation intensity over the left primary motor area: a combined EEG and TMS study. *Neuroimage*, *27*(4), 896-908. doi:10.1016/j.neuroimage.2005.05.013
- Fujiki, M., & Steward, O. (1997). High frequency transcranial magnetic stimulation mimics the effects of ECS in upregulating astroglial gene expression in the murine CNS. *Brain Res Mol Brain Res*, *44*(2), 301-308.
- Funke, K., & Benali, A. (2011). Modulation of cortical inhibition by rTMS - findings obtained from animal models. *J Physiol*, *589*(Pt 18), 4423-4435. doi:10.1113/jphysiol.2011.206573
- Gedankien, T., Fried, P. J., Pascual-Leone, A., & Shafi, M. M. (2017). Intermittent theta-burst stimulation induces correlated changes in cortical and corticospinal excitability in healthy older subjects. *Clin Neurophysiol*, *128*(12), 2419-2427. doi:10.1016/j.clinph.2017.08.034
- Gloor, P. (1985). Neuronal generators and the problem of localization in electroencephalography: application of volume conductor theory to electroencephalography. *J Clin Neurophysiol*, *2*(4), 327-354.
- Goldsworthy, M. R., Muller-Dahlhaus, F., Ridding, M. C., & Ziemann, U. (2014). Inter-subject variability of LTD-like plasticity in human motor cortex: a matter of preceding motor activation. *Brain Stimul*, *7*(6), 864-870. doi:10.1016/j.brs.2014.08.004
- Gordon, P. C., Desideri, D., Belardinelli, P., Zrenner, C., & Ziemann, U. (2018). Comparison of cortical EEG responses to realistic sham versus real TMS of human motor cortex. *Brain Stimul*. doi:10.1016/j.brs.2018.08.003
- Gray, C. M., Konig, P., Engel, A. K., & Singer, W. (1989). Oscillatory responses in cat visual cortex exhibit inter-columnar synchronization which reflects global stimulus properties. *Nature*, *338*(6213), 334-337. doi:10.1038/338334a0
- Gupta, N., Singh, S. S., & Stopfer, M. (2016). Oscillatory integration windows in neurons. *Nat Commun*, *7*, 13808. doi:10.1038/ncomms13808
- Haegens, S., Nacher, V., Luna, R., Romo, R., & Jensen, O. (2011). alpha-Oscillations in the monkey sensorimotor network influence discrimination performance by rhythmical inhibition of neuronal spiking. *Proc Natl Acad Sci U S A*, *108*(48), 19377-19382. doi:10.1073/pnas.1117190108
- Hallett, M. (2007). Transcranial magnetic stimulation: a primer. *Neuron*, *55*(2), 187-199. doi:10.1016/j.neuron.2007.06.026
- Hamada, M., Murase, N., Hasan, A., Balaratnam, M., & Rothwell, J. C. (2013). The role of interneuron networks in driving human motor cortical plasticity. *Cereb Cortex*, *23*(7), 1593-1605. doi:10.1093/cercor/bhs147
- Hari, R. (2006). Action-perception connection and the cortical mu rhythm. *Prog Brain Res*, *159*, 253-260. doi:10.1016/S0079-6123(06)59017-X
- Huang, Y. Z., Edwards, M. J., Rounis, E., Bhatia, K. P., & Rothwell, J. C. (2005). Theta burst stimulation of the human motor cortex. *Neuron*, *45*(2), 201-206. doi:10.1016/j.neuron.2004.12.033
- Huang, Y. Z., & Rothwell, J. C. (2004). The effect of short-duration bursts of high-frequency, low-intensity transcranial magnetic stimulation on the human motor cortex. *Clin Neurophysiol*, *115*(5), 1069-1075. doi:10.1016/j.clinph.2003.12.026
- Huerta, P. T., & Lisman, J. E. (1995). Bidirectional synaptic plasticity induced by a single burst during cholinergic theta oscillation in CA1 in vitro. *Neuron*, *15*(5), 1053-1063.
- Ilmoniemi, R. J., Virtanen, J., Ruohonen, J., Karhu, J., Aronen, H. J., Naatanen, R., & Katila, T. (1997). Neuronal responses to magnetic stimulation reveal cortical reactivity and connectivity. *Neuroreport*, *8*(16), 3537-3540.

- Jensen, O., & Mazaheri, A. (2010). Shaping functional architecture by oscillatory alpha activity: gating by inhibition. *Front Hum Neurosci*, *4*, 186. doi:10.3389/fnhum.2010.00186
- Keck, M. E., Sillaber, I., Ebner, K., Welt, T., Toschi, N., Kaehler, S. T., . . . Engelmann, M. (2000). Acute transcranial magnetic stimulation of frontal brain regions selectively modulates the release of vasopressin, biogenic amines and amino acids in the rat brain. *Eur J Neurosci*, *12*(10), 3713-3720.
- Keil, J., Timm, J., Sanmiguel, I., Schulz, H., Obleser, J., & Schonwiesner, M. (2014). Cortical brain states and corticospinal synchronization influence TMS-evoked motor potentials. *J Neurophysiol*, *111*(3), 513-519. doi:10.1152/jn.00387.2013
- Kičić, D., Lioumis, P., Ilmoniemi, R. J., & Nikulin, V. V. (2008). Bilateral changes in excitability of sensorimotor cortices during unilateral movement: combined electroencephalographic and transcranial magnetic stimulation study. *Neuroscience*, *152*(4), 1119-1129. doi:10.1016/j.neuroscience.2008.01.043
- Kirschstein, T., & Köhling, R. (2009). What is the source of the EEG? *Clinical EEG and Neurosc*, *40*(3), 146-149.
- Komssi, S., Kahkonen, S., & Ilmoniemi, R. J. (2004). The effect of stimulus intensity on brain responses evoked by transcranial magnetic stimulation. *Hum Brain Mapp*, *21*(3), 154-164. doi:10.1002/hbm.10159
- Laakso, I., Hirata, A., & Ugawa, Y. (2014). Effects of coil orientation on the electric field induced by TMS over the hand motor area. *Phys Med Biol*, *59*(1), 203-218. doi:10.1088/0031-9155/59/1/203
- Labedi, A., Benali, A., Mix, A., Neubacher, U., & Funke, K. (2014). Modulation of inhibitory activity markers by intermittent theta-burst stimulation in rat cortex is NMDA-receptor dependent. *Brain Stimul*, *7*(3), 394-400. doi:10.1016/j.brs.2014.02.010
- Lenz, M., Galanis, C., Muller-Dahlhaus, F., Opitz, A., Wierenga, C. J., Szabo, G., . . . Vlachos, A. (2016). Repetitive magnetic stimulation induces plasticity of inhibitory synapses. *Nat Commun*, *7*, 10020. doi:10.1038/ncomms10020
- Lopez-Alonso, V., Cheeran, B., Rio-Rodriguez, D., & Fernandez-Del-Olmo, M. (2014). Inter-individual variability in response to non-invasive brain stimulation paradigms. *Brain Stimul*, *7*(3), 372-380. doi:10.1016/j.brs.2014.02.004
- Mäki, H., & Ilmoniemi, R. J. (2010). EEG oscillations and magnetically evoked motor potentials reflect motor system excitability in overlapping neuronal populations. *Clin Neurophysiol*, *121*(4), 492-501. doi:10.1016/j.clinph.2009.11.078
- Mansur, C. G., Fregni, F., Boggio, P. S., Riberto, M., Gallucci-Neto, J., Santos, C. M., . . . Pascual-Leone, A. (2005). A sham stimulation-controlled trial of rTMS of the unaffected hemisphere in stroke patients. *Neurology*, *64*(10), 1802-1804. doi:10.1212/01.WNL.0000161839.38079.92
- Massimini, M., Ferrarelli, F., Huber, R., Esser, S. K., Singh, H., & Tononi, G. (2005). Breakdown of cortical effective connectivity during sleep. *Science*, *309*(5744), 2228-2232. doi:10.1126/science.1117256
- Massimini, M., Rosanova, M., & Mariotti, M. (2003). EEG slow (approximately 1 Hz) waves are associated with nonstationarity of thalamo-cortical sensory processing in the sleeping human. *J Neurophysiol*, *89*(3), 1205-1213. doi:10.1152/jn.00373.2002
- McAllister, S. M., Rothwell, J. C., & Ridding, M. C. (2011). Cortical oscillatory activity and the induction of plasticity in the human motor cortex. *Eur J Neurosci*, *33*(10), 1916-1924. doi:10.1111/j.1460-9568.2011.07673.x
- Mutanen, T., Nieminen, J. O., & Ilmoniemi, R. J. (2013). TMS-evoked changes in brain-state dynamics quantified by using EEG data. *Front Hum Neurosci*, *7*, 155. doi:10.3389/fnhum.2013.00155

- Neuper, C., Grabner, R. H., Fink, A., & Neubauer, A. C. (2005). Long-term stability and consistency of EEG event-related (de-)synchronization across different cognitive tasks. *Clin Neurophysiol*, *116*(7), 1681-1694. doi:10.1016/j.clinph.2005.03.013
- Nikouline, V., Ruohonen, J., & Ilmoniemi, R. J. (1999). The role of the coil click in TMS assessed with simultaneous EEG. *Clin Neurophysiol*, *110*(8), 1325-1328.
- Nikulin, V. V., Kičić, D., Kahkonen, S., & Ilmoniemi, R. J. (2003). Modulation of electroencephalographic responses to transcranial magnetic stimulation: evidence for changes in cortical excitability related to movement. *Eur J Neurosci*, *18*(5), 1206-1212.
- Nowak, D. A., Grefkes, C., Dafotakis, M., Eickhoff, S., Kust, J., Karbe, H., & Fink, G. R. (2008). Effects of low-frequency repetitive transcranial magnetic stimulation of the contralesional primary motor cortex on movement kinematics and neural activity in subcortical stroke. *Arch Neurol*, *65*(6), 741-747. doi:10.1001/archneur.65.6.741
- Nunez, P. L., & Silberstein, R. B. (2000). On the relationship of synaptic activity to macroscopic measurements: does co-registration of EEG with fMRI make sense? *Brain Topogr*, *13*(2), 79-96.
- Nunez, P. L., & Srinivasan, R. (2006). *Electric fields of the brain : the neurophysics of EEG* (2nd ed.). Oxford: Oxford University Press.
- Padberg, F., Zwanzger, P., Thoma, H., Kathmann, N., Haag, C., Greenberg, B. D., . . . Moller, H. J. (1999). Repetitive transcranial magnetic stimulation (rTMS) in pharmacotherapy-refractory major depression: comparative study of fast, slow and sham rTMS. *Psychiatry Res*, *88*(3), 163-171.
- Pascual-Leone, A., Valls-Sole, J., Wassermann, E. M., & Hallett, M. (1994). Responses to rapid-rate transcranial magnetic stimulation of the human motor cortex. *Brain*, *117* (Pt 4), 847-858.
- Pasley, B. N., Allen, E. A., & Freeman, R. D. (2009). State-dependent variability of neuronal responses to transcranial magnetic stimulation of the visual cortex. *Neuron*, *62*(2), 291-303. doi:10.1016/j.neuron.2009.03.012
- Paus, T., Sipila, P. K., & Strafella, A. P. (2001). Synchronization of neuronal activity in the human primary motor cortex by transcranial magnetic stimulation: an EEG study. *J Neurophysiol*, *86*(4), 1983-1990. doi:10.1152/jn.2001.86.4.1983
- Peinemann, A., Lehner, C., Mentschel, C., Munchau, A., Conrad, B., & Siebner, H. R. (2000). Subthreshold 5-Hz repetitive transcranial magnetic stimulation of the human primary motor cortex reduces intracortical paired-pulse inhibition. *Neurosci Lett*, *296*(1), 21-24.
- Peinemann, A., Reimer, B., Loer, C., Quartarone, A., Munchau, A., Conrad, B., & Siebner, H. R. (2004). Long-lasting increase in corticospinal excitability after 1800 pulses of subthreshold 5 Hz repetitive TMS to the primary motor cortex. *Clin Neurophysiol*, *115*(7), 1519-1526. doi:10.1016/j.clinph.2004.02.005
- Premoli, I., Bergmann, T. O., Fecchio, M., Rosanova, M., Biondi, A., Belardinelli, P., & Ziemann, U. (2017). The impact of GABAergic drugs on TMS-induced brain oscillations in human motor cortex. *Neuroimage*, *163*, 1-12. doi:10.1016/j.neuroimage.2017.09.023
- Premoli, I., Castellanos, N., Rivolta, D., Belardinelli, P., Bajo, R., Zipser, C., . . . Ziemann, U. (2014). TMS-EEG signatures of GABAergic neurotransmission in the human cortex. *J Neurosci*, *34*(16), 5603-5612. doi:10.1523/JNEUROSCI.5089-13.2014
- Quartarone, A., Bagnato, S., Rizzo, V., Morgante, F., Sant'angelo, A., Battaglia, F., . . . Girlanda, P. (2005). Distinct changes in cortical and spinal excitability following high-frequency repetitive TMS to the human motor cortex. *Exp Brain Res*, *161*(1), 114-124. doi:10.1007/s00221-004-2052-5
- Rocchi, L., Ibanez, J., Benussi, A., Hannah, R., Rawji, V., Casula, E., & Rothwell, J. (2018). Variability and Predictors of Response to Continuous Theta Burst Stimulation: A TMS-EEG Study. *Front Neurosci*, *12*, 400. doi:10.3389/fnins.2018.00400

- Rogasch, N. C., & Fitzgerald, P. B. (2013). Assessing cortical network properties using TMS-EEG. *Hum Brain Mapp*, *34*(7), 1652-1669. doi:10.1002/hbm.22016
- Romei, V., Brodbeck, V., Michel, C., Amedi, A., Pascual-Leone, A., & Thut, G. (2008). Spontaneous fluctuations in posterior alpha-band EEG activity reflect variability in excitability of human visual areas. *Cereb Cortex*, *18*(9), 2010-2018. doi:10.1093/cercor/bhm229
- Romero, J. R., Ansel, D., Sparing, R., Gangitano, M., & Pascual-Leone, A. (2002). Subthreshold low frequency repetitive transcranial magnetic stimulation selectively decreases facilitation in the motor cortex. *Clin Neurophysiol*, *113*(1), 101-107.
- Rosanova, M., Casali, A., Bellina, V., Resta, F., Mariotti, M., & Massimini, M. (2009). Natural frequencies of human corticothalamic circuits. *J Neurosci*, *29*(24), 7679-7685. doi:10.1523/JNEUROSCI.0445-09.2009
- Rutishauser, U., Ross, I. B., Mamelak, A. N., & Schuman, E. M. (2010). Human memory strength is predicted by theta-frequency phase-locking of single neurons. *Nature*, *464*(7290), 903-907. doi:10.1038/nature08860
- Salenius, S., Portin, K., Kajola, M., Salmelin, R., & Hari, R. (1997). Cortical control of human motoneuron firing during isometric contraction. *J Neurophysiol*, *77*(6), 3401-3405. doi:10.1152/jn.1997.77.6.3401
- Sauseng, P., Klimesch, W., Gerloff, C., & Hummel, F. C. (2009). Spontaneous locally restricted EEG alpha activity determines cortical excitability in the motor cortex. *Neuropsychologia*, *47*(1), 284-288. doi:10.1016/j.neuropsychologia.2008.07.021
- Siebner, H. R., Peller, M., Willloch, F., Minoshima, S., Boecker, H., Auer, C., . . . Bartenstein, P. (2000). Lasting cortical activation after repetitive TMS of the motor cortex: a glucose metabolic study. *Neurology*, *54*(4), 956-963.
- Siegle, J. H., & Wilson, M. A. (2014). Enhancement of encoding and retrieval functions through theta phase-specific manipulation of hippocampus. *Elife*, *3*, e03061. doi:10.7554/eLife.03061
- Sjöström, P. J., & Häusser, M. (2006). A cooperative switch determines the sign of synaptic plasticity in distal dendrites of neocortical pyramidal neurons. *Neuron*, *51*(2), 227-238. doi:10.1016/j.neuron.2006.06.017
- Talelli, P., Greenwood, R. J., & Rothwell, J. C. (2007). Exploring Theta Burst Stimulation as an intervention to improve motor recovery in chronic stroke. *Clin Neurophysiol*, *118*(2), 333-342. doi:10.1016/j.clinph.2006.10.014
- Van Der Werf, Y. D., & Paus, T. (2006). The neural response to transcranial magnetic stimulation of the human motor cortex. I. Intracortical and cortico-cortical contributions. *Exp Brain Res*, *175*(2), 231-245. doi:10.1007/s00221-006-0551-2
- Veniero, D., Ponzio, V., & Koch, G. (2013). Paired associative stimulation enforces the communication between interconnected areas. *J Neurosci*, *33*(34), 13773-13783. doi:10.1523/JNEUROSCI.1777-13.2013
- Vernet, M., Bashir, S., Yoo, W. K., Oberman, L., Mizrahi, I., Ifert-Miller, F., . . . Pascual-Leone, A. (2014). Reproducibility of the effects of theta burst stimulation on motor cortical plasticity in healthy participants. *Clin Neurophysiol*, *125*(2), 320-326. doi:10.1016/j.clinph.2013.07.004
- Vernet, M., Bashir, S., Yoo, W. K., Perez, J. M., Najib, U., & Pascual-Leone, A. (2013). Insights on the neural basis of motor plasticity induced by theta burst stimulation from TMS-EEG. *Eur J Neurosci*, *37*(4), 598-606. doi:10.1111/ejn.12069
- Vlachos, A., Muller-Dahlhaus, F., Rosskopf, J., Lenz, M., Ziemann, U., & Deller, T. (2012). Repetitive magnetic stimulation induces functional and structural plasticity of excitatory postsynapses in mouse organotypic hippocampal slice cultures. *J Neurosci*, *32*(48), 17514-17523. doi:10.1523/JNEUROSCI.0409-12.2012

- Wiethoff, S., Hamada, M., & Rothwell, J. C. (2014). Variability in response to transcranial direct current stimulation of the motor cortex. *Brain Stimul*, 7(3), 468-475. doi:10.1016/j.brs.2014.02.003
- Zrenner, C., Desideri, D., Belardinelli, P., & Ziemann, U. (2018). Real-time EEG-defined excitability states determine efficacy of TMS-induced plasticity in human motor cortex. *Brain Stimul*, 11(2), 374-389. doi:10.1016/j.brs.2017.11.016
- Zschocke, S., & Hansen, H.-C. (2012). *Klinische Elektroenzephalographie SpringerLink : Bücher* (3., aktualisierte und erweiterte Auflage ed.). doi:10.1007/978-3-642-19943-1

6. German summary

Die nicht-invasive Hirnstimulation (auf Englisch, non-invasive brain stimulation, NIBS) ist eine vielversprechende Methode zur Modulation von Gehirnnetzwerken. Die transkranielle Magnetstimulation (TMS) ist eine NIBS-Technik, die kortikale Neuronen in einer räumlich-zeitlichen Skala von Millimetern und Millisekunden aktivieren kann. Ihr Potential hat die TMS nicht nur für elektrophysiologische und kognitive Untersuchungen und für die Verhaltensforschung bewiesen, sondern auch für die Behandlung neurologischer und psychiatrischer Störungen. Jedoch ist die klinische Anwendung von TMS gegenwärtig noch beschränkt, da sowohl die elektrophysiologischen Antworten auf TMS als auch die klinische Besserung von Patienten, die mit TMS behandelt wurden, häufig durch eine hohe Variabilität zwischen Sitzungen und Probanden gekennzeichnet sind. Ein wesentlicher Teil dieser Variabilität kann der laufenden Hirnaktivität zum Zeitpunkt der Stimulation zugeschrieben werden.

Um den Vorteil von hirnzustandsabhängigen TMS experimentell zu beweisen, wurde im Rahmen dieser Forschungsarbeit eine TMS-Anordnung entwickelt, die die elektrische Gehirnaktivität mit Elektroenzephalographie (EEG) registriert und auf deren Grundlage TMS-Impulse auslöst. Durch die Verwendung dieser EEG-getriggerten TMS-Anordnung in Echtzeit, wird die Beurteilung der Abhängigkeit ermöglicht, die zwischen den elektrophysiologischen Antworten auf TMS des linken motorischen Kortex gesunder Probanden von der Phase der sogenannten μ -Oszillation besteht. Diese Oszillation weist eine Frequenz zwischen 8-12 Hz auf und wird im sensomotorischen Kortex generiert. Wir haben einzelne TMS-Impulse auf den negativen Peak, den positiven Peak oder die zufällige Phase der μ -Oszillation synchronisiert, um die Abhängigkeit der kortikospinalen und kortikalen Erregbarkeit von der μ -Phase zu ermitteln. Außerdem haben wir wiederholt 200 TMS-Triplets mit einer Frequenz von 100 Hz, also repetitive TMS (rTMS), und zwar entweder auf den negativen Peak, den positiven Peak oder die zufällige Phase der μ -Oszillation angewandt, um die Abhängigkeit der rTMS-induzierten dauerhaften Veränderungen in kortikospinaler und kortikaler Erregbarkeit von der μ -Phase zu bewerten. Wir haben einerseits die kortikospinale Erregbarkeit über die Amplitude der motorisch

evozierten Potentiale (MEPs) gemessen. Die MEPs wurden dabei an einem Muskel der rechten Hand aufgezeichnet. Die kortikale Erregbarkeit wurde andererseits über die Amplitude der TMS-evozierten Potentiale (TEPs) und über die Leistung der TMS-induzierten Oszillationen mit dem EEG gemessen. Darüber hinaus konnte ein Teil der Daten, die für die Beurteilung der μ -phasenabhängigen kortikalen Erregbarkeit erfasst wurden, benutzt werden, um die Unterschiede zwischen den kortikalen Antworten auf echte TMS bei Intensitäten über und unter der Ruhe-Motorschwelle (auf English, resting motor threshold, RMT), sowie auf eine realistische Scheinstimulation zu bewerten.

Mit einzelnen TMS-Impulsen am negativen Peak der laufenden μ -Oszillation wurden größere MEPs erhalten, als am positiven Peak oder an der zufälligen Phase. Außerdem wurde mit negativ-Peak-synchronisierter rTMS eine dauerhafte (> 30 Minuten) Erhöhung der MEP-Amplitude erreicht, dahingegen wurde keine signifikante Änderung der MEP-Amplitude mit positiv-Peak-synchronisierter oder mit zufälliger Phase-synchronisierter rTMS erhalten. Am negativen Peak des μ -Rhythmus wurden mit einzelnen TMS-Impulsen auch größere TEPs erzeugt als am positiven Peak. Insbesondere war die negative Auslenkung, die etwa 100 ms nach der TMS-Anwendung in dem EEG Signal auftritt, sowohl für über als auch für unter RMT-Intensitäten konsistent größer. Wichtig ist, dass evozierte Potentiale, die durch realistische Schein-TMS hervorgerufen wurden, nicht durch die Phase der μ -Oszillation moduliert wurden. Trotz der dauerhaften signifikanten Zunahme der MEP-Amplitude hat negativ-Peak-getriggerte rTMS keine der untersuchten EEG-Messdaten signifikant verändert. Schließlich hat TMS über und unter der RMT im Vergleich zu realistischer Schein-TMS TEPs mit größeren Amplituden und eine signifikante Modulation der Leistung der TMS-induzierten Schwingungsaktivität hervorgerufen.

Zusammenfassend haben wir gezeigt, dass der negative Peak des sensorimotorischen μ -Rhythmus einen Zustand hoher Erregbarkeit des Motorsystems darstellt und dass rTMS, die mit diesem Zustand hoher Erregbarkeit synchronisiert ist, bei mehr als 90% der getesteten Teilnehmer zu einem Effekt führt, der einer Langzeitpotenzierung (LTP) ähnlich ist. Bei anderen

"erregbarkeitssteigernden" NIBS-Protokollen, die die aktuelle Hirnaktivität nicht berücksichtigen, weisen nur 52-61% der getesteten Probanden einen LTP-ähnlichem Effekt auf. Diese Ergebnisse stützen die Ansicht, dass hirnzustandabhängige TMS die Variabilität zwischen Probanden verringern kann. Wir haben auch gezeigt, dass TEPs für momentane Erregbarkeitsschwankungen empfindlich sind, wohingegen komplexe molekulare und synaptische Änderungen, die auf kortikaler Ebene durch rTMS induziert werden, möglicherweise nicht immer auf makroskopischer Ebene durch EEG nachweisbar sind. Kortikale Antworten auf echte TMS des motorischen Kortex spiegeln sehr wahrscheinlich die direkte Aktivierung von Neuronen wider, und nicht die sensorisch hervorgerufene TMS-Aktivität.

Diese Erkenntnisse sind für die Verbesserung von NIBS-basierten Therapien von Hirnnetzstörungen relevant. Zukünftige Studien sind erforderlich, um zu untersuchen, ob Oszillationen in anderen klinisch relevanten Bereichen des Gehirns ebenfalls die Antworten auf TMS beeinflussen, ähnlich wie wir es im motorischen Kortex für den μ -Rhythmus beobachten konnten.

7. Declaration of contribution of others

The dissertation work was carried out at the Department of Neurology & Stroke in the University Hospital of Tübingen and at Hertie Institute for Clinical Brain Research under the supervision of Prof. Dr. Ulf Ziemann. The studies were designed in collaboration with Prof. Dr. Ulf Ziemann, Dr. Christoph Zrenner, Dr. Paolo Belardinelli and Dr. Pedro Caldana Gordon. The real-time experimental set-up was assembled by Dr. Christoph Zrenner and we together developed the real-time software. I carried out the experiments with the assistance of Dr. Paolo Belardinelli. I programmed and carried out the processing of the experimental data. Statistical analysis was performed by myself and by Prof. Dr. Ulf Ziemann, Dr. Christoph Zrenner and Dr. Pedro Caldana Gordon. I wrote the manuscripts and created all the figures of the publications in which I have first authorship. When I share first authorship with Dr. Christoph Zrenner or Dr. Pedro Caldana Gordon, I wrote part of the manuscript and created part of the figures. The use of the mentioned publications for this doctoral thesis has been approved by all authors.

I confirm that I wrote the thesis myself and that any additional source of information has been cited and acknowledged within the text.

Debora Desideri

Acknowledgments

I would like to sincerely thank my supervisor Prof. Dr. Ulf Ziemann for the unique opportunity to join his research group and for his scientific advice and guidance during the years of my Ph.D.

My gratitude goes also to the members of my Ph.D. committee Prof. Jan Born and Prof. Dr. Markus Siegel for their time and their constructive criticism during our meetings.

I am especially grateful to Dr. Christoph Zrenner and Dr. Paolo Belardinelli for their constant and invaluable support and for fostering my scientific and personal development.

I would like to thank Dr. Inka Montero for her precious help with all bureaucratic procedures and her care during my time in the Ph.D. program.

Thanks also to all my colleagues and friends in the research group for the interesting discussions in the lab meetings, the funny conversations at lunch and for promoting a cooperative and pleasant working environment.

I want to thank all the roommates I had in my years in Tübingen for making home always a nice place to go back after a long working day and for their patience and support during my process of learning German.

Thanks to all my friends in Rome for being always close to me despite the many engagements and the distance, and to the many lovely people I met during my Ph.D. years for making my stay in Tübingen the enjoyable experience it was.

Last but not least, I thank my family for their constant support and for always encouraging me to pursue my interests and passions.